Synthesis Feasibility and Efficiency of Post-modification of Multifunctional Dendrimers

CHENG, Wing Sum

A Thesis Submitted in Partial

Fulfillment of the Requirements for the

Degree of Doctor of Philosophy in

Chemistry

The Chinese University of Hong Kong

July 2010

Thesis/Assessment Committee

Professor Thomas Chung Wai Mak (Chair)
Professor Hak-Fun Chow (Thesis Supervisor)
Professor Qian Miao (Committee Member)
Professor Wayne C. Hayes (External Examiner)
Professor Ricky Man Shing Wong (External Examiner)

Dedicated to my family

Acknowledgements

I would like to express my sincere gratitude to my supervisor, Prof. Hak-Fun Chow, for his patient guidance and invaluable advice during the course of my research and preparation of this thesis.

I would like to express my thanks to my labmates, especially to Dr. Guo-Xin Wong, Dr. Chui-Man Lo and Dr. Siu-Yin Cheung for their support and helpful discussion. Thanks are also given to my dearest friend, Ms. Millie Lai, Dr. Chun-Kit Hau and Ms. Kimmy Chan who encourage me a lot throughout my studies. Special thanks are given to Mr. David T. W. Chik (HKBU) for recording the MALDI-TOF mass spectra in this thesis.

Last but not the least, I would like to say thanks to my parents, brother and sister for their encouragement and support.

July, 2010

Wing-Sum Cheng

Department of Chemistry

The Chinese University of Hong Kong

Abstract

Two layer-block G3–CCS–dendrimer **68** and G3–CSC–dendrimer **69** with dibenzylsulfide functionalities embedded in the innermost and intermediate dendritic layers, respectively, were synthesized by a convergent method. The key steps involved in their constructions were Horner–Wadsworth–Emmons olefination and thiol-mediated alkylation reaction. A third target G3–SCC–dendrimer **70**, with dibenzylsulfide moieties located in the outermost dendritic layer, could not be synthesized despite many attempts. A fourth model G3–SSS–dendrimer **136** containing 21 dibenzyl sulfone moieties in the innermost, middle and outermost layers was also prepared. All synthesized compounds were characterized by ^{1}H and ^{13}C nuclear magnetic resonance spectroscopy, mass spectrometry, elemental analysis and/or size exclusion chromatography. They were prepared in order to probe the feasibility of and the effect of dendritic shielding on two novel dendrimer synthesis methodologies, namely, dendrimer interior functional group conversion and dendrimer backbone rearrangement.

The synthetic efficiency of the dendrimer interior functional group conversion method was exemplified by converting the dibenzyl sulfide moieties in G3–CCS–dendrimer **68** and G3–CSC–dendrimer **69** to the corresponding dibenzyl sulfone under either heterogeneous (oxone in CH_2Cl_2) or homogeneous (35% H_2O_2 in CH_2Cl_2/HOAc) conditions. The effect of steric inhibition was prominent under the heterogeneous conditions as the solid oxone particles failed to penetrate into the dendrimer interior to initiate the oxidation reaction. On the other hand, dendrimers **68**, **69** and **136** could be oxidized to the corresponding dibenzyl sulfones via the dibenzyl sulfoxides under homogeneous conditions. For the first oxidation to the

dibenzyl sulfoxides, both compounds **68** and **69** proceeded with similar speed, indicating the similar steric environment between the innermost and intermediate layers of dibenzylsulfide moieties. On the other hand, the innermost dibenzyl sulfoxides in compound **68**, in comparison to the dibenzyl sulfoxides in the middle layer in compound **69**, underwent further oxidation to the dibenzyl sulfones with greater ease. This finding suggested that there were other factors, in addition to steric inhibition, in controlling the chemical reactivity of functional groups inside the dendrimer matrix. Our speculation was that the microenvironment polarity of the dendrimer interior could also play an important role in facilitating/retarding the diffusion of external chemical reagents into the interior of the dendrimer.

The synthetic efficacy of the dendrimer backbone rearrangement was examined by conducting heterogeneous Ramburg-Bäcklund rearrangements (alumina supported KOH, CBr_2F_2/THF/*t*-BuOH = 1/1/1) on dibenzylsulfone G3–$CCSO_2$–dendrimer **141** and G3–CSO_2C–dendrimer **142**. Again, steric inhibition was found to play a prominent role in dictating the chemical reactivity of the sulfone moieties under heterogeneous conditions. The innermost sulfones in compound **141** were found to be relatively inert and at most only 1 out of the 3 sulfones could undergo the rearrangement, and the major product was the starting material. On the other hand, up to 3 or 4 of the intermediate layer sulfone moieties underwent the rearrangement reaction to give the triene–tris(sulfone) **145** or tetraene–bis(sulfone) **144** products. For the first time in the literature, conclusive mass spectral evidence was obtained to unveil the detailed outcome of such complex dendrimer backbone rearrangement reactions.

摘　要

本論文報導了含二苄基硫醚的第三代層狀結構樹枝狀聚合物的合成方法及其表徵。當中，G3–CCS–dendrimer **68** 及 G3–CSC–dendrimer **69** 分別於最內層及中層含有二苄基硫醚結構。其合成方法主要依據 Horner–Wadsworth–Emmons 烯化反應和硫–烷基化反應。於最外層含二苄基硫醚的 G3–SCC–dendrimer **70** 卻在多番嘗試後仍未能以同類方法完成其合成。另外，亦成功制備了於外、中、內層共含 21 個二苄基硫醚的 G3–SSS–dendrimer **136**。所有合成產物皆經過核磁共振、質譜、凝膠色譜及元素分析。第三代層狀結構樹枝狀聚合物成功制備後便用以研究樹枝狀聚合物的內部功能基轉換及主幹重排的有效性，以及樹枝狀物的屏閉性對這兩種反應的影響。

樹枝狀聚合物的內部功能基轉換的有效性可經由 G3–CCS–dendrimer **68** 及 G3–CSC–dendrimer **69** 在 35%過氧化氫二氯甲烷醋酸溶液進行同相氧化反應或於過硫氫化鉀和二氯甲烷進行異相氧化反應。在異相反應環境，由於樹枝狀聚合物的位阻作用，固態過硫氫化鉀未能滲透入樹枝狀聚合物的內部引發反應。相反，樹枝狀聚合物 **68**、**69** 及 **136** 可在同相反應環境被氧化。樹枝狀聚合物裡的二苄基硫醚會先被氧化成二苄基亞碸，然後再被氧化成二苄基碸。當聚合物 **68** 及 **69** 進行第一步氧化反應時，兩者反應速率相當。這表明最內層及中層具有相似的位阻環境。但是，當進行第二步氧化反應時，在最內層的二苄基亞碸會比中層的更容易被氧化成二苄基碸。這現象說明功能團在樹枝狀聚合物內部的反應活性除了受位阻效應影響外，還受到其他因素影響。我們推測在樹枝狀聚合物微觀環境的極性對促進或阻礙化學試劑擴散入內部有重大影響。

樹枝狀聚合物的主幹重排的有效性可由 G3–CCSO$_2$–dendrimer **141** 及 G3–CSO$_2$C–dendrimer **142** 的 Ramburg-Bäcklund 重排反應結果得出。同樣地，位

阻效應對含碸功能團在異相反應環境中的活性也起主導作用。在主幹重排反應中， G3–$CCSO_2$–dendrimer **141** 最內層碸基的活性相對很低，只有少量原料進行了部分反應（當中 3 個含碸功能團中僅有 1 個進行反應）。相反，G3–CSO_2C–dendrimer **142** 中層碸基的活性相對較高，6 個含碸功能團中有 3 至 4 個進行反應。在本論文中，第一次通過質譜發現如此複雜的樹枝狀聚合物主幹重排反應的結果。

Table of contents Page

Chapter 3 – Synthesis and Characterization of Layer-Block Oligosulfide Dendrimers

Chapter 4 – Feasibility and Efficiency of Post-modifications of Mutifunctional Dendrimers

List of dendritic compounds involved in the synthetic schemes:

Molecular structure #	First page of appearance	Molecular structure #	First page of appearance
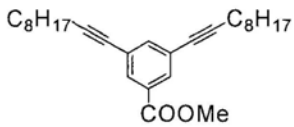 **72**	43	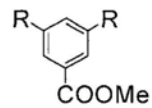 **73**	43
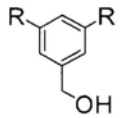 **74**	43	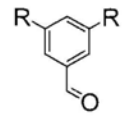 **108**	52
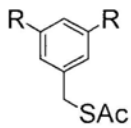 **125**	57	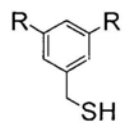 **126**	57
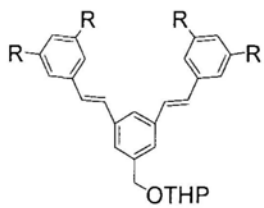 **109**	52	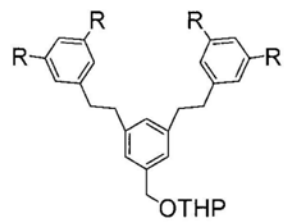 **110**	52
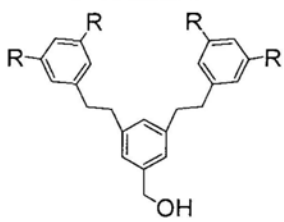 **111**	52	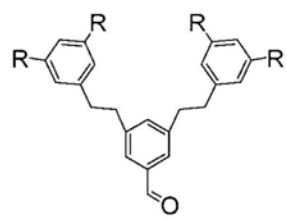 **112**	52
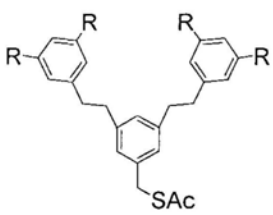 **118**	55	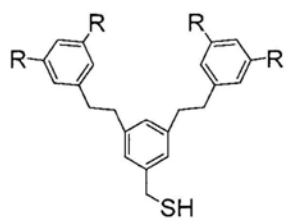 **119**	55

R = $-C_{10}H_{21}$

Molecular structure #	First page of appearance	Molecular structure #	First page of appearance
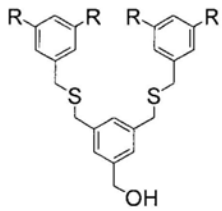 **124**	57	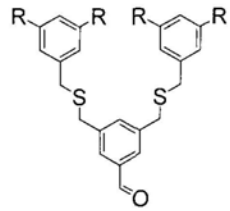 **127**	57
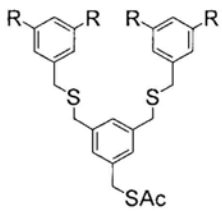 **131**	60	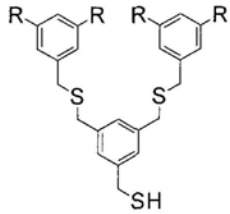 **132**	60
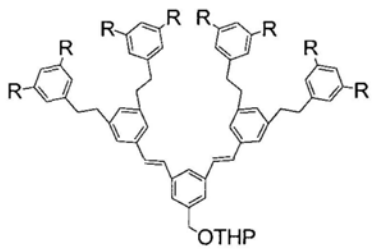 **113**	52	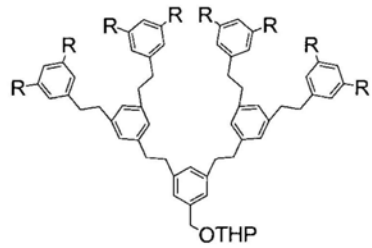 **14**	52
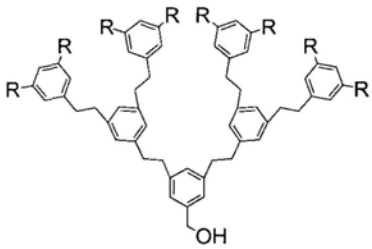 **115**	52	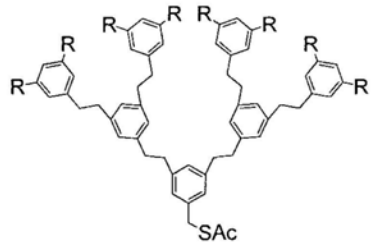 **16**	52
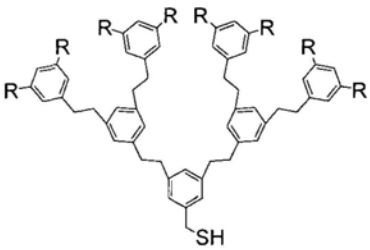 **117**	53	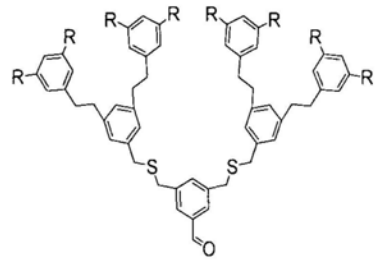 **120**	55

R = $-C_{10}H_{21}$

Molecular structure #	First page of appearance	Molecular structure #	First page of appearance
 **75**	44	 **128**	58
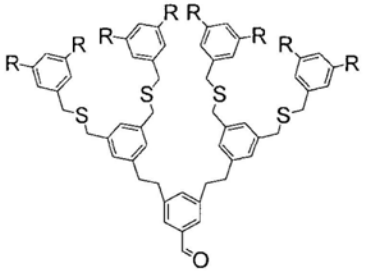 **129**	58	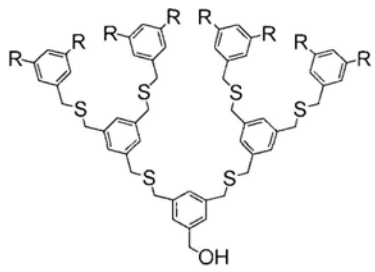 **133**	60
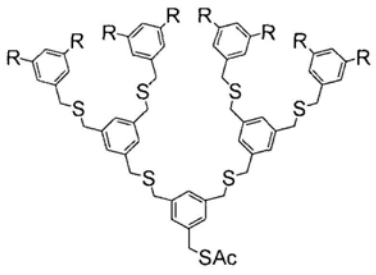 **134**	60	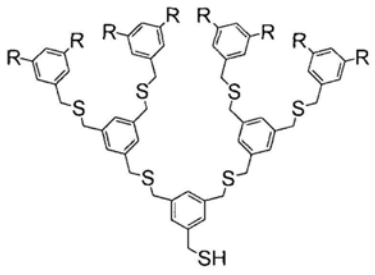 **135**	61
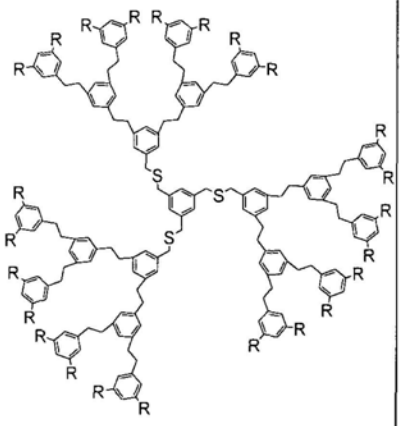 **68**	53	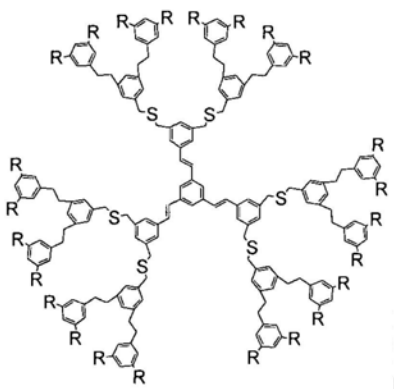 **121**	55

R = $-C_{10}H_{21}$

Molecular structure #	First page of appearance	Molecular structure #	First page of appearance
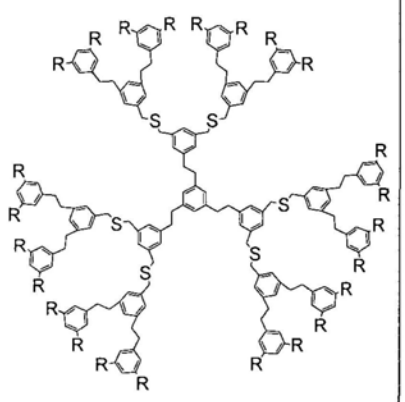 **69**	55	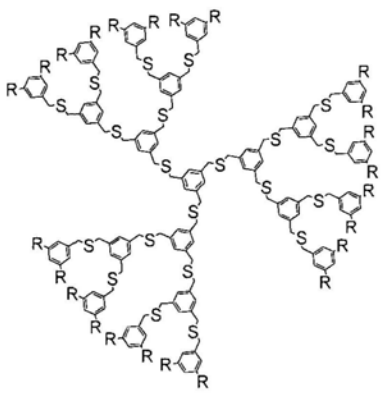 **136**	61
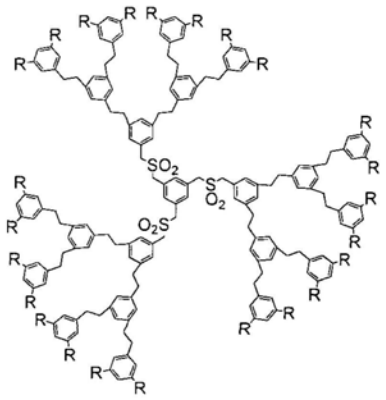 **141**	77	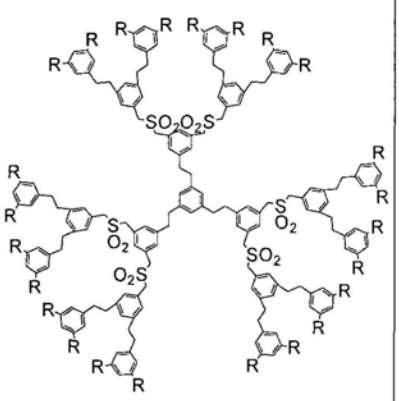 **142**	77
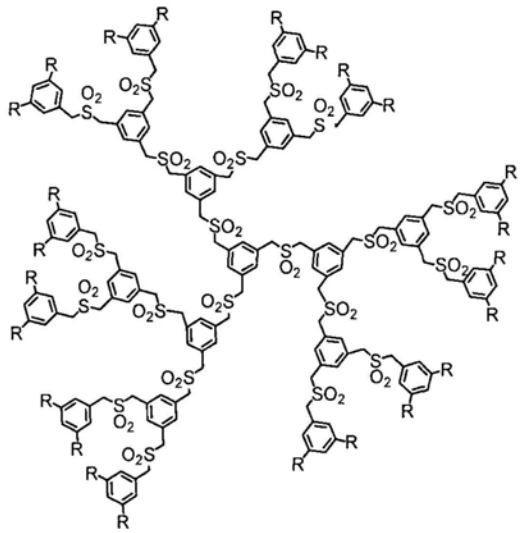 **138**			76

R = $-C_{10}H_{21}$

Abbreviations

AcOH	acetic acid	h	hour(s)
Ar	aromatic	HRMS	high resolution mass
Anal. Calcd	analytical calculated		spectrometry
a.u.	arbitrary unit(s)	HSQC	heteronuclear single quantum
Bn	benzyl		coherence
BuOH	butanol	*J*	coupling constant
^{o}C	Degree Celsius	μ	micro
cat.	catalytic	m	multiplet (NMR); milli
COSY	correlation spectroscopy	M	molar; mega
δ	chemical shift in ppm	MALDI	matrix-assisted laser
d	double (NMR)		desorption ionization
dd	doublet of doublet (NMR)	Me	methyl
DIAD	diisopropyl	MeOH	methanol
	azodicarboxylate	MeCN	acetonitrile
DME	dimethoxyethane	MHz	megahertz
DMSO	dimethylsulfoxide	mmol	millimole
ESI	electrospray ionization	M_n	number-average molecular
Et	ethyl		weight
EtOAc	ethyl acetate	mol	mole
EtOH	ethanol	mp	melting point
FAB	fast atom bombardment	MS	mass spectrometry
g	gram(s)	M_w	weight-average molecular
GPC	gel permeation		weight
	chromatography	*m/z*	mass-to-charge ratio

NMR	nuclear magnetic resonance	S_N	nucleophilic substitution
PAMAM	polyamidoamine dendrimer	*t*-Bu	tertiary butyl
PDI	polydispersity index	t	triplet (NMR)
PCC	pyridinium chlorochromate	TBAI	tetrabutylammonium iodide
Ph	phenyl	THF	tetrahydrofuran
PPI	poly(propylene imine)	THP	tetrahydropyranyl
ppm	part(s) per million	TLC	thin layer chromatography
q	quartet (NMR)	TMS	trimethylsilyl
R_f	retention factor	TOF	time of flight
s	singlet (NMR)	UV	ultraviolet

Chapter 1: Introduction to dendrimers

Dendrimer chemistry has gained increasing attention in various research fields, such as, biotechnology, medicine and nanotechnology. The term 'dendrimer' is originated from Greek (dendron = tree; meros = part) and this gives a precise description that dendrimer is a kind of molecule having a tree-like, highly branched three-dimensional architecture. The well-defined branched structure developed through an iterative synthetic method was first disclosed by Vögtle[1] in 1978. Later, Tomalia et al. reported the first family of PAMAM dendrimers[2,3] which was also known as 'starburst' polymers. Shortly thereafter Newkome's 'arborol' systems were also prepared.[4] Since then, many kinds of dendrimers with unique properties and applications have been developed. [5-10]

1.1 Dendritic structure

Dendrimers are highly ordered, globular macromolecules synthesized by a stepwise iterative approach. Basically, a dendritic structure can be divided into three distinct regions: (i) the central core, (ii) layers of repeating branching units and (iii) surface groups on the outer layers of the branching units (Figure 1).

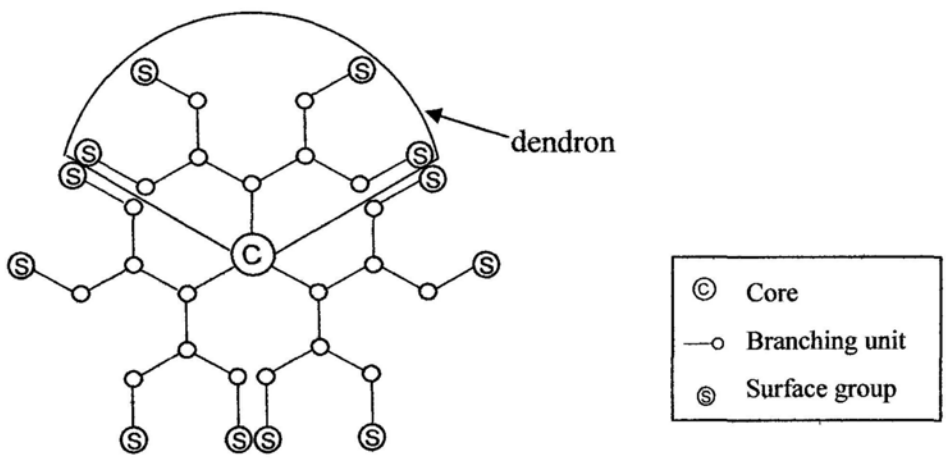

Figure 1. Schematic outline of a G3 dendrimer.

'Dendron' is referred to one of the dendritic wedges connecting to the central core. The number of dendrons present in a dendrimer molecule depends on the core multiplicity. 'Generation' is a term commonly used to express the size of a dendrimer. The number of generation equals to the number of concentric branching layers present in a dendrimer. Therefore, a dendrimer with n layers of branching units is called a n^{th} generation dendrimer and is denoted as [Gn].

Dendrimers of high generation will adopt a globular shape as the number of branching ends of the dendrimer increases exponentially with increasing generation number. Steric crowding of the branches at the surface of a dendritic molecule causes the adoption of a globular conformation.[4,11,12] When the steric effect becomes profound, complete conversion of all the surface functionalities becomes difficult after a specific generation. This is called the 'starburst effect'. However, it is also because of the spherical shape of the dendrimer that confers its interesting properties.

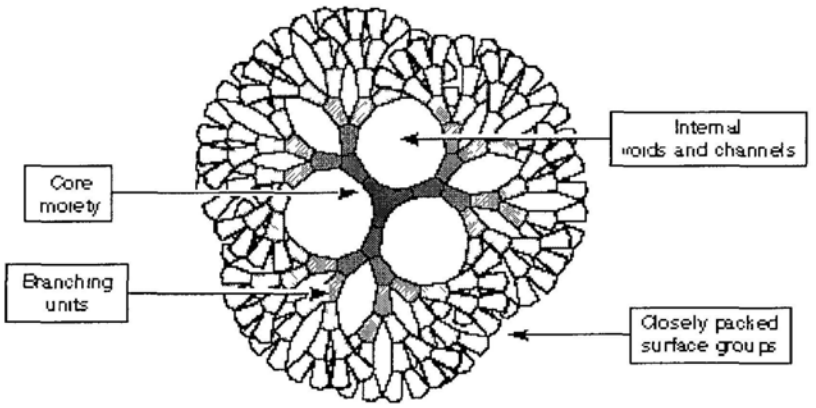

Figure 2. A 3-dimensinal representation of a dendrimer (adopted from website: www.ninger.com/dendrimer/one.htm#1.1).

Dendrimer usually has internal voids as well as closely packed surface groups (Figure 2).[13] These interior voids are shielded from the surrounding so there can be

changes of physical/ chemical properties of the internal functionalities. For examples, labile functionalities locating inside the interior may gain extra stability due to the shielding effect of the dendritic shell.[14,15] Also, the presence of internal voids inside a dendrimer would result in the formation of dendritic boxes that can encapsulate guest molecules.[16] The surface chemistry of dendrimer, on the other hand, is different from that of the internal microenvironment. By modifying the functional groups on the surface of a dendrimer, dendritic systems with different properties can be developed. Since two distinct chemical environments can occur in such a molecule, this opens up many possibilities for dendrimer applications.

1.2 Synthetic approaches of dendritic molecules

Two complementary synthetic approaches are used for the synthesis of dendrimers. They are the divergent and the convergent approaches. Both synthetic approaches involve stepwise addition and activation steps to generate higher generation dendritic molecules. By using iterative synthetic procedures, structurally perfect dendrimers with high purity and narrow polydispersity can be prepared.

1.2.1 Divergent approach

The divergent approach was first employed in dendrimer synthesis.[1–4] In this strategy, dendrimers are constructed from the central core towards the periphery (Scheme 1). In the beginning, the peripheral functionalities of the core are coupled to the reactive site of the branching unit **1** to yield the G1 dendrimer **2**. The peripheral functional groups on the branching unit are designed to be protected or unreactive to prevent uncontrolled hyperbranched polymerization. After the first coupling reaction,

the protected surface functionalities are then activated for the next stage of reaction. Activation of the peripheral groups may involve their conversion to another type of reactive functionality, or the removal of the protecting groups.

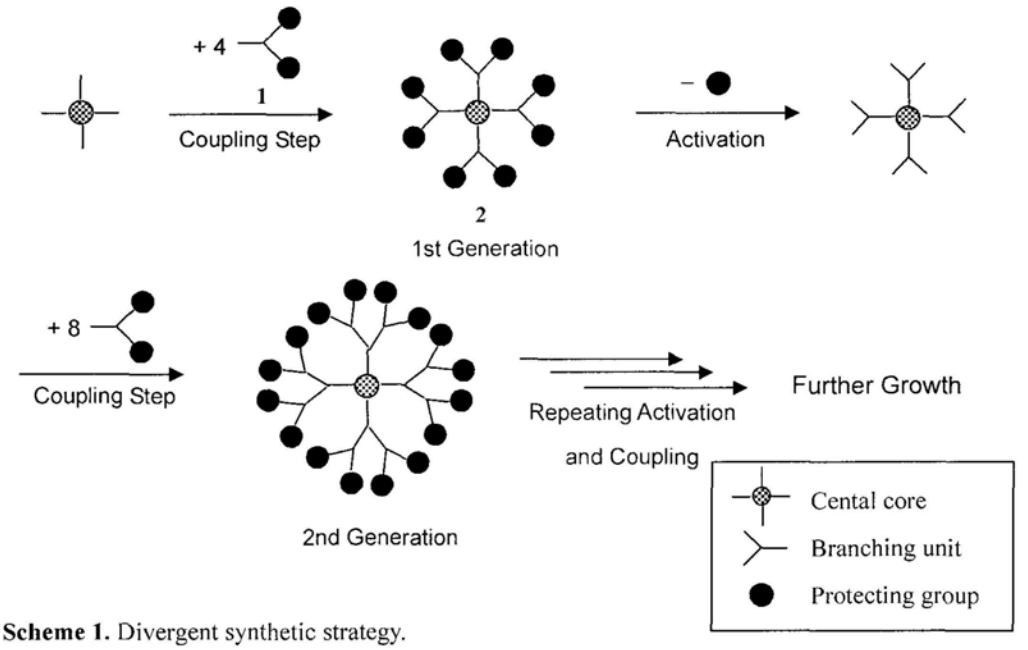

Scheme 1. Divergent synthetic strategy.

As expected, during the repetition of coupling and activation reactions, the number of reaction sites at the periphery involved in the generation growth will increase exponentially, so it is difficult to guarantee the completeness of reactions at all reaction sites even when a large excess of reagent is used. Also, any undesired molecular species resulting from side reactions as well as incomplete reactions cannot be removed easily because of their structural similarity to the intended product. Consequently, structural defects in higher generations are virtually inevitable. Nevertheless, the divergent approach is an efficient strategy to synthesize high generation dendrimers in a shorter synthetic procedure.

1.2.2 Convergent approach

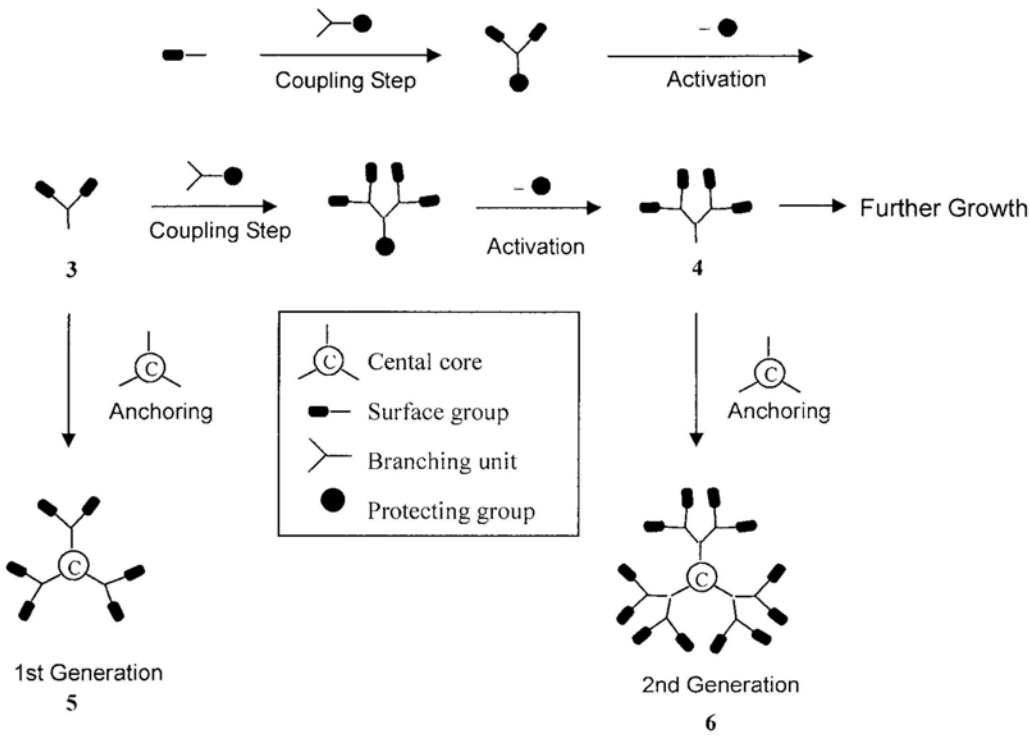

Scheme 2. Convergent synthetic strategy.

The convergent approach was first reported by Hawker and Fréchet in 1989–1990.[17–19] Contrary to the divergent approach, dendrimers are built from the periphery towards the central core (Scheme 2). Every activation and coupling reaction cycle add one new generation to a dendron. In the coupling steps, the reaction sites are located at the focal points of dendrons (*e.g.* **3** or **4**), but not the periphery of the dendrimer so the number of reaction sites is limited and is dependent on the multiplicity of the branching unit. After completion of the coupling, the single functional group located at the focal point of the dendron can be activated for further growth. Finally, dendrons of the desired generations (*e.g.* **3** or **4**) can be coupled to a polyfunctional core to yield the target dendrimer (*e.g.* **5** or **6**).

As mentioned before, only a small number of reaction sites is involved in each coupling or activation step, so the reaction can be driven to completion with a slightly excess of reagent. Also, purification is more straightforward as a missing branch will impart a large different on the size and polarity of the dendrimer. Therefore, the convergent approach provides greater structural control than the divergent approach. Dendrimers synthesized by this approach will have higher purity and can be considered as monodisperse. However, for the synthesis of high generation dendrimers, the convergent approach is a relatively slow process. Besides, when the dendrons become bulky, the focal point is too congested to be accessed by the reactive branching units. Hence, the convergent approach is more appropriate for the synthesis of low generation dendrimers.

1.2.3 Accelerated Approaches

The divergent and convergent approaches are the most commonly used methods for the synthesis of dendritic macromolecules, but they often involve tedious procedures and purification steps. Therefore, in order to speed up the synthesis of dendrimers, several accelerated approaches were developed. These strategies combine the advantages of convergent and divergent approaches so that they can reduce the number of synthetic steps required to access higher generation dendritic molecules and simplify the purification process. At the same time, the product monodispersity can usually be maintained.

1.2.3.1 Hypercore approach

The hypercore approach, also known as the "double stage convergent approach",

was first reported by Fréchet and co-workers.[20] In the first stage of this strategy, low generation dendron and a dendritic core that contains layers of branching units (hypercore) are prepared either by standard convergent or divergent approaches. In the second stage of growth, surface groups of the dendritic core are activated and coupled divergently to the focal points of dendrons.

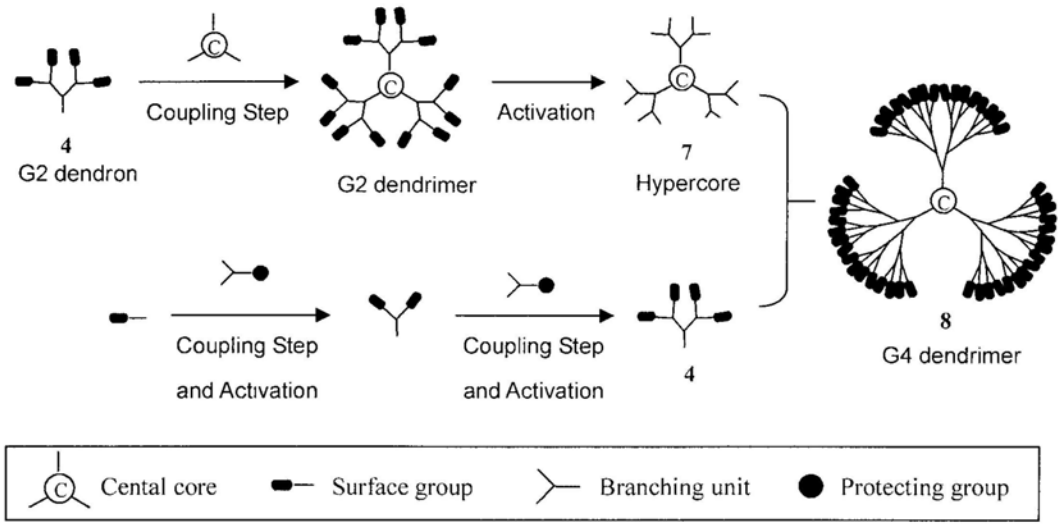

Scheme 3. The hypercore synthetic strategy.

This synthetic approach provides a more rapid and straightforward route to prepare higher generation dendrimers (Scheme 3). Hence, two or more G2 dendrons **4** are coupled to a G2 hypercore **7** to give a G4 dendrimer **8** in one step. The hypercore is less sterically hindered than the conventional core because of increased separation between the reactive sites at the periphery of the hypercore. Therefore, the higher G4 generation dendrimer **8** synthesized using this approach can be obtained in high yield.

1.2.3.2 Branched monomer approach

The branched monomer approach was another accelerated approach developed by Fréchet and co-workers in 1994.[21] The main feature of this approach involves the use of a dendritic branched monomer (*e.g.* **9**). The branched monomer is first synthesized using the convergent approach. Then, coupling and activation steps are performed just like the case using traditional branching unit. In each repetitive reaction cycle, two or more dendrimer generations can be introduced instead of just one generation as in the conventional synthetic method (Scheme 4). This strategy is very useful in the rapid preparation of higher generation dendrimers.

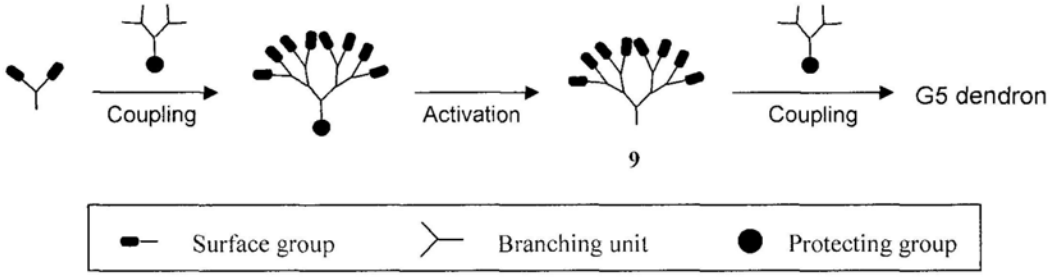

Scheme 4. Branched monomer approach.

1.2.3.3 Double Exponential Synthetic Strategy

Moore and co-worker proposed a "double exponential synthetic strategy" in 1995 that involved the use of a branching unit **12** with orthogonally protected focal and peripheral functionalities (Scheme 5).[22] The first generation dendron **10** can be modified either at the focal point or at the periphery to afford activated dendron **3** and branching unit **11**, respectively, under different chemical conditions. Coupling reaction between the protected building blocks **3** and **11** then gives a second generation dendron **12** which is then converted into two activated building blocks **4**

and **13** that again can be used to prepare a G4 dendron **14**. Each successive repetition of the activation-coupling cycle will lead to a doubling of generation number.

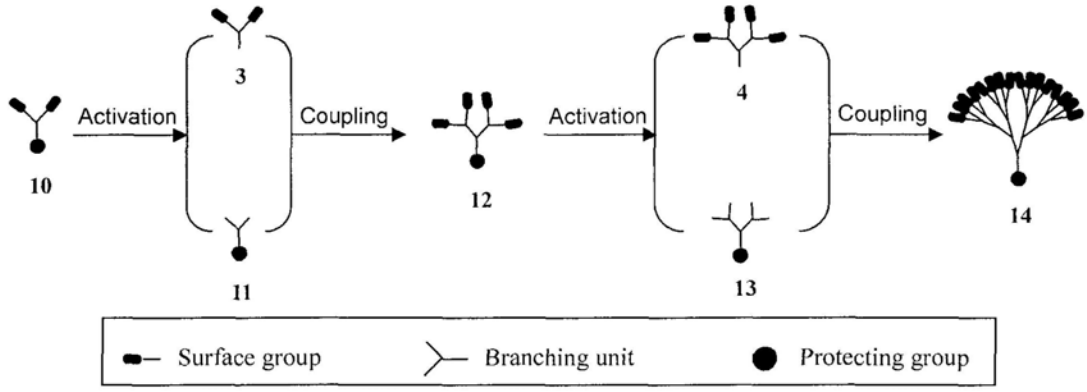

Scheme 5. Double exponential synthetic approach.

1.2.3.4 Orthogonal coupling strategy

Orthogonal coupling strategy is different from those mentioned above as it involves convergent growth with two different types of branching units. The branching units should be carefully selected so that only the focal point of one branching unit would react with the periphery of the other branching unit. Spindler and Fréchet[23] reported the first orthogonal synthesis of dendrimers. However, only a G3 dendron was prepared because of difficulties in product purification. The first orthogonal synthesis of high generation dendrimers was disclosed by Zimmerman and co-workers (Scheme 6).[24] An aryl iodide **17** was first coupled to two terminal alkyne functionalies of a brancher **16** under Sonogashira coupling conditions to yield a G2 dendron **18**. The focal alcohol functionality of **18** was then reacted with another brancher **15** by Mitsunobu reaction to yield a G3 dendron **19**. By repeating the Sonogashira and Mitsunobu reactions, dendrimer **20** consisting of alternating benzyl ester and alkynyl linkages was prepared.

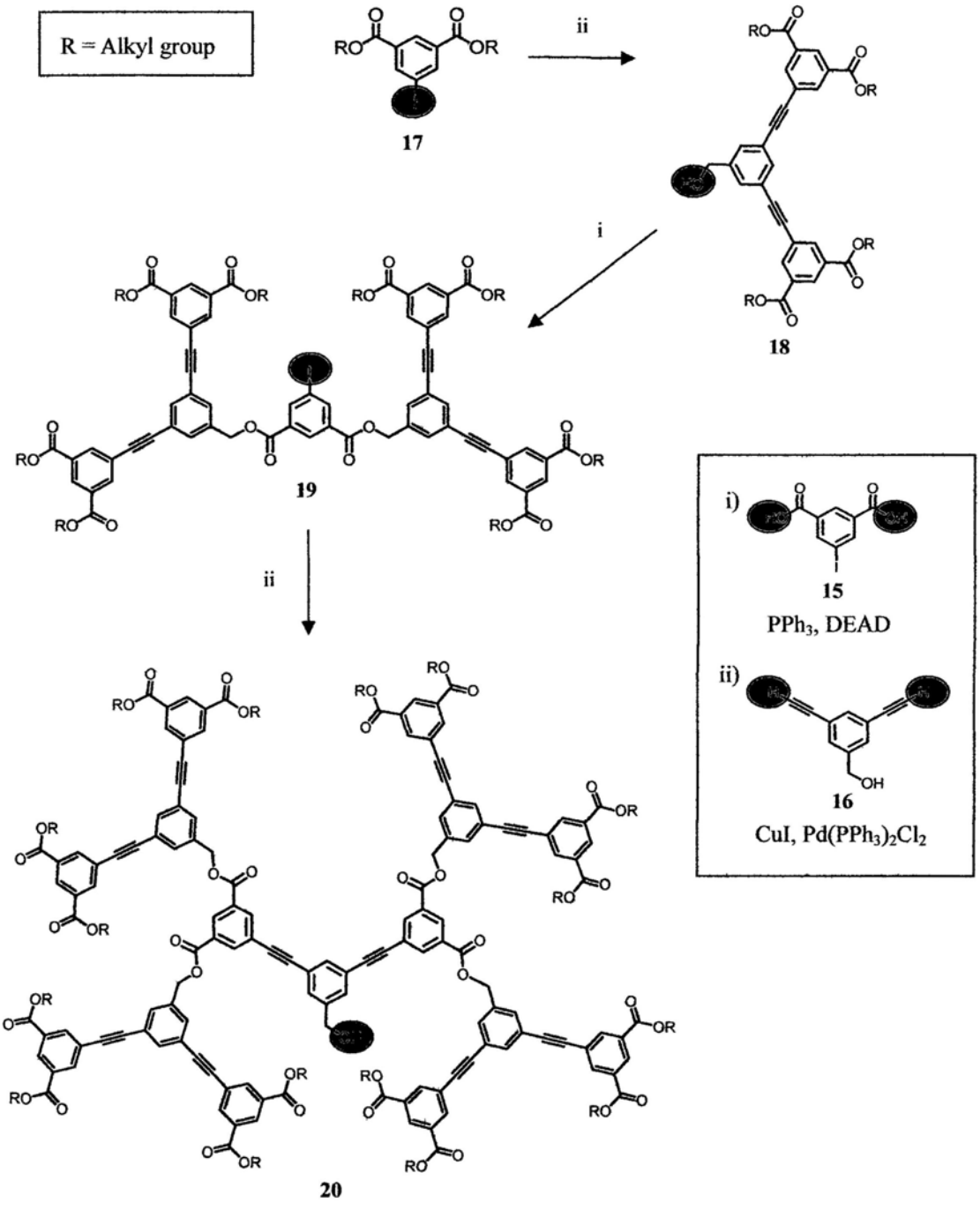

Scheme 6. An orthogonal coupling approach to dendrimers by Zimmerman (functionalities in circles of same colour can couple to each other).[24]

The advantage of using this approach is that no activation reaction is involved, and thus each coupling reaction results in the addition of one generation to the dendron generation. However, this approach is not widely applied in dendrimer synthesis as it requires two pairs of coupling functionalities that are strictly

orthogonal. This imposes a larger limitation on the choice of branching units.

1.3 Characterization of dendritic molecules

After the syntheses of dendritic molecules, it is very important to confirm their chemical compositions and homogeneity. In terms of molecular size, dendrimers are just in between small molecules and polymers so they should benefit from analytical techniques derived from both sides. Generally, dendrimers can be characterized by analytical techniques, such as, nuclear magnetic resonance (NMR) spectroscopy, mass spectrometry, elemental analyses, size exclusion chromatography (SEC), and light scattering measurement. All these techniques are jointly employed as the characterization of dendritic molecules is rather complex. One single analytical technique normally cannot provide full characterization of dendritic macromolecules. X-ray crystallography is another powerful technique that provides proof of molecular structures but it is not commonly applied in dendrimer characterization as high generation dendrimers seldom form crystals.

1.3.1 Nuclear magnetic resonance (NMR) spectroscopy

Nuclear magnetic resonance (NMR) technique is a standard tool to determine the molecular structure of organic compounds. For organic dendrimers, ^{1}H and ^{13}C NMR spectroscopy are commonly used. ^{1}H NMR spectroscopy can provide information about the chemical identity of the functional groups at the focal point and on the surface of a dendritic species. However, due to its relatively low sensitivity, the occurrence of small amount of structural defective products, especially in high generation dendrimers, cannot be easily accessed.[22] Heteronuclei

NMR spectroscopy, such as ^{15}N, ^{19}F, ^{29}Si, ^{31}P NMR are also powerful techniques to characterize dendrimers containing heteroatoms in their structure.[7b, 20, 25]

1.3.2 Mass spectrometry (MS)

Due to instrument and ionization technique limitations, molecular weight determination by mass spectrometry was confined to low molecular weight dendritic molecules in the past.[18] But recent advances in the development of mass spectrometry now allow the analysis of high molecular weight dendrimers. Electrospray ionization (ESI) and matrix-assisted laser desorption ionization (MALDI) mass spectrometry are found to be suitable for an in-depth analysis of dendrimers. For example, ESI-MS has been used to identify structural defective poly(propyleneimine) (PPI)[26] and polyamidoamine (PAMAM) dendrimers.[28-30] MALDI–TOF–MS studies on the structural defects of high generation Newkome-type dendrimers had also been reported.[31-33]

1.3.3 Size exclusion chromatography (SEC)

Size exclusion chromatography (SEC) is a commonly employed polymer characterization technique and it is also used in dendrimer chemistry. First SEC is an efficient method for the purification of dendrimers as the desired dendrimer can be separated from other side products and impurities based on size difference. Second, it can provide information about the molecular weight distributions of dendritic species. Third, a structurally pure dendrimer will give a narrow SEC peak with a polydispersity index (PDI) of less that 1.05. However, a dendrimer cannot be regarded as monodisperse based only on the PDI value of the SEC peak. Even having

a PDI value close to 1.0, the sample may still be a mixture of dendritic species of similar sizes.[22]

1.3.4 Miscellaneous

Other analytical techniques are also applied in the studies of dendrimers. For examples, infra-red spectroscopy[34] and UV-Visible spectroscopy[35] have been employed to monitor chemical transformations occurring within the dendritic architecture. Optical polarimetry[36] and circular dichroism[37] are used in the characterization of chiral dendrimers. Small angle X-ray scattering (SAXS),[38a-b] wide-angle X-ray scattering (WAXS),[38c] small angle neutron scattering (SANS)[39] and laser light scattering techniques (LLS)[40] can also provide information about the molecular weight and aggregations of different dendrimers. Besides, atomic force microscopy (AFM),[41a] scanning electron microscopy (SEM)[41b] and transmission electron microscopy (TEM)[11] are also important imaging techniques for the visualization of dendrimer morphology.

1.4 Properties and Applications

Dendrimers show unique physical and chemical properties due to their molecular uniformity, multifunctional surface and the presence of internal cavities. Hence, they are very useful in a wide variety of applications. It is obvious that the property of a dendrimer is closely related to the functionalities present in the framework. Therefore, by modifying the surface, interior and core, the property of a dendrimer could be tuned to suit different applications. There are numerous applications of dendrimers already reported in the literature.[8-10] They cover a wide variety of aspects in different

research fields so that a thorough and extensive review is not appropriate here as this thesis is focused on the development of new synthetic methodologies of dendrimer. Hence, we will only present a brief summary on the applications of dendrimers.

1.4.1 Medicinal applications

The use of dendrimers in biology and medicine has been described in several excellent reviews.[42] The most useful attribute of dendrimers is their multivalency. The terminal functional groups are closely packed in higher generation dendrimers therefore concentrated loadings of drugs or spectroscopic labels for therapeutic and imaging applications can be achieved. For example, the surface groups of a G3.5 carboxylate-terminated PAMAM dendrimer **21** can be conjugated with cisplatin to function as an anticancer drug carrier which has higher solubility in water and lower toxicity.[43a] PAMAM dendrimers can also be used as carriers for magnetic resonance imaging (MRI) contrast reagents.[43b] For example, the terminal amines of a G6 PAMAM dendrimer were conjugated with a metal chelator which could form stable complexes with gadolinium. These dendrimer–gadolinium complexes enhanced the quality of conventional MR images and 3D time of flight MR angiograms. Hydrophobic metalloporphyrin **22** encapsulated by poly(glutamic acid) dendrons could function as a water-soluble oxygen sensor *in vivo*.[43c] Dendrimers have also been used in tissue engineering. It was reported that a G2 PPI dendrimer **23** could serve as a crosslinking adjuvant for the formation of collagen gel.[43d] Such a dendrimer crosslinked collagen gel showed improved optical and mechanical properties that made it possible to be used as a corneal tissue-engineering scaffold.

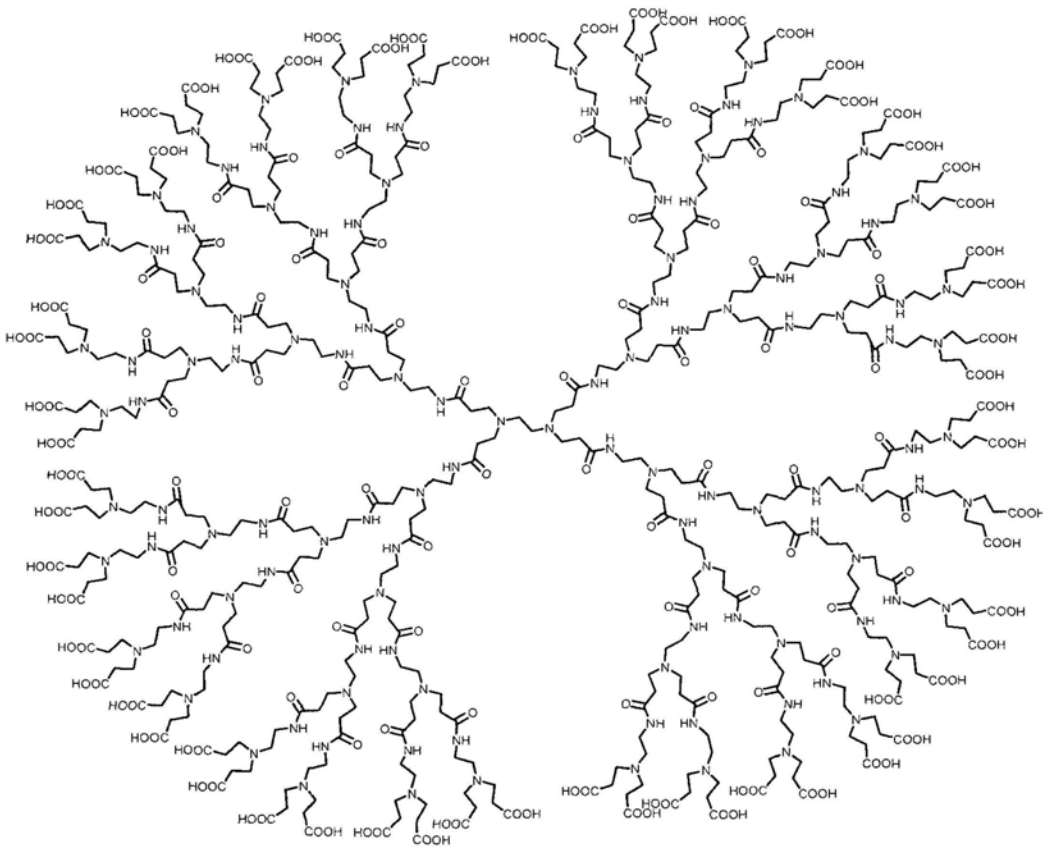

21

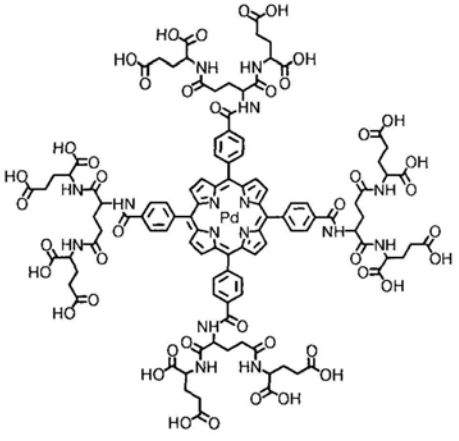

22

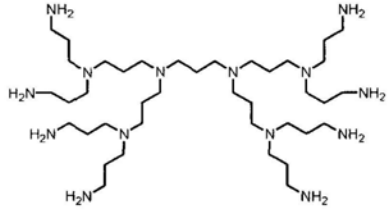

23

Figure 3. Molecular structures of a PAMAM dendrimer **21**, a metalloporphyrin **22** encapsulated by poly(glutamic acid) dendrons and a PPI dendrimer **23**.

1.4.2 Host–Guest Chemistry

Dendrimers exhibit increasing congestion from the core towards the periphery so this characteristic makes them attractive candidates for guest encapsulation. Encapsulation can take place either in the interior or on the periphery. For example, Newkome[44] and coworkers prepared a hydrocarbon-based dendrimer **24** containing multiple carboxylate surface groups. The resulting dendrimer has a gross structure resembles to that of a micelle. This "unimolecular micelle" was used to bind to different lipophilic probes such as diphenylhexatriene, phenol blue and pinacyanol chloride. Jansen *et al.*[45] also reported the topological trapping of guest molecules by a modified PPI "dendritic box" **25**. The soft-core, hard-shell dendritic framework could trap a variety of dye molecules such as eriochrome black T and rose bengal in its interior cavities.

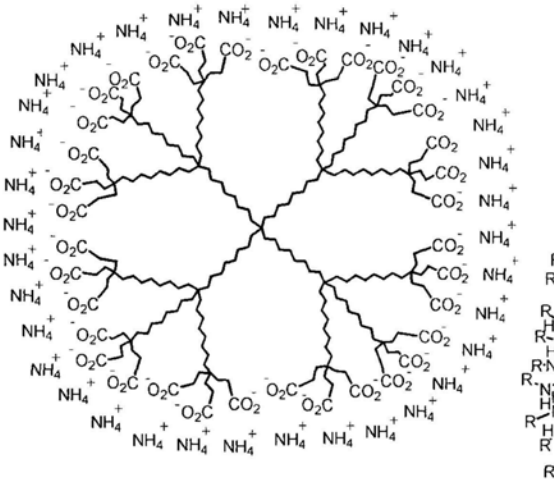

24

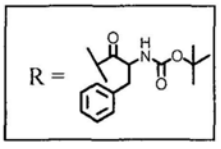

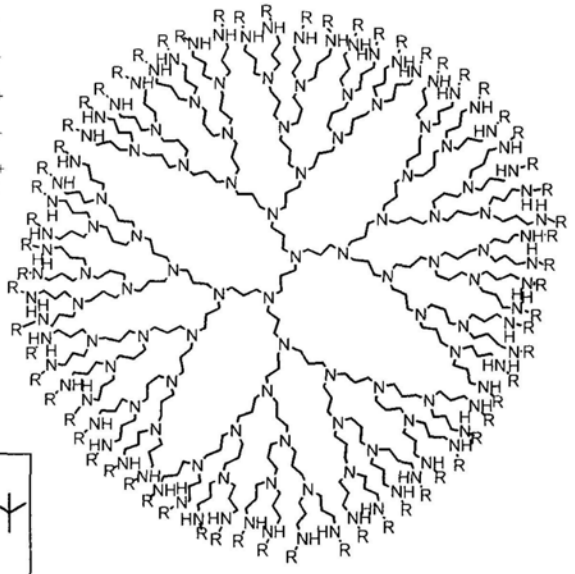

25

Figure 4. A hydrocarbon-based dendrimer **24** which served as a "unimolecular micelle" and a modified PPI "dendritic box" **25** which was used to trap a variety of dye molecules.

1.4.3 Catalysis

Dendrimers possess nanoscopic dimensions but they can be molecularly dissolved so that they can be used to fill the gap between homo- and heterogeneous catalysis. The catalytic site(s) may be placed at a particular, isolated position, like the core or the exterior of a dendrimer.[8,9] The solubility of the catalyst can also be tuned and this can facilitate catalyst recycling via precipitation or ultrafiltration. For example, Seebach and co-workers reported a chiral TADDOL dendritic catalyst derived from dendrimer **26** which catalyzed the nucleophilic addition of diethyl zinc to benzaldehyde (Figure 5).[46a] The catalytic site was incorporated near the core of a Fréchet-type dendrimer. Reetz *et al.* also reported that G3 PPI dendrimers with the periphery modified by biphenylphosphine ligands could form complexes with $Pd(CH_3)_2(PhCN)_2$ which can catalyze the Heck reaction.[46b]

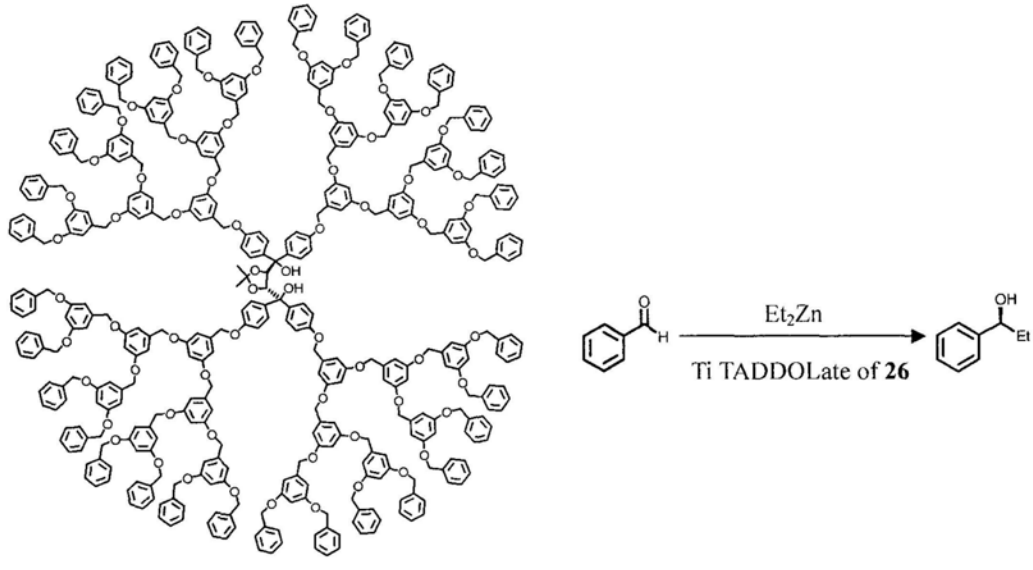

26

Figure 5. A TADOL dendritic catalyst derived from dendrimer **26** that catalyze the nucleophilic addition of diethyl zinc to benzaldehyde .

1.4.4 Miscellaneous

There are also studies in the use of dendrimers for other applications. For examples, PAMAM dendrimers can be applied in coating[47a] and ink industries.[47b] They have also been studied for use as low-dielectric materials,[48] as templates for the growth of single-wall carbon nanotubes.[49] Poly(arylene) dendrimer **27** was used as additives in gold nanoparticle formation,[50] and PPI dendrimer **28** was used in dye industry.[51] Dendrimers have also been explored in terms of their electronic and optoelectronic applications. Hence, they could function as light harvesting system **29**,[52] liquid crystal **30**,[53] organic light-emitting diode (OLED) **31** and solar cell.[10]

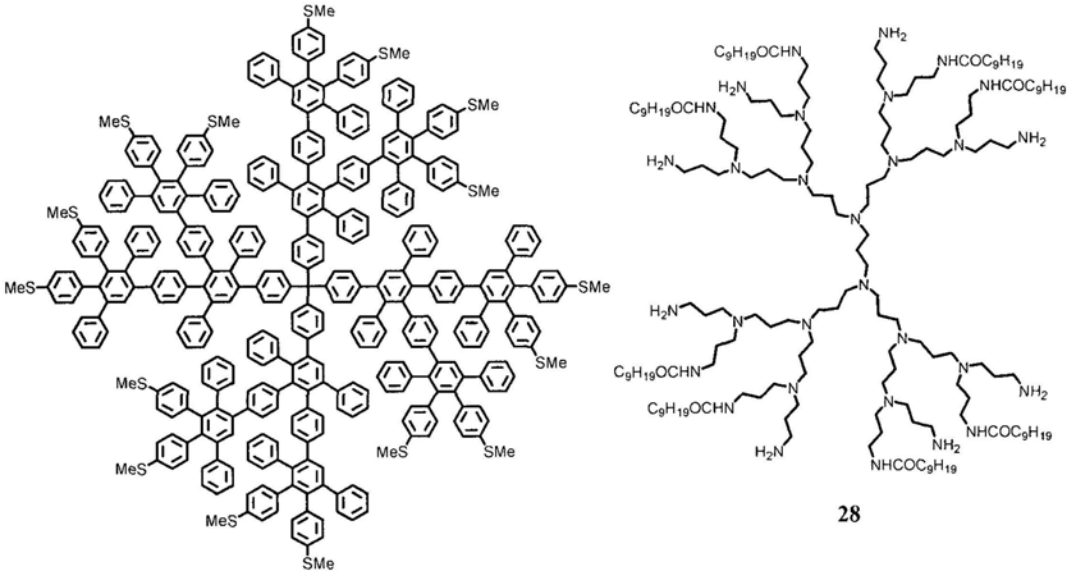

27 **28**

Figure 6. Structures of a poly(arylene) dendrimer **27** and a PPI dendrimer **28**.

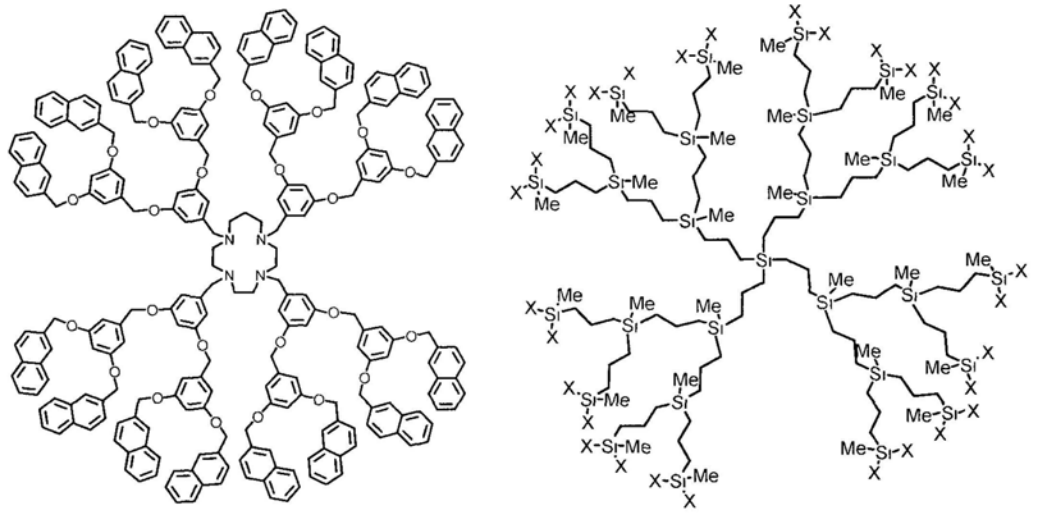

29

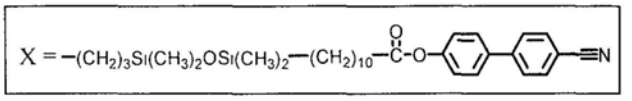

30

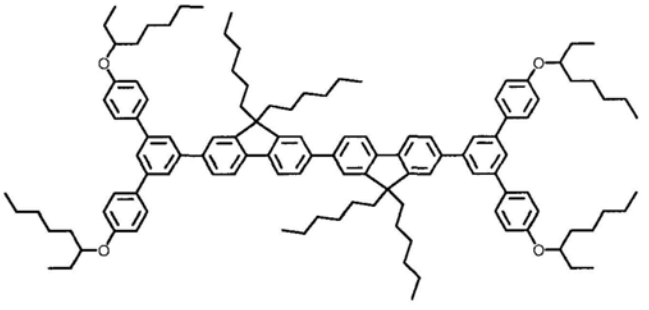

31

Figure 7. Dendritic systems served as light harvesting system **29**, liquid crystal **30** and organic light-emitting diode (OLED) **31**.

Chapter 2: Post-synthetic modifications of dendrimers

Dendrimers are a new class of macromolecules having different properties and applications. As mentioned in Chapter 1, functionalization of a dendrimer would alter its properties and thus be tailored for different applications. This can be accomplished either by pre-modification or post-modification strategies. In the pre-modification strategy, branched monomer units with the designate functionality will be used in the construction of dendritic framework. However, this strategy is not always practicable when the required building blocks are difficult to prepare or the functional moieties cannot withstand the various conditions during the iterative synthesis. Alternatively, post-modification can be to modify dendrimers. In the post-modification approach, monomer units bearing a functional "handle" are used to build up the dendrimer. After the construction of dendrimer, the functional "handle" will be used for further derivatizations through chemical reactions to produce the target functionalized dendrimer. Of course, functional groups can be introduced at the periphery, in the interior, or in the core of the dendrimer depending on the location of the function "handles". This thesis is focused on the synthetic feasibility of dendrimer post-modifications, hence a thorough review on this topic will be given first.

2.1 Post-synthetic modifications at the dendritic periphery

Post-synthetic modifications at the dendritic periphery were frequently found in dendritic catalysts synthesis. Several examples of metal containing dendritic catalysts were reported in literature[54]. For example, in 1994, Koten *et al.* reported nickel-containing metallodendrimers that were prepared by conversion of the surface

aryl bromide functionalities (*e.g.* **32**) into the corresponding Ni complexes (*e.g.* **33**).[55] The reaction relied on multiple oxidative additions of $Ni(PPh_3)_4$ into the arylbromide functionalities. These metallodendrimers could be used as homogeneous catalysts for the Kharasch addition (Scheme 7).

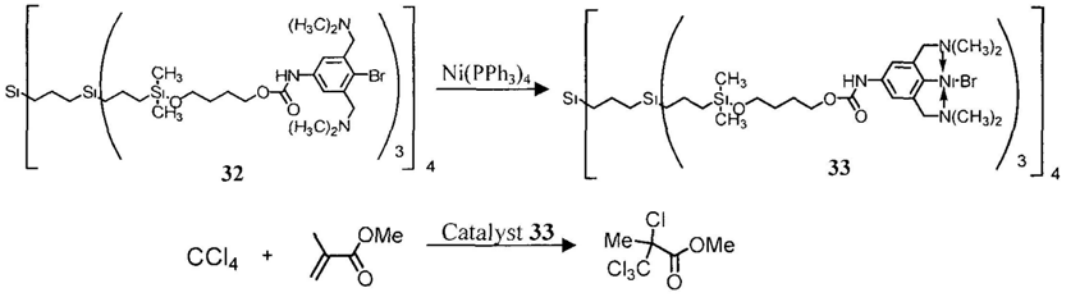

Scheme 7. van Koten's Ni-terminated macromolecular catalysts for the Kharasch addition of polyhalogenoalkanes to C - C double bonds.

Koten and co-workers also reported that 4-bromophenyl-functionalized carbosilane dendrimer **34** could undergo polylithiation to give the 4-lithiophenyl-functionalized dendrimer **35** in quantitative yield which was then reacted with different electrophiles to yield a variety of periphery-modified dendrimers. (Scheme 8).[56] As lithiated dendrimers are good precursors to prepare functionalized dendrimers, Moss *et al.* also reported the synthesis and isolation of lithiated carbosilane-based dendrimers.[57]

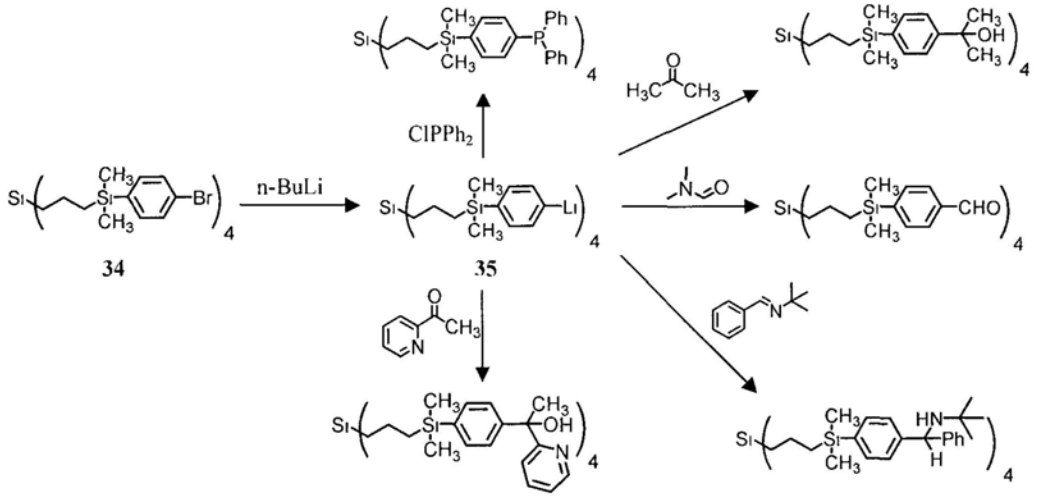

Scheme 8. Periphery modifications of carbosilane dendrimer through polylithiation.

Nithyanandhan and Jayaraman showed another example to functionalize dendrimers through multiple halogen-lithium exchange reactions. The bromophenyl group functionalized G1 to G3 poly(alkyl aryl ether) dendrimers (*e.g.* G2 **36**) were post-modified to give oligolithiated derivatives by treatment with *n*-butyllithium (Scheme 9).[58] The lithiated species were then reacted either with D_2O or with CO_2 to obtain the corresponding deuterated **37a** and carboxylic acid functionalized dendrimers **37b**. To avoid imperfections in the dendrimer, the metal-halogen exchange process should be exceed > 99.9% and the following reactions with electrophiles should have high efficiency.

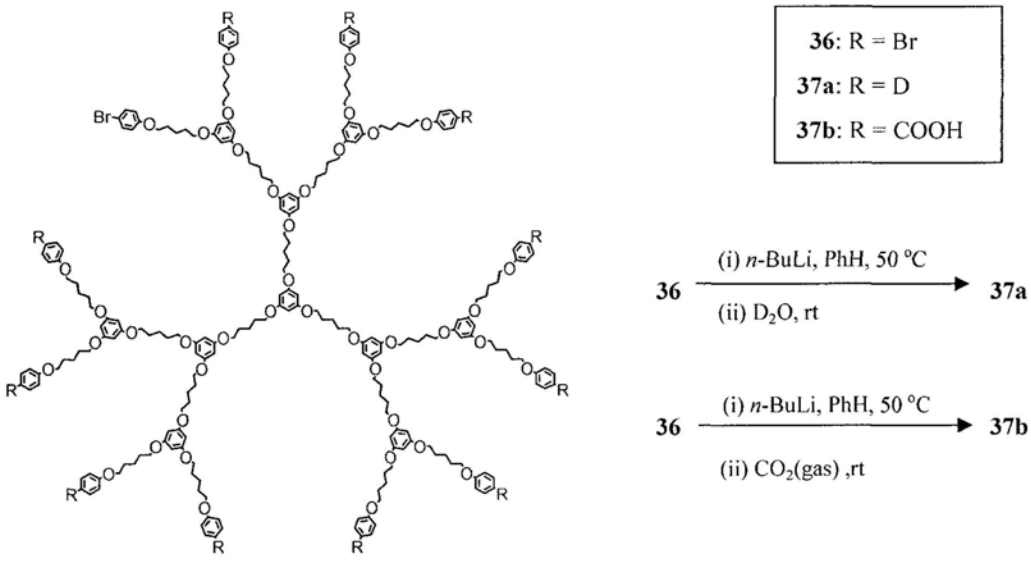

Scheme 9. Post-modification of bromophenyl group functionalized G2 dendrimer **36**.

Periphery post-modification can also be found in the synthesis of dendritic host system. Meijer and co-workers reported a series of oligoethyleneglycol-terminated PPI dendrimers **39** which served as water-soluble dendritic hosts to trap xanthene dyes (Scheme 10).[59] The transformation again depended on the high coupling efficiency of the multiple ester formation reactions.

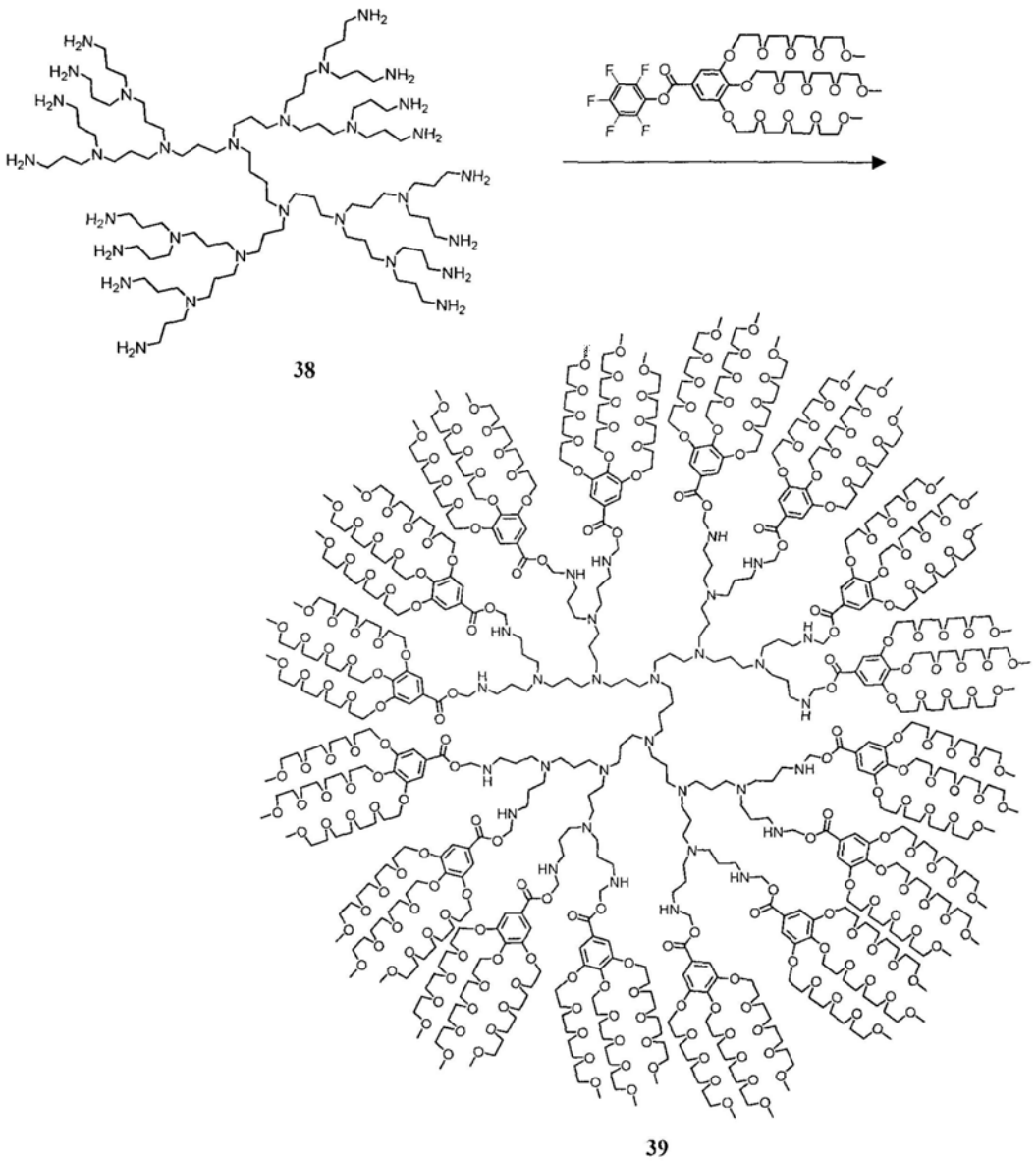

Scheme 10. Synthesis of a G3-oligoethyleneglycol-terminated poly(propylene imine) dendrimers via post-synthetic modification at the surface functionalities.

Most of the surface group modifications were achieved through covalent bonding but modifications using non-covalent interactions are advantageous because of their reversibility. Chechik and Crooks[60] showed an example of dendrimer periphery modifications based on the formation of ion pairs between fatty acids and amine–terminated PAMAM dendrimers (*e.g.* **40**) (Scheme 11). The modified

dendrimer **41** was used as a phase transfer agent to transport encapsulated molecules through aqueous and organic phases.

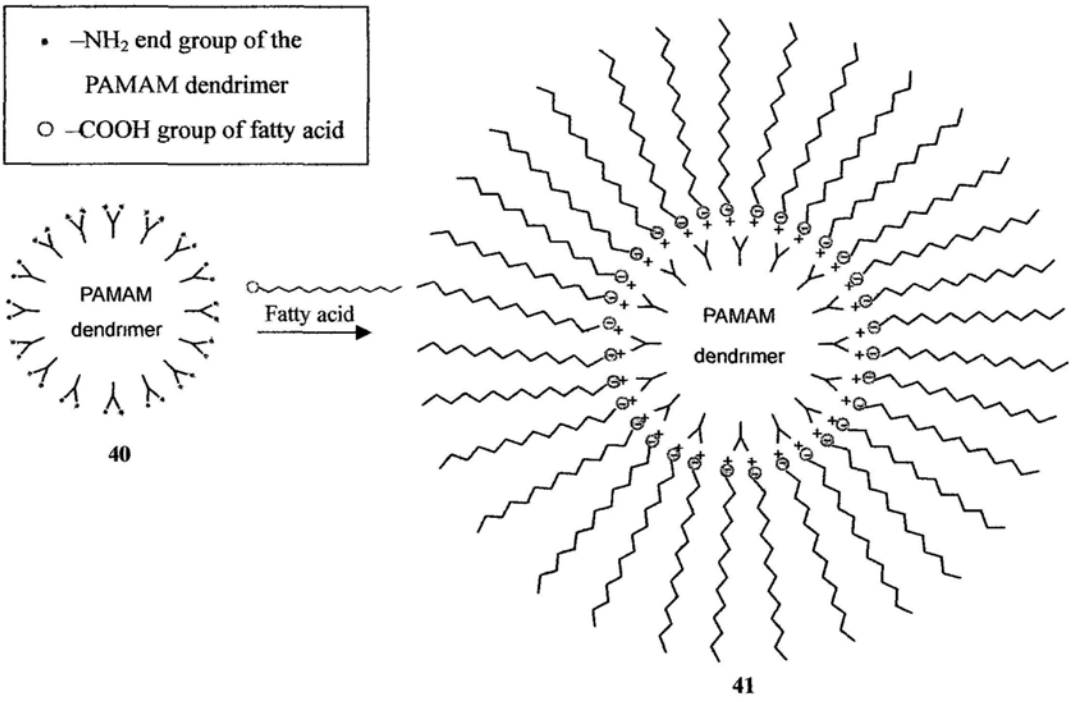

Scheme 11. Non-covalent periphery modifications of a PAMAM dendrimer.

2.2 Post-synthetic modifications at the dendritic interior

From synthetic considerations, introducing functional groups is much easier to the dendrimer periphery than to the interior backbone. However, functionalization on the dendritic backbone can enhance the level of sophistication of the dendritic macromolecule.[61] The local nanoenvironment within the dendrimer can be greatly influenced by the functionalities present in the dendritic interior. Therefore the facile conversion of interior functional moieties can allow one to quickly prepare and fine tune the interior properties from a particular dendritic skeleton. Lochmann *et al.*[62] first reported the interior modification of Fréchet-type dendrons in 1993 (Scheme 12). The dendron **42** was first metalated with superbases, followed by reaction with

electrophiles to yield multifunctionalized dendron **44**. There were 31 benzylic and 15 aromatic reactive sites, but only a maximum of 34 could be functionalized. Since metallation was generally not efficient and low yielding, therefore the product formed was a complex mixture of compounds.

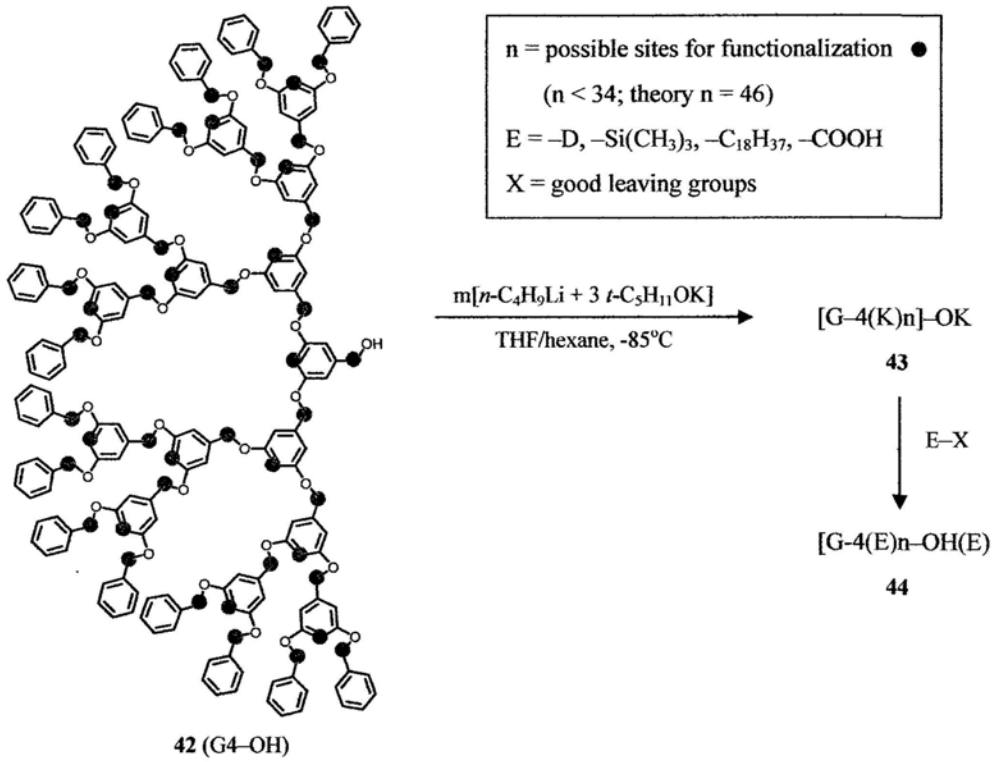

Scheme 12. Multisite interior functionalized Fréchet-type dendrons prepared via metalation by superbases and reaction with electrophiles.

Upon functionalization, the new dendrimer possessed enhanced hydrophilic or hydrophobic behavior, For example, when the metalated **42** was reacted with CO_2, the resulting poly(carboxylic acid) became soluble in water. But when it was reacted with octadecyl bromide, a hydrophobic product which was soluble in hexane was obtained. Therefore interior conversion is a convenient method to change the properties of dendrimers in a few steps.

Twyman[63] also reported a post-synthetic modification of a water-soluble dendrimer **45** (Scheme 13). In this example, the dendrimer was reacted with excess benzyl bromide to yield the internal functionalized dendrimer **46**. However, not all tertiary nitrogens could be quaternalized even under prolonged reaction time in the presence of an excess reagent. Besides, it was found that many isomers were formed in the reaction.

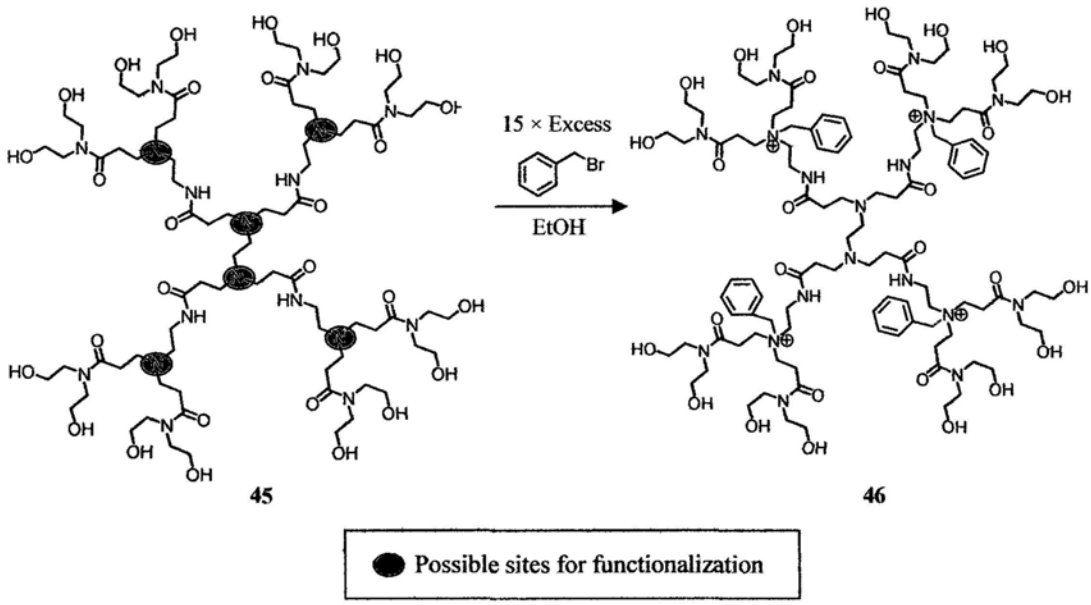

Scheme 13. Post-synthetic interior modification of the water-soluble dendrimer **45**.

Fréchet and co-workers reported the synthesis of poly(aryl ether) dendrimers **47** containing allyl groups which could be converted to a wide range of functional groups through olefin metathesis (Scheme 14).[64] The allyl group was chosen because it would remain intact during the growth of the dendrimer. Subsequent post-synthetic intermolecular cross-coupling reactions with various allyl containing functionalities in the presence of ruthenium-based catalysts then gave the target products **48a** or **48b**. Incidentally, intramolecular metathesis between dendritic branches resulted in cross-linking.

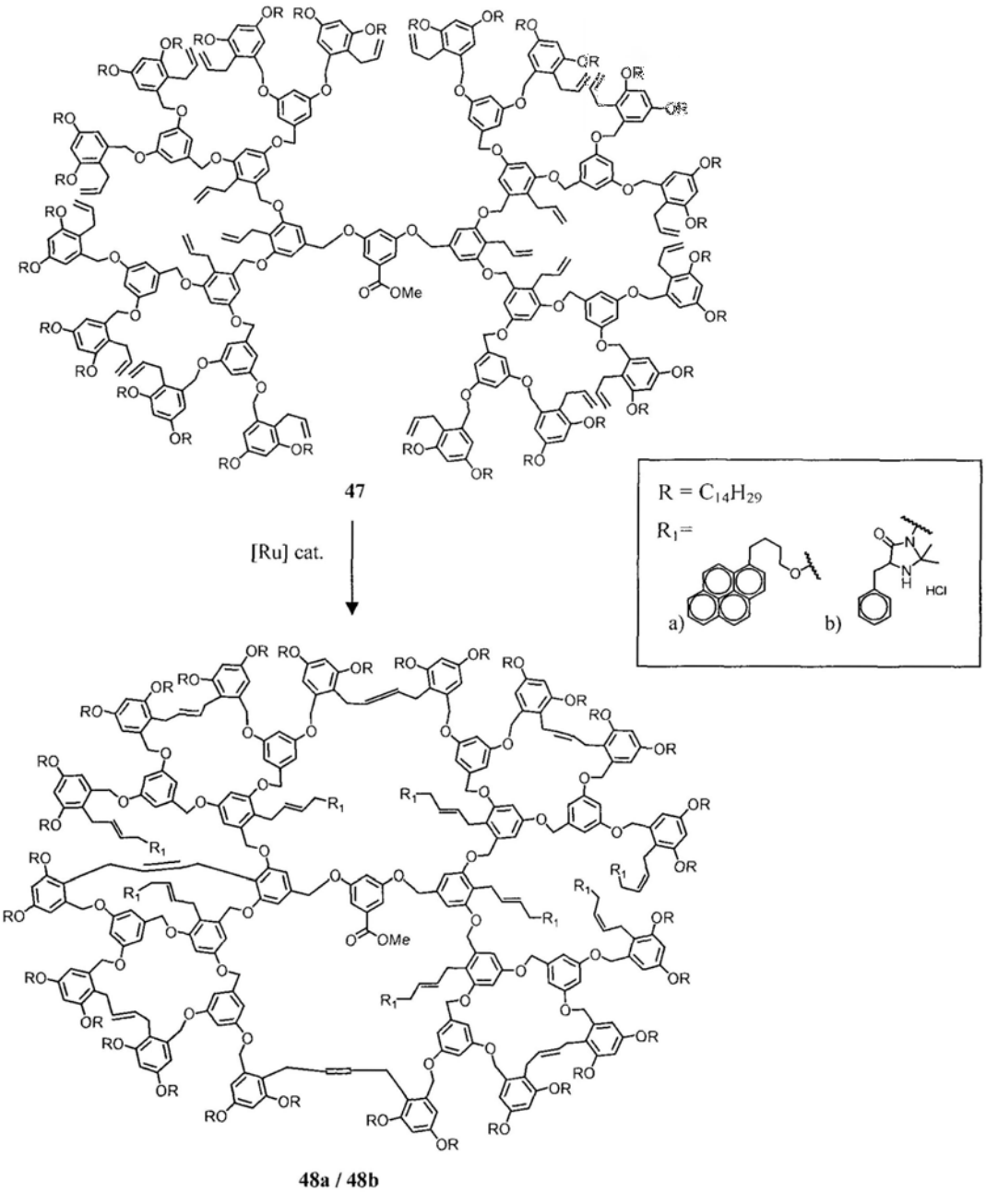

Scheme 14. Post-synthetic modifications of dendrimer **47** through olefin metathesis.

Similar controllable internal postmodifications could also be found in other dendritic systems. Müllen and co-workers reported the synthesis of polyphenylene dendrimers (*e.g.* G2 **49**) bearing multiple benzophenones at the branches.[65] The embedded keto groups were reacted with organolithium reagents to yield different

alcohol products **50** (Scheme 15). It was found that bulky reactants like pyrene could be introduced to the rigid dendritic backbone > 99.9%. On the other hand, a structurally similar G1 and G2 polyphenylene dendrimers with a benzophenone located at the core failed to give quantitative conversion when they were reacted with aryl- and alkyllithium reagents.[66] Besides, it was found that the modification of the core with aryl- or alkyllithium reagents was only possible for molecules smaller than biphenyl because of spatial shielding.

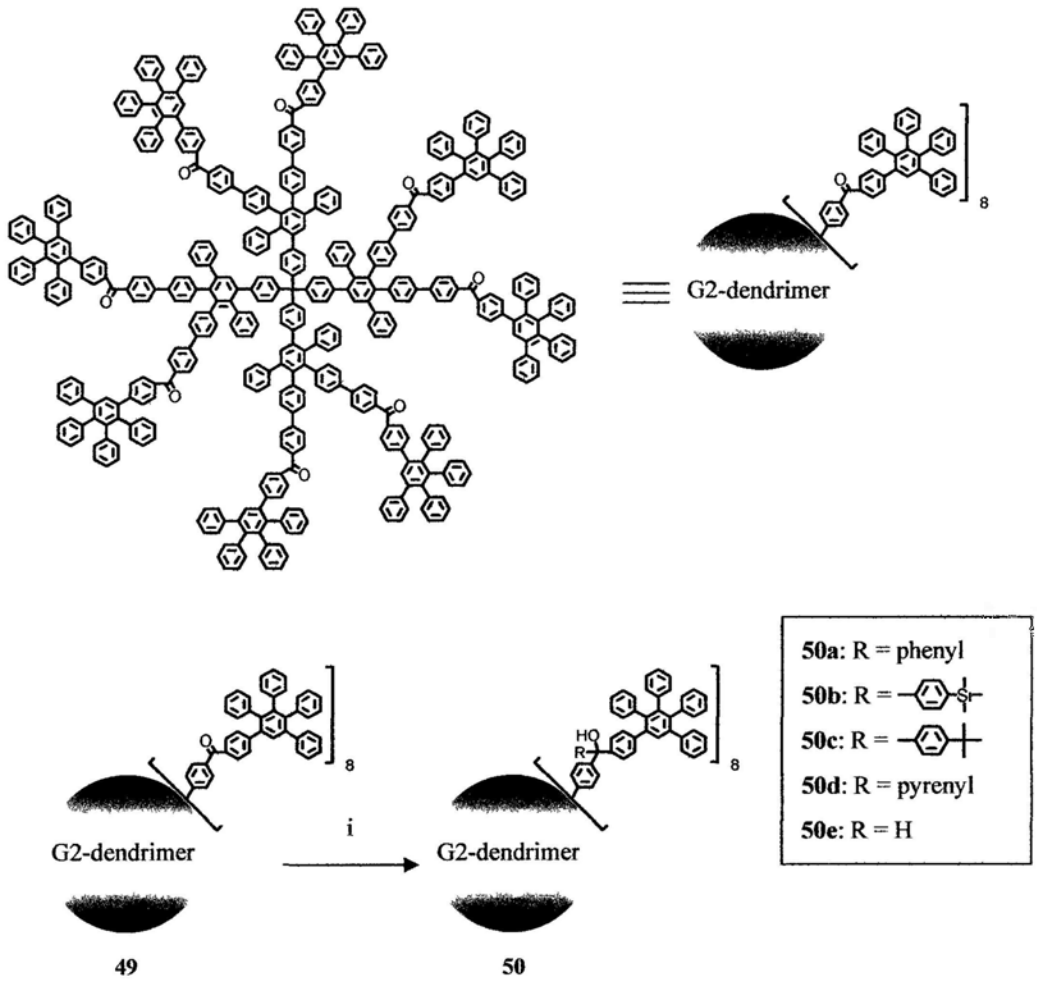

Scheme 15. Post-modification of G2 polyphenylene dendrimer **49**. (i) **50a** C_6H_5Li, THF, 70 °C; **50b–d** *tert*-butyllithium, 1-bromo-4-trimethylsilyl-benzene/ 1-bromo-4-*tert*-butylbenzene/ 1-bromopyrene, respectively, THF, 70 °C; **50e** $LiAlH_4$, THF, 70 °C.

Salamończyk and coworkers reported the chemical modification of a series of G1 to G4 selenophosphate dendrimer (*e.g.* G2 **51**).[67] The G3 dendrimer was subjected to multiple functional group transformations from P=Se to the P=O moieties on treatment with bulky *t*-BuOOSiMe$_3$. From the ^{31}P NMR analysis, it was believed that oxidation occurred at the periphery branching first, and then at the interior site once the oxidant could penetrate into the dendritc structure.

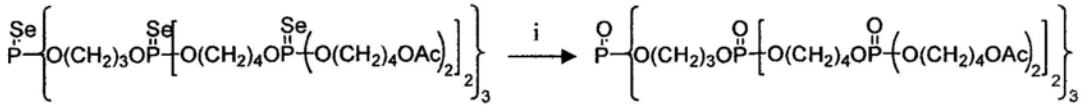

51 **52**

Scheme 16. The oxygenation of G2 selenophosphate dendrimer **51**. (i) *t*-BuOOSiMe$_3$, CH_2Cl_2.

Chu and Imae[68] showed the synthesis of a PAMAM dendrimer **53** in which 1,3-diamino-2-propanol was used as a branch component so that many secondary alcohol functional groups were embedded internally within the dendritic framework (Scheme 17). The alcohol groups were later oxidized to the corresponding ketone dendrimer **54** by either chemical or electrochemical oxidation. It was confirmed by ^{1}H and ^{13}C NMR analyses that all internal secondary alcohols could undergo chemical transformations successfully. As a dehydrogenation process was involved during the oxidation reaction of alcohol units, dendrimer **53** may serve as a "hydrogen donor" and have potential applications in the field of fuel cells and biosensors.

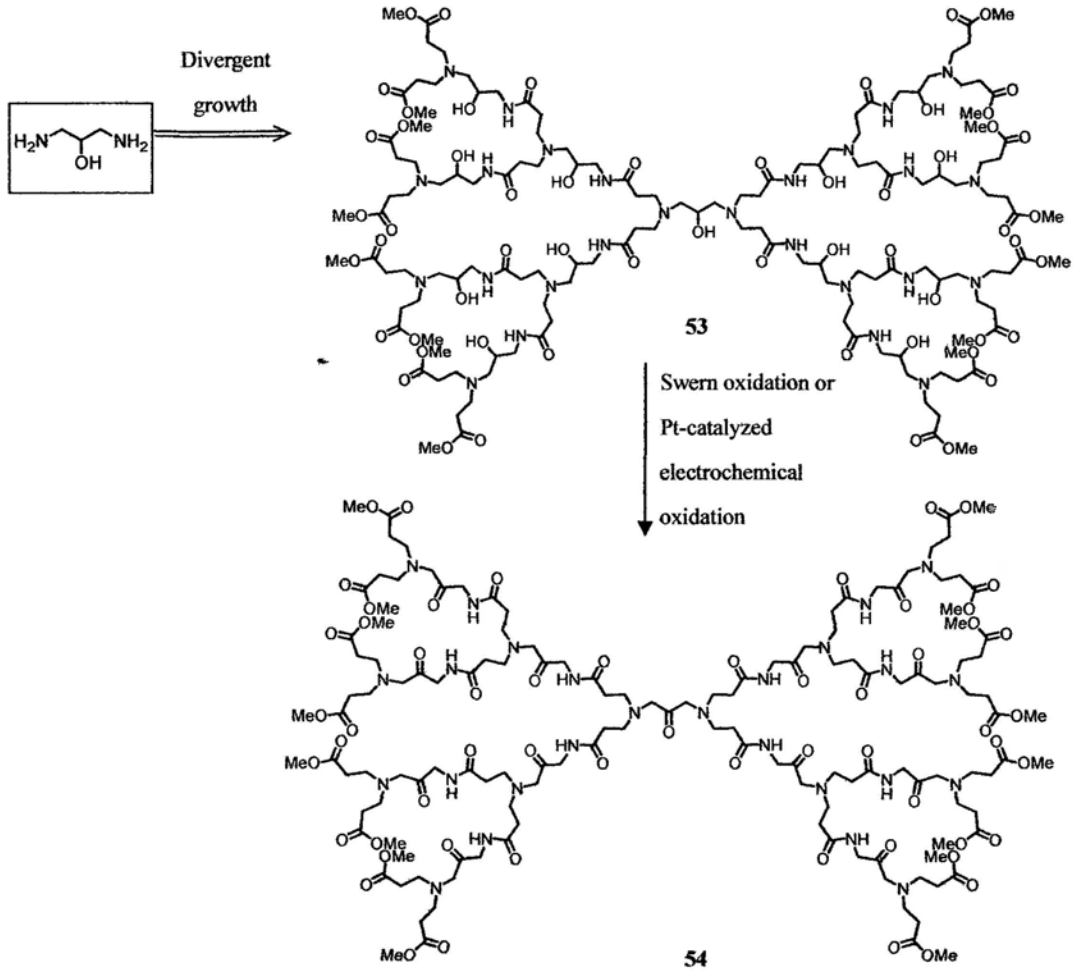

Scheme 17. Post-modification of PAMAM dendrimer **53**.

Chow and coworkers also reported an example of dendrimer interior functional group conversion. G1 to G3-oligo(dibenzyl sulfide) dendrimers (*e.g.* G3 **55**) were synthesized through traditional convergent approach. These dendrimers have many $-CH_2SCH_2-$ branches embedded inside the structure. The sulfide mioieties were later converted into the corresponding sulfone moieties under different oxidation conditions to give oligo(dibenzylsulfone) dendrimer (*e.g.* **56**) (Scheme 18).[69] It was found that interior functional group conversions from G1 to G3-oligo(dibenzyl sulfide) dendrimers to the corresponding oligo(dibenzyl sulfone) dendrimers depended on the reaction conditions. In oxidative conditions involving

heterogeneous reagents such as oxone in MeOH or in CH_2Cl_2 were unsuccessful. While smooth conversion to the corresponding oligosulfone **56** was realized in homogenous conditions using 35% H_2O_2, acetic acid and CH_2Cl_2. It should be noted that from G1 to G3 dendrimer, the number of the sulfide moieties involved in the transformations increased from 3 to 21. Although the sulfide groups at inner layers were highly shielded from G2 and G3 dendrimers, all sulfide moieties could be fully oxidized to sulfone groups under homogenous conditions. However, the problems encountered under these unsuccessful heterogeneous oxidation conditions revealed that there were other factors that could affect such multiple interior functional group conversions.

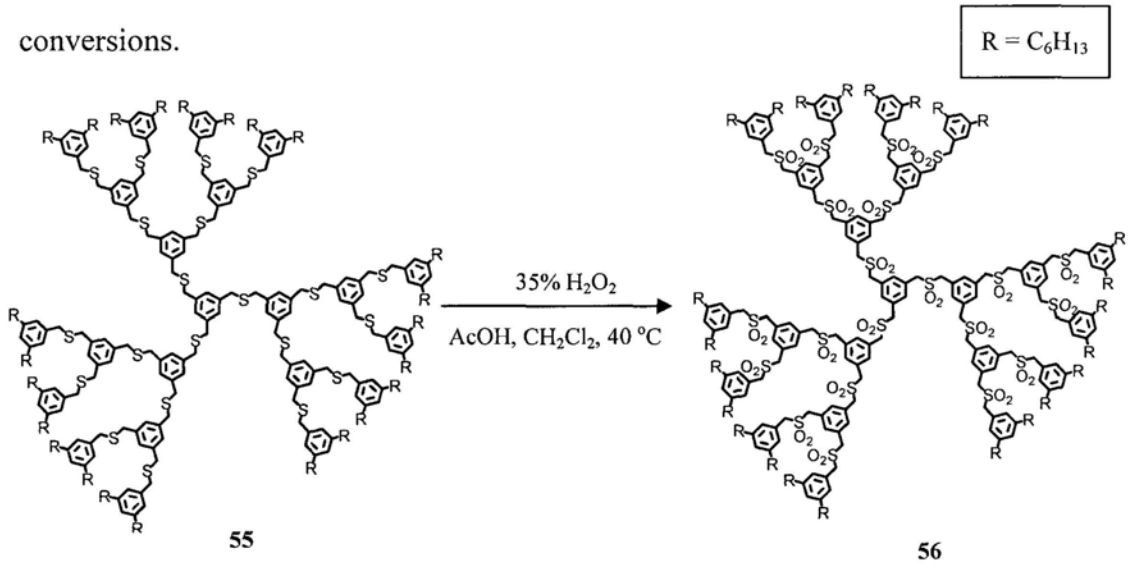

Scheme 18. Interior functional group transformations from oligo(dibenzyl sulfide) dendrimer to oligo(dibenzyl sulfone) dendrimer.

To selectively modify one or several internal functionalities at particular positions, an alternative methodology using embedded functional "handles" was developed. However, since the positions of the anchor groups determine the sites of post-modification, the structure of the dendrimer is always complicated and this may pose additional synthetic challenges. In addition, the anchor groups chosen should be able to tolerate the reaction conditions during the synthesis of dendrimer.

Using this strategy, Bo and coworkers[70] reported a method that could modify functional moieties at specific positions inside the interior of a dendrimer. Fréchet-type G3-dendrimers (**58a–c**) with one aryl bromide unit embedded in either the first **58c**, second **58b** or third **58a** layer of a G3 dendrimer. (Scheme 19). The aryl bromide was chosen to serve as functional "handle" as it could undergo Suzuki coupling with boronic acid **57** even in a congested reaction environment to furnish the various internal functionalized dendrimers **59a,b,c**. From the NMR analyses, the conversions of these coupling steps (**59a–c**) were all over 95%. Therefore, the idea of having bromide as anchor groups on the dendritic backbone for post-modification was proved to be successful and this idea was further developed by other research groups.[61]

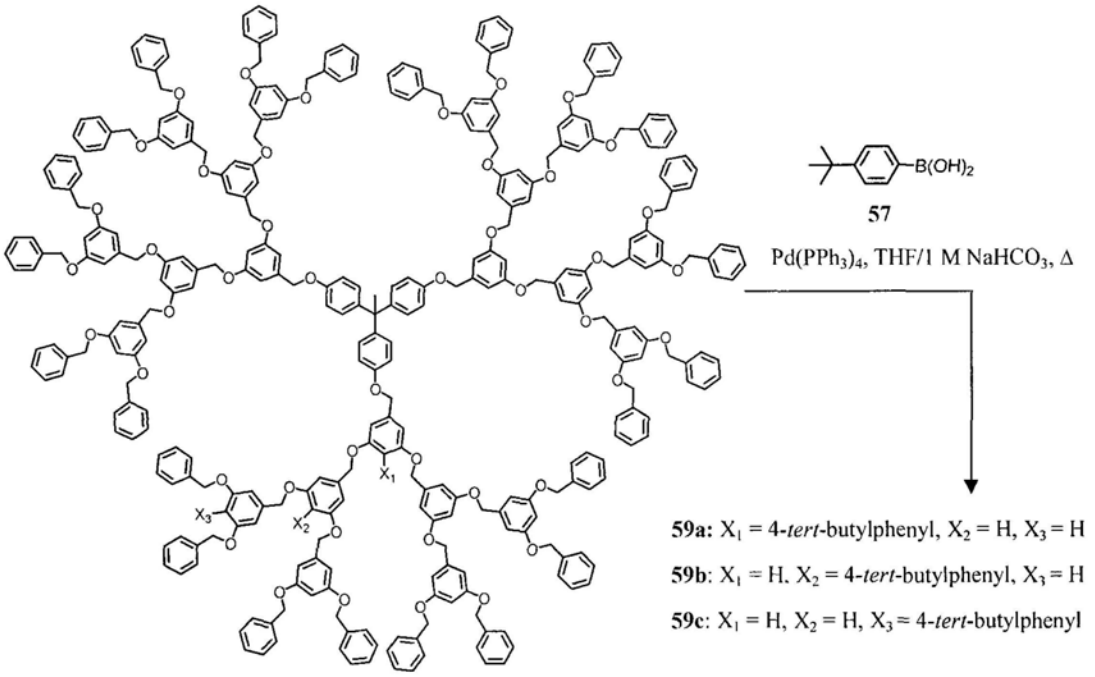

59a: X_1 = 4-*tert*-butylphenyl, X_2 = H, X_3 = H

59b: X_1 = H, X_2 = 4-*tert*-butylphenyl, X_3 = H

59c: X_1 = H, X_2 = H, X_3 = 4-*tert*-butylphenyl

58a: X_1 = Br, X_2 = H, X_3 = H

58b: X_1 = H, X_2 = Br, X_3 = H

58c: X_1 = H, X_2 = H, X_3 = Br

Scheme 19. Post-modification of the interior of a dendrimer via Suzuki cross-coupling.

Gade and coworkers[71] reported another example of post-modification at specific location inside a dendrimer. Phenyl–Si bonds were introduced at different position of several carbosilane dendrimers. For the one with the phenyl–Si bond at the core (*e.g.* G3 **60**), quantitative cleavage of the phenyl–Si unit at the dendritic core could be achieved by triflic acid to get the silyl triflate derivative **61** (Scheme 20). This silyl triflate derivative was readily substituted by anionic nucleophilies to give various products **62a**/ **62b**. For the one having several phenyl–Si groups located at the branching points and at the periphery (*e.g.* **63**), all phenyl moieties could be removed by triflic acid. The resulting product could also react with suitable nucleophile to get the desired functionalized dendrimer **64**.

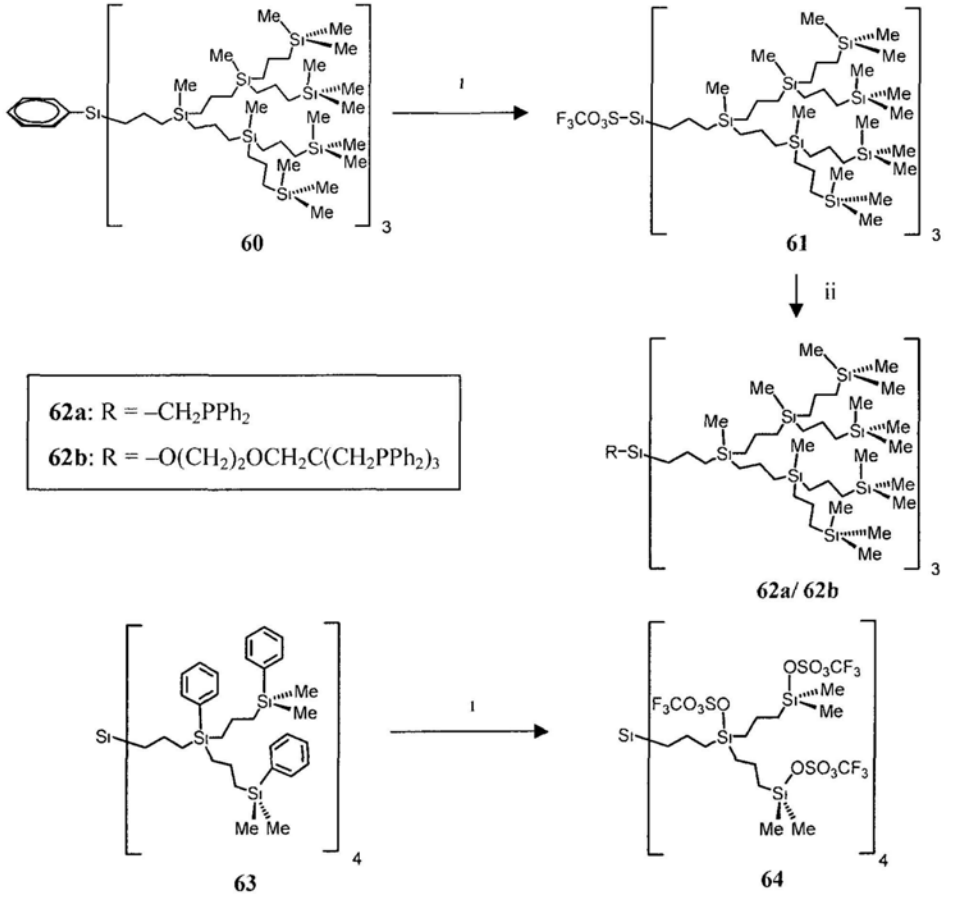

Scheme 20. Post-modification of phenyl-functionalized carbosilane dendrimers **60** and **63**. (i) F_3CSO_3H, toluene; (ii) **62a**: $Ph_3SnCH_2PPh_2$, PhLi; **62b**: $(Ph_2PCH_2)_3CCH_2O(CH_2)_2OH$, *n*-BuLi.

As the reactive sites are located within the dendritic framework, the feasibility of the interior post-modification method is greatly dependent on the structure of the dendrimers. Hence, there are studies to analyze the accessibility of guest molecules to the interior of a dendrimer. For example, Thayumanavan reported the synthesis of G1 to G4 benzyl ether dendrons (*e.g.* G4 **65**) in which photochemically active anthracene unit was incorporated at different location (Figure 8).[72a] The photochemical quenching properties of the anthracene group in the various dendrons were studied. For dendrons of the same generation (*e.g.* G4 **65a–e**), it was found that anthracene unit near the dendritic core was less accessible. Besides, the accessibility of the periphery anthracene in the highest generation G4 dendron is less than that in the interior of lower generation dendrons. It was believed that the backfolding of the G4 dendron would result in burying of the anthracene moiety and thus showed a lower quenching rate.

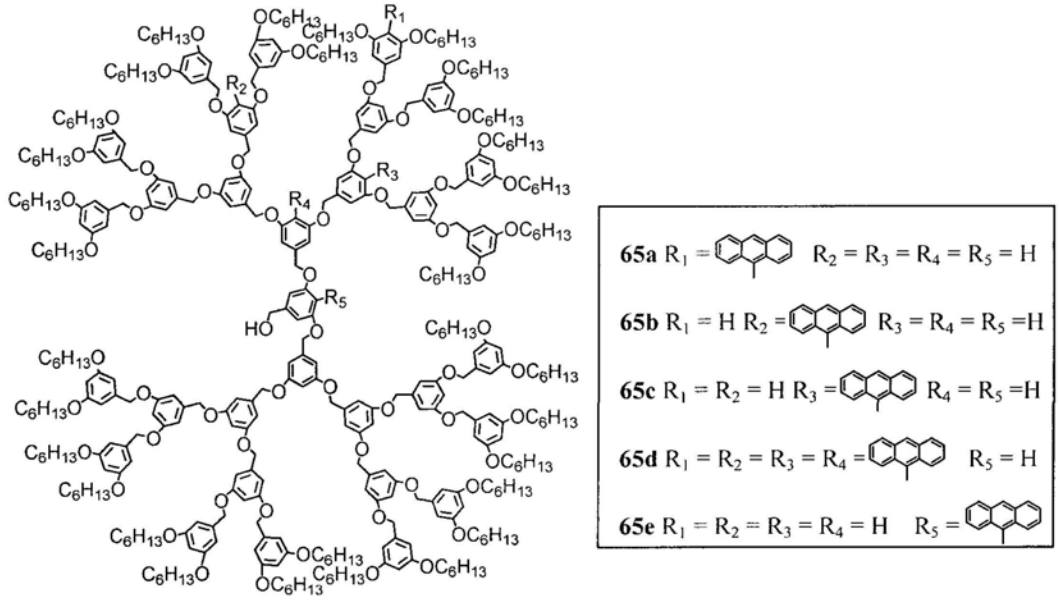

Figure 8. Benzyl ether dendrons with anthracene served to probe the accessibility of the dendrimer.

Simanek and co-worker reported another example to probe the dendrimer accessibility based on a thiol–disulfide exchange process.[73] A series of dendrimers

bearing disulfide-linked dansyl group (*e.g.* **66**) at different locations were synthesized. In the presence of dithiothreitol, thiol-disulfide exchange occurred which led to the release of the dansyl groups. By comparing the exchange rate in different dendrimers, it was found that the thiol-disulfide exchange rate was affected by the size of dendrimers as well as the locations of the dansyl group. The rate of exchange decreased when the size of dendrimer increased. Also, the exchange process occurred more readily at the periphery of the dendrimer than that near the core.

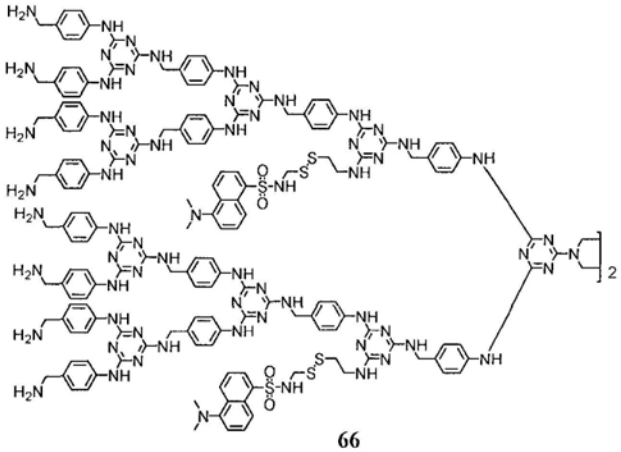

66

Figure 9. Dendrimer **66** bearing dansyl groups was used to study the accessibility of dendrimer.

2.3 Post-synthetic modifications by multiple dendritic backbone rearrangements

The synthetic strategy mentioned here is a completely different post-modification method to synthesize dendrimers. It is different from the conventional methodologies discussed in the last section. Generally, the interior post-modification of a dendrimer mostly involves functional group transformations without changing the dendritic backbone. However, the approach described here involves dendrimer backbone rearrangements that produce a new dendrimer of a totally different dendritic skeleton. Hence, the term "dendrimer metamorphosis" was used to describe this modification method.[69]

The examples given were the skeletal rearrangements of the previously mentioned G1 to G3 oligosulfone dendrimers (*e.g.* G3 **56**) to the corresponding G1 to G3-(phenylenevinylene) dendrimers (*e.g.* G3 **67**) via a heterogeneous Ramberg-Bäcklund (RB) reaction.[69] Again, multiple rearrangements were involved in these transformations (Scheme 21). As it turned out, multiple rearrangements were successful with the smaller size G1– and G2 dendrimers, in which three and nine rearrangement reactions, respectively took place in one single molecule. On the other hand, under similar reaction conditions, it was found that the corresponding 21-ene could not be obtained despite numerous attempts. According to ^{1}H NMR evidence, there was still the presence of benzylic protons adjacent to the SO_2 moiety, suggesting not all the 21 sulfone moieties in the G3-oligosulfone dendrimer **56** could be successfully converted into the alkene functionalities. However, the exact structure of the products was not determined.

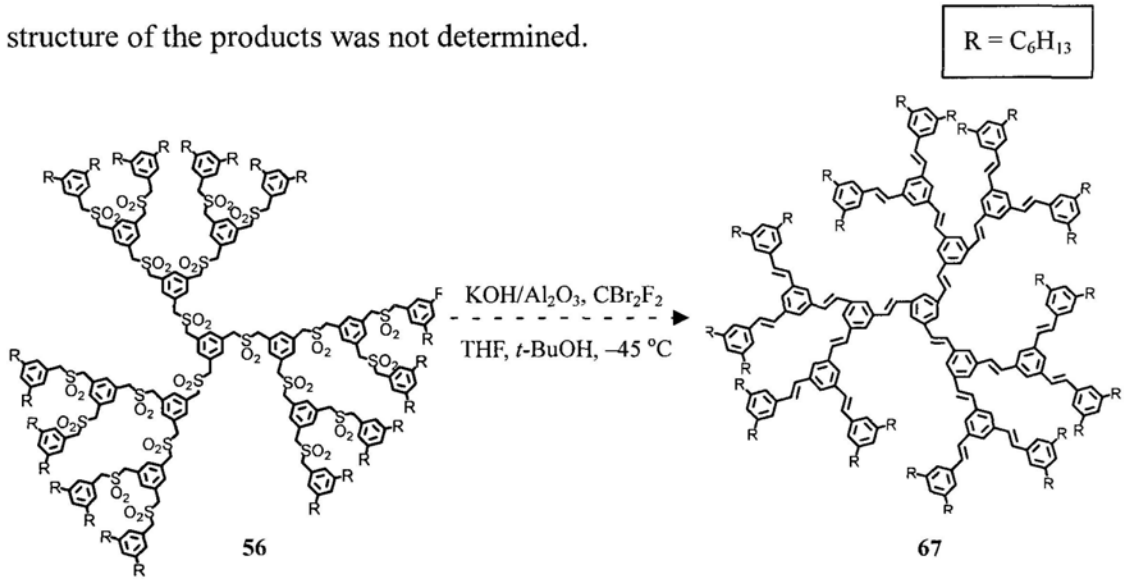

Scheme 21. Dendrimer metamorphosis from oligo(dibenzyl sulfone) dendrimers to oligo(phenylenevinylene) dendrimers.

It appeared that dendrimer shell shielding effect as well as heterogeneous reaction conditions were possible reasons for the failure of the complete conversion of 21 sulfone units to the G3 oligo(phenylenevinylene) dendrimer. Besides, during

the RB reactions, the three-atom –C–S–C– linkers of the dendrimer (*e.g.* **56**) were converted to two-atom ethylene linkers. Hence, it was likely that the sulfone functionalities near the dendritic surface would react in preference to the interior ones. This would lead to a shrinking of the dendritic shell which could prevent the interior sulfone moieties from the reactions. However, due to the presence of many sulfone moieties inside the whole dendrimer structure, it was difficult to pinpoint the location where the dendritic backbone rearrangements failed to occur. Therefore, the extent of the dendritic shielding effect towards the chemical transformations on the different locations (*e.g.* periphery, internal) within the dendrimer framework could not be accessed.

2.4 Aims of the project

Having reviewed the various post-modification approaches, one can immediately identify their advantages as compared to the divergent and convergent methods. First, a new kind of dendrimer, containing another type of functionality, can be prepared in one single step from an existing dendrimer precursor without resorting to multi-step synthesis. Secondly, the post-modification approaches can facilitate the preparation of dendrimers that are difficult to synthesize due to incompatible coupling chemistry via the divergent and convergent procedures. For example, while the previously mentioned oligo(sulfide) dendrimer **55** can be conveniently constructed by nucleophilic substitution of a benzyl bromide with a thiolate, the same coupling strategy cannot be used to form the oligo(sulfone) dendrimer **56** from the same benzyl bromide. Hence, the post-modification approach can offer a complimentary route to the convergent and divergent protocols.

Despite these favorable attributes, it is important to realize that there are also limitations of the post-modification strategies. There are key issues that need to be carefully studied in order to define the scope and feasibility of such novel strategies. First, in case where multiple functional group conversions are involved, there is always the question of the completeness of such multiple transformations. Analytically, it is difficult to differentiate the fully converted species from those partially converted species as they possess very similar spectroscopic, physical and chemical properties. Second, the extent of site encapsulation due to the dendrimer shell on the interior functionalities remains to be clarified. Although there are already studies to probe the interior accessibility of dendrimers by photochemical[72a-c] and chemical methods,[73] a thorough analysis by varying the location of the reactive functionality as well as the reaction conditions should provide additional insights of the synthetic hurdles that need to be surpassed in order to make the post-modification approaches practicable.

In this thesis, three different G3 dendrimers **68–70** having sulfide moieties located at different concentric layers were carefully designed and prepared. The periphery of these dendrimers is decorated with an inert layer of hydrocarbon shell. In contrast to the G3 oligosulfide dendrimer **55** prepared earlier, in which three concentric layers of sulfides were present in the same dendritic molecule, the sulfide moieties in each of the new G3 dendrimers **68–70** are shielded to different extent from the exterior according to their locations inside the dendrimers. By examining the relative oxidation efficiencies of the differentially located sulfides in the three G3 dendrimers **68–70** under various conditions, we should be able to address the dendritic shell shielding effect on their accessibility by other molecular species. We will also subject the three corresponding G3 sulfone products to the Ramberg

Bäcklund (RB) rearrangement conditions and to identify structural factors that led to the failure in our previous RB reaction involving the G3 oligosulfone dendrimer **56**. Such investigations should provide us with additional insights in the synthetic feasibility of dendrimer interior functional group conversion and dendrimer metamorphosis.

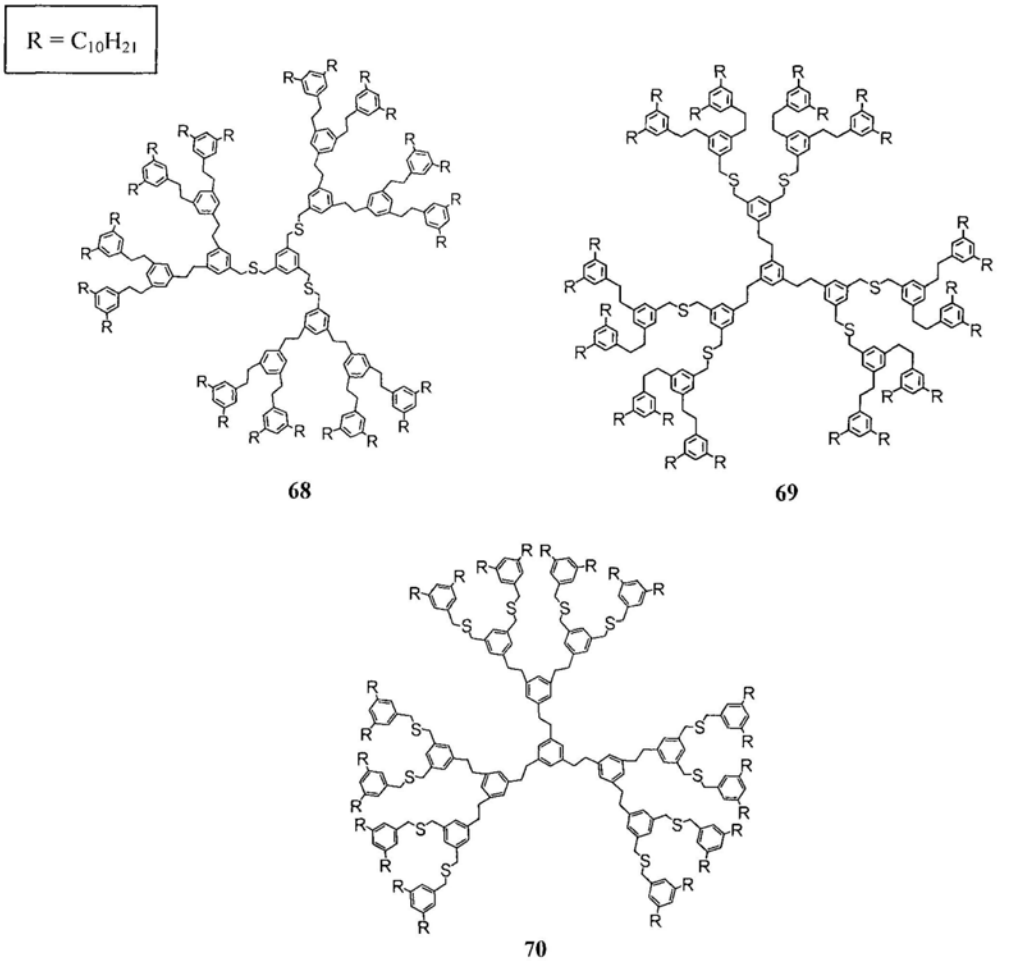

Figure 10. Structures of the three target layer-block dendrimers **68**–**70**.

In the next chapter we will disclose the synthetic design and the synthetic routes to the three target compounds.

Chapter 3: Synthesis and characterization of layer-block oligosulfide dendrimers

3.1 Synthetic design

In order to find out factors affecting dendrimer interior functional group conversion and dendrimer metamorphosis, dendrimers that possess reactive functional groups at specific locations inside the dendritic structure should be used as targets for study. In our previous investigation,[69] it was found that the dendritic backbone rearrangements via Ramberg–Bäcklund (RB) reaction did not proceed completely only in the G3–prototype dendrimer, therefore we decide to focus our attention mainly on the G3 substrates. In order to pinpoint the exact site of chemical transformation, layer-block dendrimers were designed as experimental templates in which the reactive sulfide or sulfone functionalities were embedded at concentric layers away from the central core (Figure 6). By studying the relative reaction rates of the chemical transformations of the reactive interior functional groups in these layer block dendrimers, we should be able to identify whether steric shielding effect plays any important role in dictating their relative reactivities. In other words, do functional groups that are located closer to the central core react more slowly than those located near the dendrimer surface? Secondly, by changing the reaction conditions from homogeneous to heterogeneous, we should be able to learn whether phase separation is another synthetic hurdle in these post-modification strategies.

Figure 11. Simplified diagram for layer-block G3–dendrimers.

3.1.1 Dendritic surface

In order to study the dendritic shell shielding effect, the reactive sulfide or sulfone moieties should be well-shielded. To achieve this goal, a C–10 long alkyl chain was chosen as the surface group of our target G3 substrates. Based on computer simulations[12,74] as well as experimental studies on different dendrimers,[75] it was found that the end groups would not simply locate at the dendritic surface, but usually back-folded towards the core to some extent. The degree of backfolding depends on the actual dendritic structure and secondary interactions between the end groups, such as π–π interaction, hydrogen-bonding interaction, and/or electrostatic repulsion.[76] If the end groups do not have strong secondary interactions between each other, they would distribute throughout the dendrimer architecture if the dendrimer is structurally flexible. Therefore, using long alkyl chains as surface groups in our dendritic systems can ensure effective shielding of the reactive interior functional groups.

3.1.2 Linker of the dendrimer

Two types of linker, one reactive and the other inert with respect to the transformation chemistry, would be used in the layer-block dendrimer system. For

the reactive layer, the linker is the same as that of the oligo(dibenzyl sulfide) dendrimers, i.e., a $-CH_2SCH_2-$ group that can be oxidized to the sulfone ($-CH_2SO_2CH_2-$) linker, which in turn can be converted to the corresponding vinylene (–CH=CH–) linker via Ramberg–Bäcklund rearrangement. For the inert layer, the selected linker has to fulfill some criteria. Firstly, the linker should be inert to the reaction conditions employed in the dendrimer synthesis, as well as the interior functional group transformation reactions, *e.g.* sulfide oxidation reaction and the RB reaction. Secondly, as we wish to monitor the progress of the interior functional group transformations by ^1H NMR experiment, so the proton signals of the inert linker should not overlap with the signals due to the reactive $-CH_2SCH_2-$ linker. Thirdly, the length of the inert linker should be a part of consideration. Ideally, it is best to be a three-atom spacer, similar to the $-CH_2SCH_2-$ linker so that the experimental models would have higher similarity to the prototype dendrimer **55** in our previous study. Unfortunately, due to the synthetic difficulties (*vide infra*), a two-atom ethylene linker is chosen instead and details will be discussed in the next section.

3.2 Preparation of branching units, dendrons and dendrimers

The convergent approach was employed to prepare the target G3 layer-block dendrimers **68**–**70**. The surface groups were added to the branching unit through Sonogashira coupling between 1-decyne and methyl 3,5-diiodobenzoate **71** in the presence of $PdCl_2(PPh_3)_2$ and CuI under basic conditions[77] to give methyl 3,5-di-(dec-1-ynyl)benzoate **72** in 96% yield (Scheme 22). The triple bonds of **72** were subsequently saturated by catalytic hydrogenation using 10% palladium on charcoal to afford the di-*n*-decyl substituted benzoate **73** in 85% yield. The ester was

then reduced to the corresponding G1–alcohol **74** by lithium aluminium hydride ($LiAlH_4$) in 93% yield.

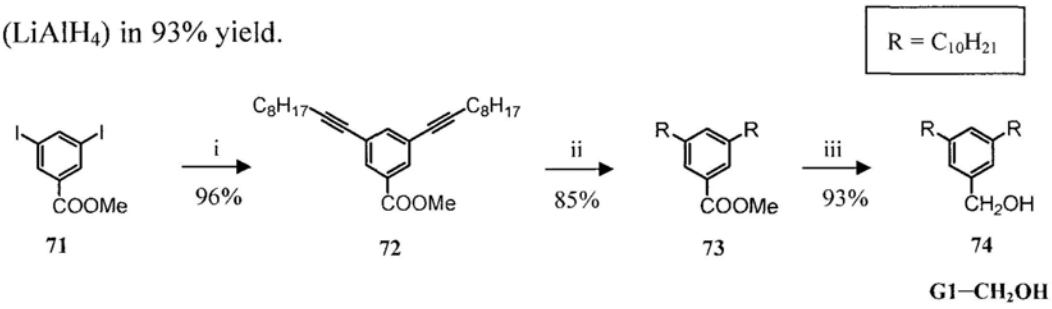

Scheme 22. Synthesis of G1–alcohol **74**. Reagents and conditions: (i) 1-decyne, $PdCl_2(PPh_3)_2$, CuI, NEt_3, THF, 20 °C; (ii) H_2, 10% Pd/C, THF, MeOH, 20 °C; (iii) $LiAlH_4$, THF, 0–20 °C.

Once the G1–alcohol was obtained, the –OH group at the focal point was transformed to other functional groups that were capable of coupling to different branching units to yield various G2 dendrons. Methods of introducing the oligosulfide linker $–CH_2SCH_2–$ had been reported by Chow's group[69] and they were also applied in this study. For the inert linker, several linkage systems had been tried and these are reported in details in the next section.

As there are a number of dendritic molecules involved in the synthetic scheme, a notation system is used to simplify the discussion in this thesis. All dendrons are named in a format of "Gn–B–F" whereas Gn represents the number of generation of the dendron, B indicates the type of branches involved and F refers to the functional group present at the focal point. Using the G3 dendron **75** as an example (Figure 12), counting from the surface towards the focal point, branches $–CH_2SCH_2–$ are encountered in the outer layer and –CH=CH– are found in the inner layer, therefore the notation "SC=C" is used to name the branch. The functional group at the focal point of dendron **75** was a dimethyl acetal $–CH(OMe)_2$. Therefore, dendron **75** has a notation of $G3–SC=C–CH(OMe)_2$. For the cases of our target dendrimers, they were

all named as "G3–B–dendrimer" instead.

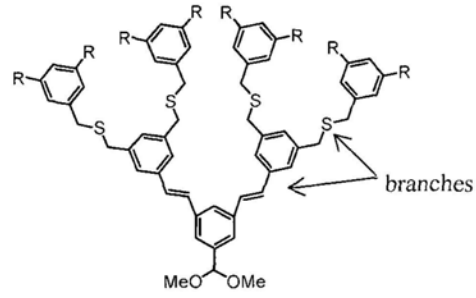

75

branches	Short notations
$-CH_2SCH_2-$	S
$-CH_2CH_2-$	C
$-CH=CH-$	C=C

Figure 12. Structure of G3 dendron **75** and the notations for various branches.

3.2.1 Choices of inert linker

3.2.1.1 $-CH_2OCH_2-$ linker

In our first attempt, a three-atom linker $-CH_2OCH_2-$ that was inert to the sulfide oxidation and RB reaction conditions was chosen as the linkage group. The G1–alcohol **74** was first converted to the alkoxide anion using sodium hydride and then reacted with a TBDPS-protected branching unit **76** to obtain the G2 dendron **77** (Scheme 23). However, the yield of this reaction was low (29%).

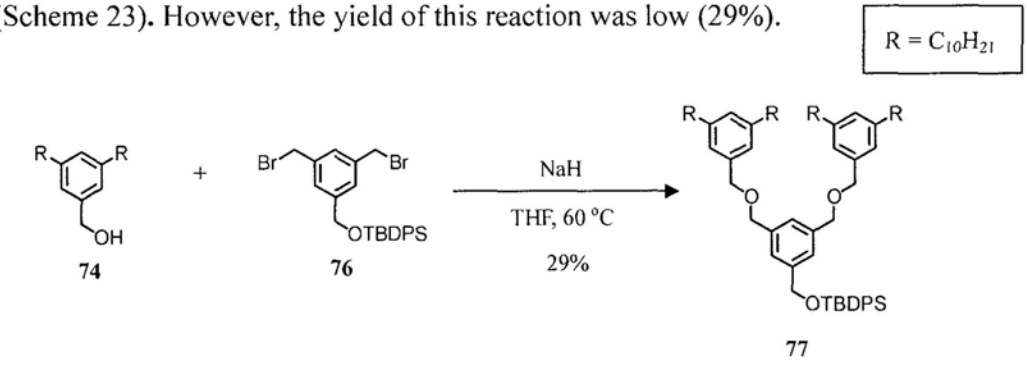

Scheme 23. Synthesis of G2 dendron **77** with –COC– linkage.

In fact, similar coupling reactions under different reaction conditions had been reported in literature but the results were mostly unsatisfactory (25–45%).[78] It appeared that the William coupling reaction was not an effective way to give

dibenzyl ethers. In addition, in our case it was found that the TBDPS group was partially cleaved during the reaction and an uncontrolled hyperbranched polymerization occurred to give a complex mixture of products. As a result, the yield was very low and product purification was very difficult.

3.2.1.2 $-CH_2CH_2CH_2-$ linker

The 3-atom propylene linker is not commonly found in dendrimer system as its construction is not straightforward. Schlüter *et al.* reported both divergent and convergent synthetic approaches for the preparation of lower generation G1– and G2–phenylenepropylene dendrons.[79] However, both methods were found not feasible in our case. For the divergent method, structural defects may result as twelve identical transformations will be involved in the synthesis of our target G3 dendrimers. Hence, the alternative convergent approach was adopted. The key step used in the introduction of the 3-carbon spacer was a modified Suzuki-type coupling between a substituted propylene borane **79** and an aryl iodide. When monomer **78** was coupled to the known organoborane **79**,[79] it was found that the desired product **80** and its styryl isomer **81** were obtained as an inseparable mixture (Scheme 24). Furthermore, the undesirable side product **81** was formed in 50% yield.

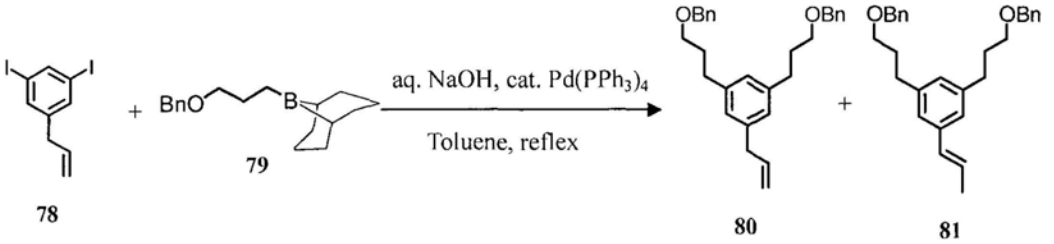

78 79 80 81

Scheme 24. Synthesis of phenylenepropylene dendron via a convergent approach.

We therefore tried to introduce the propylene linker using another method. The

G1–alcohol **74** was first converted to the corresponding bromide **82** in 97% yield in the presence of CBr_4 and triphenylphosphine (Scheme 25). It was then reacted with TMS-acetylenyl magnesium bromide to afford alkyne **83**. The carbon chain at the focal point was then already extended to contain three atoms. The TMS group was then removed by K_2CO_3 so that the free acetylene **84** could be used to couple with a branching aryl dihalide unit **86**. Unfortunately, isomerization of the triple bond occurred during desilylation and allene **85** was obtained instead.

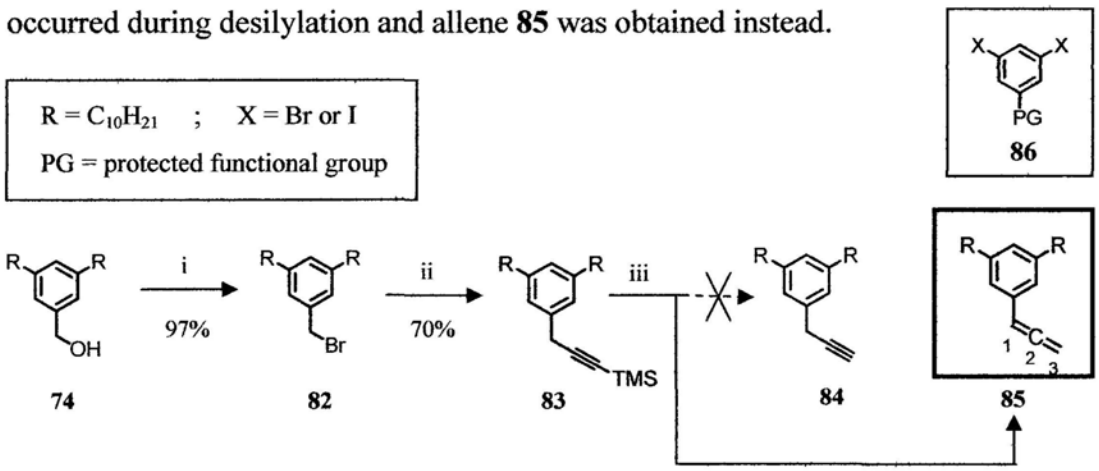

Scheme 25. Synthetic approach to intermediate **84** using Grignard reaction. Reagents and conditions: (i) CBr_4, PPh_3, THF, 20 °C; (ii) TMSC≡C–MgBr, CuI, THF, 60 °C; (iii) K_2CO_3, MeOH, THF, 20 °C.

The ^{13}C NMR spectrum of compound **85** showed a characteristic peak at 209.9 ppm, which was due to the allenic carbon and was consistent with the value reported in the literature.[80] The ^{1}H NMR of compound **85** also showed the presence of a doublet and a triplet at 5.13 ppm and 6.12 ppm, respectively, confirming the presence of the allene unit.

As the terminal acetylene **84** could not be obtained, another synthetic pathway involving the Wittig reaction was used (Scheme 26). The G1–bromide **82** was reacted with TMSCN in order to introduce one additional carbon atom to the focal point. The cyanide **87** obtained was then hydrolyzed, reduced and brominated to

afford the corresponding bromide **90**. The corresponding phosphonium salt **91** was prepared by reacting compound **90** with triphenylphosphine.

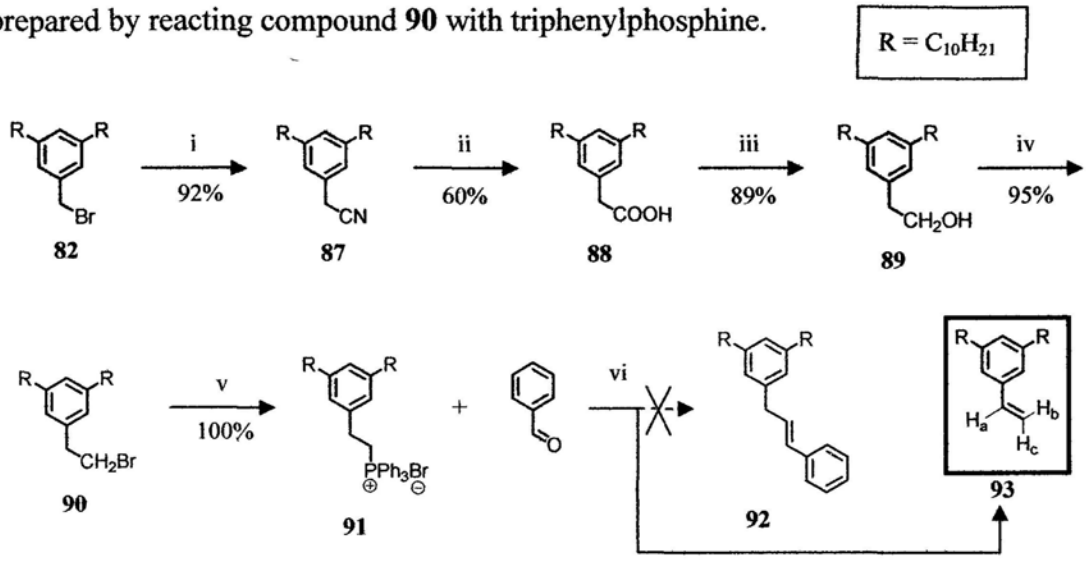

Scheme 26. Synthetic approach to intermediate **92** using Wittig reaction. Reagents and conditions: (i) TMSCN, TBAF, MeCN, 80 °C; (ii) 40% NaOH, H_2O_2, THF, EtOH; (iii) $LiAlH_4$, THF, 0–20 °C; (iv) CBr_4, PPh_3, THF, 20 °C; (v) PPh_3, DMF, 100 °C; (vi) NaH, THF, reflux.

In a model experiment, benzaldehyde was first used to couple to compound **91** in order to test the feasibility of this synthetic method. However, it was found that base-promoted elimination of the triphenylphosphine occurred and only alkene **93** could be obtained. The structure of compound **93** was proven by ^1H NMR spectroscopic analysis. The ^1H NMR spectrum showed a characteristic doublet of doublet (dd) signal at 6.68 ppm (J_{trans}= 17.7 Hz; J_{cis} = 10.8 Hz) which was due to the proton H_a. Two dd signals were also observed at 5.72 ppm (J_{trans} = 17.7 Hz; J_{gem} = 0.9 Hz) and 5.20 ppm (J_{cis} = 11 Hz; J_{gem} = 0.6 Hz) which corresponded to protons H_b and H_c, respectively.

Since it was problematic to introduce the propylene group as the linker, so a two-atom ethylene linker was used instead. Although it was one atom less, it should not have much influence on our study of the dendritic shielding effect. The relative reactivities of the different interior sulfide moieties could still be assessed. The

synthesis of our target dendrimers could be simplified when the ethylene group was used as the linker because many synthetic methods to poly(phenyleneethylene) dendrimers had been reported.[81]

3.2.1.3 $-CH_2CH_2-$ linker

According to the literature[82], the Horner–Wadsworth–Emmons (HWE) reaction was the most commonly used method to connect dendrons and branching unit via the –CH=CH– linker. Therefore this strategy was applied to our synthetic scheme (Scheme 27). A dendron **94** with an aldehyde functional group locating at the focal point will be used to couple to diphosphonate **95** to yield the next higher generation dendron **96**. The double bonds in dendron **96** are then saturated to afford the flexible $-CH_2CH_2-$ linkers and the focal point protecting group can then be removed for further growth of dendrimer.

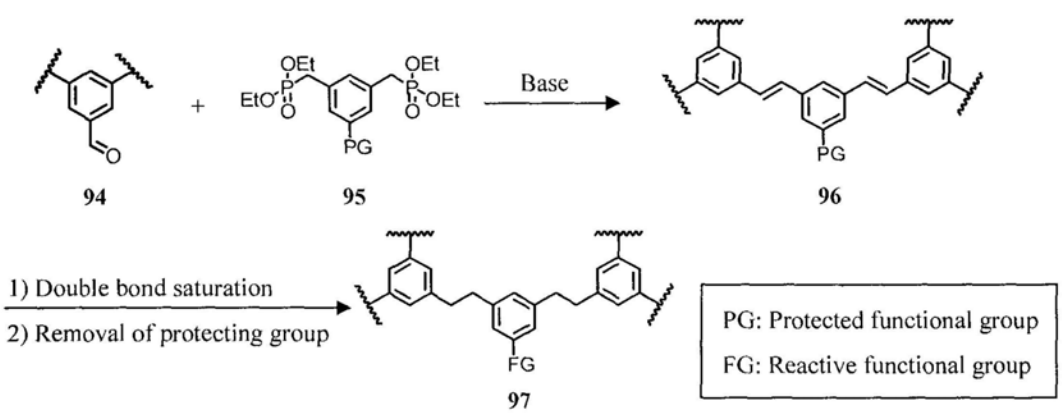

Scheme 27. Horner–Wadsworth–Emmons (HWE) approach to phenylenevinylene dendrons.

3.2.2 Synthesis of various branchers

Three different branching units **104**, **105** and **107** were used during the growth of dendrons. Branchers **104** and **107** were used in HWE coupling reactions. Their

focal point was protected either as a –THP group or a dimethyl acetal group. Reasons for using different protecting groups will be explained later. Brancher **105** was a dibromide which could react with thiols to afford a higher generation dendron with C–S–C branches. They were all prepared from commercially available trimesic acid (Scheme 28).[82]

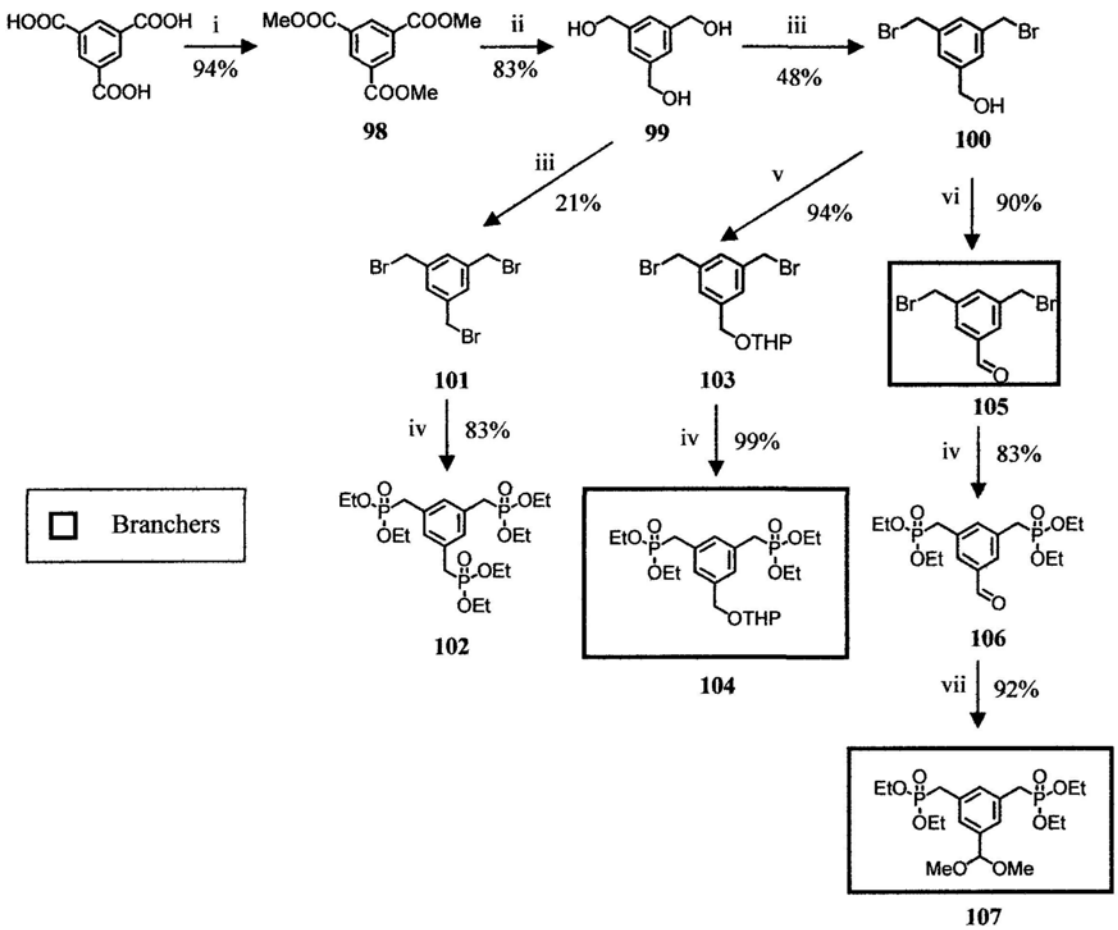

Scheme 28. Synthesis of various branchers **104**, **105**, **107** and core unit **101**, **102**. Reagents and conditions: (i) MeOH, conc. H_2SO_4, reflux; (ii) $LiAlH_4$, THF, 0–20 °C; (iii) CBr_4, PPh_3, THF, 20 °C; (iv) $P(OEt)_3$, 100 °C; (v) DHP, PPTS, CH_2Cl_2, 20 °C; (vi) PCC/silica gel, CH_2Cl_2, 0–20 °C; (vii) montmorillonite K 10, $CH(OMe)_3$, MeOH, 20 °C.

Esterification of trimesic acid using methanol and concentrated sulfuric acid gave the corresponding methyl triester **98**, which was then reduced by $LiAlH_4$ to afford 1,3,5-tris(hydromethyl)benzene **99**. The triol **99** was brominated to obtain a mixture of dibromide **100** and tribromide **101** in 48% and 21% yield, respectively

using 2.2 equivalents of CBr_4 and PPh_3. The tribromide **101** could be used as the core unit itself or further reacted with triethyl phosphite to yield a tris(phosphonate) **102** in 83% yield.

For the dibromide **100**, the remaining –OH group was either reacted with dihydropyran in the presence of pyridium *p*-toluenesulfonate (PPTS) to yield a THP-protected dibromide **103** (94%) or oxidized by pyridinium chlorochromate (PCC) in CH_2Cl_2 to afford the corresponding aldehyde **105** (90%). Compounds **103** and **105** were reacted with triethyl phosphite to give the diphosphonates **104** and **106** in 99% and 83% yield, respectively. The aldehyde group of **106** was then protected as a dimethyl acetal to obtain the brancher **107** in 92% yield. This was an essential step because if compound **106** was used to couple with other dendrons under the HWE conditions, self-coupling of **106** would also occur to give a crosslinked polymer network.

Since the sulfide moieties were introduced at different concentric layers, the synthesis of the various layer block dendrimers would not be as straightforward as that of Chow's type oligo(dibenyl sulfide) dendrimers. However, the type of reactions involved were mostly the same except the order of the reaction sequence. Two key coupling methods were used. When the dendron and the branching unit were connected by a two carbon $-CH_2CH_2-$ linker, a reaction cycle involving sequential HWE coupling–double bond saturation was employed. On the other hand, when a sulfide $-CH_2SCH_2-$linker was involved, a Mitsunobu type alcohol to thiol transformation followed by a simple S_N2 thioalkylation reaction were used (Scheme 29).

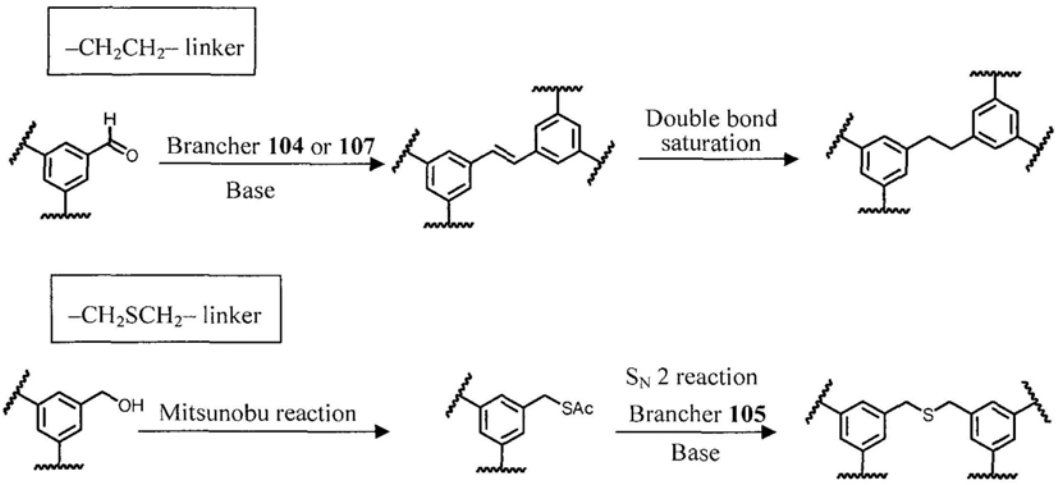

Scheme 29. Reaction cycles involved in the growth of dendons.

3.2.3 Synthesis of G3–CCS–dendrimer 68 with sulfide linkers in the innermost layer

For the convergent preparation of the G3–CCS–dendrimer **68** bearing three sulfide moieties embedded in the innermost dendritic layer, one required a G3 dendron **116** having two inert $-CH_2CH_2-$ layers with a focal point CH_2SH functionality for anchorage to the tribromide central core **101** (Scheme 30). Hence, the G1–alcohol **74** was first oxidized with PCC in CH_2Cl_2 to give the corresponding aldehyde **108** which was then coupled with the diphosphonate brancher **104** to obtain the unsaturated G2 dendron **109** in 74% yield. The two double bonds in compound **109** were then saturated by catalytic hydrogenation in the presence of 10% Pd–C and K_2CO_3. The inorganic base was used to prevent the cleavage of the THP protecting group during hydrogenation. After that, removal of THP group was performed in the presence of HCl to give the G2–alcohol **111** in 74% yield. The free hydroxyl group of the dendron **111** was then oxidized with PCC again to provide G2–aldehyde **112** in 81% yield. HWE olefination was repeated again between the aldehyde **112** and the

brancher **104** to give a THP–protected G3 dendron **113** in 60% yield. Then, catalytic hydrogenation followed by acid-catalyzed removal of the THP group gave the G3–alcohol **115**. At this stage, the focal point CH_2OH group of **115** was converted to the corresponding thioacetate **116** by Mitsunobu reaction in order to introduce the innermost sulfide linker.

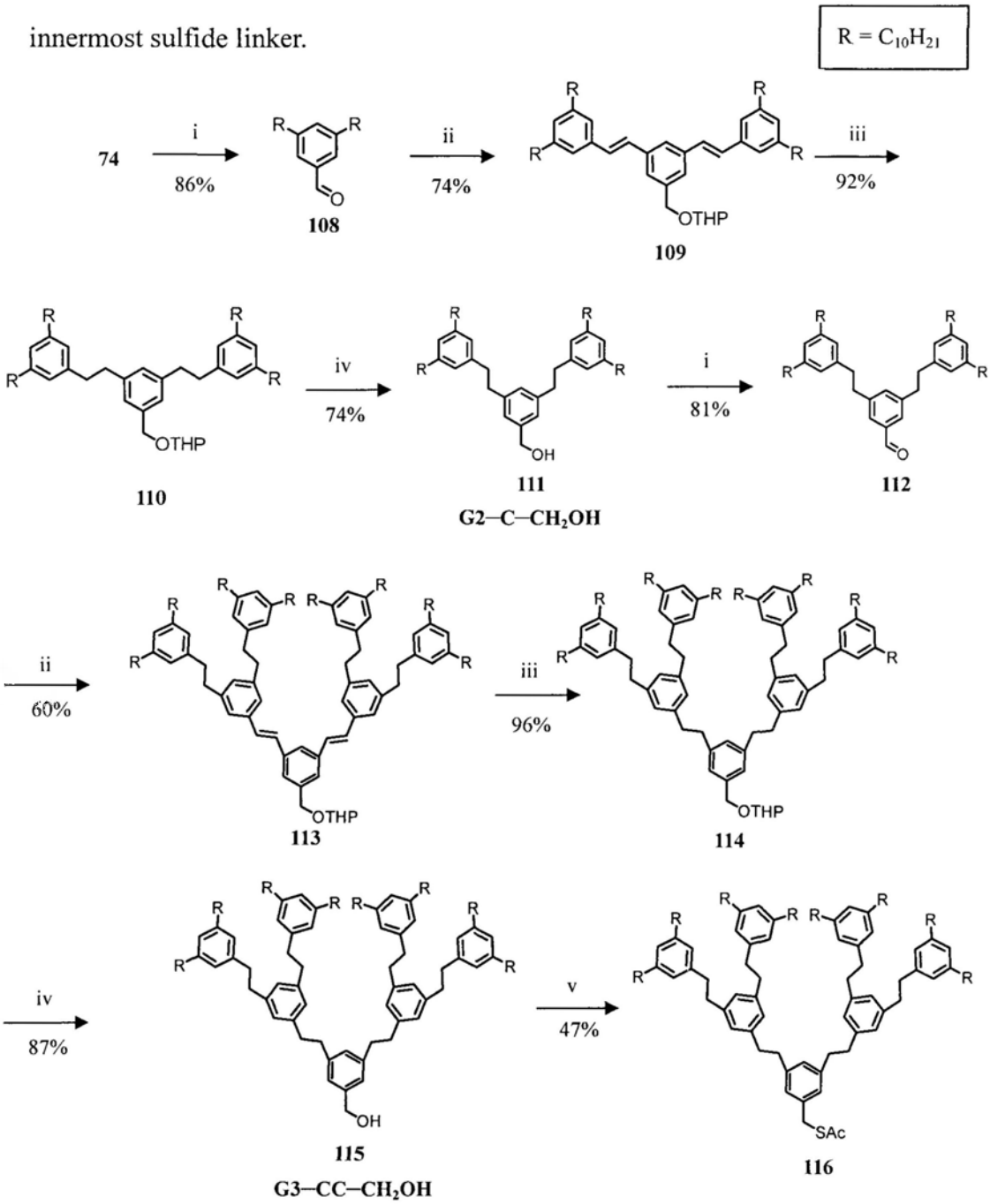

Scheme 30. Synthesis of G3–CCS–dendrimer **68**. Reagents and conditions: (i) PCC/silica gel, CH_2Cl_2, 0–20 °C; (ii) **104**, NaH, THF, reflux; (iii) 10% Pd/C, K_2CO_3, THF, 20 °C; (iv) conc. HCl, THF, EtOH, 20 °C; (v) AcSH, DIAD, PPh_3, THF, 0–20 °C.

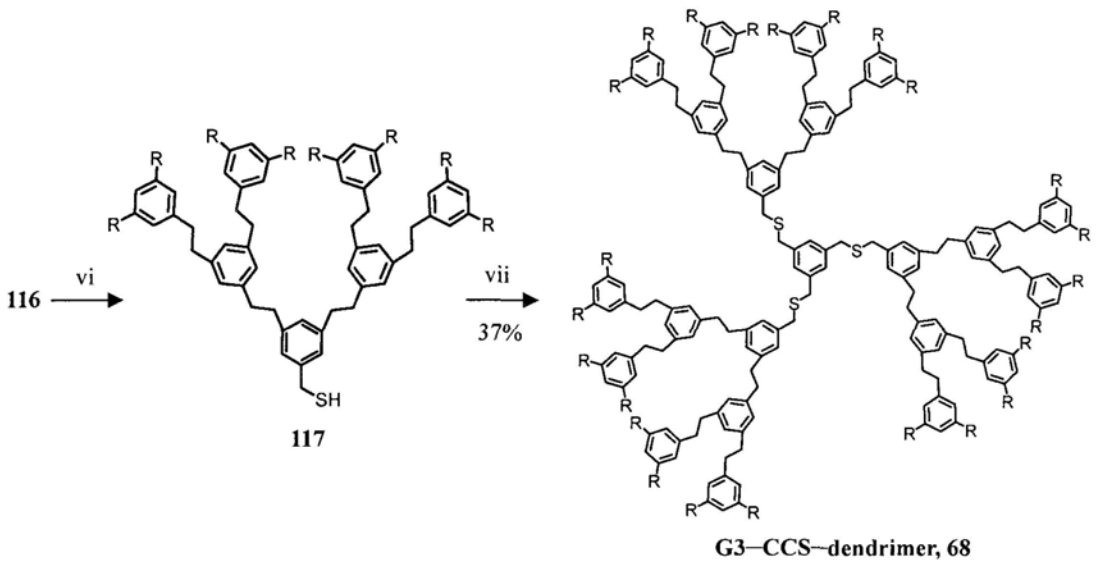

Scheme 30 (ctd). Synthesis of G3–CCS–dendrimer **68**. Reagents and conditions: (vi) NaOMe, MeOH, THF, 20 °C; (vii) **101**, NaOH, TBAI, MeOH, THF, 20 °C.

The coupling reaction between the G3 dendron **116** and the tribromide core **101** proved to be difficult. Generally, the acetyl group of the dendritic thioacetate is first removed by sodium methoxide and an S_N2 thioalkylation is then performed in the presence of a dibromide brancher to obtain the desired higher generation dendron. Unfortunately, when one tried to synthesize the G3–CCS–dendrimer **68** under the same experimental conditions, only unidentifiable products were obtained. Hence, another reported procedure was then tried,[83] in which the *in situ* generated thiol **117**, 1,8-diazabicyclo[5.4.0]undec-7-ene (DBU) and the tribromide **101** were mixed in benzene and stirred at room temperature. However, the target product **68** still could not be obtained.

Phase transfer (PT) reaction has proven to be an effective method to prepare umsymmetrical thioethers.[84] Ferreira and coworkers reported the synthesis of aryl alkyl sulfides from the corresponding disulfides under phase transfer conditions.[85] The disulfide bond was found to cleave and give the thiolate anion in the presence of hydroxide anion. The arylthiolate anion was then reacted with the alkylating agent in

the presence of phase transfer catalyst (PTC) to give the desired thioether. Since dendritic disulfide was always obtained as a by-product (due to facile oxidation of the *in situ* generated thiol **117**) during the coupling reaction between thioacetate **116** and tribromide **101**, it was therefore possible to prepare the target dendrimer **68** under the PT conditions. Hence, the acetyl group in compound **116** was removed by sodium methoxide *in situ* and the resulting thiol **107** was immediately reacted with the trifunctional core 1,3,5-tris(bromomethyl)benzene **101** in the presence of sodium hydroxide and TBAI to yield the G3–CCS–dendrimer **68** in 37% yield. This dendrimer processes three sulfide groups locating at the innermost dendritic layer. Although the product yield was low, the G3–CCS–dendrimer **68** could be obtained in pure form.

3.2.4 Synthesis of G3–CSC–dendrimer 69 with sulfide linkers in the middle layer

For the convergent preparation of the G3–CSC–dendrimer **69** bearing six sulfide moieties embedded in the middle dendritic layer, one needs to secure the synthesis of a G2 dendron **119** having one inert $-CH_2CH_2-$ layer with a focal point CH_2SH functionality. This compound was prepared by the G2–alcohol **111** via a Mitsunobu reaction (Scheme 31). Hence, alcohol **111** was converted to the corresponding thioacetate **118** in the presence of thioacetic acid, DIAD and triphenylphosphine in 43% yield. The middle $-CH_2SCH_2-$ layer was then prepared by coupling reaction of the thiol **119**, generated *in situ* from compound **118** by treatment with NaOMe, with the dibromide brancher **105** to give the G3–aldehyde **120** in 39% yield. The G3–aldehyde **120** was then reacted with the tris(phosphonate) core **102** in the presence of sodium hydride to afford the unsaturated G3–CSC=C–dendrimer **121**.

This product had six sulfide moieties located in the middle dendritic layer and three double bonds in the inner layer.

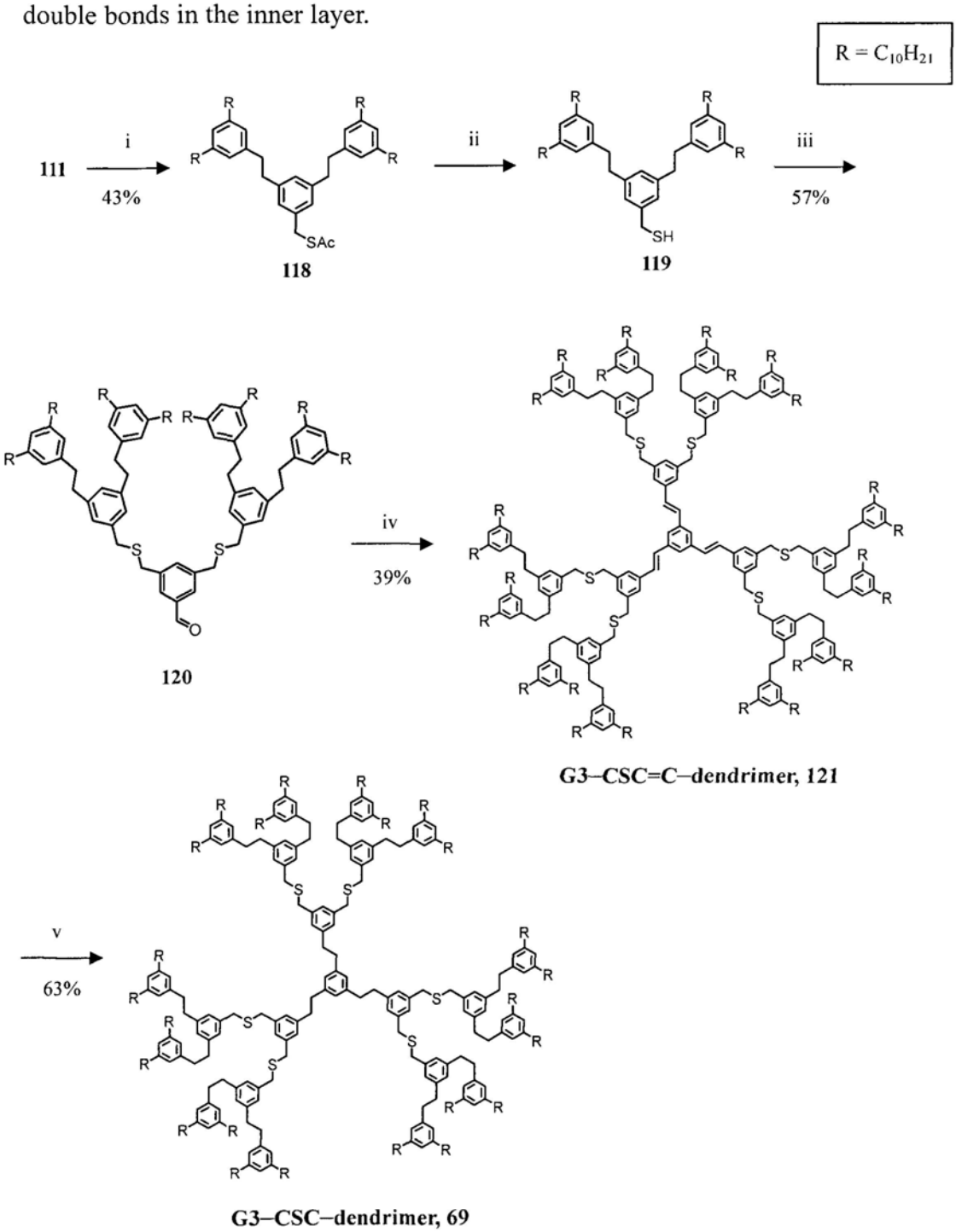

Scheme 31. Synthesis of G3–CSC–dendrimer **69**. Reagents and conditions: (i) AcSH, DIAD, PPh_3, THF, 0–20 °C; (ii) NaOMe, MeOH, THF, 20 °C; (iii) **105**, MeOH, THF, 20 °C; (iv) **102**, NaH, THF, reflux; (v) $TsNHNH_2$, aq. NaOAc, DME, $CHCl_3$, 85 °C.

Entry	Reagents and conditions	Results
1	H_2, Pd/C, THF, 20 °C	Breakdown of the dendrimer (Cleavage of C–S bond)
2	H_2, K_2CO_3, Pd/C, THF, 20 °C	
3	$NaBH_4$, Pd/C, AcOH, THF, 20 °C	
4	LAH, 20 °C	No reaction
5	LAH, 50 °C	Breakdown of the dendrimer (Cleavage of C–S bond)
6	N_2H_4, $CuSO_4$, 40 °C	

Table 1. Attempts tried for the saturation of carbon–carbon double bond in dendrimer **121**.

The three double bonds were then subjected to saturation to give the $-CH_2CH_2-$ linker. As our first attempt, catalytic hydrogenation using palladium on charcoal (Table 1, entries 1 and 2) was tried. However, it was found that the desired product could not be obtained. It appeared that the C–S bonds underwent cleavage reactions much faster than C=C saturation. We also tried to generate hydrogen gas by mixing sodium borohydride and acetic acid (entry 3).[86] Unfortunately, this method was also unsuccessful in reducing the C=C bonds. As an alternative, we used lithium aluminium hydride ($LiAlH_4$) as the reducing agent (entries 4 and 5). However, no reaction was found when the reaction was performed at 20 °C. When the reaction temperature was raised to 50 °C, cleavage of the dendrimer skeleton again occurred. We then resolved to use diimide as a reducing agent, which was generated *in situ* from hydrazine in the presence of atmospheric oxygen and copper(II) sulfate (entry 6). The diimine, in principle, should react with the alkene through a cyclic transition state to yield the saturated product **69**. Hence, the unsaturated dendrimer **121** was treated with a mixture of $CuSO_4$ and hydrazine at 40 °C. However, the saturated product could not be obtained. Therefore, another experimental condition was tried.

The diimine was generated *in situ* by using $TsNHNH_2$ and sodium acetate. Finally, it was found that the double bonds in the innermost layer of the G3–dendrimer **121** could be saturated to give the target G3–CSC–dendrimer **69** in 63% yield.

3.2.5 Attempted synthesis of G3–SCC–dendrimer 70 with sulfide linkers in the outermost layer

The G1–alcohol **74** was converted to the corresponding G1–thioacetate **125** via Mitsunobu reaction, followed by coupling reaction with the dibromo branching agent **105** to yield the G2 dendron **127** (Scheme 32). Initially, the synthetic method reported by Chow was applied and another dibromo branching unit **122** was employed for generation growth (Route a). However, it was found out that G2–alcohol **124**, prepared via $LiAlH_4$ reduction of the ester **123**, could only be oxidized by PCC to give the G2–aldehyde **127** in 24% yield. As a result, we tried to conduct the coupling reaction using another branching unit, 3,5-bis(bromomethyl)benzaldehyde **105**. In this manner, the G2 aldehyde dendron **127** was obtained in 47% yield directly from the thiol **126**.

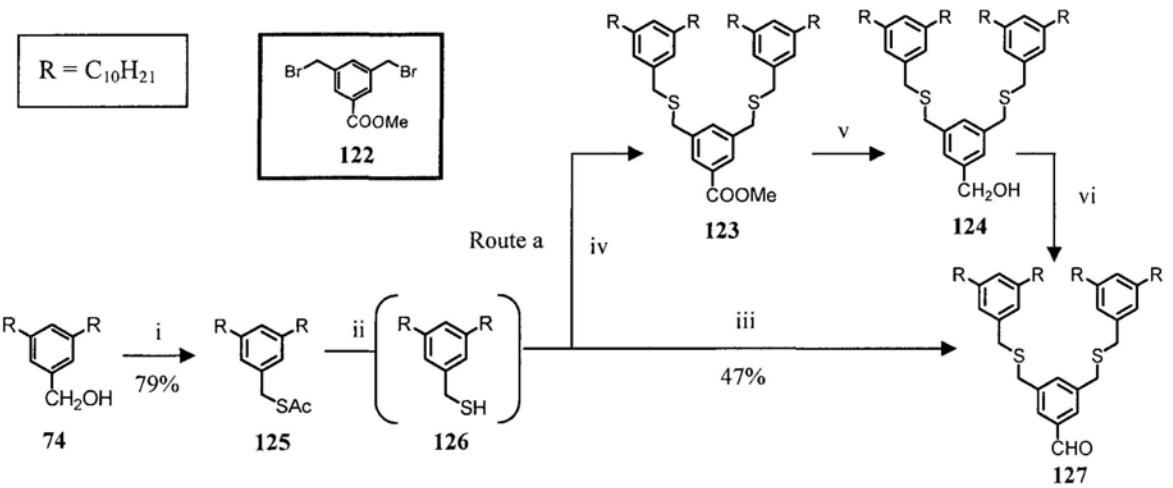

Scheme 32. Synthesis of G2 dendron **127**. Reagents and conditions: (i) AcSH, DIAD, PPh_3, THF, 0–20 °C; (ii) NaOMe, MeOH, THF, 20 °C; (iii) **105**, MeOH, THF, 20 °C; (iv) **122**, MeOH, THF, 20 °C; (v) $LiAlH_4$, THF, 0–20 °C; (vi) PCC/silica gel, CH_2Cl_2, 0–20 °C.

The aldehyde **127** was then coupled to the bisphosphonate branching unit **107** under HWE conditions to afford the unsaturated G3 dendron **128** in 52% yield (Scheme 33). Surprisingly, the double bonds of **128** could be hydrogenated using $CuSO_4$ and NH_2NH_2 to give the corresponding saturated G3 dendron **129** in 66% yield. The presence of the sulfur atoms did not create any complication, this was in sharp contrast to the hydrogenation reaction with the G3–CSC=C–dendrimer **121**.

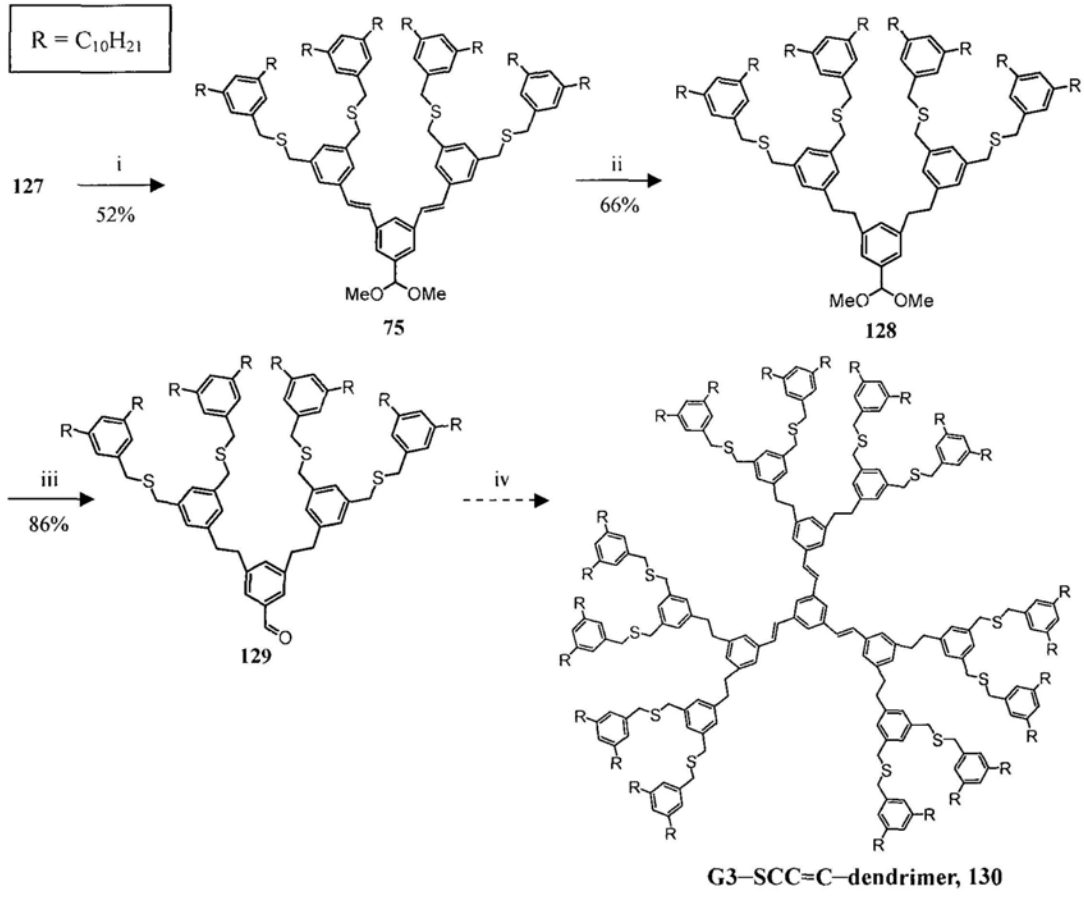

Scheme 33. Attempted synthesis of G3–SCC–dendrimer **70**. Reagents and conditions: (i) **107**, NaH, THF, reflux; (ii) N_2H_4, $CuSO_4$, THF, 40 °C; (iii) 20% H_2SO_4, THF, 20 °C; (iv) **102**, NaH, THF, reflux.

The focal point acetal group in **128** was then removed under acidic condition to yield G3–aldehyde **129** in 86% yield. However, when compound **129** was reacted with the trisphosphonate core **102**, only a complex mixture was obtained despite

numerous attempts. According to ^{1}H NMR analysis, there were signals (δ 3.2–3.3 and δ 4.0–4.1) due to the presence of residual ethyl phosphonate moiety. It appeared that the HWE reaction was incomplete and at most only two dendrons could be anchored to the central core. This suggested that the failure of the HWE reactions was most likely due to steric retardation. As we compared the results of the different HWE reactions, it was found that coupling efficiency was greatly reduced as the size of the dendron increased. For example, the G1–aldehyde **108** could be coupled to the diphosphonate brancher to yield G2 dendron in 74% yield but the product yield was dropped to 50–60% in cases of bulkier G2–aldehydes (*e.g.* **112** or **127**). The yield was even lower (39%) when the G3 dendron G3–CS–CHO **120** was coupled to the trifunctional triphosphonate core **102** as three, instead of two G3 dendrons were anchored to such a small central core. Although G3–CS–CHO **120** and G3–SC–CHO **129** were both G3 dendrons and possessed similar structure, the G3–SC–CHO dendron was sterically more congested near the focal point as the linker in the inner layer of G3–aldehyde **129** were $-CH_2CH_2-$ which had one atom less when compared to that (*i.e.* $-CH_2SCH_2-$) in compound **120**. Besides, the triphosphonate core **102** was a very bulky reagent, it was envisaged that even G3 dendron **129** could couple to the core **102** once, further coupling reactions would become very difficult due to the steric inhibition.

Looking back at the synthesis of G3–CCS–dendrimer **68**, although the linker in the inner layer of G3–CC–CH_2SH **117** was also $-CH_2CH_2-$, the reaction between the thiol and the tribromide core **101** was straight forward. This is because the tribromide was less bulky than the triphosphonate **102**, hence the target dendrimer **68** could still be prepared successfully. As the G3–SCC=C–dendrimer **130** could not be obtained after many trials, our study could only focus on the two target dendrimers **68** and **69**.

3.2.6 Synthesis of G3–SSS–dendrimer 136

We also prepared the corresponding G3–SSS–dendrimer **136** with three sulfide layers as a model compound in order to probe the optimal conditions for the internal functional group conversions. The synthesis began with the G1–CH_2SAc **125** (Scheme 34). The acetyl group in compound **125** was removed by sodium methoxide in a mixture of THF and MeOH to generate the corresponding thiol **126** which was immediately coupled to the dibromide branching unit **100** to give the G2–S–CH_2OH in 85% yield. The focal point CH_2OH group was then converted to corresponding thioacetate by Mitsunobu reaction in 85% yield. Using the same synthesis sequence, G3–SS–CH_2OH **133** was prepared from G2–thioacetate in 44% yield and it was converted to the G3–thioacetate **134** in 82% yield. Finally, the acetyl group in compound **134** was removed by sodium methoxide to give the corresponding thiol **135** which was then coupled to the tribromide core **101** to get the target G3–SSS–dendrimer **136** in 74% yield.

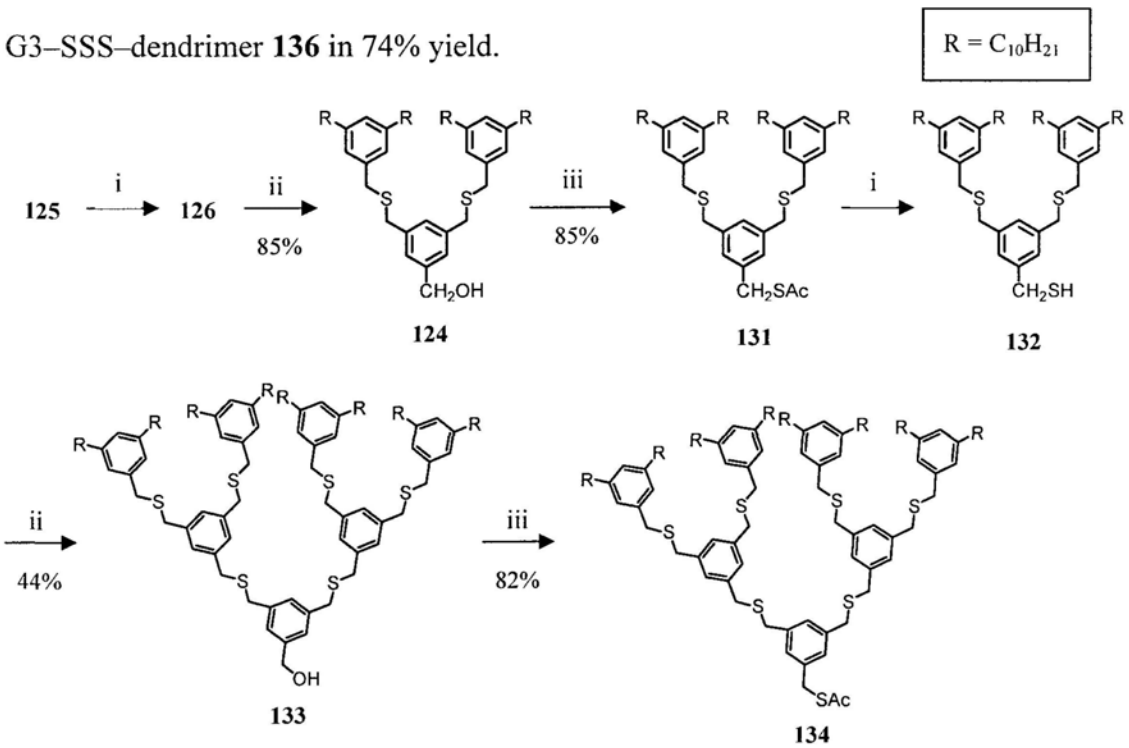

Scheme 34. Synthesis of G3–SSS–dendrimer **136**. Reagents and conditions: (i) NaOMe, MeOH, THF, 20 °C; (ii) **100**, MeOH, THF, 20 °C; (iii) AcSH, DIAD, PPh_3, THF, 0–20 °C.

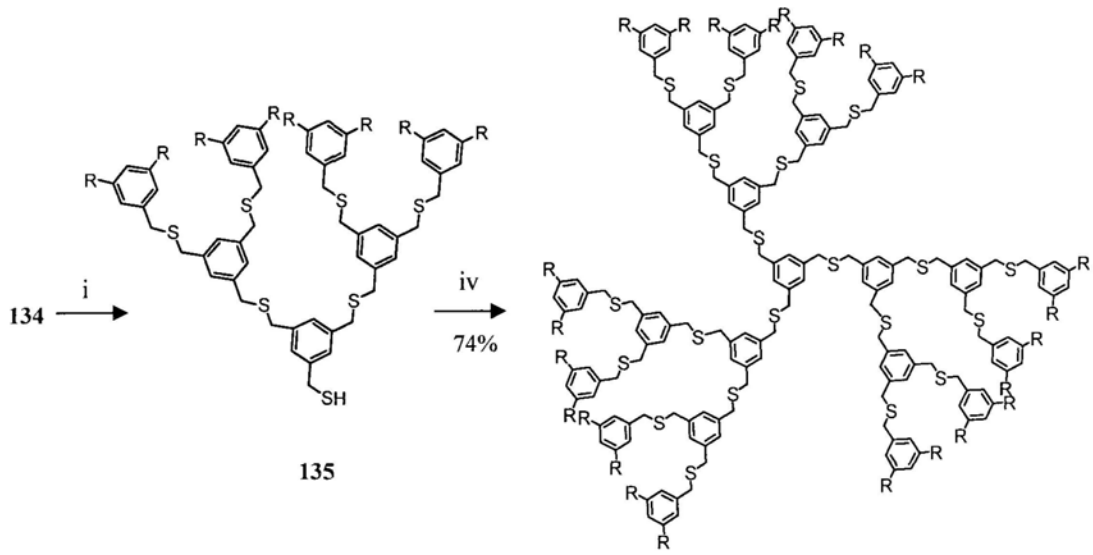

Scheme 34 (ctd.). Synthesis of G3–SSS–dendrimer **136**. Reagents and conditions: (i) NaOMe, MeOH, THF, 20 °C; (iv) **101**, MeOH, THF, 20 °C.

3.3 Structural characterization of dendrons and dendrimers

The two target layer-block dendrimers **68**, **69** and their precursor molecules were characterized by proton (^{1}H) and carbon (^{13}C) nuclear magnetic resonance spectroscopy (NMR), mass spectrometry (MS) and gel permeation chromatography (GPC). 2-Dimensional NMR techniques were also used to provide signal peaks assignment when nessessary.

3.3.1 ^{1}H NMR spectroscopy

Due to the structural similarity of the dendritic molecules, several common spectral features were found in the ^{1}H NMR spectra. First, four sets of characteristic peaks due to the proton signals of the decyl surface group, were found to locate between δ 0.8 ppm to δ 2.6 ppm. Hence, the methyl signal was found as a triplet to at

δ 0.9, whereas the benzylic protons were situated at δ 2.6 ppm as a triplet. The protons at the internal position were found as two multiplets at δ 1.3 and 1.6 ppm. Second, proton signals due to functional groups at the dendritic focal point were found at the region from δ 3.0 – δ 10 ppm (Figure 13) and the positions of these characteristic proton signals depended only on the nature of the focal point group, but independent of the generation. Therefore, these characteristic signals can serve as a tool for identification of chemical transformations occurred at the focal point.

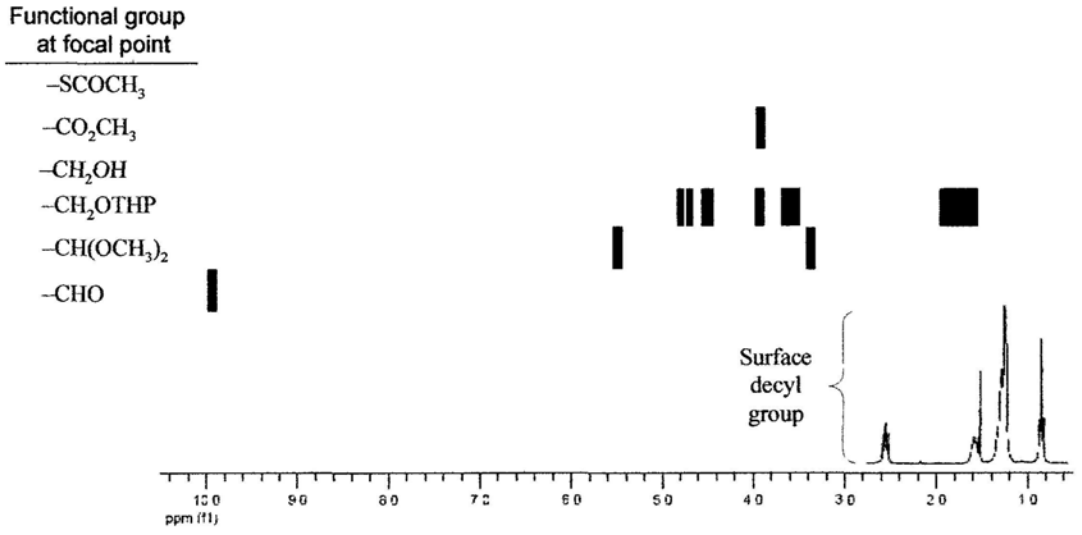

Figure 13. Chemical shift position of the characteristic proton signals (300 MHz, $CDCl_3$) due to functionalities at the focal point.

There are only three types of branches (–CC–, –CSC–, –C=C–) in all the dendritic molecules, and they give rise to proton signals in different regions. For the saturated –CH_2CH_2– branch, proton signals are located at about δ 2.8–2.9. For the –CH_2SCH_2–branch, the chemical shift of the proton signals are at about δ 3.5–3.6, which is more downfield shifted as compared to the saturated –CH_2CH_2– branch due to the presence of the sulfur atom. For the –CH=CH– branch, as they are connected to the aromatic branchers and are part of a conjugated system, the proton signals are downfield shifted and located at about δ 6.8–6.9. Signals due to the aromatic

branchers of the dendritic molecules can be observed at the downfield region from δ 6.8 to δ 8.0 ppm.

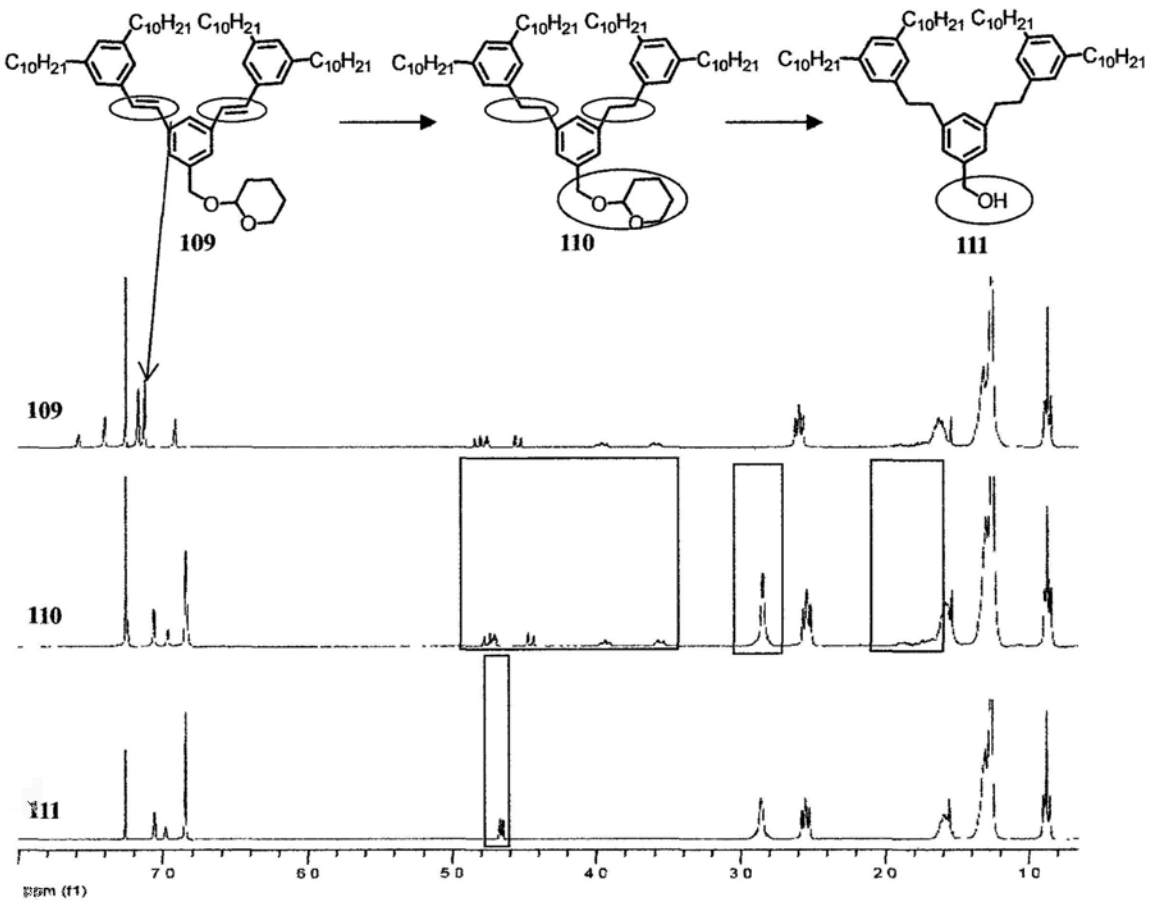

Figure 14. Stacked ^{1}H NMR spectra (300 MHz, $CDCl_3$) for G2 dendrons **109–111**.

^{1}H NMR spectroscopy was also a useful tool to elucidate the chemical transformation of the functional group at the focal point or at the branches. For example, in the synthesis of saturated G2–C–OTHP **110**, saturation of the carbon-carbon double bonds could be monitored by ^{1}H NMR spectroscopy (Figure 14). Before the reaction, the AB system due to the double bonds was observed at the δ 7.1– 7.2 ppm. When the hydrogenation was completed, the vinylene HC=CH signal disappeared and a new board proton signal at δ 2.8 ppm was found which was due to the ^{1}H signal on the $-CH_2CH_2-$ linker. The ^{1}H signals of the diastereotropic benzyl protons near the –OTHP group were found as two doublets at 4.55 and 4.82.

After removing the THP protecting group at the focal point, the signals due to the THP moiety disappeared, and the benzylic protons adjacent to the OH group now became a doublet at δ 4.66 ppm in G2–C–CH_2OH dendron **111**.

2D NMR spectroscopy was also used to aid structural assignments. For example, in the ^1H NMR spectrum of THP-protected G2 dendron **109**, there were two peaks at about δ 7.13 and δ 7.17 ppm, both of which had a relative integration of 4. It was difficult to distinguish which one was due to the protons of the double bonds and which was due to the aromatic protons on the surface branchers. Therefore, 2-dimensional heteronuclear single quantum coherence (HSQC) NMR spectroscopy was used to probe additional information on the proton-carbon connectivity (Figure 15). This technique can relate a particular ^{13}C signal to its corresponding ^1H signal by showing a cross peak at the 2D NMR spectrum. From the spectrum, ten ^{13}C signals were found from δ 122 ppm to δ 144 ppm which were due to the carbon atoms on the aromatic rings and the double bonds, and there were only six sp^2-hybridized carbon signals that had correlation to the proton signals. It was found that there were two non-equivalent carbon signals at δ 128 and δ 130 ppm that possessed a cross peak with the proton signal at δ 7.13, hence this proton signal must be due to the olefinic hydrogen (in blue ellipse).

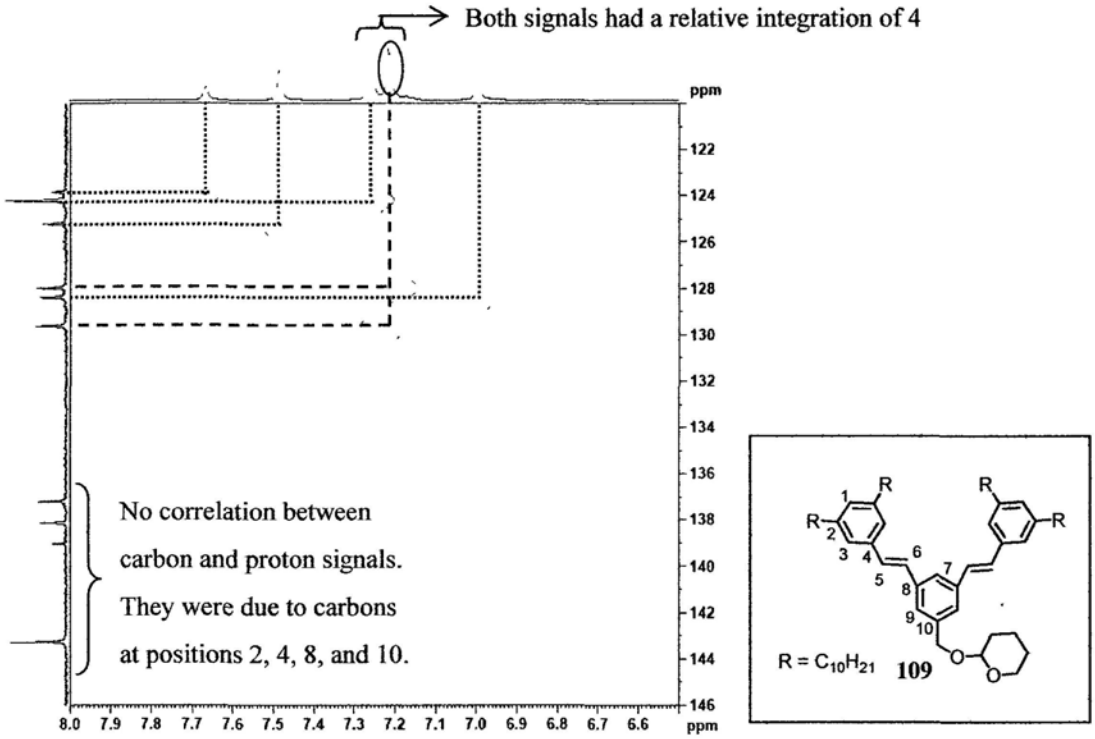

Figure 15. Partial HSQC NMR spectrum (400 MHz, $CDCl_3$) of THP protected G2 dendron **109**.

For the G3 series of dendrons, ^{1}H NMR spectroscopic analysis again provides valuable information on their structure. The stacked ^{1}H NMR spectra of the G3 dendrons **75**, **128**–**129** are shown in Figure 16. After saturation of the double bonds in dendron **75**, the proton signals due to the outer branches –CH_2SCH_2– as well as the focal point protecting group –$CH(OCH_3)_2$ were shifted towards the upfield region slightly. As expected, the proton signals of the –CH_2CH_2– branches for both the G2 and G3 dendrons were found at the same chemical shift of 2.9 ppm. The benzylic proton signals adjacent to the S atom were found to locate at about δ 3.6 ppm. After deprotection of the dimethyl acetal group, an aldehyde peak located at δ 10.0 was found. At the same time, the signals of the –CH_2CH_2– branches were resolved into multiplets at around δ 3.0.

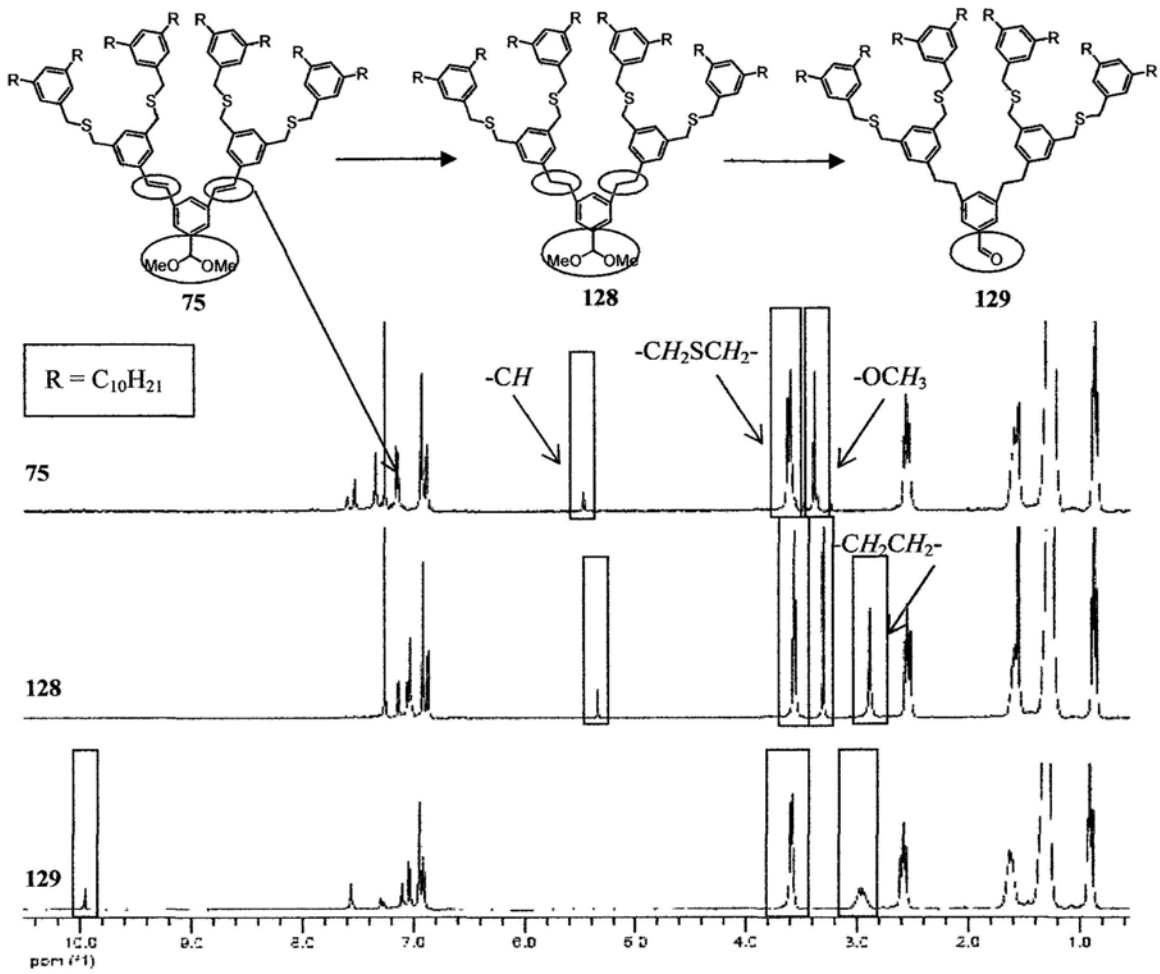

Figure 16. Stacked ^{1}H NMR spectra (300 MHz, $CDCl_3$) for G3 dendrons, **75**, **128**–**129**.

Figure 17 showed the stacked ^{1}H NMR spectra of G3–CCS–dendrimer **68** and G3–CSC–dendrimer **69**. For G3–CCS–dendrimer, the proton peaks due to $-CH_2CH_2-$ of two different dendritic layers were almost merge together and were located at about δ 2.84 and 2.86 ppm. For G3–CSC–dendrimer, the proton signals of the $-CH_2CH_2-$ branches were found as two clear board peaks at δ 2.80 and 2.87 ppm. The benzylic proton signals adjacent to the S atom were found to locate at about δ 3.6 ppm which was similar to those sulfide containing dendrons.

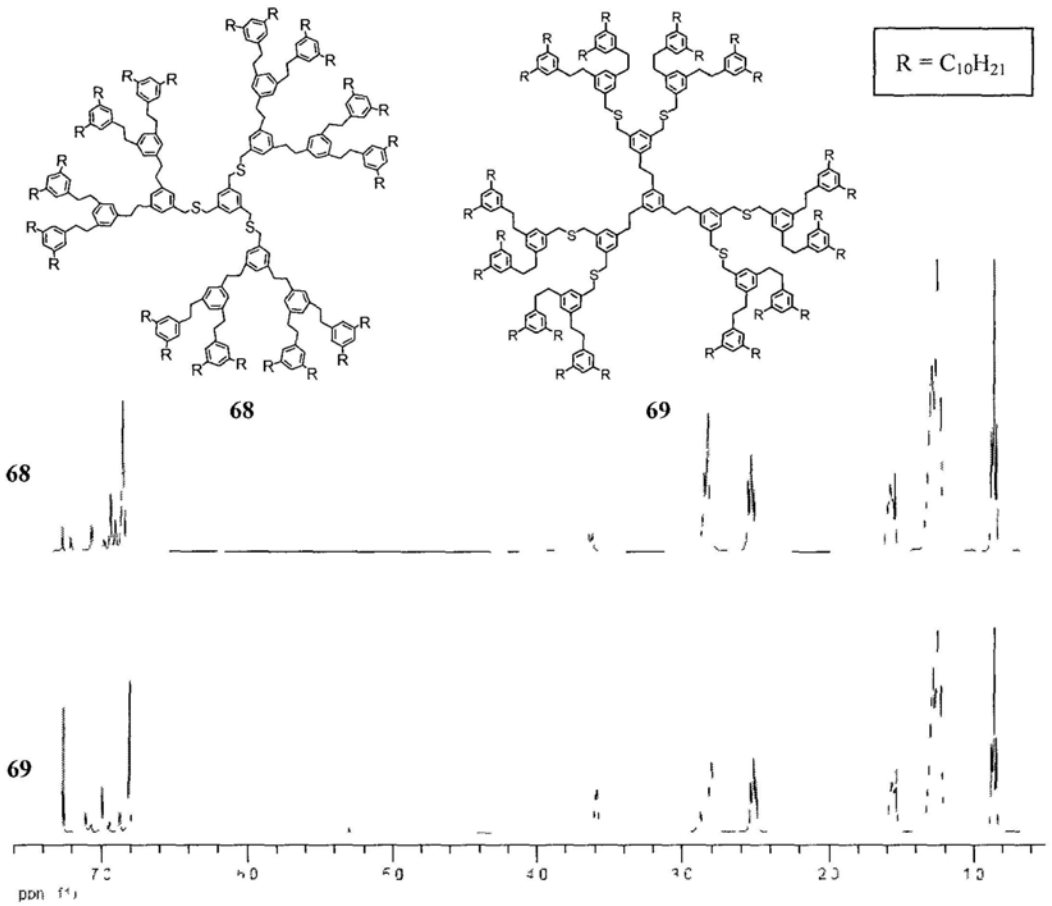

Figure 17. Stacked ^{1}H NMR spectra (400 MHz, $CDCl_3$) for G3–CCS–dendrimer **68**, G3–CSC–dendrimer **69**.

3.3.2 ^{13}C NMR spectroscopy

^{13}C NMR spectroscopy is a very useful characterization technique in the structural identification of symmetrical dendritic molecules. Hence, all dendritic molecules were characterized by this technique. For most dendrons, the signals fell into two distinct regions. Those due to the decyl surface groups were observed at the upfield region from δ 14 ppm to δ 36 ppm. Signal overlappings were commonly encountered because of the very similar chemical environment of the aliphatic carbon atoms. The ^{13}C signals due to the aromatic carbons were found to spread between δ 123–144 ppm in the downfield region.

The ^{13}C signals due to $-CH_2SCH_2-$ and $-CH_2CH_2-$ branches are at about δ 35 ppm and δ 38 ppm, respectively. These signal peaks usually overlap with the signals due to the surface group. For the branches –CH=CH–, the respective carbon signals were found at about δ 127 to 130 ppm, which overlapped with the aromatic carbon signals. Figure 18 showed the ^{13}C NMR spectrum of G3–CSC=C–dendrimer **121** which indicated the various types of carbon signals in the different regions.

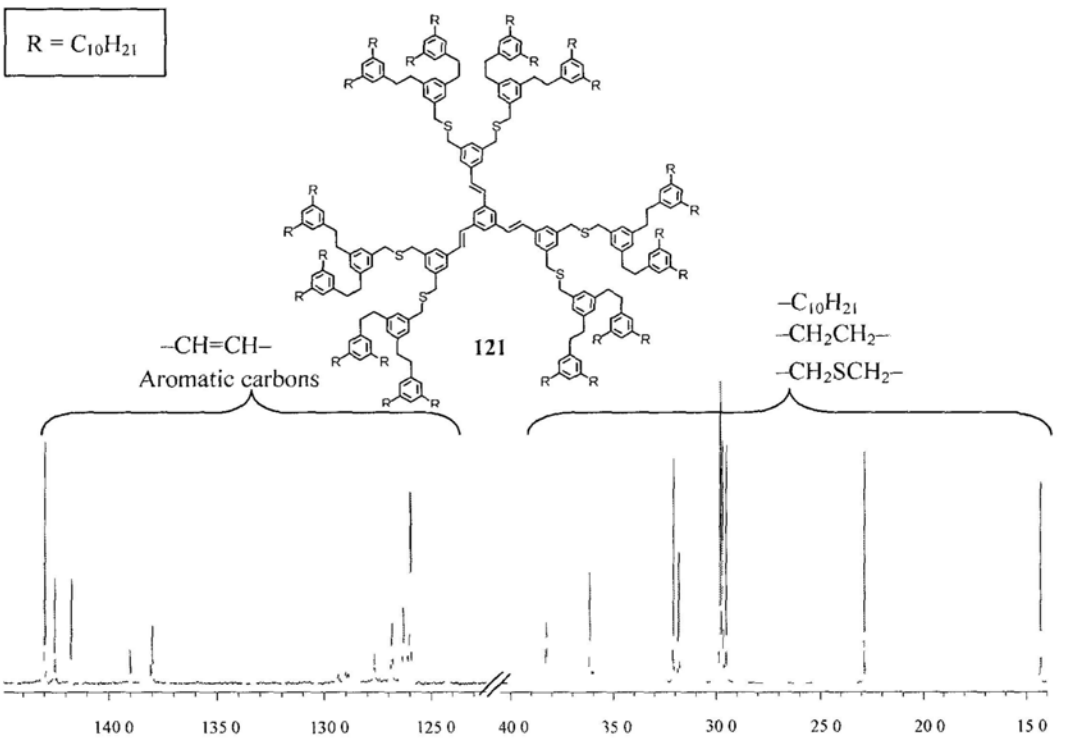

Figure 18. ^{13}C NMR spectrum (300 MHz, $CDCl_3$) for the G3–CSC=C– dendrimer **121**.

The functional groups at the focal point also exhibited the respective carbon signals at different regions (Figure 19). Generally, signals due to the carbonyl groups from the thioacetate, aldehyde or methyl ester were found at chemical shift values higher than δ 160 ppm, while other carbon signals due to the functionalities at the focal point were mainly located from δ 50 ppm to δ 110 ppm. Furthermore, it was found that the chemical shift values of these characteristic carbon signals did not change significantly in different dendrimer generations.

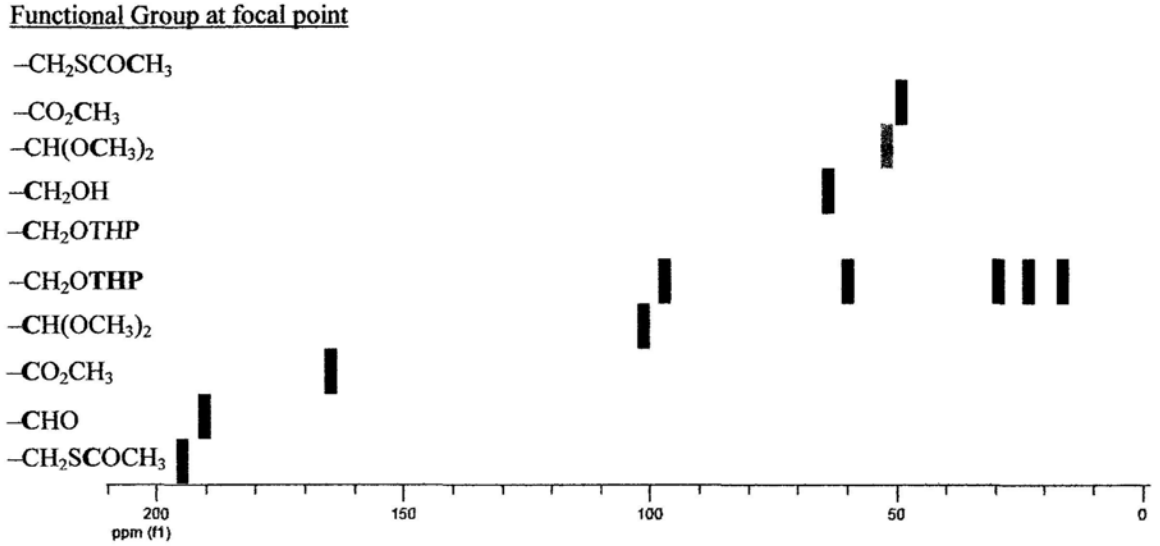

Figure 19. Location of carbon signals (300 MHz, $CDCl_3$) due to different functional group at the dendritic focal point.

3.3.3 Mass spectrometry

Mass spectrometry is a commonly used technique in the characterization of dendritic compounds as the presence of defects could be observed from the spectrum. Two kinds of soft ionization techniques were employed in our study. They were electrospray ionization (ESI) and the matrix-assisted laser desorption/ionization-time (MALDI). Peaks of the molecular ions could be located in all spectra of the dendritic compounds and they showed peaks matching the calculated molecular weight. The experimental results of the mass spectral data were summarized in Table 2.

G1–dendron	Ionization method	Theoretical Value [a]	Measued value [a]
72	ESI	431.2921	431.2931
73	ESI	439.3547	439.3545
74	ESI	411.3597	411.3600
108	ESI	409.3441	409.3450
125	ESI	469.3475	469.3486

Table 2. Mass-to-charge ratio for G1 to G3 dendritic species. [a] the theoretical value and the measured value was based on molecular weight of $[M+Na]^+$.

G2–dendron	Ionization method	Theoretical Value[a]	Measued value
109	MALDI-TOF	979.8241	979.8289
110	MALDI-TOF	983.8554	983.8544
111	ESI	899.7979	899.7965
112	MALDI-TOF	897.7822	897.7833
118	ESI	957.7857	957.7848
124	ESI	963.7421	963.7418
127	MALDI-TOF	961.7264	961.7241
131	MALDI-TOF	1021.7298	1021.7314
G3–dendron	Ionization method	Theoretical Value	Measued value
75	MALDI-TOF	2045.5632	2045.5632
113	MALDI-TOF	1957.7039	1957.7106
114	MALDI-TOF	1961.7352	1961.7329
115	ESI	1877.6777	1877.6790
116	MALDI-TOF	1935.6654	1935.6646
120	ESI	1939.6062	1939.6072
128	MALDI-TOF	2049.5921	2049.5888
129	MALDI-TOF	2003.5503	2003.5577
133	MALDI-TOF	2069.5100	2069.5105
134	MALDI-TOF	2127.4982	2127.5001
G3–dendrimer[†]	Ionization method	Theoretical Value	Measued value
68[b]	MALDI-TOF	5728	5728
69	MALDI-TOF	5847	5846
121	MALDI-TOF	5840	5840
136	MALDI-TOF	6305	6305

Table 2 *(ctd)*. Mass-to-charge ratio for G1 to G3 dendritic species. [†] The value was obtained by low resolution mass spectrometry; [a] the theoretical value and the measured value was based on molecular weight of $[M+Na]^+$; [b] unless otherwise stated, values of molecular weight was due to $[M]^+$

Most of the prepared compounds were also characterized by high resolution mass spectrometry (HRMS) unless the molecular weight of the dendritic species was too high that only low resolution mass spectra could be obtained. From the mass spectra, fragments due to the cleavage of dendrons or protected groups were also

found. Figure 20 shows the mass spectrum of the molecular ion peak $[M+Na]^+$ as well as the dimeric peak $[2M+Na]^+$. Besides, there was a peak found with mass to charge ratio (*m/z*) at 856.7411. This was due to the cleavage of the protecting group –OTHP at the dendritic focal point.

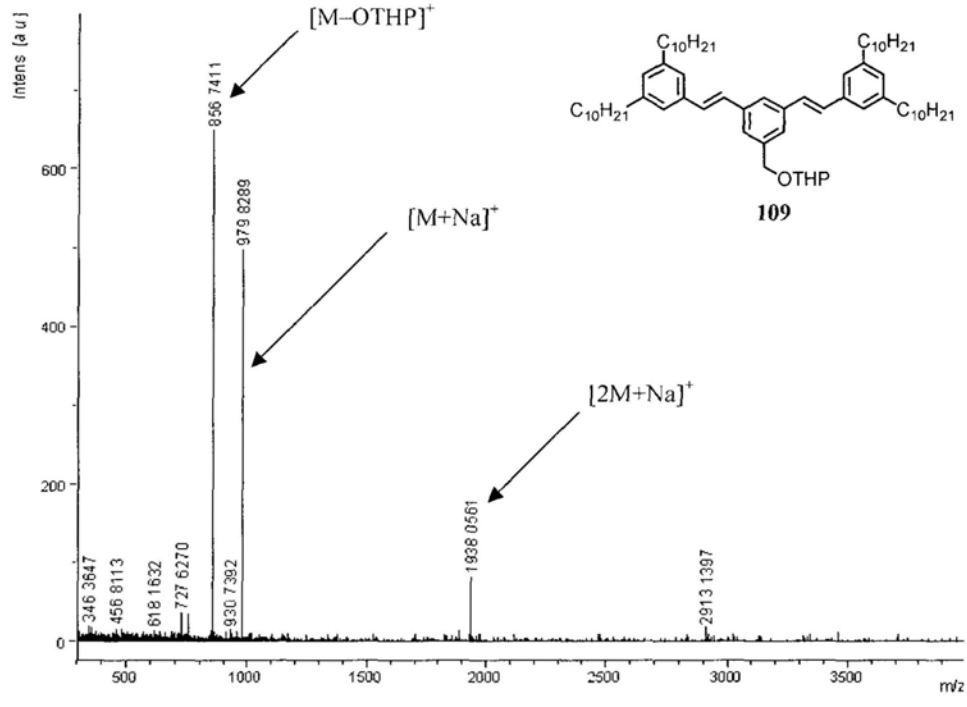

Figure 20. Mass spectrum (MALDI–TOF) of G2 dendron **109**.

Figure 21 shows the mass spectrum of the G3–CSC=C–dendrimer **121**. The molecular ion peak $[M+Na]^+$ at *m/z* 5839.8861 was found. Other dendritic fragment ion peaks could also be observed at *m/z* 4980.3390 and 4087.9300 which were due to the cleavage of one or two G2 dendrons. Also, it was found that the cleavage was commonly occurred at the C–S bond.

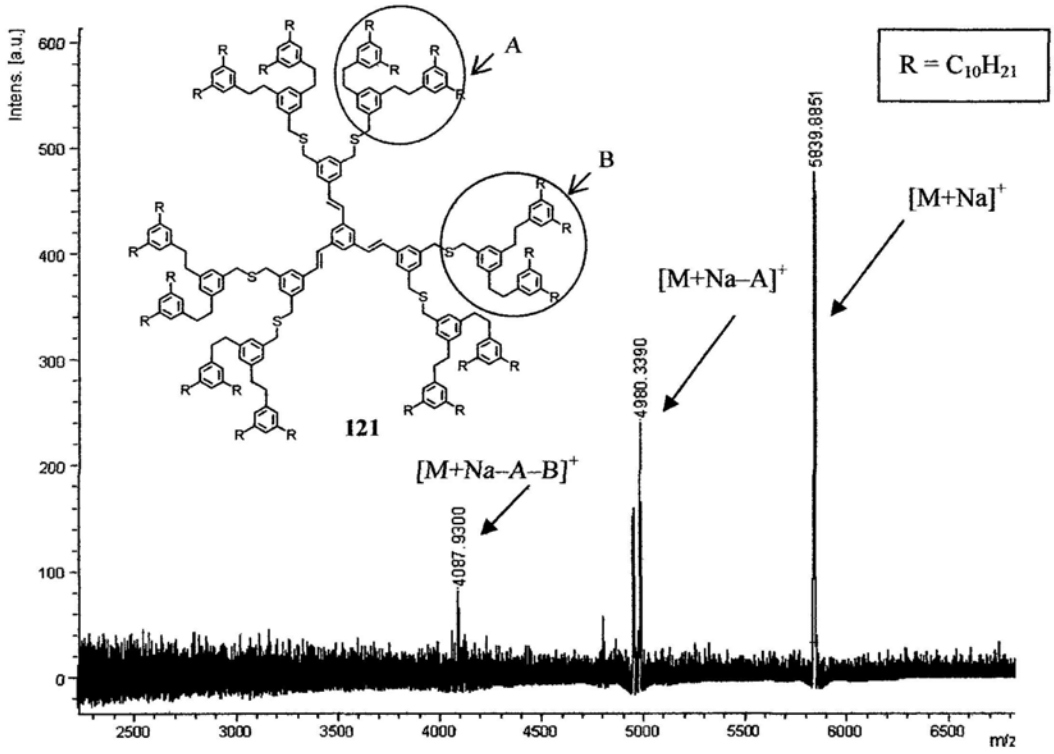

Figure 21. Mass spectrum (MALDI–TOF) of G3–CSC≡C–dendrimer **121**.

3.3.4 Gel permeation chromatography (GPC)

Gel permeation chromatography, also known as size exclusion chromatography (SEC), is a popular technique for the determination of the molecular weight distribution of polymers. GPC separation is based on the hydrodynamic volume of the analytes. Analytes with smaller size will be trapped in the porous column more easily, so they will be retained within the column and thus possess a longer retention time. Conversely, larger analytes will have a shorter retention time. Since analytes different in size will have different retention time, GPC is also a convenient tool to access the purity of dendrimers. Polydispersity index (PDI) is defined as the ratio of weight average molar mass (M_w) and number average molar mass (M_n). For dendritic molecules, PDI below 1.03 can be regarded as monodisperse. Using polystyrenes as the calibration standards, the molecular weight of the analyte can also be estimated.

Table 3 summarized the GPC results of the prepared dendritic molecules. All samples showed narrow molecular weight distribution of <1.02. As expected, dendritic molecules of the same generation will have similar retention time. Hence, the G1 to G3 dendron series possess retention time of 34 min, 32 min, and 30 min respectively while the G3 dendrimer had retention time at about 28 min (Figure 22).

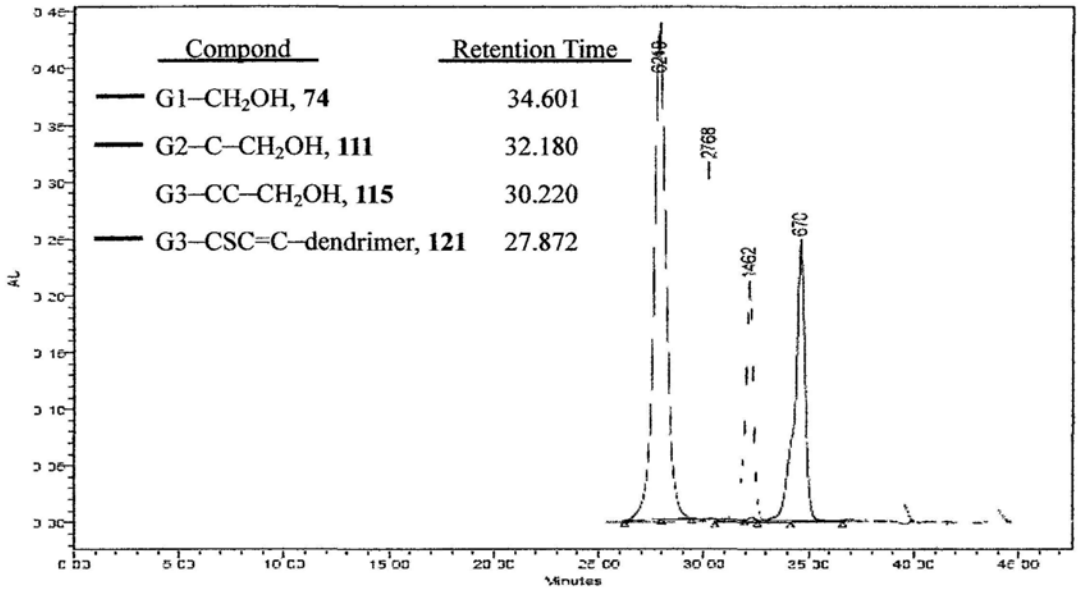

Figure 22. Stacked GPC chromatograms for selected dendritic species.

3.4 Summary

Two target dendrimers G3–CCS–dendrimer **68** and G3–CSC–dendrimer **69** were synthesized and characterized. A third target dendrimer G3–SCC–dendrimer **70**, with organosulfide moieties located in the outermost dendritic layer, could not be synthesized despite numerous attempts. It may due to the severe steric hindrance of the dendrimer interior towards external reagents. Hence, our study was focused on the two target dendrimer **68** and **69**. A model dendrimer G3–SSS–dendrimer **136** was also synthesized in order to find out the optimum reaction conditions for the interior functional group conversions.

G1 dendron	Retention time (min)	M_n (Daltons)	M_w (Daltons)	Polydispersity (M_w/M_n)
72	34.844	625	629	1.01
73	34.746	647	654	1.01
74	34.601	688	696	1.01
108	34.798	635	639	1.01
125	34.585	681	685	1.01
G2 dendron	Retention time (min)	M_n (Daltons)	M_w (Daltons)	Polydispersity (M_w/M_n)
109	32.014	1557	1572	1.01
110	32.167	1485	1494	1.01
111	32.183	1483	1494	1.01
112	32.306	1416	1424	1.01
118	32.198	1474	1483	1.01
124	32.236	1481	1498	1.01
127	32.328	1406	1420	1.01
131	32.239	1451	1459	1.01
G3 dendron	Retention time (min)	M_n (Daltons)	M_w (Daltons)	Polydispersity (M_w/M_n)
75	30.263	2750	2772	1.01
113	30.179	2820	2839	1.01
114	30.253	2753	2769	1.01
115	30.220	2815	2837	1.01
116	30.265	2740	2756	1.01
120	30.339	2677	2694	1.01
128	30.406	2632	2660	1.01
129	30.423	2607	2622	1.01
133	30.302	2712	2731	1.01
134	30.288	2727	2743	1.01
G3 dendrimer	Retention time (min)	M_n (Daltons)	M_w (Daltons)	Polydispersity (M_w/M_n)
68	28.261	6305	6385	1.01
69	28.981	5060	5092	1.01
121	27.872	6131	6217	1.01
136	28.009	6025	5908	1.02

Table 3. GPC results (retention time, M_n, M_w, PDI) of prepared dendritic compounds.

Chapter 4: Feasibility and efficiency of post-modifications of multifunctional dendrimers

4.1 Oxidation from sulfides to sulfones inside the dendritic skeleton

4.1.1 Oxidation under homogeneous conditions

In order to compare the relative reactivities of the same functionalities at different locations inside the dendrimer, the layer-block oligosulfide dendrimers **68** and **69** and the model compound **136** were subjected to oxidation under either homogeneous or heterogeneous reaction conditions. For the homogeneous condition, the reagents used were 35% H_2O_2 in CH_2Cl_2/AcOH (10/1). For the heterogeneous condition, the reagent oxone in CH_2Cl_2 was employed to oxidize the dendrimers.

^{1}H NMR spectroscopy was used to probe the relative reactivity of the sulfide oxidation in the different dendrimers. During oxidation, the sulfide was first converted to the corresponding sulfoxide, and finally to the sulfone. As a result, the chemical shift value of the benzylic proton signals adjacent to the sulfur atom will change according to the oxidation state of the sulfur atom. For sulfide, the benzylic protons appear as a singlet at about δ 3.5–3.6 ppm. When the sulfide is oxidized to the corresponding sulfoxide, the proton signals will become multiplets located at δ 3.7–4.0 ppm due to the chiral sulfoxide environment. When all the sulfoxides are oxidized to the sulfones, the proton signals are normally found as singlets at about δ 4.1–4.3 ppm. Hence, the relative integration values of the regions δ 3.5–3.6, δ 3.7–4.0 and δ 4.1–4.3 can provide information on the extent of the two oxidation processes.

For the model G3 dendrimer **136**, due to the presence of many sulfide moieties within the structure, it was therefore impossible to find out which of those oxidized faster than the others. What we would like to find out were the optimal reaction temperature and reagent concentration under which the reaction proceeded in a conversion rate that was not too fast or too slow for easy monitoring. In the end, it was found that all 21 sulfide functionalities could be oxidized in the presence of 35% H_2O_2 (3.0 equiv. per sulfone moiety) in CH_2Cl_2/AcOH (10/1) to the corresponding G3–$SO_2SO_2SO_2$–dendrimer **138** at 32 °C in a period of 10 h (concentration of G3–SSS–dendrimer = 1.7 mM). As a result, the reaction temperature for all sulfide oxidation reactions was set to 32.0 ± 0.1 °C. The structural identity of the product **138** was proven by ^{1}H NMR spectroscopy and mass spectrometry (Figure 23), in which the molecular ion peak $[M]^+$ was found to have a mass to charge ratio (*m/z*) of 6978.

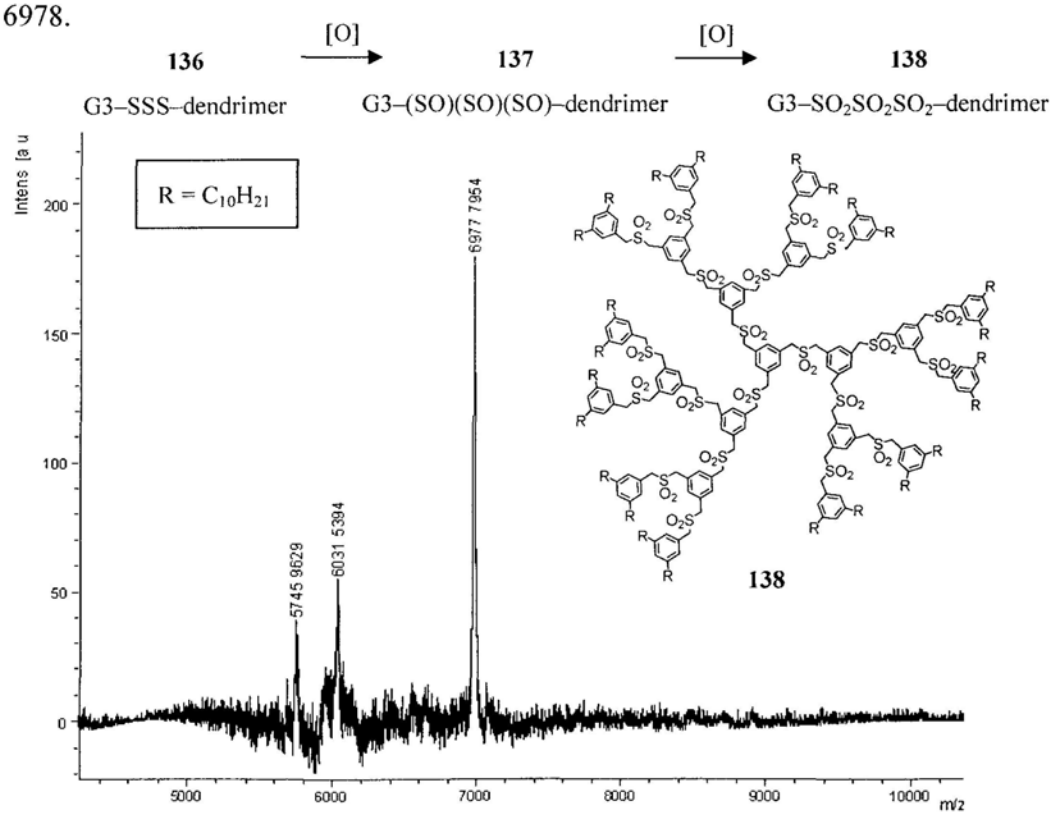

Figure 23. Mass spectrum (MALDI–TOF) of G3–$SO_2SO_2SO_2$–dendrimer **138**.

For the two layer block dendrimers **68** and **69**, the oxidation reactions were conducted under a standardized condition using 9.0 equiv. of 35% H_2O_2 per sulfone moiety and at a dendrimer concentration of 1.7 mM. The progress of the oxidation processes was monitored by taking aliquots from the reaction mixture at specific time intervals for ^1H NMR analyses. From the relative integrations of the proton signal peaks due to benzylic proton adjacent to the sulfide, sulfoxide and sulfone moieties, their ratios in the product mixture were then worked out (Figure 24).

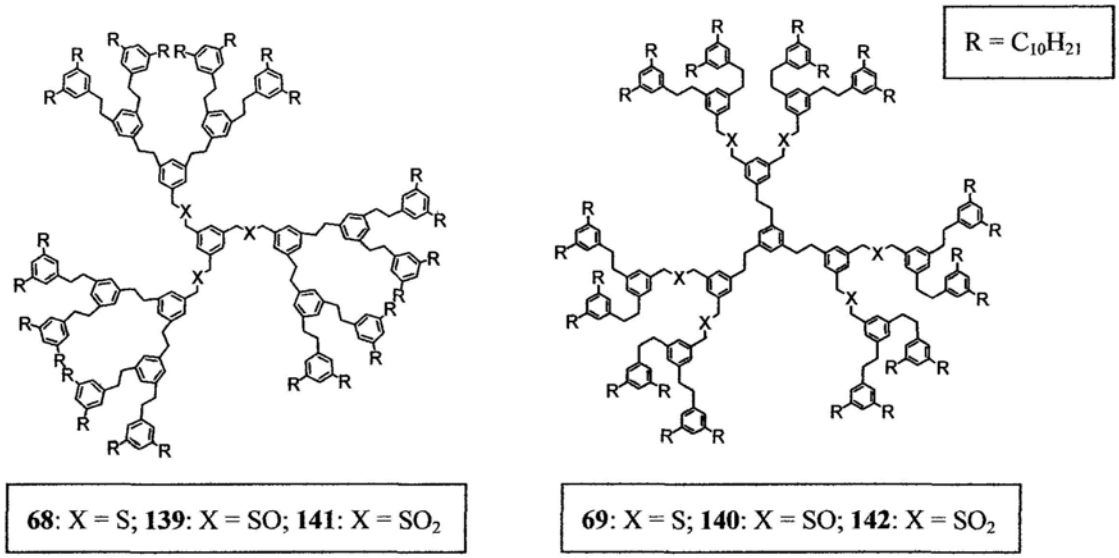

68 (G3–CCS–dendrimer) $\xrightarrow{[O]}$ **139** (G3–CC(SO)–dendrimer) $\xrightarrow{[O]}$ **141** (G3–CCSO$_2$–dendrimer)

69 (G3–CSC–dendrimer) $\xrightarrow{[O]}$ **140**(G3–C(SO)C–dendrimer) $\xrightarrow{[O]}$ **142** (G3–CSO$_2$C–dendrimer)

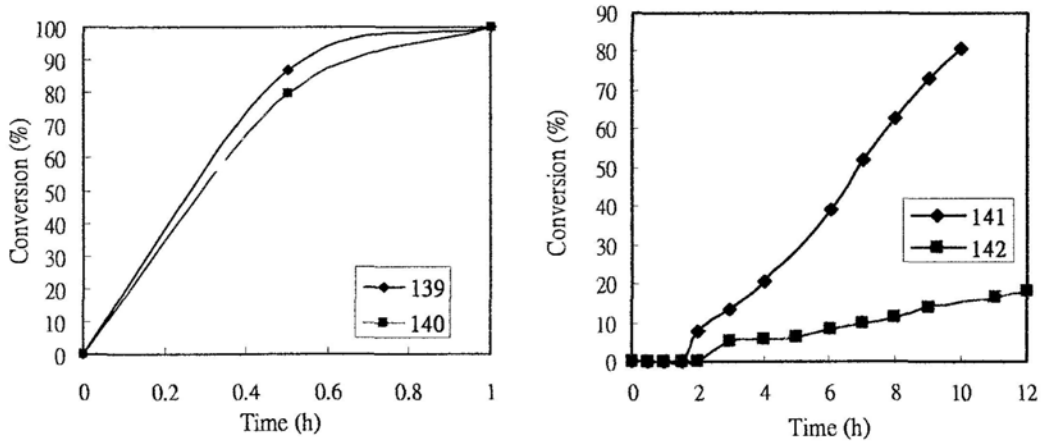

Figure 24. Plots of percentage conversion of a) sulfide to sulfoxide in G3 dendrimers **68** and **69**; b) sulfoxide to sulfone in G3 dendrimers **139** and **140**.

Interestingly, there was little difference in terms of the oxidation rate from the sulfide to the sulfoxide state for these two dendrimers, suggesting that there was little difference in terms of the steric environment between the sulfides in the intermost and in the middle layers. On the other hand, the sulfone functionalities in the G3–CC(SO)–dendrimer **139** were oxidized much quicker than those in the G3–C(SO)C–dendrimer **140**. Hence, after 10 h, about 80% of **139** had already been converted to the corresponding sulfone **141** while the conversion of **140** remained at 16%. The lack of reactivity of the sulfoxides in the intermediate layer was unexpected if one considered all 21 sulfoxide moieties could be transformed into the corresponding 21 sulfone functionalities within 10 h in the case of the G3–SSS–dendrimer **136**. Hence, there are other factors, in addition to steric shielding, that are in operation in this transformation. One possible cause for this anomaly could be due to the difference in microenvironment polarity of the dendrimers. As the sulfoxide functionality is very polar, hence G3–(SO)(SO)(SO)–dendrimer **137** should be much more polar than the other two dendrimers with less number of sulfoxide groups. As the oxidant H_2O_2 is also polar, an increase in the dendrimer polarity would enhance the diffusion of polar reagents into the interior of the dendrimer and thus compound **136** could be oxidized at a faster rate. Having said that, it was still unclear to us as to why the inner most sulfoxides in G3–CC(SO)–dendrimer **139** oxidized much faster than those in the G3–C(SO)C–dendrimer **140**.

As mentioned previously, about 80% sulfoxide moieties in dendrimer **139** were oxidized to sulfone moieties in 10 hours, and complete oxidation could be achieved in 24 hours. However, only 15% of sulfoxide groups in dendrimer **140** were converted to sulfone groups in 10 hours and the oxidation was not completed even after 48 hours. Hence, the reaction mixture was warmed at 40 °C for 12 h to drive the

oxidation to completion.

The structure of the oligosulfone dendrimers **141** and **142** were confirmed by ^{1}H and ^{13}C NMR and mass spectroscopy, and their purity by gel permeation chromatography. For both compounds, the most notable changes in their ^{1}H NMR spectra were the downfield shift of the benzylic proton signals adjacent to the sulfone moiety (Figure 25). They appeared as two board singlets located at about δ 4.1–4.2 ppm. In the ^{13}C NMR spectra of G3–CSO_2C–dendrimer **142**, the signals of benzylic carbons adjacent to the sulfone group were found at δ 57–60. However, those signals of the G3–$CCSO_2$–dendrimer **141** were too weak to be detected.

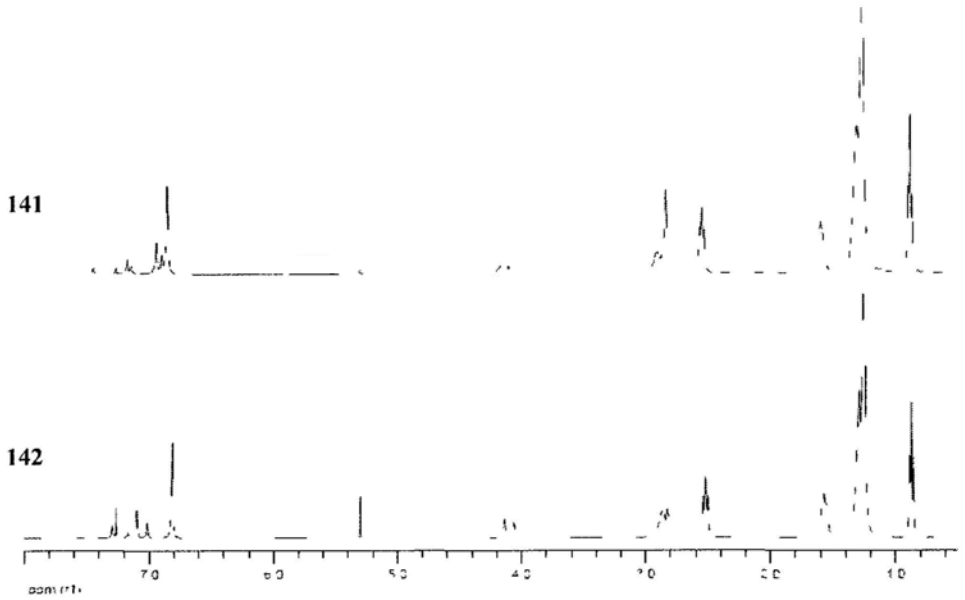

Figure 25. Stacked ^{1}H NMR spectra (400 MHz, $CDCl_3$) of G3–$CCSO_2$–dendrimer **141** and G3–CSO_2C–dendrimer **142**.

The sulfone dendrimers **141** and **142** was also characterized by mass spectrometry. Hence, the molecular ion peak for compound **141** and **142** was found at 5824.2, and 6016.6 ,respectively.

The purity of the G3 oligosulfone dendrimers **141** and **142** was assessed by GPC (Figure 26). The GPC chromatograms showed a major peak with a PDI of 1.01 and a retention time (~28.3 min) similar to that of their precursor oligosulfide G3 dendrimers **68** and **69** (~28.3 and 29.0 min), indicating both the oligosulfides and oligosulfones had a similar hydrodynamic radius.

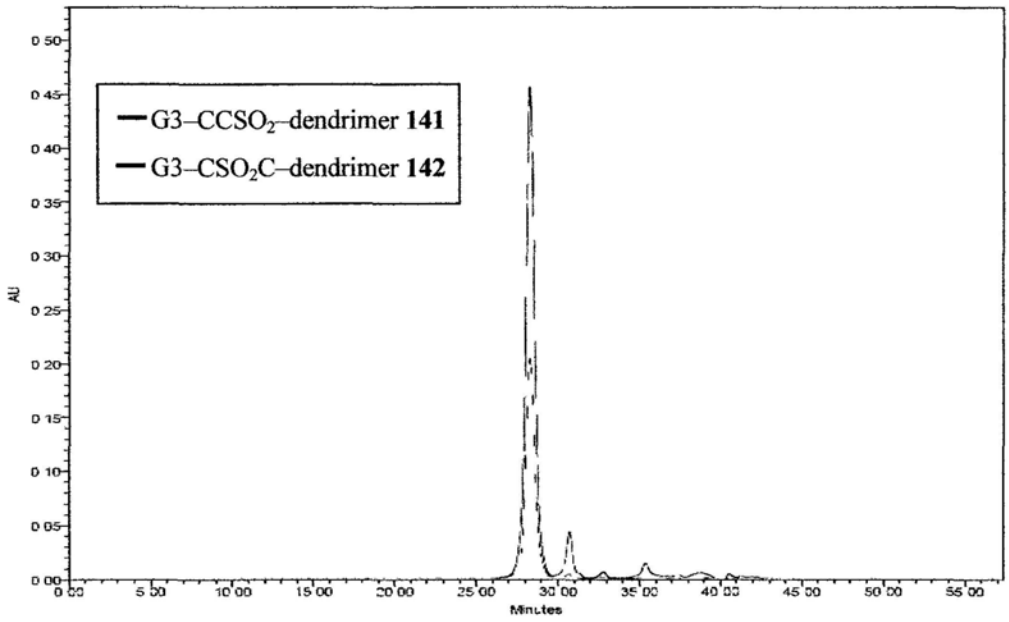

Figure 26. Stacked GPC chromatograms for G3 dendrimers **141** and **142**.

4.1.2. Oxidation under heterogeneous conditions

When the oxidation reactions were switched to heterogeneous conditions using oxone powder (3 equiv. per sulfide) in CH_2Cl_2 at 32.0 ± 0.1 °C, none of the sulfide functionalities inside the G3–CCS–dendrimers could be oxidized to the corresponding sulfoxide after 5 days as determined by ^1H NMR spectroscopy. It appeared that phase separation between the dendrimer and the reagent greatly hindered chemical transformations within the dendrimers. As a result, the heterogeneous oxidation method was not applied to other G3 dendrimers.

4.2 Backbone rearrangements within dendrimers

Once the syntheses of G3–$CCSO_2$–dendrimer **141** and G3–CSO_2C–dendrimer **142** were secured by the interior functional group conversion method, they were then subjected to Ramberg-Bäcklund (RB) rearrangement using Chan's modified conditions (KOH/Al_2O_3, CBr_2F_2) in THF/*t*-BuOH at –45 °C.[87] Based on previous studies,[88] dendritic backbone rearrangement of dibenzyl sulfones was a facile process and completed in 10 min at this temperature. In addition, prolonging the reaction time did not increase the product yield, while raising the reaction temperature to 0–25 °C led to a reduction of the product yield due to decomposition of the stilbene system in the presence of the strong base KOH at higher temperature. Hence, excess amount of powdered alumina-supported KOH (~200 mg; containing about 70 mg of KOH) was added a solution (2.5 mM) of the above layer block dendrimers in CBr_2F_2/THF/*t*-BuOH (1/1/1) at –45 °C for 10 min. For the G3–$CCSO_2$–dendrimer **141**, the products found were a mixture of the starting material (*i.e.* no RB rearrangement occurred) and a compound **143** that was formed by a single RB rearrangement process. Figure 27 showed the mass spectrum of the crude product obtained from the RB reaction of dendrimer **141**, the peak with mass to charge ratio (*m/z*) at 5796.7 was due to the single RB rearrangement product [**143** + K]$^+$, while the peak located at 5865.5 was due to the starting tris(sulfone) [**141** + K]$^+$.

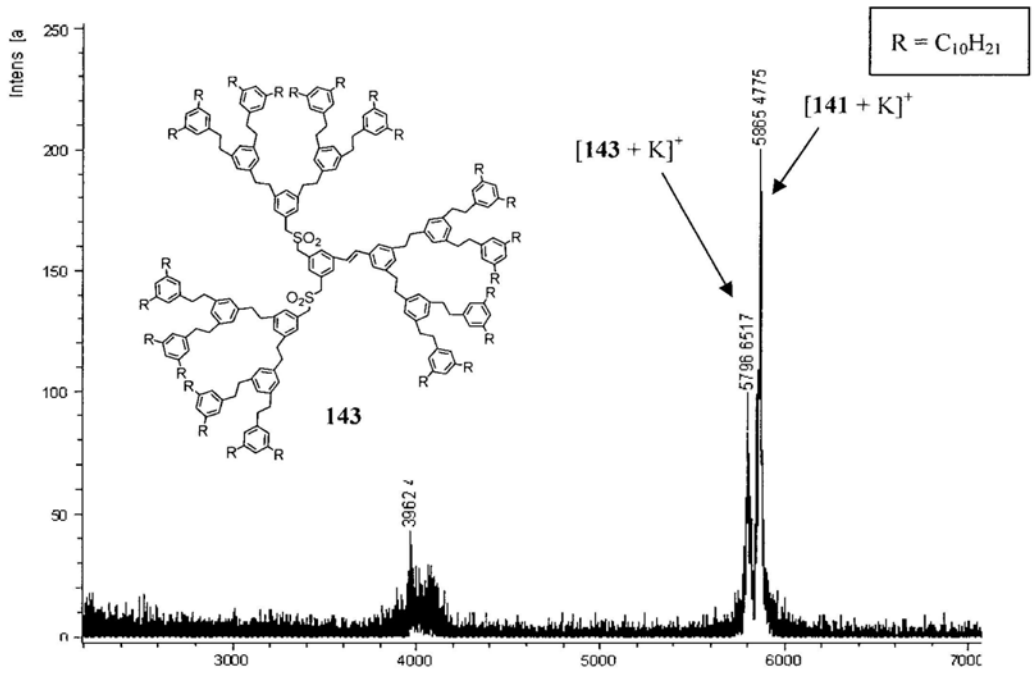

Figure 27. Mass spectrum of the crude product after RB reaction of G3–$CCSO_2$–dendrimer **141**.

For the G3–CSO_2C–dendrimer **142,** there were six sulfone functionalities inside the dendrimer skeleton. After the reaction, the crude product was subjected to mass spectral analysis (Figure 29). Two major peaks were found in the spectrum. The first was a peak with a *m/z* ratio of 5752.6 due to a dendrimer **144** which possessed four newly formed double bonds after RB reactions. The second was a fragmentation peak (*m/z* 4896.4) coming from a dendrimer **145** with three double bonds.

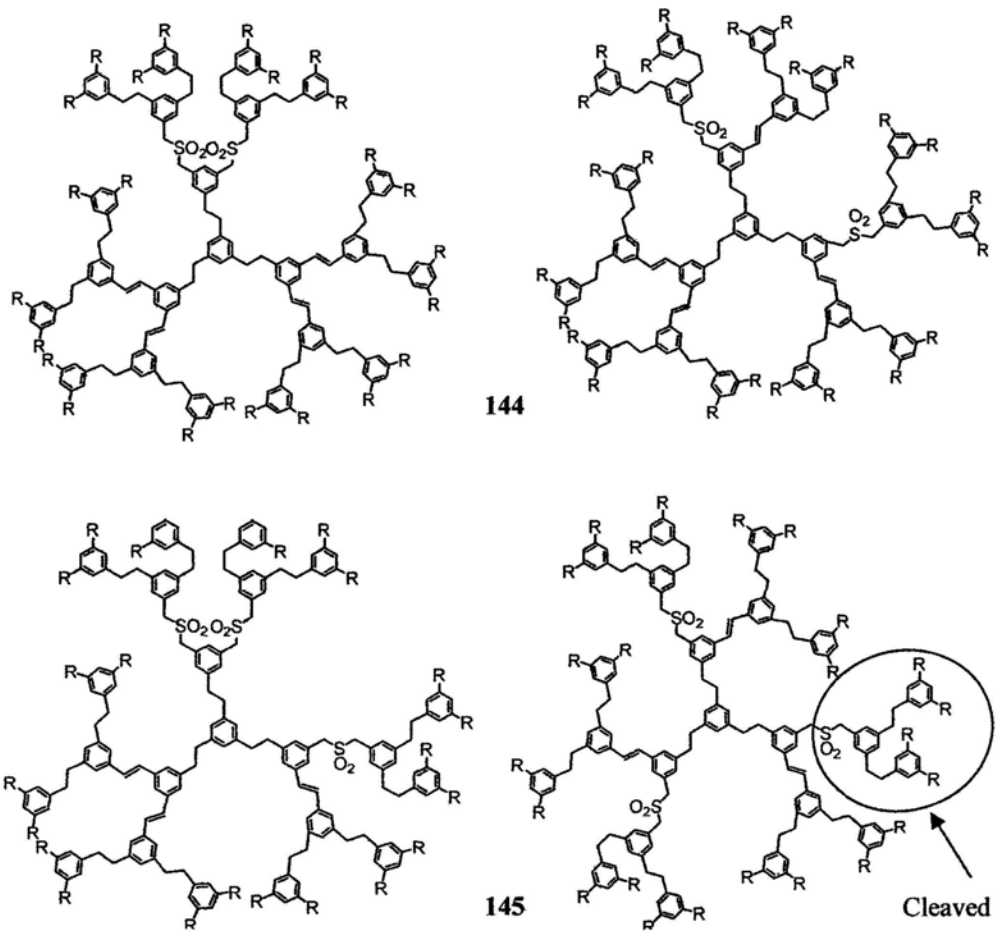

Figure 28. Structure of G3–dendrimr **144** and **145**.

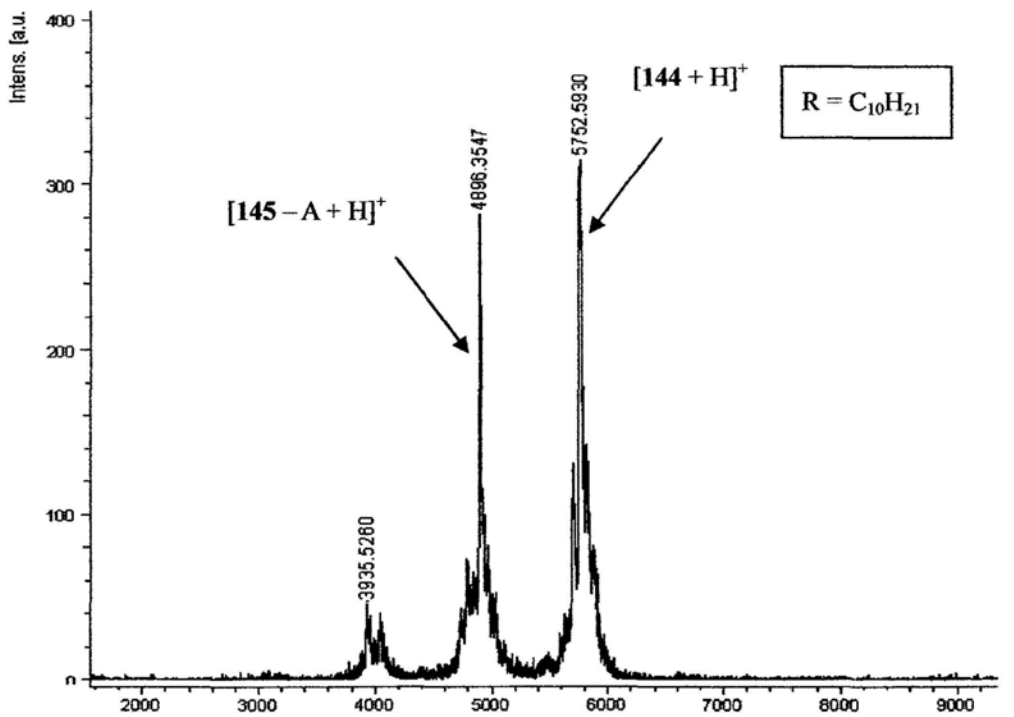

Figure 29. Mass spectrum of the crude product after RB reaction of G3–CSO_2C–dendrimer **142**.

Comparing the Ramberg Bäcklund rearrangement results of the two dendrimers, it was found that rearrangements of the dendritic skeleton to form new double bonds occurred more readily on the middle dendritic layer than on the innermost layer. Most of the innermost sulfone moieties remained unreacted in the G3–$CCSO_2$–dendrimer **141**, or at most only one sulfone could undergo RB reaction. On the other hand, at least three sulfone moieties in the same dendrimer molecule rearranged successfully to yield the corresponding double bonds for G3–CSO_2C–dendrimer **142**. In this case it could be clearly seen that steric effect played a significant retarding role in reactions that are heterogeneous in nature, as the solid alumina particles were too large to penetrate into the dendritic interior to initiate the reaction. This problem became more prominent in the case of the G3–$CCSO_2$–dendrimer **141**.

4.3 Summary

Under homogeneous reaction conditions, G3–CCS–dendrimer **68** and G3–CSC–dendrimer **69** showed similar oxidation rate from the sulfide to the sulfoxide state. However, the sulfoxide functionalities in the G3–CC(SO)–dendrimer **139** were oxidized much faster than those in the G3–C(SO)C–dendrimer **140**. Besides, it was found that oxidation reactions performed under heterogeneous conditions were not favored. When G3–$CCSO_2$–dendrimer **141** and G3–CSO_2C–dendrimer **142** were subjected to Ramberg Bäcklund rearrangements, the rearrangement efficiency was greatly affected by steric shielding effect. Most of the 'more shielded' innermost sulfone moieties in dendrimer **141** failed to react while at least three 'less shielded' middle layer sulfones in dendrimer **142** underwent rearrangements.

Chapter 5: Conclusions

Two layer-block G3–CCS–dendrimer **68** and G3–CSC–dendrimer **69** with organosulfide moieties embedded in the innermost and middle dendritic layers, respectively, were synthesized and characterized. A third target G3–SCC–dendrimer **70**, with organosulfide moieties located in the outermost dendritic layer, could not be synthesized despite many attempts. These compounds were prepared in order to probe the feasibility of two new dendrimer synthesis methodologies, namely, dendrimer interior functional group conversion and dendrimer backbone rearrangement.

The inability to prepare G3–SCC–dendrimer **70** already suggested that these dendritic molecules had a very compact architecture and hence the accessibility of the dendrimer interior by external reagents was subjected to severe steric inhibition. Hence for reactions that were heterogeneous in nature, the synthetic efficiencies of both the interior functional group conversion and dendrimer backbone rearrangement were low. This was exemplified in the case of the oxone-mediated interior functional group oxidation, in which the organosulfide moieties inside the inner dendritic shell of G3–CCS–dendrimer **68** were inert to the reaction conditions. In contrast, an ordinary small organosulfide molecule could undergo oxone-promoted oxidation to give the corresponding organosulfone with ease. The failure to have all the sulfone functionalities inside a dendrimer undergone a heterogeneous RB rearrangement in the cases of G3–$CCSO_2$–dendrimer **141** and G3–CSO_2C–dendrimer **142** provided further examples on the steric shielding effect on functional group reactivity. More interestingly, there was an observed difference between the dendrimer backbone

rearrangement efficiency between the 'more shielded' innermost sulfone moieties in G3–$CCSO_2$–dendrimer **141** and the 'less shielded' middle layer sulfone functionalities in G3–CSO_2C–dendrimer **142**. As it turned out, most of the sulfones in dendrimer **141** failed to react, and at most only one could undergo the rearrangement to give the mono-ene–bis(sulfone) product **143**. On the other hand, at least three or four of the six sulfones reacted to give either the triene–tris(sulfone) **145** or tetraene–bis(sulfone) compounds **144**. More importantly, this was the first time in the literature where conclusive mass spectral evidence was obtained to unveil the detailed outcome of such complex reactions.

On the other hand, the picture appeared to be very complex for reactions that were conducted under homogeneous conditions. One anomaly was that the innermost sulfoxides in G3–CC(SO)–dendrimer **139** were found to possess higher reactivity towards homogeneous H_2O_2-mediated oxidation as compared to the intermediate layer sulfoxides in G3–C(SO)C–dendrimer **140** under identical reaction conditions. Perhaps more intriguingly, G3–SSS–dendrimer **136**, despite having three innermost, six middle and twelve outermost sulfide moieties, could be completely and smoothly oxidized to the corresponding G3–$SO_2SO_2SO_2$–dendrimer **138** in a comparatively shorter period of time. We have no obvious explanation for the observed phenomena, but tempted to suggest that the polarity of the microenvironment, amongst other factors such as steric shielding, may contribute to the observed anomaly. Previously it had been shown by Kaifer[89] and Meijer[90] that the strength of hydrogen bond bindings could be significantly altered by the microenvironment of the dendrons. In this study we also found that in some occasions the chemical reactivity of the functionalities inside a dendritic molecule could not be simply rationalized by steric inhibition, and there were findings that the microenvironment polarity of the

dendrimer itself could also play an important role in dictating the efficiency of chemical transformations.

In summary, dendrimer interior functional group conversion and dendrimer backbone rearrangement are new and novel synthetic strategies for the preparation of new dendritic molecules. However, steric inhibition at the interior of the dendrimer, plus the difficulties in ensuring complete multiple functional group transformations are two hurdles that needed to be further addressed. In addition, one should also examine the role of microenvironment polarity through further studies in the future.

Chapter 6: Experimental Procedures

6.1 General Information

All reagents were purchased from commercial suppliers (Acros or Aldrich) and used without further purification. All reactions were performed under N_2 atmosphere unless otherwise noted. All glasswares were dried in an oven prior to use. Tetrahydrofuran (THF) was freshly distilled from sodium benzophenone ketyl before use. Dichloromethane and acetonitrile were distilled from calcium hydride prior to use. Silica gel for flash chromatography is Merck 60 (70-230 mesh) silica gel. Thin layer chromatography (TLC) was performed on silica gel sheets 60 F_{254} purchased from E. Merck.

All nuclear magnetic resonance (NMR) spectra were recorded either on a Bruker DPX spectrometer at 300 MHz (^{1}H) and 75.5 MHz (^{13}C) or a Bruker Advance II NMR spectrometer at 400 MHz (^{1}H) and 100 MHz (^{13}C). Chloroform-*d* (dried over molecular sieve 4Å) was used as solvent unless otherwise stated. All chemical shifts are reported in ppm (δ) and coupling constants (*J*) in Hz. Melting points were measured on an Electrothermal IA9000 digital melting point apparatus and are uncorrected. Mass spectra were obtained by electrospray ionization (ESI) or fast atom bombardment (FAB) on a Finnigan Mat 95XL mass spectrometer or by matrix assisted laser desorption/ ionization time of flight mass spectrometry (MALDI–TOF) on a Bruker Daltonics autoflex III TOF Analyzer with high resolution reflectron time-of-flight (refTOF) mass spectrometer. The reported molecular mass (*m/z*) is the most abundant monoisotopic mass unless otherwise specified. Size exclusion chromatography (SEC) analyses was performed using Waters® Styragel columns

(HR1, HR2, HR3 and HR4 7.8 x 300 mm in serial) at 40°C using THF as eluent (flow rate = 1.0 mL/min) on a Waters® HPLC 515 pump equipped with a Waters® 2489 UV/Vis detector. Elemental analysis was carried out at MEDAC Ltd, Science Center, Cooper's Hill Lane, Englefield Green, Egham, Surrey TW20 0LB, United Kingdom.

6.2 Synthesis of dendrons and dendrimers

3,5-Diiodobenzoic acid.[87]

3,5-Diaminobenzoic acid (9.98 g, 66 mmol) was dissolved in HCl solution (250 mL, 2.4 M) and cooled to –10°C for 15 min. A solution of sodium nitrite (9.83 g, 142 mmol) in water (50 mL) was added slowly and stirred for 5 min. After that, a solution of potassium iodide (23.71 g, 143 mmol) in water (50 mL) was added. The mixture was stirred at 0°C for a further 10 min and then heated to 90°C for 20 min. The reaction mixture was allowed to cool to 20°C and sodium bisulfite (~2 g) was added to destroy the excess iodine. The remaining brown solid was filtered and then redissolved in 90% aqueous ethanol (300 mL). Decolorizing charcoal was added and the solution was brought to boiling and filtered. The filtrate was concentrated under reduced pressure and cold water (250 mL) was added to precipitate the product. After the solution was cooled in ice bath for 10 min, it was filtered to give the product as a brown solid (15.68 g, 64%). M.p: 231–233 °C (lit.[88]: 233 °C). R_f: 0.24 (EtOAc); ^{1}H NMR (300Mz; DMSO-d_6; COOH not observed): 8.19 (d, J = 1.5 Hz, 2 H, Ar*H*), 8.35 (t, J = 1.5 Hz, 1 H, Ar*H*); ^{13}C NMR (75 MHz; DMSO-d_6): 96.1, 134.3, 137.0, 148.2, 164.7.

Methyl 3,5-diiodobenzoate (71).[87]

3,5-Diiodobenzoic acid (30.62 g, 82 mmol) was dissolved in methanol (600 mL). Concentrated sulfuric acid (2 mL) was then added slowly and the reaction mixture was heated to 65 °C for 18 h. The excess solvent was then evaporated and the resulting solution was neutralized by saturated Na_2CO_3 solution. The product was then extracted with CH_2Cl_2 (150 mL × 3) and the combined organic layers was dried ($MgSO_4$), filtered and concentrated *in vacuo*. The residue was purified by flash

chromatography on silica gel (eluent: hexane/EtOAc = 10/1) to give the ester (22.89 g, 72%) as a white solid. M.p: 94–97 °C (lit.[87]: 94 °C). R_f: 0.47 (hexane/EtOAc = 50/1); ^{1}H NMR (300 MHz): 3.92 (s, 3 H, CO_2CH_3), 8.23 (t, J = 1.7 Hz, 1 H, Ar*H*), 8.32 (d, J = 1.5 Hz, 2 H, Ar*H*), ^{13}C NMR (75 MHz): 52.8, 94.5, 133.2, 137.7, 149.2, 164.1.

Methyl 3,5-di-(dec-1-ynyl)benzoate (72).

A mixture of methyl 3,5-diiodobenzoate **71** (15.00 g, 39 mmol), 1-decyne (40.0 mL, 222 mmol), bis(triphenylphosphine)palladium(II) dichloride (2.74 g, 3.9 mmol), copper(I) iodide (0.38 g, 2.0 mmol), and triethylamine (25 mL) in dry THF (200 mL) was stirred at 20 °C for 72 h. The mixture was filtered through a short pad of silica gel and washed with ethyl acetate (200 mL). The solvent was concentrated *in vacuo* and the residue was purified by column chromatography on silica gel (eluent: hexane/EtOAc = 200/1 gradient to 80/1) to give the product (15.14 g, 96%) as a brown oil. R_f: 0.41 (hexane/EtOAc = 40/1); ^{1}H NMR (300 MHz): 0.89 (t, J = 6.6 Hz, 6 H, CH_2CH_3), 1.18–1.53 (m, 20 H), 1.53–1.68 (m, 4 H), 2.39 (t, J = 7.1 Hz, 4 H, $C{\equiv}CCH_2$), 3.91 (s, 3 H, CO_2CH_3), 7.57 (t, J = 1.5 Hz, 1 H, Ar*H*), 7.93 (d, J = 1.8 Hz, 2 H, Ar*H*); ^{13}C NMR (75 MHz): 14.0, 19.3, 22.7, 28.7, 28.9, 29.2, 29.2, 31.9, 52.0, 79.2, 91.7, 124.7, 130.3, 131.4, 138.3, 165.6; MS (ESI): *m/z* 431 [$(M + Na)^+$, 100%]. HRMS (ESI): calcd for $(M + Na)^+$, 431.2921; found, 431.2931. Anal. Calcd (%) for $C_{28}H_{40}O_2$: C, 82.30; H, 9.87. Found: C, 82.64; H, 10.09.

Methyl 3,5-di-(*n*-decyl)benzoate (73).

A mixture of methyl 3,5-di-(dec-1-ynyl)benzoate **72** (16.79 g, 41 mmol) and 10% Pd/C (1.7 g) in THF/MeOH (300 mL) was stirred under H_2 at atmospheric pressure at 20 °C. After 72 h, the mixture was filtered through a pad of Celite. The filtrate was concentrated *in vacuo* and the residue was purified by column chromatography on

silica gel (eluent: hexane/EtOAc = 80/1) to give compound (14.51 g, 85%) as a pale yellow oil. R_f: 0.21 (hexane/EtOAc = 40/1); ^{1}H NMR (300 MHz): 0.88 (t, J = 6.6 Hz, 6 H, CH_2CH_3), 1.14–1.38 (m, 28 H), 1.54–1.68 (m, 4 H), 2.61 (t, J = 7.8 Hz, 4 H, $ArCH_2$), 3.91 (s, 3 H, CO_2CH_3), 7.18 (s, 1 H, Ar*H*), 7.67 (s, 2 H, Ar*H*); ^{13}C NMR (75 MHz): 14.2, 22.8, 29.4, 29.5, 29.6, 29.7, 29.7, 31.6, 32.0, 35.9, 52.0, 127.0, 130.1, 133.4, 143.1, 167.6; MS (ESI): *m/z* 439 [(M + Na)$^+$, 100%]. HRMS (ESI): calcd for (M + Na)$^+$, 439.3547; found, 439.3545. Anal. Calcd (%) for $C_{28}H_{48}O_2$: C, 80.71; H, 11.61. Found: C, 80.93; H, 11.91.

G1–CH_2OH (74).

To a stirred suspension of $LiAlH_4$ (1.53 g, 40 mmol) in dried THF (50 mL) was added dropwise a solution of methyl 3,5-di-(*n*-decyl)benzoate **73** (16.88 g, 41 mmol) in THF (100 mL) at 0°C. The mixture was allowed to stir at 20 °C and the reaction progress was monitored by TLC until all the starting material disappeared (3–5 h). The excess hydride was then quenched by the addition of ice water (5 mL). The product was extracted with ethyl acetate, saturated NaCl solution, and dried ($MgSO_4$). The organic solvent was filtered and concentrated *in vacuo*. The residue was purified by flash chromatography on silica gel (eluent: hexane/EtOAc = 50/1 gradient to 30/1) to give the target compound as a yellow oil (14.68 g, 93%). R_f: 0.21 (hexane/EtOAc = 10/1); ^{1}H NMR (300 MHz): 0.88 (t, J = 6.8 Hz, 6 H, CH_2CH_3), 1.18–1.40 (m, 28 H), 1.52–1.67 (m, 5 H, O*H* and CH_2), 2.57 (t, J = 7.8 Hz, 4 H, $ArCH_2$), 4.65 (d, J = 6 Hz, 2 H, CH_2OH), 6.93 (s, 1 H, Ar*H*), 7.00 (s, 2 H, Ar*H*); ^{13}C NMR (75 MHz): 14.2, 22.8, 29.5, 29.6, 29.7, 29.8, 29.8, 31.7, 32.0, 36.1, 65.5, 124.5, 128.0, 140.8, 143.3; MS (ESI): *m/z* 411 [(M + Na)$^+$, 100%]. HRMS (ESI): calcd for (M + Na)$^+$, 411.3597; found, 411.3600. Anal. Calcd (%) for $C_{27}H_{48}O$: C, 83.44; H, 12.45. Found: C, 83.12; H, 12.49.

General Procedure for the synthesis of dendritic aldehydes Gn–CHO from the dendritic benzyl alcohols Gn–CH_2OH

To a stirred solution of Gn–CH_2OH in CH_2Cl_2 at 0 °C was added slowly a mixture of finely ground PCC/silica gel in portions. After that, the reaction mixture was allowed to stir at 20 °C for 2–6 h. The completeness of the reaction was monitored by TLC. When the reaction was finished, the reaction mixture was filtered by a short pad of silica gel. The filtrate was then concentrated and purified by column chromatography.

G1–CHO (108). Starting from G1–CH_2OH **74** (5.31 g, 14 mmol), PCC (4.26 g, 27 mmol) in CH_2Cl_2 (30 mL), compound G1–CHO (4.56 g, 86%) was obtained as a colorless oil after column chromatography (eluent: hexane/EtOAc = 100/1 gradient to 50/1) and became a white solid when standing under vacuum. M.p: 31–36°C. R_f: 0.21 (hexane/EtOAc = 50/1); ^{1}H NMR (300 MHz; CD_2Cl_2): 0.88 (t, J = 6.8 Hz, 6 H, CH_3), 1.19–1.39 (m, 28 H), 1.56–1.69 (m, 4 H), 2.65 (t, J = 7.7 Hz, 4 H, ArCH_2), 7.29 (s, 1 H, Ar*H*), 7.50 (s, 2 H, Ar*H*), 9.95 (s, 1 H, CHO); ^{13}C NMR (75 MHz): 14.2, 22.8, 29.4, 29.5, 29.6, 29.7, 29.7, 31.5, 32.0, 35.7, 127.3, 135.1, 136.7, 143.9, 193.0; MS (ESI): *m/z* 409 [(M + Na)$^+$, 100%]. HRMS (ESI): calcd for (M + Na)$^+$, 409.3441; found, 409.3450.

G2–C–CHO (112). Starting from G2–C–CH_2OH **111** (2.84 g, 3.2 mmol), PCC (1.00 g, 6.4 mmol) in CH_2Cl_2 (15 mL), compound G2–C–CHO (2.30 g, 81%) was obtained as a colorless oil after column chromatography (eluent: hexane/EtOAc = 100/1). R_f: 0.67 (hexane/EtOAc = 30/1); ^{1}H NMR (300 MHz): 0.88 (t, J = 6.8 Hz, 12 H, CH_3), 1.18–1.40 (m, 56 H), 1.50–1.66 (m, 8 H), 2.54 (t, J = 7.8 Hz, 8 H, ArCH_2), 2.78–3.00 (m, 8 H, ArCH_2CH_2Ar), 6.81 (s, 4 H, Ar*H*), 6.85 (s, *2* H, Ar*H*), 7.21 (s, 1 H,

Ar*H*), 7.54 (s, 2 H, Ar*H*), 9.95 (s, 1 H, C*H*O); ^{13}C NMR (75 MHz; one signal was not resolvable due to signal overlapping): 14.2, 22.8, 29.5, 29.6, 29.7, 29.8, 29.8, 31.8, 32.1, 36.1, 37.9, 38.0, 126.0, 126.5, 127.5, 135.3, 136.8, 141.0, 143.0, 192.4; MS (MALDI–TOF): calcd for $(M + Na)^+$, 897.7822; found, 897.7833. Anal. Calcd (%) for $C_{63}H_{102}O$: C, 86.43; H, 11.74. Found: C, 86.38; H, 11.57.

General Procedure for the Horner–Wadsworth–Emmons reactions

Sodium hydride was added to a stirred solution of the phosphonates and Gn–CHO in THF at 20 °C. The reaction mixture was refluxed for 18 h. After hydrolysis with water, the mixture was extracted with CH_2Cl_2. The combined organic layers was then washed with saturated NaCl solution, dried ($MgSO_4$), filtered and concentrated *in vacuo*. The residue was purified by flash chromatography on silica gel to give the alkene.

G3–SC=C–CH(OMe)$_2$ (75). Starting from G2–S–CHO **127** (2.47 g, 2.6 mmol), bisphosphonate **107** (0.60 g, 1.3 mmol) and 60% sodium hydride (0.39 g, 9.8 mmol) in THF (10 mL), compound G3–SCC=CH(OMe)$_2$ **75** (1.39 g, 52 %) was obtained as a yellow liquid after column chromatography (eluent: hexane/EtOAc = 50/1). R_f: 0.13 (hexane/EtOAc = 50/1); ^{1}H NMR (300 MHz): 0.86 (t, J = 6.6 Hz, 24 H, CH_3), 1.14–1.44 (m, 112 H), 1.51–1.68 (m, 16 H), 2.56 (t, J = 7.7 Hz, 16 H, ArCH_2), 3.39 (s, 6 H, OCH_3), 3.60 (s, 8 H, CH_2S), 3.63 (s, 8 H, CH_2S), 5.46 (s, 1 H, OC*H*), 6.88 (s, 4 H, Ar*H*), 6.91 (s, 8 H, Ar*H*), 7.13 (s, 2 H, Ar*H*), 7.15 (s, 4 H, Ar*CHCH*Ar), 7.34 (s, 4 H, Ar*H*), 7.53 (s, 2 H, Ar*H*), 7.60 (s, 1 H, Ar*H*); ^{13}C NMR (75 MHz; one signal was not resolvable due to signal overlapping): 14.3, 22.8, 29.5, 29.6, 29.7, 29.8, 31.7, 32.0, 35.7, 36.0, 36.0, 52.7, 102.8, 124.3, 124.9, 126.0, 126.6, 127.5, 128.7, 129.0. 129.3,

137.7, 137.7, 137.8, 139.1, 139.1, 143.2; HRMS (MALDI–TOF): *m/z* calcd for $(M + Na)^+$, 2045.5632; found, 2045.5632. Anal. Calcd (%) for $C_{137}H_{216}O_2S_4$: C, 81.32; H, 10.76. Found: C, 80.92; H, 10.50.

G2–C=C–OTHP (109). Starting from G1–CHO **108** (7.73 g, 20 mmol), bisphosphonate **104** (4.92 g, 10 mmol) and 60% sodium hydride (2.4 g, 60 mmol) in THF (60 mL), compound G2–C=C–OTHP **109** (7.09 g, 74%) was obtained as a yellow liquid after column chromatography (eluent: Hexane/EtOAc = 80/1 gradient to 50/1). R_f: 0.24 (hexane/EtOAc = 30/1); ^{1}H NMR (300 MHz): 0.88 (t, J = 6.6 Hz, 12 H, CH_3), 1.15–1.43 (m, 56 H), 1.56–1.98 (m, 14 H), 2.60 (t, J = 7.7 Hz, 8 H, $ArCH_2CH_2$), 3.53–3.65 (m, 1 H, OCH_ACH_B), 3.90–4.03 (m, 1 H, OCH_ACH_B), 4.55 (d, J = 12 Hz, 1 H, ArCHHO), 4.76 (t, J = 3.5 Hz, 1 H, OCHO), 4.82 (d, J = 12 Hz, 1 H, ArCHHO), 6.92 (s, 2 H, ArH), 7.13 (s, 4 H, CH=CH), 7.17 (s, 4 H, ArH), 7.41 (s, 2 H, ArH), 7.58 (s, 1 H, ArH); ^{13}C NMR (75 MHz): 14.3, 19.5, 22.8, 25.6, 29.5, 29.6, 29.7, 29.8, 29.8, 30.7, 31.7, 32.1, 36.1, 62.1, 68.8, 97.7, 123.8, 124.2, 125.2, 127.9 (C=), 128.3, 129.6 (C=), 137.2, 138.1, 139.0, 143.2; HRMS (MALDI-TOF): *m/z* calcd for $(M + Na)^+$, 979.8241; found, 979.8289. Anal. Calcd (%) for $C_{68}H_{108}O_2$: C, 85.29; H, 11.37. Found: C, 85.23; H, 11.22.

G3–CC=C–OTHP (113). Starting from G2–C–CHO **112** (2.30 g, 2.6 mmol), bisphosphonate **104** (0.67 g, 1.4 mmol) and 60% sodium hydride (0.23 g, 5.9 mmol) in THF (10 mL), compound G3–CC=C–OTHP (1.53 g, 60%) was obtained as a pale yellow liquid after column chromatography (eluent: hexane/EtOAc = 50/1). R_f: 0.45 (hexane/EtOAc = 25/1); ^{1}H NMR (300 MHz): 0.90 (t, J = 6.6 Hz, 24 H, CH_3), 1.12–1.43 (m, 112 H), 1.47–2.10 (m, 22 H), 2.59 (t, J = 7.7 Hz, 16 H, $ArCH_2$), 2.79–3.02 (m, 16 H, $ArCH_2CH_2Ar$), 3.55–3.67 (m, 1 H, OCHH), 3.93–4.05 (m, 1 H,

OCH*H*), 4.59 (d, *J* = 12.3 Hz, 1 H, ArC*H*HO), 4.80 (t, *J* = 3.5 Hz, 1 H, OC*H*O), 4.87 (d, *J* = 12 Hz, 1 H, ArCH*H*O), 6.89 (s, 12 H, Ar*H*), 6.97 (s, 2 H, Ar*H*), 7.12 (d, *J*= 16.5 Hz, 2 H, C=C*H*), 7.19 (d, *J* = 16.5 Hz, 2 H, C*H*=C) 7.25 (s, 4 H, Ar*H*), 7.44 (s, 2 H, Ar*H*), 7.61 (s, 1 H, Ar*H*); ^{13}C NMR (75 MHz): 14.3, 19.5, 22.9, 25.7, 29.5, 29.7, 29.7, 29.8, 29.8, 30.8, 31.8, 32.1, 36.2, 38.3, 38.4, 62.3, 68.9, 97.9, 123.9, 124.5, 125.3, 126.0, 126.4, 128.3, 128.5, 129.5, 137.4, 138.1, 139.1, 141.8, 142.6, 143.1; HRMS (MALDI–TOF): *m/z* calcd for $(M + Na)^+$, 1957.7039; found, 1957.7106. Anal. Calcd (%) for $C_{140}H_{220}O_2$: C, 86.89; H, 11.46. Found: C, 87.24; H, 11.55.

G3–CSC=C–dendrimer (121). Starting from G3–CS–CHO **120** (1.42 g, 0.7 mmol), triphosphonate **102** (0.13 g, 0.2 mmol), 60% sodium hydride (0.02 g, 0.5 mmol) in THF (3 mL), the target G3–CSC=C–dendrimer **121** was obtained as a colorless liquid (0.56 g, 39%) after purification by column chromatography (eluent: hexane/ CH_2Cl_2 = 7/1 gradient to 4/1). R_f: 0.24 (hexane/CH_2Cl_2 = 7/1) ^{1}H NMR (300 MHz): 0.91 (t, *J* = 6.6 Hz, 72 H, C*H*$_3$), 1.19–1.43 (m, 336 H), 1.49–1.69 (m, 48 H), 2.56 (t, *J* = 7.7 Hz, 48 H, ArC*H*$_2$), 2.74–2.97 (m, 48 H, ArC*H*$_2$C*H*$_2$Ar), 3.66 (s, 12 H, C*H*$_2$S), 3.68 (s, 12 H, C*H*$_2$S), 6.85 (s, 36 H, Ar*H*), 6.94 (s, 6 H, Ar*H*), 7.05 (s, 12 H, Ar*H*), 7.17 (s, 3 H, Ar*H*), 7.20 (s, 6 H, ArC*H*C*H*Ar), 7.45 (s, 6 H, Ar*H*), 7.56 (s, 3 H, Ar*H*); ^{13}C NMR (75 MHz): 14.3, 22.6, 22.9, 23.1, 29.5, 29.7, 29.7, 29.8, 31.8, 32.1, 32.3, 36.0, 36.2, 38.3, 124.2, 126.0, 126.1, 126.3, 126.8, 127.7, 128.9, 129.0, 129.3, 137.9, 138.0, 138.1, 139.0, 141.7, 142.5, 143.0; HRMS (MALDI-TOF): *m/z* calcd for $(M + Na)^+$, 5839.9042; found, 5839.8851. Anal. Calcd (%) for $C_{414}H_{648}S_6$: C, 85.47; H, 11.23. Found: C, 85.78; H, 11.54.

General procedure for the saturation of C=C double bonds by Pd-C catalyzed hydrogenation

To a stirred mixture of the unsaturated dendron and K_2CO_3 in THF, 10% palladium on charcoal was added and the reaction mixture was stirred under H_2 atmosphere (1 atm) at 20 °C for 3 h. The mixture was then filtered with a short pad of celite and the filtrate was concentrated under reduced pressure. The crude product was purified by silica gel chromatography to afford the desired product.

G2–C–OTHP (110). Starting from G2–C=C–OTHP **109** (7.09 g, 7.4 mmol), 10% Pd/C (0.73 g) and K_2CO_3 (1.14 g, 8.3 mmol) in THF (200 mL), compound G2–C–OTHP **110** (6.52 g, 92%) was obtained as a colorless oil after column chromatography (eluent: hexane/EtOAc = 50/1). R_f: 0.21 (hexane/EtOAc = 30/1); ^{1}H NMR (300 MHz): 0.88 (t, J = 6.5 Hz, 12 H, CH_3), 1.16–1.42 (m, 56 H), 1.47–1.96 (m, 14 H), 2.55 (t, J = 7.8 Hz, 8 H, ArCH_2), 2.74–2.95 (m, 8 H, ArCH_2CH_2Ar), 3.50–3.62 (m, 1 H, OC*H*H), 3.86–4.00 (m, 1 H, OCHC*H*), 4.46 (d, J = 11.7 Hz, 1 H, ArC*H*HO), 4.71 (t, J = 3.3 Hz, 1 H, OC*H*O), 4.76 (d, J = 11.7 Hz, 1 H, ArCH*H*O), 6.85 (s, 6 H, Ar*H*), 6.97 (s, 1 H, Ar*H*), 7.01 (s, 2 H, Ar*H*); ^{13}C NMR (75 MHz; two aliphatic signals were not resolvable due to signal overlapping): 14.2, 19.4, 22.8, 25.7, 29.5, 29.6, 29.7, 29.8, 30.6, 31.8, 32.1, 36.1, 38.2, 61.7, 68.8, 97.4, 125.6, 125.9, 126.1, 127.9, 138.2, 141.6, 142.0, 142.6; HRMS (MALDI-TOF): *m/z* calcd for $(M + Na)^+$, 983.8554; found, 983.8544. Anal. Calcd (%) for $C_{68}H_{112}O_2$: C, 84.93; H, 11.74. Found: C, 85.02; H, 11.58.

G3–CC–OTHP (114). Starting from G3–CC=C–OTHP **113** (1.53 g, 0.8 mmol), 10% Pd/C (0.16 g) and K_2CO_3 (0.35 g, 2.5 mmol) in THF (100 mL), compound

G3–CC–OTHP **114** (1.47 g, 96 %) was obtained as a colorless oil after column chromatography (eluent: hexane/EtOAc = 50/1). R_f: 0.16 (hexane/EtOAc = 30/1); ^{1}H NMR (300 MHz): 0.87 (t, J = 6.6 Hz, 24 H, CH_3), 1.01–1.41 (m, 112 H), 1.47–1.93 (m, 22 H), 2.55 (t, J = 7.8 Hz, 16 H, ArCH_2), 2.72–2.87 (m, 16 H, ArCH_2CH_2Ar of the outermost layer), 2.87–2.96 (m, 8 H, ArCH_2CH_2Ar of the inner layer), 3.50–3.62 (m, 1 H, OCHH), 3.88–4.00 (m, 1 H, OCHH), 4.48 (d, J = 11.7 Hz, 1 H, ArCHHO), 4.73 (t, J = 3.5 Hz, 1 H, OCHO), 4.79 (d, J = 12 Hz, 1 H, ArCHHO), 6.85 (s, 4 H, ArH), 6.86 (s, 8 H, ArH), 6.92 (s, 2 H, ArH), 6.93 (s, 4 H, ArH), 7.05 (s, 1 H, ArH), 7.10 (s, 2 H, ArH); ^{13}C NMR (75 MHz; two aliphatic and one aromatic signals were not resolvable due to signal overlapping): 14.3, 19.5, 22.9, 25.7, 29.5, 29.7, 29.7, 29.8, 29.8, 30.7, 31.8, 32.1, 36.2, 38.3, 38.4, 62.2, 69.1, 97.8, 125.8, 126.0, 126.3, 126.4, 128.0, 138.4, 141.9, 142.1, 142.3, 142.4, 143.0; HRMS (MALDI–TOF): *m/z* calcd for $(M + Na)^+$, 1961.7352; found, 1961.7329. Anal. Calcd (%) for $C_{140}H_{224}O_2$: C, 86.71; H, 11.64. Found: C, 86.69; H, 11.44.

General procedure for the removal of the tetrahydropyranyl group

To a stirred solution of protected dendron in THF/MeOH solution (1:1) was added concentrated HCl (37%) slowly. The reaction mixture was stirred until all the starting material was consumed as checked by TLC analysis. After that, the mixture was neutralized by saturated Na_2CO_3 solution. The mixture was then extracted with CH_2Cl_2, followed by washing with saturated NaCl solution. The collected organic layers were dried ($MgSO_4$), filtered and concentrated *in vacuo*. The residue was purified by flash chromatography on silica gel to give the alcohol.

G2–C–CH_2OH (111). Starting from G2–C–OTHP **110** (5.74 g, 6.0 mmol), concentrated HCl (3 mL) in THF/MeOH solution (15 mL), compound G2–C–CH_2OH **111** (3.90 g, 74 %) was obtained as a colorless liquid after column chromatography (eluent: hexane/EtOAc = 50/1 gradient to 30/1) After standing at 20 °C under vacuum, a white solid was obtained. M.p: 32–34 °C; R_f: 0.34 (hexane/EtOAc = 10/1); ^{1}H NMR (300 MHz): 0.88 (t, J = 6.6 Hz, 12 H, CH_3), 1.20–1.40 (m, 56 H), 1.51–1.67 (m, 9 H, $ArCH_2CH_2$ + OH), 2.55 (t, J = 7.8 Hz, 8 H, $ArCH_2$), 2.77–2.95 (m, 8 H, $ArCH_2CH_2Ar$), 4.66 (d, J = 6 Hz, 2 H, $ArCH_2OH$), 6.85 (s, 6 H, Ar*H*), 6.98 (s, 1 H, Ar*H*), 7.06 (s, 2 H, Ar*H*); ^{13}C NMR (75 MHz; one aliphatic signal was not resolvable due to signal overlapping): 14.3, 22.9, 29.5, 29.6, 29.7, 29.8, 29.8, 31.8, 32.1, 36.1, 38.3, 65.5, 124.8, 126.0, 126.3, 128.1, 141.1, 141.7, 142.5, 142.9; MS (ESI): *m/z* 900 [$(M + Na)^+$, 100%]. HRMS (ESI): calcd for $(M + Na)^+$, 899.7979; found, 899.7965. Anal. Calcd (%) for $C_{63}H_{104}O$: C, 86.23; H, 11.95. Found: C, 86.60; H, 12.28.

G3–CC–CH_2OH (115). Starting from G3–CC–OTHP **114** (1.40 g, 0.7 mmol), concentrated HCl (1 mL) in THF/MeOH solution (20 mL), compound G3-CC-CH_2OH **115** (1.16 g, 87 %) was obtained as a pale yellow oil after column chromatography (eluent: hexane/EtOAc =100/1). R_f: 0.33 (hexane/EtOAc = 20/1); ^{1}H NMR (300 MHz): 0.87 (t, J = 6.6 Hz, 24 H, CH_3), 1.17–1.46 (m, 112 H), 1.51–1.69 (m, 17 H, $ArCH_2CH_2$ + OH), 2.55 (t, J = 7.8 Hz, 16 H, $ArCH_2$), 2.85 (s, 16 H, outer $ArCH_2CH_2Ar$), 2.88 (s, 8 H, inner $ArCH_2CH_2Ar$), 4.68 (d, J = 6.3 Hz, 2 H, $ArCH_2OH$), 6.85 (s, 12 H, Ar*H*), 6.92 (s, 6 H, Ar*H*), 7.05 (s, 1 H, Ar*H*), 7.08 (s, 2 H, Ar*H*); ^{13}C NMR (75 MHz; four signals were not resolvable due to signal overlapping): 14.3, 22.9, 29.5, 29.7, 29.7, 29.8, 29.8, 31.8, 32.1, 36.2, 38.4, 65.6, 124.9, 126.0, 126.3, 126.4, 128.1, 141.2, 141.9, 142.0, 142.4, 142.7, 143.0; MS (ESI): *m/z* 1878 [$(M + Na)^+$, 100%]. HRMS (ESI): calcd for $(M + Na)^+$, 1877.6777; found, 1877.6790.

Anal. Calcd (%) for $C_{135}H_{216}O$: C, 87.40; H, 11.73. Found: C, 87.20; H, 11.62.

General procedure for the synthesis of dendritic thioacetates Gn–CH_2SAc from dendritic benzyl alcohols Gn–CH_2OH

DIAD was added to a solution of triphenylphosphine in dry THF at 0 °C. After 10 min, a solution of the dendritic alcohol Gn–CH_2OH and thiolacetic acid in dry THF was then added dropwise and the reaction mixture was stirred at 20 °C for 2 h. The solvent was evaporated under reduced pressure and hexane was added to precipitate the triphenylphosphine oxide formed. The reaction mixture was filtered and the filtrate was concentrated *in vacuo*. The crude product was purified by silica gel chromatography to afford the desired product.

G3–CC–CH_2SAc (116). Staring from G3–CC–CH_2OH **115** (1.05 g, 0.6 mmol), DIAD (0.2 mL, 1.0 mmol), thiolacetic acid (0.1 mL, 1.1 mmol) and triphenylphosphine (0.30 g, 1.1 mmol) in THF (5 mL), compound G3–CC–CH_2SAc **116** (0.51 g, 47 %) was obtained after column chromatography (eluent: hexane/EtOAc = 100/1 gradient to 50/1) as a yellow liquid. R_f: 0.25 (hexane:EtOAc = 30/1); ^1H NMR (300 MHz): 0.88 (t, J = 6.5 Hz, 24 H, CH_3), 1.15–1.41 (m, 112 H), 1.51–1.68 (m, 16 H), 2.36 (s, 3 H, CO_2CH_3), 2.56 (t, J = 7.7 Hz, 16 H, $ArCH_2$), 2.71–2.98 (m, 24 H, $ArCH_2CH_2Ar$), 4.12 (s, 2 H, CH_2CO_2SAc), 6.86 (s, 4 H, Ar*H*), 6.87 (s, 8 H, Ar*H*), 6.93 (s, 6 H, Ar*H*), 7.01 (s, 3 H, Ar*H*); ^{13}C NMR (75 MHz; two aliphatic signals were not resolvable due to signal overlapping): 14.3, 22.8, 29.5, 29.7, 29.7, 29.8, 29.8, 30.5, 31.8, 32.1, 33.6, 36.2, 38.3, 38.4, 126.0, 126.2, 126.3, 126.4, 126.7, 127.8, 137.7, 142.0, 142.0, 142.4, 142.8, 143.1, 195.4; HRMS (MALDI–TOF): *m/z* calcd for $(M+Na)^+$, 1935.6654; found, 1935.6646. Anal. Calcd (%) for $C_{137}H_{218}OS$: C,

86.00; H, 11.48. Found: C, 85.93; H, 11.78.

G2–C–CH_2SAc (118). Staring from G2–C–CH_2OH **111** (2.69 g, 3.1 mmol), DIAD (1.2 mL, 6.1 mmol), thiolacetic acid (0.4 mL, 6.2 mmol) and triphenylphosphine (1.61 g, 6.2 mmol) in THF (10 mL), compound G2–C–CH_2SAc **118** (1.24 g, 43 %) was obtained after column chromatography (eluent: hexane/EtOAc = 100/1) as a yellow liquid. R_f: 0.42 (hexane/EtOAc = 30/1); ^{1}H NMR (300 MHz): 0.88 (t, J = 6.6 Hz, 12 H, C*H*$_3$), 1.18–1.41 (m, 56 H), 1.51–1.67 (m, 8 H), 2.36 (s, 3 H, C*H*$_3$COS), 2.55 (t, J = 7.8 Hz, 8 H, ArC*H*$_2$), 2.76–2.88 (m, 8 H, ArC*H*$_2$C*H*$_2$Ar), 4.09 (s, 2 H, C*H*$_2$SAc), 6.84 (s, 6 H, Ar*H*), 6.92 (s, 1 H, Ar*H*), 6.97 (s, 2 H, Ar*H*); ^{13}C NMR (75 MHz; two signals were not resolvable due to signal overlapping): 14.3, 22.8, 29.5, 29.6, 29.7, 29.8, 29.8, 30.3, 31.8, 32.1, 33.6, 36.1, 38.2, 125.9, 126.3, 126.6, 127.8, 137.5, 141.6, 142.6, 142.9, 195.0; MS (ESI): *m/z* 958 [(M+Na)$^+$, 100%]. HRMS (ESI): calcd for (M + Na)$^+$, 957.7857; found, 957.7848. Anal. Calcd (%) for $C_{65}H_{106}OS$: C, 83.44; H, 11.42. Found: C, 83.37; H, 11.35.

G1–CH_2SAc (125). Staring from G1–CH_2OH **74** (15.47 g, 40 mmol), DIAD (15.7 mL, 80 mmol), thiolacetic acid (5.7 mL, 80 mmol) and triphenylphosphine (20.90 g, 80 mmol) in THF (300 mL), compound G1–CH_2SAc **125** (14.04 g, 79 %) was obtained after column chromatography (eluent: hexane/EtOAc = 100/1 gradient to 50/1) as a yellow liquid. R_f: 0.42 (hexane/EtOAc = 30/1); ^{1}H NMR (300 MHz): 0.88 (t, J = 6.6 Hz, 6 H, C*H*$_3$), 1.17–1.38 (m, 28 H), 1.48–1.64 (m, 4 H), 2.35 (s, 3 H, C*H*$_3$COS), 2.53 (t, J = 7.8 Hz, 4 H, ArC*H*$_2$), 4.08 (s, 2 H, C*H*$_2$SAc), 6.87 (s, 1 H, Ar*H*), 6.90 (s, 2 H, Ar*H*); ^{13}C NMR (75 MHz; one aliphatic signal was not resolvable due to signal overlapping): 14.2, 22.8, 29.5, 29.6, 29.6, 29.8, 30.4, 31.6, 32.1, 33.6, 36.0, 126.3, 127.7, 137.2, 143.4, 195.3; MS (ESI): *m/z* 469 [(M + Na)$^+$, 100%].

HRMS (ESI): calcd for $(M + Na)^+$, 469.3475; found, 469.3486. Anal. Calcd (%) for $C_{29}H_{50}OS$: C, 77.96; H, 11.28. Found: C, 77.74; H, 11.39.

G2–S–CH_2SAc (131). Staring from G2–S–CH_2OH **124** (4.06 g, 4.3 mmol), DIAD (1.7 mL, 8.6 mmol), thiolacetic acid (0.6 mL, 8.4 mmol) and triphenylphosphine (2.27 g, 8.7 mmol) in THF (30 mL), compound G2–S–CH_2SAc **131** (3.66 g, 85 %) was obtained after column chromatography (eluent: hexane/EtOAc = 100/1) as a yellow liquid. R_f: 0.21 (hexane:EtOAc = 80/1); ^{1}H NMR (300 MHz): 0.87 (t, J = 6.6 Hz, 12 H, C*H*$_3$), 1.16–1.46 (m, 56 H), 1.52–1.68 (m, 8 H), 2.35 (s, 3 H, C*H*$_3$COS), 2.55 (t, J = 7.7 Hz, 8 H, ArC*H*$_2$), 3.55 (s, 8 H, C*H*$_2$S), 4.09 (s, 2 H, C*H*$_2$SAc), 6.87 (s, 2 H, Ar*H*), 6.91 (s, 4 H, Ar*H*), 7.08 (s, 2 H, Ar*H*), 7.12 (s, 1 H, Ar*H*); ^{13}C NMR (75 MHz; one signal was not resolvable due to signal overlapping): 14.2, 22.8, 29.5, 29.6, 29.7, 29.8, 30.3, 31.7, 32.0, 33.4, 35.4, 35.8, 36.0, 126.5, 127.4, 128.2, 128.8, 137.7, 137.9, 139.1, 143.1, 194.7; HRMS (MALDI–TOF): *m/z* calcd for $(M+Na)^+$, 1021.7298; found, 1021.7314. Anal. Calcd (%) for $C_{65}H_{106}OS_3$: C, 78.09; H, 10.69. Found: C, 77.73; H, 11.08.

G3–SS–CH_2SAc (134). Staring from G3–SS–CH_2OH **133** (1.00 g, 0.5 mmol), DIAD (0.2 mL, 1.0 mmol), thiolacetic acid (70 μL, 1.0 mmol) and triphenylphosphine (0.26 g, 1.0 mmol) in THF (10 mL), compound G3–SS–CH_2SAc **134** (0.85 g, 82 %) was obtained after column chromatography (eluent: hexane/EtOAc = 60/1) as a pale yellow liquid. R_f: 0.33 (hexane:EtOAc = 30/1); ^{1}H NMR (300 MHz): 0.87 (t, J = 6.6 Hz, 24 H, C*H*$_3$), 1.15–1.40 (m, 112 H), 1.49–1.65 (m, 16 H), 2.32 (s, 3 H, C*H*$_3$COS), 2.53 (t, J = 7.8 Hz, 16 H, ArC*H*$_2$), 3.53 (s, 4 H, C*H*$_2$S), 3.56 (s, 12 H, C*H*$_2$S), 3.58 (s, 8 H, C*H*$_2$S), 4.07 (s, 2 H, C*H*$_2$SAc), 6.86 (s, 4 H, Ar*H*), 6.91 (s, 8 H, Ar*H*), 7.08 (s, 4 H, Ar*H*), 7.12 (s, 4 H, Ar*H*) 7.16 (s, 1 H, Ar*H*); ^{13}C NMR (75 MHz; one aliphatic

carbon signal was not resolvable due to signal overlapping): 14.2, 22.8, 29.5, 29.6, 29.7, 29.7, 30.4, 31.7, 32.0, 33.3, 35.3, 35.4, 35.6, 35.9, 36.0, 126.5, 127.4, 128.3, 128.5, 128.6, 128.8, 137.6, 138.1, 138.5, 138.9, 138.9, 143.1, 194.8; HRMS (MALDI–TOF): *m/z* calcd for $(M+Na)^+$, 2127.4982; found, 2127.5001. Anal. Calcd (%) for $C_{137}H_{218}OS_7$: C, 78.15; H, 10.43. Found: C, 77.94; H, 10.43.

General procedure for the coupling reactions between the dendritic thioacetate Gn-CH_2SAc and the branching units/core

To a stirred solution of dendritic thiolacetate in THF/ MeOH (1:1) was added NaOMe and the mixture was stirred at 20 °C for 5 min. A solution of the branching unit/core in THF was added into the reaction mixture. The mixture was stirred at 20 °C for 4–18 h. Water was then added to the reaction mixture and extraction was performed using CH_2Cl_2 followed by washing with saturated NaCl solution. The collected organic layers were dried ($MgSO_4$) and filtered. The filtrate was concentrated under reduced pressure and the residue was purified by flash chromatography on silica gel to give the desired product.

G3–CS–CHO (120). Starting from G2–C–CH_2SAc **118** (0.63 g, 0.7 mmol), branching unit **105** (0.10 g, 0.3 mmol) and NaOMe (0.07 g, 1.3 mmol) in THF/MeOH (2 mL). The product **120** was obtained as a pale yellow liquid (0.37 g, 57%) after purification by liquid chromatography (eluent: hexane = 100/1). R_f: 0.86 (hexane/EtOAc = 40/1); ^{1}H NMR (300 MHz): 0.92 (t, J = 6.5 Hz, 24 H, CH_3), 1.17–1.46 (m, 112 H), 1.54–1.72 (m, 16 H), 2.59 (t, J = 7.5 Hz, 16 H, $ArCH_2$), 2.77–2.98 (m, 16 H, $ArCH_2CH_2Ar$), 3.62 (s, 4 H, CH_2S), 3.67 (s, 4 H, CH_2S), 6.88 (s, 12 H, Ar*H*), 6.97 (s, 2 H, Ar*H*), 7.01 (s, 4 H, Ar*H*), 7.54 (s, 1 H, Ar*H*), 7.68 (s, 2 H,

Ar*H*), 10.01 (s, 1 H, C*H*O); ^{13}C NMR (75 MHz): 14.3, 22.9, 29.5, 29.7, 29.7, 29.8, 29.8, 31.8, 32.1, 35.3, 36.0, 36.2, 38.2, 38.3, 126.0, 126.3, 126.8, 127.8, 129.0, 135.7, 136.9, 137.6, 140.0, 141.7, 142.6, 143.0, 191.9; MS (ESI): *m/z* 1940 [$(M+Na)^+$, 100%]. HRMS (ESI): calcd for $(M+Na)^+$, 1939.6062; found, 1939.6072. Anal. Calcd (%) for $C_{135}H_{214}OS_2$: C, 84.57; H, 11.25. Found: C, 84.54; H, 11.64.

G2–S–CH_2OH (124). Starting from G1–CH_2SAc **125** (1.10 g, 2.5 mmol), 3,5-bis(bromomethyl)benzyl alcohol **100** (0.34 g, 1.2 mmol) and NaOMe (0.27 g, 5 mmol) in THF/MeOH (10 mL), the product was obtained as a pale yellow liquid (0.93 g, 85%) after purification by liquid chromatography (eluent: hexane/EtOAc = 20/1). R_f: 0.30 (hexane/EtOAc = 15/1); ^{1}H NMR (300 MHz): 0.87 (t, J = 6.6 Hz, 12 H, CH_3), 1.18–1.38 (m, 56 H), 1.51–1.65 (m, 9 H, O*H* and CH_2), 2.54 (t, J = 7.8 Hz, 8 H, ArCH_2), 3.57 (s, 4 H, CH_2S), 3.59 (s, 4 H, CH_2S), 4.67 (d, J = 6 Hz, 2 H, CH_2OH), 6.87 (s, 2 H, Ar*H*), 6.91 (s, 4 H, Ar*H*), 7.15 (s, 3 H, Ar*H*); ^{13}C NMR (75 MHz; two aliphatic carbon signals were not resolvable due to the signal overlapping): 14.3, 22.8, 29.5, 29.6, 29.7, 29.8, 31.7, 32.1, 35.7, 36.0, 65.2, 126.3, 126.5, 127.4, 129.1, 137.7, 139.0, 141.5, 143.2; MS (ESI): *m/z* 964 [$(M+Na)^+$, 100%]. HRMS (ESI): calcd for $(M+Na)^+$, 963.7421; found, 963.7418. Anal. Calcd (%) for $C_{63}H_{104}OS_2$: C, 80.36; H, 11.13. Found: C, 80.52; H, 11.45.

G2–S–CHO (127). Starting from G1–CH_2SAc **125** (10.98 g, 24.6 mmol), 3,5-bis(bromomethyl)benzaldehyde **105** (3.60 g, 12.3 mmol) and NaOMe (4.00 g, 73.7 mmol) in THF/MeOH (30 mL), the product **127** was obtained as a yellow liquid (5.37 g, 47 %) after purification by liquid chromatography (eluent: hexane/EtOAc = 100/1 gradient to 80/1). R_f: 0.34 (hexane/EtOAc = 30/1); ^{1}H NMR (300 MHz): 0.87 (t, J = 6.6 Hz, 12 H, CH_3), 1.15–1.39 (m, 56 H), 1.50–1.66 (m, 8 H), 2.55 (t, J = 7.8 Hz,

8 H, ArCH_2), 3.57 (s, 4 H, CH_2S), 3.63 (s, 4 H, CH_2S), 6.88 (s, 2 H, Ar*H*), 6.89 (s, 4 H, Ar*H*), 7.48 (s, 1 H, Ar*H*), 7.63 (s, 2 H, Ar*H*), 9.97 (s, 1 H, C*H*O); ^{13}C NMR (75 MHz; two aliphatic carbon signals were not resolvable due to signal overlapping): 14.3, 22.8, 29.5, 29.6, 29.7, 29.8, 31.7, 32.0, 35.2, 36.0, 126.5, 127.6, 128.9, 135.6, 136.9, 137.3, 140.0, 143.3, 191.8; HRMS (MALDI–TOF): *m/z* calcd for $(M+Na)^+$, 961.7264; found, 961.7241. Anal. Calcd (%) for $C_{63}H_{102}OS_2$: C, 80.53; H, 10.94. Found: C, 80.31; H, 11.14.

G3–SS–CH$_2$OH (133). Starting from G2–S–CH$_2$SAc **131** (2.36 g, 2.4 mmol), 3,5-bis(bromomethyl)benzyl alcohol **100** (0.33 g, 1.1 mmol) and NaOMe (0.37 g, 6.9 mmol) in THF/MeOH (15 mL), the product **133** was obtained as a colorless liquid (1.01 g, 44%) after purification by liquid chromatography (eluent: hexane/EtOAc = 20/1). R_f: 0.14 (hexane/EtOAc = 20/1); ^{1}H NMR (300 MHz): 0.87 (t, J = 6.8 Hz, 24 H, CH_3), 1.15–1.40 (m, 112 H), 1.46–1.66 (m, 16 H), 1.82 (t, J = 6.2 Hz, 1 H, O*H*), 2.54 (t, J = 7.7 Hz, 16 H, ArCH_2), 3.56 (s, 16 H, CH_2S), 3.57 (s, 8 H, CH_2S), 4.60 (d, J = 6.3 Hz, 2 H, CH_2OH), 6.87 (s, 4 H, Ar*H*), 6.91 (s, 8 H, Ar*H*), 7.08(s, 2 H, Ar*H*), 7.11 (s, 6 H, Ar*H*), 7.20 (s, 1 H, Ar*H*); ^{13}C NMR (75 MHz; one aromatic and two aliphatic signals were missing due to signal overlapping): 14.3, 22.8, 29.5, 29.6, 29.7, 29.8, 31.7, 32.1, 35.5, 35.5, 35.7, 36.0, 65.0, 126.5, 127.5, 128.5, 128.6, 129.0, 137.7, 138.6, 138.8, 138.8, 141.7, 143.2; HRMS (MALDI–TOF): *m/z* calcd for $(M+Na)^+$, 2069.5100; found, 2069.5101. Anal. Calcd (%) for $C_{135}H_{216}OS_6$: C, 79.19; H, 10.63. Found: C, 78.81; H, 10.49.

G3–SSS–dendrimer (136). Starting from G3–SS–CH2SAc **134** (0.67 g, 0.32 mmol), 1,3,5-tris(bromomethyl)benzene **101** (34 mg, 96 μmol), and NaOMe (31 mg, 0.57 mmol) in THF/MeOH (5 mL), the product **136** was obtained as a colorless liquid

(0.45 g, 74%) after purification by liquid chromatography (eluent: hexane/EtOAc = 60/1). R_f: 0.6 (hexane/EtOAc = 20/1); ^{1}H NMR (300 MHz): 0.86 (t, J = 6.5 Hz, 72 H, CH_3), 1.14–1.38 (m, 336 H), 1.46–1.65 (m, 48 H), 2.52 (t, J = 7.7 Hz, 48 H, ArCH_2), 3.43–3.74 (m, 84 H, CH_2S), 6.85 (s, 12 H, ArH), 6.90 (s, 24 H, ArH), 7.05 (s, 6 H, ArH), 7.08 (s, 3 H, ArH), 7.13 (s, 15 H, ArH + ArH), 7.16 (s, 6 H, ArH); ^{13}C NMR (75 MHz; six aromatic carbon and six aliphatic carbon signals were not resolvable due to signal overlapping): 14.3, 22.8, 29.5, 29.7. 29.7, 29.8, 31.7, 32.1, 35.8, 36.1, 126.6, 127.4, 128.5, 128.6, 137.7, 138.7, 138.9, 143.2; LRMS (MALDI–TOF): *m/z* calcd for M^+, 6304.987; found, 6304.7219. Anal. Calcd (%) for $C_{414}H_{654}S_{21}$: C, 78.87; H, 10.45. Found: C, 78.42; H, 10.18.

G3–SC–CH(OMe)$_2$ (128).

A mixture of G3–SC=C–CH(OMe)$_2$ **75** (2.21 g, 1.1 mmol), copper(II) sulfate (0.10 g, 0.6 mmol) and hydrazine (1.3 mL) in THF (1 mL) was stirred at 40 °C for 18 h under open air. After that, the reaction mixture was concentrated under reduced pressure and the residue was extracted with ethyl acetate (3mL × 3). The organic layer was washed with saturated NaCl and then dried ($MgSO_4$), filtered and concentrated *in vacuo*. Compound **128** (1.46 g, 66%) was obtained as a colorless oil after column chromatography (eluent: hexane/EtOAc = 50/1). R_f: 0.16 (hexane/EtOAc = 40/1); ^{1}H NMR (300 MHz): 0.87 (t, J = 6.6 Hz, 24 H, CH_3), 1.14–1.40 (m, 112 H), 1.49–1.66 (m, 16 H), 2.54 (t, J = 7.8 Hz, 16 H, ArCH_2), 2.83–2.95 (m, 8 H, ArCH_2CH_2Ar), 3.30 (s, 6 H, OCH_3), 3.56 (s, 8 H, CH_2S), 3.57 (s, 8 H, CH_2S), 5.34 (s, 1 H, OCH), 6.87 (s, 4 H, ArH), 6.91 (s, 8 H, ArH), 7.03 (s, 5 H, ArH + ArH), 7.06 (s, 2 H, ArH), 7.13 (s, 2 H, ArH); ^{13}C NMR (75 MHz; two aliphatic signals were not resolvable due to signal overlapping): 14.3, 22.8, 29.5, 29.6, 29.7, 29.8, 31.7, 32.0, 35.8, 36.0, 36.0, 38.1, 52.7, 103.3, 124.5, 126.5, 127.4, 127.5, 127.9, 128.8, 137.8, 138.3, 138.6, 141.9, 142.3,

143.1; HRMS (MALDI–TOF): *m/z* calcd for $(M + Na)^+$, 2049.5921; found, 2049.5888. Anal. Calcd (%) for $C_{137}H_{220}O_2S_4$: C, 81.16; H, 10.94. Found: C, 81.22; H, 11.17.

G3–SC–CHO (129).

To a stirred solution of G3–SC–$CH(OMe)_2$ **128** (1.36 g, 0.7 mmol) in THF (5 mL) was added 20% aqueous H_2SO_4 (10 mL) slowly. The reaction mixture was stirred until all the starting material was consumed and it was confirmed by ^1H NMR analysis. The mixture was neutralized by saturated Na_2CO_3 solution and then extracted by ethyl acetate, followed by washing with saturated NaCl solution. The collected organic layers were dried ($MgSO_4$), filtered and concentrated *in vacuo*. The residue was purified by liquid chromatography (eluent: Hexane/EtOAc = 40/1) on silica gel to give a pale yellow liquid (1.13 g, 86%). R_f: 0.43 (hexane/EtOAc = 40/1); ^1H NMR (300 MHz): 0.91 (t, J = 6.5 Hz, 24 H, CH_3), 1.19–1.45 (m, 112 H), 1.54–1.70 (m, 16 H), 2.58 (t, J = 7.7 Hz, 16 H, $ArCH_2$), 2.84–3.08 (m, 8 H, $ArCH_2CH_2Ar$), 3.58 (s, 8 H, CH_2S), 3.60 (s, 8 H, CH_2S), 6.91 (s, 4 H, Ar*H*), 6.94 (s, 8 H, Ar*H*), 7.02 (s, 4 H, Ar*H*), 7.10 (s, 2 H, Ar*H*), 7.29 (s, 1 H, Ar*H*), 7.57 (s, 2 H, Ar*H*), 9.96 (s, 1 H, C*H*O); ^{13}C NMR (75 MHz): 14.3, 22.8, 29.5, 29.6, 29.7, 29.8, 31.7, 32.0, 35.8, 36.0, 36.0, 37.7, 37.8, 126.5, 127.4, 127.6, 127.8, 127.9, 135.1, 136.9, 137.7, 138.7, 141.7, 142.9, 143.1, 192.5; HRMS (MALDI–TOF): *m/z* calcd for $(M + Na)^+$, 2003.5577; found, 2003.5503; Anal. Calcd (%) for $C_{135}H_{214}OS_4$: C, 81.83; H, 10.89. Found: C, 82.00; H, 11.18.

G3–CCS–dendrimer (68).

A mixture of G3–CC–CH_2SAc **116** (88 mg, 46 μmol) and the tribromide **101** (5 mg,

14 μmol), NaOMe (5 mg, 93 μmol) and NaOH (0.2 g, 5 mmol) in THF/MeOH (2 /2 mL) was stirred for 18 h at 20 °C. The reaction mixture was then washed with water and then extracted with CH_2Cl_2 (10 mL ×3). The combined organic layers was then washed with saturated NaCl, dried ($MgSO_4$) and filtered. The filtrate was then evaporated *in vacuo* and afforded the target compound a colorless liquid (30 mg, 37%) after liquid chromatography (eluent: Hexane/CH_2Cl_2 = 6/1). R_f: 0.2 (hexane/ CH_2Cl_2 = 7/1); ^{1}H NMR (400 MHz): 0.88 (t, J = 6.6 Hz, 72 H, CH_3), 1.18–1.40 (m, 336 H), 1.52–1.66 (m, 48 H), 2.55 (t, J = 7.6 Hz, 48 H, ArCH_2), 2.84 (s, 48 H, outer ArCH_2CH_2Ar), 2.86 (s, 24 H, inner ArCH_2CH_2Ar), 3.63 (s, 6H, CH_2S), 3.65 (s, 6 H, CH_2S), 6.84 (s, 12 H, Ar*H*), 6.85 (s, 24H, Ar*H*), 6.90 (s, 6 H, Ar*H*), 6.93 (s, 12H, Ar*H*), 6.97 (s, 3H, Ar*H*), 7.06 (s, 6 H, Ar*H*), 7.21 (s, 3 H, Ar*H*); ^{13}C NMR (75 MHz; six signals were missing due to signal overlapping): 14.3, 22.9, 29.5, 29.7, 29.7, 29.8, 30.4, 31.8, 32.1, 36.2, 38.4, 125.9, 126.2, 126.3, 126.8, 127.5, 128.6, 138.1, 138.9, 141.9, 142.1, 142.4, 142.6, 143.0 ; HRMS (MALDI–TOF): *m/z* calcd for M^+, 5727.817; found, 5727.9678. Anal. Calcd (%) for $C_{414}H_{654}S_3$: C, 86.81; H, 11.51. Found: C, 86.83; H, 11.17.

G3–CSC–dendrimer (69).

To a stirred solution of G3–CSC=C–dendrimer **121** (0.36 g, 62 μmol) and *p*-toluenesulfono hydrazide ($TsNHNH_2$) (0.34 g, 1.8 mmol) warmed in DME/THF (3/3 mL) at 80 °C was added an aqueous solution of sodium acetate (2.5 mL, 0.7 M in H_2O) over a 24 h period. The completeness of the reaction was monitored by ^{1}H NMR spectroscopy. When the reaction was finished, the reaction mixture was extracted by CH_2Cl_2. The organic layer was washed with saturated NaCl and then dried ($MgSO_4$), filtered and concentrated under reduced pressure. Compound **69** (0.23 g, 63%) was obtained as a colorless liquid after column chromatography (eluent: hexane/CH_2Cl_2 =

8/1 gradient to 3/1). R_f: 0.53 (hexane/ CH_2Cl_2 = 4/1); ^{1}H NMR (400 MHz): 0.86 (t, J = 6.6 Hz, 72 H, CH_3), 1.12–1.38 (m, 336 H), 1.49–1.64 (m, 48 H), 2.52 (t, J = 7.8 Hz, 48 H, ArCH_2), 2.72–2.93 (m, 60 H, ArCH_2CH_2Ar), 3.59 (s, 12 H, CH_2S), 3.60 (s, 12 H, CH_2S), 6.81 (s, 36 H, Ar*H* +Ar*H*), 6.87 (s, 6 H, Ar*H*), 6.94 (s, 3 H, ArH), 6.99 (s, 12 H, Ar*H*), 7.07 (s, 3 H, Ar*H*), 7.11 (s, 6 H, Ar*H*); ^{13}C NMR (100 MHz; five aliphatic signals and one aromatic signal were not resolvable due to signal overlapping): 14.3, 22.9, 29.5, 29.7, 29.7, 29.8, 31.8, 32.1, 36.0, 36.2, 38.3, 126.0, 126.3, 126.8, 127.1, 127.6, 127.9, 138.1, 138.6, 141.8, 142.1, 142.5, 142.7, 143.0; LRMS (MALDI–TOF): *m/z* calcd for $(M + Na)^+$, 5847.0018; found, 5846.1679. Anal. Calcd (%) for $C_{414}H_{654}S_6$: C, 85.38; H, 11.32. Found: C, 85.43; H, 11.53.

6.3 Synthesis of the branching units of the dendrimers

Trimethyl benzene-1,3,5-tricarboxylate (98).[89]

Trimesic acid (20.09 g, 96 mmol) was dissolved in methanol (300 mL). Concentrated sulfuric acid (1 mL) was then added slowly and the reaction mixture was heated to 80 °C for 18 h. The reaction mixture was cooled down to 20 °C and neutralized with saturated Na_2CO_3 solution. Some product was precipitated out upon cooling and the reaction mixture was then filtered while the filtrate was concentrated under reduced pressure. The filtered product was redissolved in CH_2Cl_2 and combined with the concentrated filtrate. The mixture was then extracted with CH_2Cl_2 (150 mL × 3). The combined organic layers were dried ($MgSO_4$), filtered and concentrated *in vacuo* to give a white solid (22.69 g, 94%). M.p: 146 °C (lit.[89] 144–145 °C). R_f: 0.44 (hexane/EtOAc = 1/1); ^{1}H NMR (300 MHz): 3.98 (s, 9 H, CO_2CH_3), 8.86 (s, 3 H, Ar*H*); ^{13}C NMR (75 MHz): 53.1, 131.6, 135.0, 165.8.

1,3,5-Tris(hydroxymethyl)benzene (99).[89]

To a heated (~50 °C) suspension of $LiAlH_4$ (9.22 g, 243 mmol) in dried THF (300 mL) was added dropwise through a dropping funnel a solution of trimethyl benzene-1,3,5-tricarboxylate **98** (20.71 g, 82 mmol) in THF (300 mL). The reaction mixture was heated to 60 °C for 48 h and then cooled in an ice-bath. Water was added dropwise to destroy the excess $LiAlH_4$. The reaction mixture was filtered and the filtrate was collected. The solid residue was then extracted with THF for several times until most of the product was extracted. The combined organic layers were concentrated *in vacuo* to give the crude product which was purified by column chromatography (eluent: EtOAc) to give a white solid (11.45 g, 83%). M.p: 77–78 °C (lit.[89] 75–76 °C). R_f: 0.12 (EtOAc); ^{1}H NMR (300 MHz; DMSO-d_6): 4.47 (d, J = 5.7 Hz, 6 H, ArCH_2OH), 5.14 (t, J = 5.7 Hz, 3 H, ArCH$_2$OH), 7.12 (s, 3 H, ArH); ^{13}C NMR (75 MHz; DMSO-d_6): 63.2, 123.1, 142.2.

3,5-Bis(bromomethyl)benzyl alcohol (100) and 1,3,5-Tris(bromomethyl)benzene (101).[82]

To a solution of 1,3,5-Tris(hydroxymethyl)benzene **99** (6.49 g, 39 mmol) and CBr_4 (28.13 g, 85 mmol) in acetonitrile at 0 °C was added PPh_3 (22.68 g, 86 mmol) in small portions. Then, the reaction mixture was stirred at 20 °C for 3 to 5 h. The mixture was concentrated under reduced pressure and the residue was purified by column chromatography on silica gel (eluent: hexane/EtOAc = 5/1 gradient to 1/1) to give the tribromide **101** as a white solid (2.92 g, 21%). M.p: 98 °C (lit.[82] 96 °C). R_f: 0.48 (hexane/EtOAc = 7/1); ^{1}H NMR (300 MHz): 4.46 (s, 6 H, ArCH_2Br), 7.36 (s, 3 H, ArH); ^{13}C NMR (75 MHz): 32.3, 129.7, 139.1. Further elution gave the dibromide **100** as a white solid (5.46 g, 48%). M.p: 93–94 °C. R_f: 0.1 (hexane/EtOAc = 5/1); ^{1}H NMR (300 MHz): 1.75 (t, J = 6 Hz, 1 H, ArCH$_2$OH), 4.48 (s, 4 H, ArCH_2Br), 4.71 (d,

J = 5.7 Hz, 2 H, ArCH_2OH), 7.34 (s, 3 H, ArH); ^{13}C NMR (75 MHz): 32.9, 64.6, 127.5, 128.9, 138.8, 142.4.

DiCH$_2$Br–OTHP (103).

To a solution of 3,5-bis(bromomethyl)benzyl alcohol **100** (4.52 g, 15.4 mmol) in CH_2Cl_2 was added 3,4-dihydro-2H-pyran (2.1 mL, 23.0 mmol) and PPTS (0.39 g, 1.5 mmol) and the reaction mixture was stirred at 20 °C for 2 to 6 h. The solvent was evaporated under reduced pressure and the residue was purified by column chromatography (eluent: hexane/EtOAc = 20/1) to afford a colorless liquid (5.48 g, 94%). R_f: 0.45 (hexane/EtOAc = 5/1); ^{1}H NMR (300 MHz): 1.45–1.97 (m, 6 H), 3.50–3.62 (m, 1 H, OCHH), 3.83–3.97 (m, 1 H, OCHH), 4.48 (s, 4 H, ArCH_2Br), 4.48 (d, J = 12.3 Hz, 1 H, ArCHH), 4.71 (t, J = 3.5 Hz, 1 H, OCHO), 4.77 (d, J = 12.3 Hz, 1 H, ArCHH), 7.33 (s, 2 H, ArH), 7.34 (s, 1 H, ArH); ^{13}C NMR (75 MHz): 19.4, 25.5, 30.6, 32.9, 62.3, 68.2, 98.1, 128.3, 128.8, 138.5, 139.9; MS (FAB): m/z 377 [(M(^{79}Br) + H)$^+$, 8%]. HRMS (FAB): calcd for (M+H)$^+$, 378.9726; found, 378.9709. Anal. Calcd (%) for $C_{14}H_{18}Br_2O_2$: C, 44.47; H, 4.80. Found: C, 44.60; H, 4.84.

3,5-Bis(bromomethyl)benzaldehyde (105).[82]

To a stirred solution of 3,5-bis(bromomethyl)benzyl alcohol **100** (5.45 g, 19 mmol) in CH_2Cl_2 at 0 °C was added slowly a finely ground mixture of PCC/silica gel (5.86 g, 38 mmol) in portions. The reaction mixture was allowed to stir at 20 °C for 2 to 6 h. The completeness of the reaction was monitored by TLC. When the reaction was finished, the reaction mixture was filtered through a short pad of silica gel. The filtrate was then concentrated and purified by column chromatography on silica gel (eluent: hexane/EtOAc = 9/1) to give a white solid (4.87 g, 90%). M.p: 103–105 °C. R_f: 0.34 (hexane/EtOAc = 5/1); ^{1}H NMR (300 MHz): 4.53 (s, 4 H, ArCH_2Br), 7.69 (s, 1 H,

Ar*H*), 7.84 (s, 2 H, Ar*H*), 10.02 (s, 1 H, ArC*H*O); ^{13}C NMR (75 MHz): 31.7, 129.9, 135.2, 137.3, 139.6, 191.1.

General procedure for the synthesis of phosphonate

A stirred mixture of the benzyl bromide and triethyl phosphite was heated to 100 °C for 6 h. After the reaction, the product was purified by column chromatography.

1,3,5-Tris(diethoxyphosphorylmethyl)benzene (102).[82] Starting from 1,3,5-tris(bromomethyl)benzene **101** (0.22 g, 0.6 mmol) and triethyl phophite (0.35 mL, 2.0 mmol), compound **102** (0.29 g, 83 %) was obtained as a colorless liquid after column chromatography. R_f: 0.1 (EtOAc); ^{1}H NMR (300 MHz): 1.14 (t, J = 7.1 Hz, 18 H, CH_3), 2.91 (d, J = 22.2 Hz, 6 H, $ArCH_2$), 3.84–3.98 (m, 12 H, CH_2CH_3), 7.03 (d, J = 2.1 Hz, 3 H, Ar*H*); ^{13}C NMR (75 MHz): 16.3 (m), 33.3 (d, J = 138 Hz), 62.1 (m), 129.7 (m), 132.1 (m).

DiP(OEt)2–OTHP (104). Starting from $DiCH_2Br$–OTHP **103** (5.48 g, 14 mmol) and triethyl phosphite (5.5 mL, 32 mmol), compound **104** (7.06 g, 99%) was obtained as a pale yellow liquid after column chromatography (eluent: EtOAc gradient to EtOAc/EtOH = 5/1). R_f: 0.34 (EtOAc/EtOH = 5/1); ^{1}H NMR (300 MHz): 1.24 (t, J = 7.1 Hz, 12 H, CH_3), 1.40–1.93 (m, 6 H), 3.13 (d, J = 21.6 Hz, 4 H, ArCH_2), 3.47–3.59 (m, 1 H, OC*H*H), 3.80–3.94 (m, 1 H, OCH*H*), 3.94–4.10 (m, 8 H, OCH_2CH$_3$), 4.44 (d, J = 12 Hz, 1 H, ArC*H*H), 4.69 (t, J = 3.3 Hz, 1 H, OC*H*O), 4.74 (d, J = 12 Hz, 1 H, ArCH*H*), 7.14 (s, 1 H, Ar*H*), 7.18 (s, 2 H, Ar*H*); ^{13}C NMR (75 MHz): 16.0 (m), 18.9, 25.1, 30.1, 33.2 (d, J = 138 Hz), 61.6 (m), 61.7 (m), 68.1, 97.3, 127.4 (t, J = 4.9 Hz), 130.0 (t, J = 6.6 Hz), 131.6 (t, J = 6.0 Hz), 138.5 (t, J = 3.1 Hz); MS (FAB): *m/z* 493

[M^+, 40%]. HRMS (FAB): calcd for M^+, 493.2115; found, 493.2109.

3,5-Bis(diethoxyphosphorylmethyl)benzaldehyde (106).[82] Starting from 3,5-Bis(bromomethyl)benzaldehyde **105** (2.42 g, 8.3 mmol) and triethyl phosphite (3 mL, 17.3 mmol), compound **106** (2.81 g, 83%) was obtained as a colorless liquid after column chromatography (eluent: EtOAc gradient to EtOAc/EtOH = 5/1). R_f: 0.1 (EtOAc); ^{1}H NMR (300 MHz): 1.14 (t, J = 7.1 Hz, 12 H, CH_3), 3.10 (d, J = 21.9 Hz, 4 H, ArCH_2), 3.83–4.02 (m, 8 H, CH_2), 7.41 (s, 1 H, Ar*H*), 7.60 (s, 2 H, Ar*H*), 9.87 (s, 1 H, C*H*O); ^{13}C NMR (75 MHz): 16.3 (m), 33.2 (d, J = 138 Hz), 62.2 (m), 129.4 (t, J = 4.8 Hz), 133.3 (m), 136.7 (t, J = 2.9 Hz), 137.0 (t, J = 6.4 Hz).

3,5-Bis(diethoxyphosphorylmethyl)benzaldehyde dimethyl acetal (107).[82]

A mixture of montmorillonite K 10 (3.62 g) and trimethyl orthoformate (4.6 mL, 42 mmol) was stirred at 20 °C for 15 min. Then, a solution of the aldehyde **106** (2.80 g, 6.9 mmol) in methanol (15 mL) was added and stirred for 6 h. The progress of the reaction was monitored by ^{1}H NMR. When the reaction was completed, the montmorillonite was filtered and washed with methanol. The filtrate collected was evaporated under reduced pressure and the product (2.88 g, 92%) was obtained as a colorless liquid. R_f = 0.21 (EtOAc); ^{1}H NMR (300 MHz): 1.24 (t, J = 7.1 Hz, 12 H, CH_3), 3.14 (d, J = 21.6 Hz, 4 H, ArCH_2), 3.30 (s, 6 H, OCH_3), 3.92 – 4.10 (m, 8H, OCH_2), 5.36 (s, 1 H, C*H*), 7.20 (s, 1 H, Ar*H*), 7.27 (s, 2 H, Ar*H*); ^{13}C NMR (75 MHz): 16.0 (m), 33.2 (d, J = 137 Hz), 52.0, 61.6 (m), 102.1, 126.5(m), 130.8 (m), 131.6 (m), 138.2.

6.4 Post-modification of multifunctional dendrimers

A) Relative reactivity of interior functional group conversions from G3-oligo(sulfide) dendrimers to G3-oligo(sulfone) dendrimers

Heterogeneous reaction conditions

Oxone was added to a solution of G3-oligo(sulfide) dendrimer in CH_2Cl_2 and stirred at 32 °C. At different time intervals, an aliquot was taken from the reaction mixture, washed with water and then extracted by CH_2Cl_2. The organic layer was then evaporated under reduced pressure. The residue was then subjected to ^{1}H NMR analysis to determine the extent of the reaction.

Homogeneous reaction conditions

A mixture of the G3-oligo(sulfide) dendrimer and 35% hydrogen peroxide (10 mol. equiv per sulfide) in CH_2Cl_2/HOAc (10/1) was stirred at 32 °C. The reaction was monitored by ^{1}H NMR analysis. At different time intervals, a portion of the reaction mixture was washed with saturated Na_2CO_3 solution and then extracted with CH_2Cl_2. The organic layer was evaporated under reduced pressure.

G3–3SO_2–dendrimer (141). Starting with G3–CCS–dendrimer **68** (50 mg, 9 μmol), 35% H_2O_2 (22 μl, 26 mmol), compound **141** was obtained as a colorless liquid (50 mg, 99%) after liquid chromatography (eluent: CH_2Cl_2/hexane = 2/1). R_f: 0.1 (CH_2Cl_2 / = 2/1); ^{1}H NMR (400 MHz): 0.86 (t, J = 6.8 Hz, 72 H, CH_3), 1.15–1.38 (m, 336 H), 1.48–1.67 (m, 48 H), 2.53 (t, J = 7.8 Hz, 48 H, ArCH_2), 2.81 (s, 48H, outer ArCH_2CH_2Ar), 2.88 (s, 24 H, inner ArCH_2CH_2Ar), 4.09 (s, 6H, CH_2SO_2), 4.15 (s, 6 H, CH_2SO_2), 6.83 (s, 36 H, Ar*H*), 6.88 (s, 6H, Ar*H*), 6.92 (s, 12 H, Ar*H*), 7.12 (s, 3H,

Ar*H*), 7.15 (s, 6H, Ar*H*), 7.42 (s, 3 H, Ar*H*); ^{13}C NMR (100 MHz; three signals were not resolvable due to signal overlapping): 14.3, 22.9, 23.0, 29.5, 29.7, 29.7, 29.8, 29.9, 31.0, 31.8, 32.1, 36.2, 38.1, 38.2, 38.4, 125.9, 126.2, 126.3, 126.5, 127.5, 128.6, 128.8, 141.8, 141.9, 142.4, 143.0, 143.3 ; LRMS (MALDI–TOF): *m/z* calcd for $(M + H)^+$, 5824.8214; found, 5824.1822. Anal. Calcd (%) for $C_{414}H_{654}S_3O_6$: C, 85.38; H, 11.32. Found: C, 85.14; H, 11.63.

G3–6SO$_2$–dendrimer (142). Starting with G3–CSC–dendrimer **69** (47 mg, 8 μmol), 35% H_2O_2 (42 μl, 0.5 mmol), compound **142** was obtained as a colorless liquid (46 mg, 94%) after liquid chromatography (eluent: CH_2Cl_2/hexane = 2/1). R_f: 0.1 (CH_2Cl_2/ = 2/1); ^{1}H NMR (400 MHz, CD_2Cl_2): 0.86 (t, *J* = 6.6 Hz, 72 H, C*H*$_3$), 1.15–1.40 (m, 336 H), 1.47–1.64 (m, 48 H), 2.50 (t, *J* = 7.6 Hz, 48 H, ArC*H*$_2$), 2.72–2.95 (m, 60H, ArC*H*$_2$C*H*$_2$Ar), 4.08 (s, 12H, C*H*$_2$SO$_2$), 4.11 (s, 12 H, C*H*$_2$SO$_2$), 6.80 (s, 36 H, Ar*H*), 6.95 (s, 3 H, Ar*H*), 7.01 (s, 6H, Ar*H*), 7.07 (s, 12 H, Ar*H*), 7.18 (s, 3H, Ar*H*), 7.27 (s, 6H, Ar*H*); ^{13}C NMR (100 MHz; three aliphatic and two aromatic signals were not resolvable due to signal overlapping): 14.3, 22.8, 29.5, 29.7, 29.7, 29.8, 31.8, 32.1, 36.2, 38.0, 38.1, 57.4, 59.0, 126.0, 126.4, 127.5, 128.0, 128.6, 129.7, 132.1, 141.5, 141.7, 143.0, 143.1, 143.6 ; LRMS (MALDI–TOF): *m/z* calcd for M^+, 6017.0128; found, 6016.5551. Anal. Calcd (%) for $C_{414}H_{654}O_{12}S_3$: C, 82.65; H, 10.96. Found: C, 82.23; H, 10.39.

G3–21SO$_2$–dendrimer (138).Starting from G3–SSS–dendrimer **136** (88 mg, 14 μmol), 35% H_2O_2 (250 μl, 2.9 mmol), compound **138** was obtained as a white solid (54 mg, 55%) after purified by precipitation using CH_2Cl_2/ MeOH. M.p: 195–196 °C ^{1}H NMR (300 MHz,): 0.87 (t, *J* = 6.3 Hz, 72 H, C*H*$_3$), 1.14–1.38 (m, 336 H), 1.46–1.65 (m, 48 H), 2.57 (m, 48 H, ArC*H*$_2$), 3.95–4.65 (m, 84 H, C*H*$_2$SO$_2$, 7.02 (s,

12 H, Ar*H*), 7.05 (s, 24 H, Ar*H*), 7.31 (s, 6 H, Ar*H*), 7.61 (s, 21 H, Ar*H*), 7.71 (s, 3 H, Ar*H*); ^{13}C NMR (75 MHz; four aliphatic and eight aromatic signals were not resolvable due to signal overlapping): 14.7, 23.3, 30.0, 30.1, 30.1, 30.3, 32.1, 32.5, 36.4, 57.2, 57.6, 60.2, 127.7, 128.8, 129.4, 130.0, 135.0, 144.4; LRMS (MALDI–TOF): *m/z* calcd for M^+, 6976.9618; found, 6977.7954. Anal. Calcd (%) for $C_{414}H_{654}S_6O_{12}$: C, 71.27; H, 9.45. Found: C, 71.34; H, 9.01.

B) Dendritic Metamorphosis from G3-oligo(sulfone) dendrimers to G3-oligo(phenylenevinylene) by the Ramberg-Bäcklund Rearrangement

Finely divided KOH/Al_2O_3 was added to a rapidly stirred solution of the G3-oligo-(sulfone) dendrimer in THF/*t*-BuOH/CBr_2F_2 (1/1/1) at -45 °C. After 10 min, the mixture was filtered through a pad of Celite and washed with CH_2Cl_2. The filtrate was evaporated under reduced pressure to give the crude product.

References

1) Buhleier, E. W.; Wehner, W.; Vögtle, F. *Synthesis* **1978**, 155–158.

2) Tomalia, D. A.; Baker, H.; Dewald, J. R.; Hall, M.; Kallos, G.; Martin, S.; Roeck, J.; Ryder, J.; Smith, P. *Polym. J. (Tokyo)* **1985**, *17*, 117–132.

3) Tomalia, D. A.; Baker, H.; Dewald, J. R.; Hall, M.; Kallos, G.; Martin, S.; Roeck, J.; Ryder, J.; Smith, P. *Macromolecules* **1986**, *19*, 2466–2468.

4) Newkome, G. R.; Yao, Z.; Baker, G. R.; Gupta, V. K. *J. Org. Chem.* **1985**, *50*, 2003–2004.

5) Newkome, G. R.; Moorefield, C. N.; Vögtle, F. *Dendritic Molecules: Concepts, Syntheses and Perspectives*; VCH: Weinheim, Germany, 1996.

6) Tomalia, D. A.; Hedstrand, D, M.; Wilson, L. R. *Encyclopedia of Polymer Science and Engineering, Index Volume*; Wiley: New York, 1990; p 42–92.

7) For a review on phosphorus- and silicon- based dendrimers: a) Gudat, D. *Angew. Chem., Int. Ed. Engl.* **1997**, *36*, 1951–1955. b) Majoral, J. -P.; Caminade, A. -M. *Chem Rev.* **1999**, *99*, 845–880.

8) Bosman, A. W.; Janssen, H. M.; Meijer, E. W. *Chem. Rev.* **1999**, *99*, 1665–1688.

9) Grayson, S. M.; Fréchet, J. M. J. *Chem. Rev.* **2001**, 101, 3819–3867.

10) Burn. P. L.; Lo, S. C. *Chem. Rev.* **2007**, *107*, 1097–1116.

11) Newkome, G. R.; Yao, Z.; Baker, G. R.; Gupta, V. K.; Russo, P. S.; Saunders, M. J. *J. Am. Chem. Soc.* **1986**, *108*, 849–850.

12) Naylor, A. M.; Goddard, W. A., III; Kiefer, G. E.; Tomalia, D. A. *J. Am. Chem. Soc.* **1989**, *111*, 2339–2341.

13) Caminati, G.; Turro, N.J.; Tomalia, D. A. *J. Am. Chem. Soc.* **1990**, *112*, 8515–8522.

14) Enomoto, M.; Aida, T. *J. Am. Chem. Soc.* **1999**, *121*, 874–875.

15) Jiang, D. –L.; Aida, T. *Chem. Commun.* **1996**, *13*, 1523–1524.

16) Chow, H. –F.; Leung, C. –F.; Wang, G. –X.; Yang, Y. –Y. *C. R. Chime* **2003**, *6*, 735–745 and references therein.

17) Fréchet, J. M. J.; Jiang, Y.; Hawker, C. J.; Philippides, A. E. *Proc. IUPAC Int. ymp., Macromol. (Seoul)* **1989**, 19–20.

18) Hawker, C. J.; Fréchet, J. M. J. *J. Am. Chem. Soc.* **1990**, *112*, 7638–7647.

19) Hawker, C. J.; Fréchet, J. M. J. *J. Chem. Soc., Chem. Commun.* **1990**, 1010–1013.

20) Wooley, K. L.; Hawker, C. J.; Fréchet, J. M. J. *J. Am. Chem. Soc.* **1991**, *113*, 4252–4261.

21) Wooley, K. L.; Hawker, C. J.; Fréchet, J. M. J. *Angew. Chem., Int. Ed.* **1994**, *33*, 82–85.

22) Kawaguchi, T.; Walker, K. L.; Wilkins, C. L.; Moore, J. S. *J. Am. Chem. Soc.* **1995**, *117*, 2159–2165.

23) Spindler, R.; Fréchet, J. M. J. *J. Chem. Soc., Perkin Trans 1* **1993**, 913–918.

24) Zeng, F.; Zimmerman, S. C. *J. Am. Chem. Soc.* **1996**, *118*, 5326–5327.

25) Chow, H. –F.; Chan, I. Y. –K.; Mak, C. C.; Ng, M. –K. *Tetrahedron* **1996**, *52*, 4277–4290.

26) Hummelen, J. C.; van Dongen, J. L. J.; Meijer, E. W. *Chem. Eur. J.* **1997**, 3, 1489–1493.

27) Kallos, G. J.; Tomalia, D. A.; Hedstrand, D. M.; Lewis, S.; Zhou, J. *Rapid Commun. Mass Spectrom.* **1991**, *5*, 383–386.

28) Schwartz, B. L.; Rockwood, A. L.; Smith, R. D.; Tomalia, D. A.; Spindler, R. *Rapid Commun. Mass Spectrom.* **1995**, *9*, 1552–1555.

29) Dvornic, P. R.; Tomalia, D. A. *Macromol. Symp.* **1995,** *98*, 403–428.

30) Tolic, P. T.; Anderson, G. A.; Smith, R. D.; Brothers, H. M., II; Spindler, R.; Tomalia, D. A. *Int. J. Mass Spectrom. Ion Proc.* **1997**, *165/166*, 405–418.

31) Dandliker, P. J.; Diederich, F.; Gross, M.; Knobler, C. B.; Louati, A.; Sanford, E. M. *Angew. Chem., Int. Ed. Engl.* **1994**, *33*, 1739–1742.

32) Dandliker, P. J.; Diederich, F.; Gisselbrecht, J. -P.; Louati, A.; Gross, M. *Angew. Chem., Int. Ed. Engl.* **1995**, *34*, 2725–2728.

33) Mattei, S.; Walliman, P.; Kenda, B.; Amrein, W.; Diederich, F. *Helv. Chim. Acta* **1997**, *80*, 2391–2417.

34) de Brabander-van den Berg, E. M. M.; Nijenhuis, A.; Mure, M.; Keulen, J.; Reintjens, R.; Vandenbooren, F.; Bosman, B.; de Raat, R.; Frijns, T.; van den Wal, S.; Castelijns, M.; Put, J.; Meijer, E. W. *Macromol. Symp.* **1994**, *77*, 51–62.

35) Achar, S.; Puddephatt, R. J.; *Angew. Chem., Int. Ed. Engl.* **1994**, *33*, 847–849.

36) Chen, Y. M.; Chen, C. F.; Xi, F. *Chirality* **1998**, *10*, 661–666.

37) Rosini, C.; Superchi, S.; Peerlings, H. W. I.; Meijer, E. W. *Eur. J. Org. Chem.* **2000**, 61–71.

38) a) Omotowa, B. A.; Keefer, K. D.; Kirchmeier, R. L.; Shreeve, J. M. *J. Am. Chem. Soc.* **1999**, *121*, 11130–11138. b) Prosa, T. J.; Bauer, B. J.; Amis, E. J.; Tomalia, D. A.; Scherrenberg, R. *J. Polym. Sci., Part B, Polym. Phys.* **1997**, *35*, 2913–2924. c) Cho, B. –K.; Jain, A.; Nieberle, J.; Mahajan, S.; Wiesner, U. *Macromolecules* **2004**, *37*, 4227–4234.

39) Pötschke, D.; Ballauff, M.; Lindner, P.; Fischer, M.; Vögtle, F. *Macromolecules* **1999**, *32*, 4079–4087.

40) a) Rietveld, I. B.; Smit, J. A.M. *Macromolecules* **1999**, *32*, 4608–4614. b) Li, X.; He, X.; Ng, A. C. H.; Wu, C.; Ng, D. K. P. *Macromolecules* **2000**, *33*, 2119–2123.

41) a) Veerman, J. A.; Levi, S. A.; van Veggel, F. C. J. M.; Reinhoudt, D. N.; van Hulst, N. F. *J. Phys. Chem., A* **1999**, *103*, 11264–11270. b) Widmer, I.; Hubler, U.; Stöhr, M.; Merz, L.; Güntherodt, H. –J.; Hermann, B. A.; Samori, P.; Rabe, J. P.; Rheiner, P. B.; Greiveldinger, G.; Murer, P. *Helv. Chim. Acta* **2002**, *85*, 4255–4263.

42) a) Svenson, S.; Tomalia, D. A. *Advancd drug delivery review* **2005**, *57*, 2106–2129. b) Lee, C. C.; MacKay, J. A.; Fréchet, J. M. J.; Szoka, F. C. *Nat. Biotechnol.* **2005**, *23*, 1517–1526. c) Tolia, G. T; Choi, H. H. *Pharm. Tech.* **2008**, *32*, 88–98.

43) a) Malik, N.; Evagorou, E. G.; Duncan, R. *Anticancer Drugs*, **1999**, *10*, 767–776. b Wiener, E. C.; Brechbiel, M. W.; Brothers, H.; Magin, R. L.; Gansow, O. A.; Tomalia, D. A.; Lauterbur, P. C. *Magn. Reson. Med.* **1994**, *31*, 1–8. c Dunphy, I.; Vinogradov, S. A.; Wilson, D. F. *Anal. Biochem.* **2002**, *310*, 191–198. d) Duan, X.; Sheardown, H. *Biomaterials*, 2006, 27, 4608–4617.

44) Newkome, G. R.; Moorefield, C. N.; Baker, G. R.; Saunders, M. J.; Grossman, S. H. *Angew. Chem., Int. Ed. Engl.* **1991**, *30*, 1178–1181.

45) a) Jansen, J. F. G. A.; de Brabander-van den Berg, E. M. M.; Meijer, E. W. *Science* **1994**, *265*, 1226–1229. b) Jansen, J. F. G. A.; de Brabander-van den Berg, E. M. M.; Meijer, E. W. *New Molecular architectures and functions, Proceedings of the OUMS 1995*, Toyonaka, Osaka, Japan; June 2–5,1995; Springer-Verlag: Berlin Heidelberg, 1996.

46) a) Rheiner, P. B.; Seebach, D. *Chem. Eur. J.* **1999**, *5*, 3221–3236. b) Reetz, M. T.; Lohmer, G.; Schwickardi, R. *Angew. Chem., Int. Ed. Engl.* **1997**, *36*, 1526–1529.

47) a) Pan, B.F.; Cui, D.X.; Xu, P.; Huang, T.; Li, Q.; He, R.; Gao, F. *J. Biomed. Pharm. Eng.* **2007**, 13–16. b) Kohli, N.; Dvornic, P. R.; Kaganove, S. N.; Worden, R. M.; Lee, I. *Macromol. Rapid Commun.* **2004**, 25, 935–941.

48) Yu, S.; Wong, T. K. S.; Hu, X.; Pita, K. *Chem. Phys. Lett.* **2004**, *384*, 63–67.

49) Amama, P. B.; Maschmann, M. R.; Fisher, T. S.; Sands, T. D. *J. Phys. Chem. B* **2006**, *110*, 10636–10644.

50) Tanaka,Y.; Nemoto,T.; Naka, K.; Chujo, Y. *Polym.Bull. (Berlin)* **2000**, *45*, 447–450.

51) Burkinshaw, S. M.; Mignanelli, M.; Froehling, P. E.; Bide, M. J. *Dyes Pigm.* **2000**, *47*, 259–267.

52) Giansante, C.; Ceroni, P.; Balzani, V.; Vögtle, F. *Angew. Chem.* **2008**, *120*, 5502–5505.

53) Z. E. Hughes; M. R. Wilson; L. M. Stimson *Soft Matte* **2005**, *1*, 436–443.

54) Newkome, G. R.; He, E.; Moorefield, C. N. *Chem. Rev.* **1999**, *99*, 1689–1746.

55) Knapen, J. W. J.; van der Made, A. W.; de Wilde, J. C.; van Leeuwen, P. W. W. N. M.; Wijkens, P.; Grove, D. M.; van Koten, G. *Nature* **1994**, *372*, 659–663.

56) Wijkens, P.; Jastrzebski, J. T. B. H.; van der Schaaf, P. A.; Kolly, R.;, Hafner, A.; van Koten, G. *Org. Lett.* **2000**, *2*, 1621–1624.

57) Meijboom, R.; Hutton, A. T.; Moss, J. R. *Organometallics* **2003**, *22*, 1811–1815,

58) Nithyanandhan, J.; Jayaraman, N *Tetrahedron* **2006**, *62*, 6228–6235.

59) Baars, M. W. P. L.; Kleppinger, R.; Koch, M. H. J.; Yeu, S. –L.; Meijer, E.W. *Angew. Chem. Int. Ed.* **2000**, *39*, 1285–1288.

60) Chechik, V.; Zhao, M.; Crooks, R. M. *J. Am. Chem. Soc.* **1999**, *121*, 4910–4911.

61) Hecht, S. *J. Polym. Sci. A* **2003**, *41*, 1047–1058.

62) Lochmann, L.; Wooley, K. L.; Ivanova, P. T.; Fréchet, J. M. J. *J. Am. Chem. Soc.* **1993**, *115*, 7043–7044.

63) L. J. Twyman *Tetrahedron Lett.* **2000**, *41*, 6875–6878.

64) Liang, C. O.; Fréchet, J. M. J. *Macromolecules*, **2005**, *38*, 6276–6284.

65) Bernhardt, S.; Baumgarten, M.; Wagner, M.; Müllen, K *J. Am. Chem. Soc.* **2005,** *127*, 12392–12399.

66) Bernhardt, S.; Baumgarten, M.; Müllen, K *Eur. J. Org. Chem.* **2006**, 2523–2529.

67) Salamończyk, G. M.; Kuźnikowski, M.; Poniatowska, E *Chem. Comm.* **2001**, 2202–2203.

68) Chu, C. C.; Imae, T. *Macromolecules*, **2009**, *42*, 2295–2299.

69) Chow, H. –F; Ng, M. –K; Leung, C. –W; Wang, G. –X *J. Am. Chem. Soc.* **2004,** *126*, 12902–12915.

70) Bo, Z.; Schäfer, A.; Franke, P.; Schlüter, A. D. *Org. Lett.* **2000**, *2*, 1645–1648.

71) Tuchbreiter, A.; Werner, H.; Gade, L. H. *Dalton Trans.* **2005**, 1394–1402.

72) a) Sivanandan, K.; Aathimanikandan, S. V.; Arges, C. G.; Bardeen, C. J.; Thayumanavan, S. *J. Am. Chem. Soc.* **2005**, *127*, 2020–2021. b) Rozhkov, V.; Wilson, D.; Vinogradov, S. *Macromolecules* **2002**, *35*, 1991–1993. c) Aathimanikandan, S. V.; Sandanaraj, B. S.; Arges, C. G.; Bardeen, C. J.; Thayumanavan, S. *Org. Lett.* **2005**, *7*, 2809–2812.

73) Zhang, W.; Tichy, S. E.; Pérez, L. M.; Maria, G. C.; Lindahl, P. A.; Simanek, E.E. *J. Am. Chem. Soc.* **2003**, *125*, 5086–5094.

74) a) Lescanec, R. L.; Muthukumar, M. *Macromolecules* **1990**, *23*, 2280–2288. b) Boris, D.; Rubinstein, M. *Macromolecules* **1996**, *29*, 7251–7260. c) Miklis, P.; Çagin, T.; Goddard, W. A., III *J. Am. Chem. Soc.* **1997**, *119*, 7458–7462. d) Cavallo, L.; Fraternali, F. *Chem. Eur. J.* **1998**, *4*, 927–934.

75) a) Mourey, T. H.; Turner, S. R.;Rubinstein, M.; Fréchet, J. M. J.; Hawker, C. J.; Wooley, K. L. *Macromolecules* **1992**, *25*, 2401–2406. b) Meltzer, A. D.; Tirrel, D. A.; Jones, A. A.; Inglefield, P. T. *Macromolecules* **1992**, *25*, 4549–4552. c) Scherrenberg, R.; Coussens, B.; van Vliet, P.; Edouard, G.; Brackman, J.; de Brabander, E.; Mortensen, K. *Macromolecules* **1998**, *31*, 456–461.

76) a) Percec, V.; Johansson, G.; Ungar, G.; Zhou, J. *J. Am. Chem. Soc.* **1996**, *118*, 9855–9866. b) Balagurusamy, V. S. K.; Ungar, G.; Percec, V.; Johansson, G. *J. Am. Chem. Soc.* **1997**, *119*, 1539–1555. c) Duan, R. G.; Miller, L. L.; Tomalia, D. A. *J. Am. Chem. Soc.* **1995**, *117*, 10783–10784. d) Miller, L. L.; Kunugi, Y.; Canavesi, A.; Rigaut, S.; Moorefield, C. N.; Newkome, G. R. *Chem. Mater.* **1998**, *10*, 1751–1754. e) Bosman, A. W.; Bruining, M. J.; Kooijman, H.; Spek, A. L.; Janssen, R. A. J.; Meijer, E. W. *J. Am. Chem. Soc.* **1998**, *120*, 8547–8548.

77) a) Takahashi, S.; Kuroyama, Y.; Sonogashira, K.; Hagihara, N *Synthesis* **1980**, 627–630. b) Davidson, L.; Freebairn, K. W.; Russell, A. T.; Trivedi, H. S.; Hayes, W. C. *Synlett* **2002**, 251–254. c) Davidson, L.; Blencowe, A.; Drew, M. G.. B.; Freebairn, K. W.; Hayes, W. *J. Mater. Chem.* **2003**, *13*, 758–766.

78) a) Soomro, S. A.; Benmouna, R.; Berger, R.; Meier, H. *Eur. J. Org. C*hem. **2005**, 3586–3593. b) Rajakumar, P.; Ganesan, K. *Syn. Comm.* **2004**, *34*, 2209–2017.

79) Beinhoff, M.; Karakaya, B.; Schlüter, A. D. *Synthesis* **2003**, *1*, 79–90.

80) Janssen, R. H. A. M.; Lousberg, R. J. J. Ch.; de Bie, M. J. A. *Rec. Trav. Chim.* **1981**, *100*, 85–94.

81) a) Meier, H.; Lehmann, M. *Angew. Chem., Int. Ed.* **1998**, *37*, 643–645. b) Pillow, J. N. G.; Halim, M.; Lupton, J. M.; Burn, P. L.; Samuel, I. D. W. *Macromolecules* **1999**, *32*, 5985–5993. c) Deb, S. K.; Maddux, T. M.; Yu, L. *J. Am. Chem. Soc.* **1997**, *119*, 9079–9080.

82) Díez-Barra, E.; García-Martínez, J. C.; Merino, S.; del Rey, R.; Rodríguez-López, J.; Sánchez-Verdú, P.; Tejeda, J *J. Org. Chem.* **2001**, *66*, 5664–5670.

83) Ono, N; Miyake, H; Saito, T; Kaji, A. *Synthesis* **1980**, 952–953.

84) a) Herriott, A. W.; Picker, D. *J. Am. Chem. Soc.* **1975**, *97*, 2345–2349. b) Herriott, A. W.; Picker, D. *Synthesis* **1975**, 447–448.

85) Ferreira, J. T. B.; Comasseto, J. V.; Braga, A. L. *Syn. Comm.* **1982**, *12*, 595–600.

86) Tran, A. T.; Huynh, V. A.; Friz, E. M.; Whitney, S. K.; Cordes, D. B. *Tetrahedron Lett.* **2009**, *50*, 1817–1819.

87) Chan, T.-L.; Fong, S.; Li, Y.; Man, T.-O.; Poon, C.-D. *J. Chem. Soc., Chem. Commun.* **1994**, 1771-1772.

88) Chi-Wing Leung, *M. Phil. Thesis*, The Chinese University of Hong Kong, 1999.

89) Sun, H.; Kaifer, A. E. *Org. Lett.* **2005**, *7*, 3845–3848.

90) a) de Greef, T. F. A.; Nieuwenhuizen, M. M. L.; Stals, P. J. M.; Fitié, C. F. C.; Palmans, A. R. A.; Sijbesma, R. P.; Meijer, E. M. *Chem. Commun.* **2008**, 4306–4308; b) de Greef, T. F. A.; Nieuwenhuizen, M. M. L.; Sijbesma, R. P.; Meijer, E. W. *J. Org. Chem.* **2010**, *75*, 598–610.

91) Endres, A.; Maas, G. *Tetrahedron* **2002**, *58*, 3999–4005

92) Skulski, L.; Lulinski, P. *Bull. Chem. Soc. Jpn.* **1997**, *70*, 1665–1669

93) Castaldi, M. P.; Gibson,S. E.; Rudd, M.; White, A J. P. *Chem. Eur. J.* **2006**, *12*, 138–148

List of ^{1}H NMR and ^{13}C NMR Spectra of Dendritic Compounds

1H

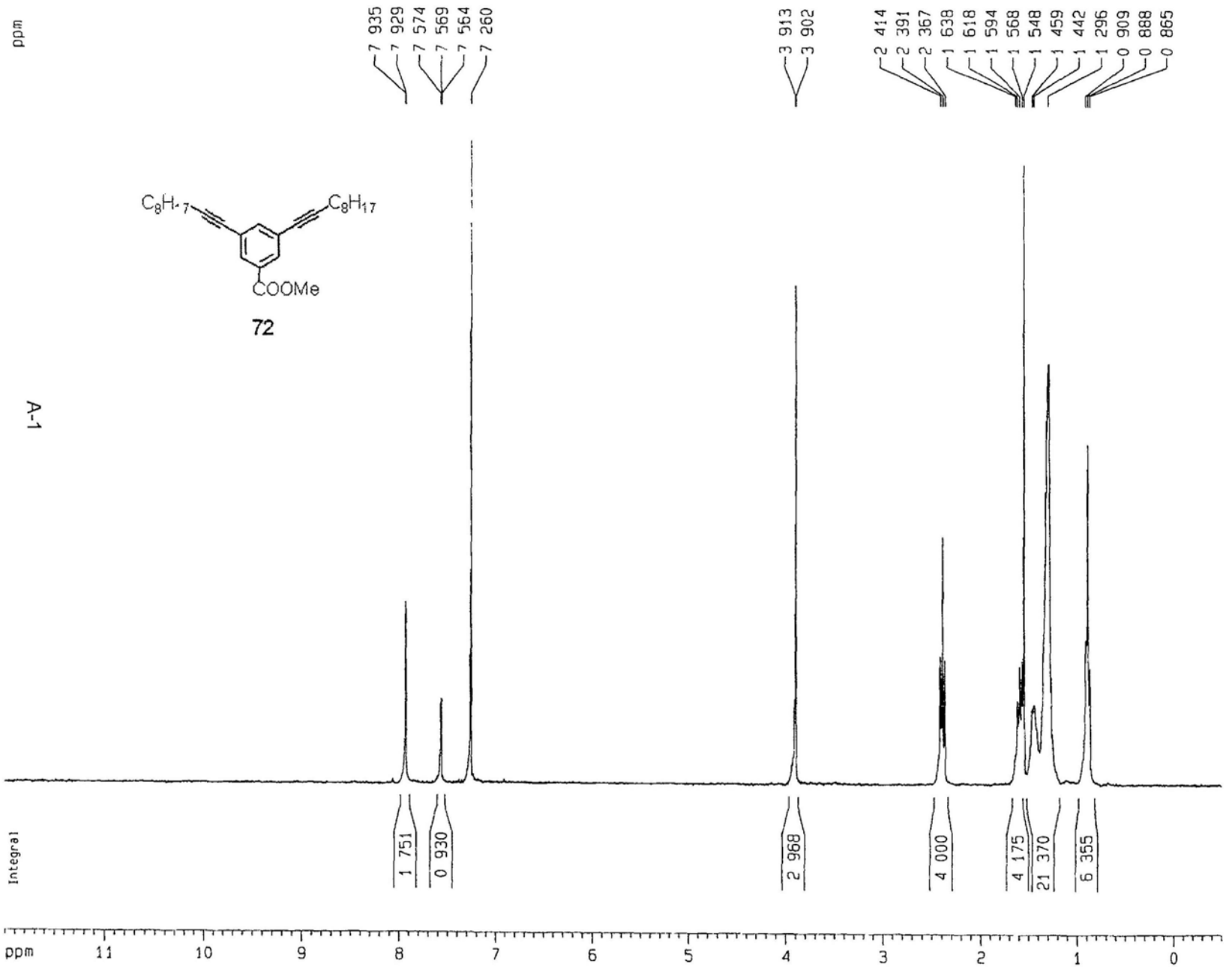

Current Data Parameters
NAME jan031
EXPNO 1
PROCNO 1

F2 - Acquisition Parameters
Date_ 20071205
Time 9 21
INSTRUM dpx300
PROBHD 5 mm BBO BB-1H
PULPROG zg
TD 32768
SOLVENT CDCl3
NS 8
DS 0
SWH 8992 806 Hz
FIDRES 0 274439 Hz
AQ 1 8219508 sec
RG 512
DW 55 600 usec
DE 79 43 usec
TE 0 0 K
D1 5 00000000 sec
MCREST 0 00000000 sec
MCWRK 0 01500000 sec

======== CHANNEL f1 ========
NUC1 1H
P1 5 00 usec
PL1 -2 00 dB
SFO1 300 1312000 MHz

F2 - Processing parameters
SI 32768
SF 300 1300066 MHz
WDW EM
SSB 0
LB 0 30 Hz
GB 0
PC 1 00

1D NMR plot parameters
CX 22 00 cm
CY 11 57 cm
F1P 12 000 ppm
F1 3601 56 Hz
F2P -0 500 ppm
F2 -150 07 Hz
PPMCM 0 56818 ppm/cm
HZCM 170 52841 Hz/cm

C13

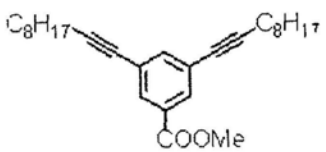

72

A-2

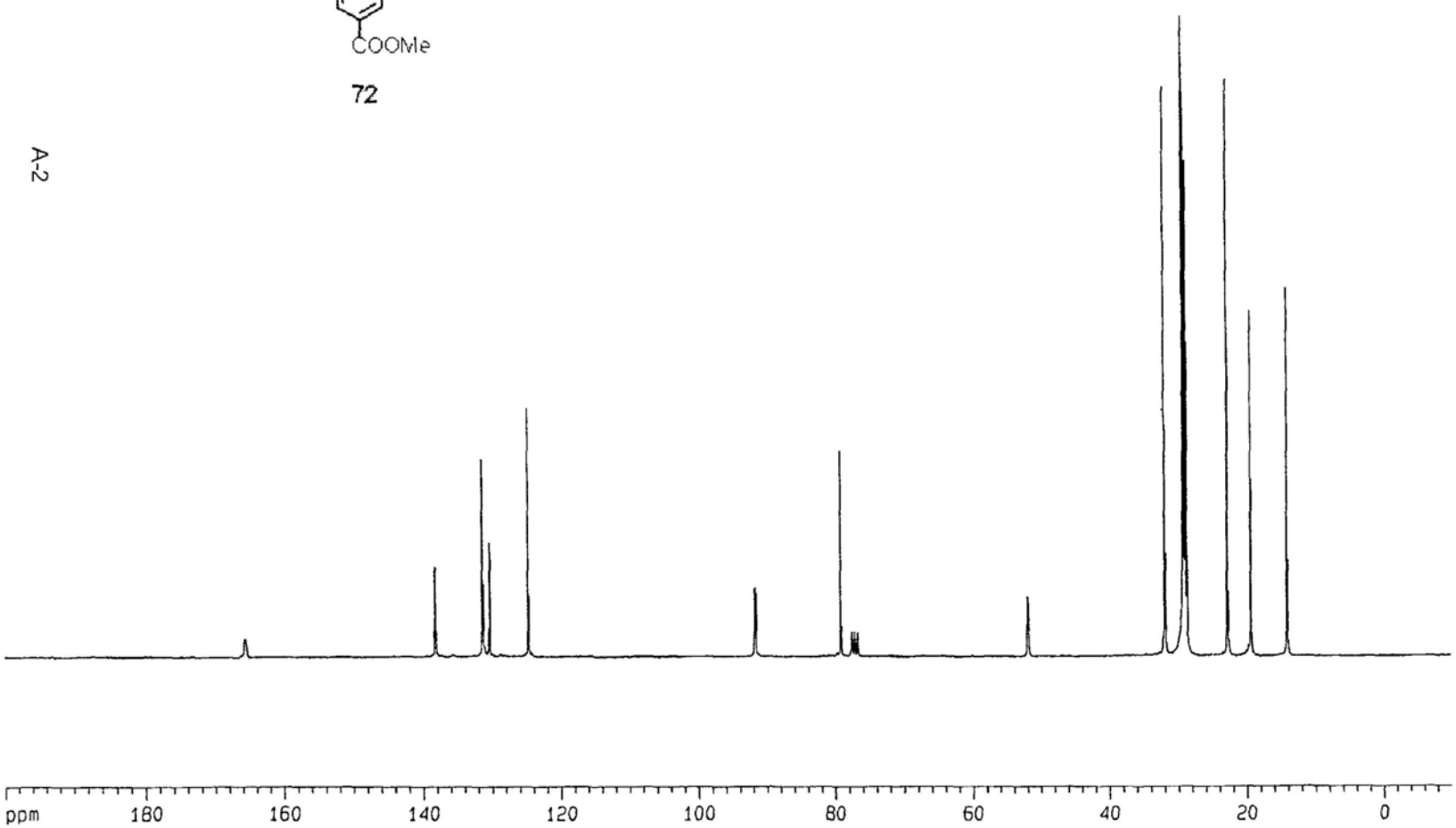


```
Current Data Parameters
NAME            jan031-c
EXPNO                  1
PROCNO                 1

F2 - Acquisition Parameters
Date_          20071205
Time               9 33
INSTRUM          dpx300
PROBHD   5 mm BBO BB-1H
PULPROG            zgdc
TD                65536
SOLVENT           CDCl3
NS                  467
DS                    0
SWH          22675.736 Hz
FIDRES        0.346004 Hz
AQ            1.4451188 sec
RG                 8192
DW               22.050 usec
DE                6.00 usec
TE                 0.0 K
D1            1.00000000 sec
d11           0.03000000 sec
MCREST        0.00000000 sec
MCWRK         0.01500000 sec

======== CHANNEL f1 ========
NUC1                13C
P1                3.00 usec
PL1              -6.00 dB
SFO1         75.4745111 MHz

======== CHANNEL f2 ========
CPDPRG2         waltz16
NUC2                1H
PCPD2          100.00 usec
PL2            120.00 dB
PL12            19.00 dB
SFO2        300.1315007 MHz

F2 - Processing parameters
SI                 65536
SF          75.4677465 MHz
WDW                   EM
SSB                   0
LB                3.00 Hz
GB                    0
PC                 1.40

1D NMR plot parameters
CX               22.00 cm
CY                9.70 cm
F1P             200.000 ppm
F1            15093.55 Hz
F2P             -10.000 ppm
F2             -754.68 Hz
PPMCM            9.54545 ppm/cm
HZCM           720.37384 Hz/cm
```

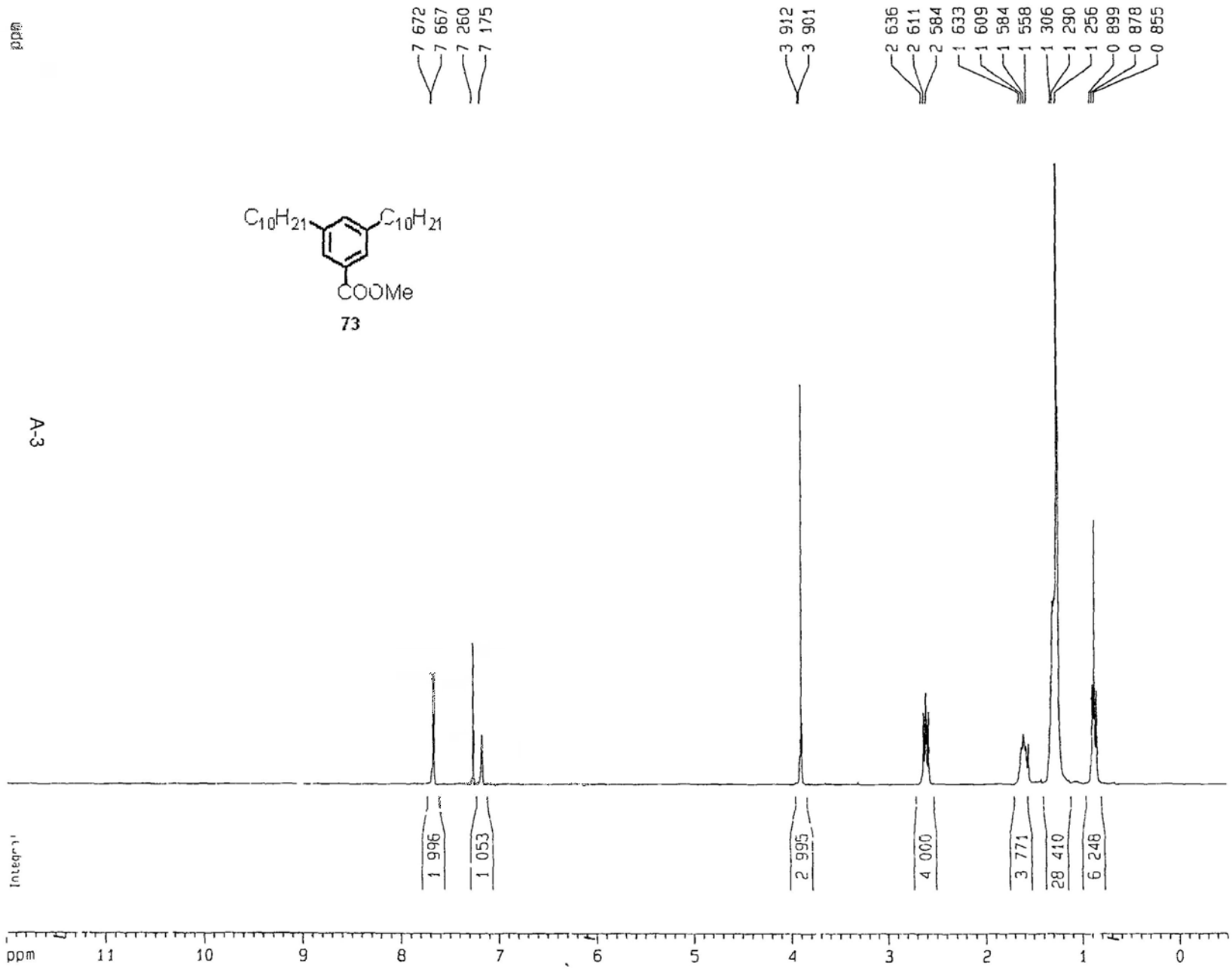

Current Data Parameters

NAME	jan032
EXPNO	1
PROCNO	1

F2 - Acquisition Parameters

Date_	20070908
Time	8 48
INSTRUM	dpx300
PROBHD	5 mm BBO BB-1H
PULPROG	zg
TD	32768
SOLVENT	CDCl3
NS	8
DS	0
SWH	8992 806 Hz
FIDRES	0 274439 Hz
AQ	1 8219508 sec
RG	228 1
DW	55 600 usec
DE	79 43 usec
TE	0 0 K
D1	5 00000000 sec
MCREST	0 00000000 sec
MCWRK	0 01500000 sec

======== CHANNEL f1 ========

NUC1	1H
P1	5 00 usec
PL1	-2 00 dB
SFO1	300 1312000 MHz

F2 - Processing parameters

SI	32768
SF	300 1300063 MHz
WDW	EM
SSB	0
LB	0 30 Hz
GB	0
PC	1 00

1D NMR plot parameters

CX	22 00 cm
CY	11 17 cm
F1P	12 000 ppm
F1	3601 56 Hz
F2P	-0 500 ppm
F2	-150 07 Hz
PPMCM	0 56818 ppm/cm
HZCM	170 52841 Hz/cm

C13

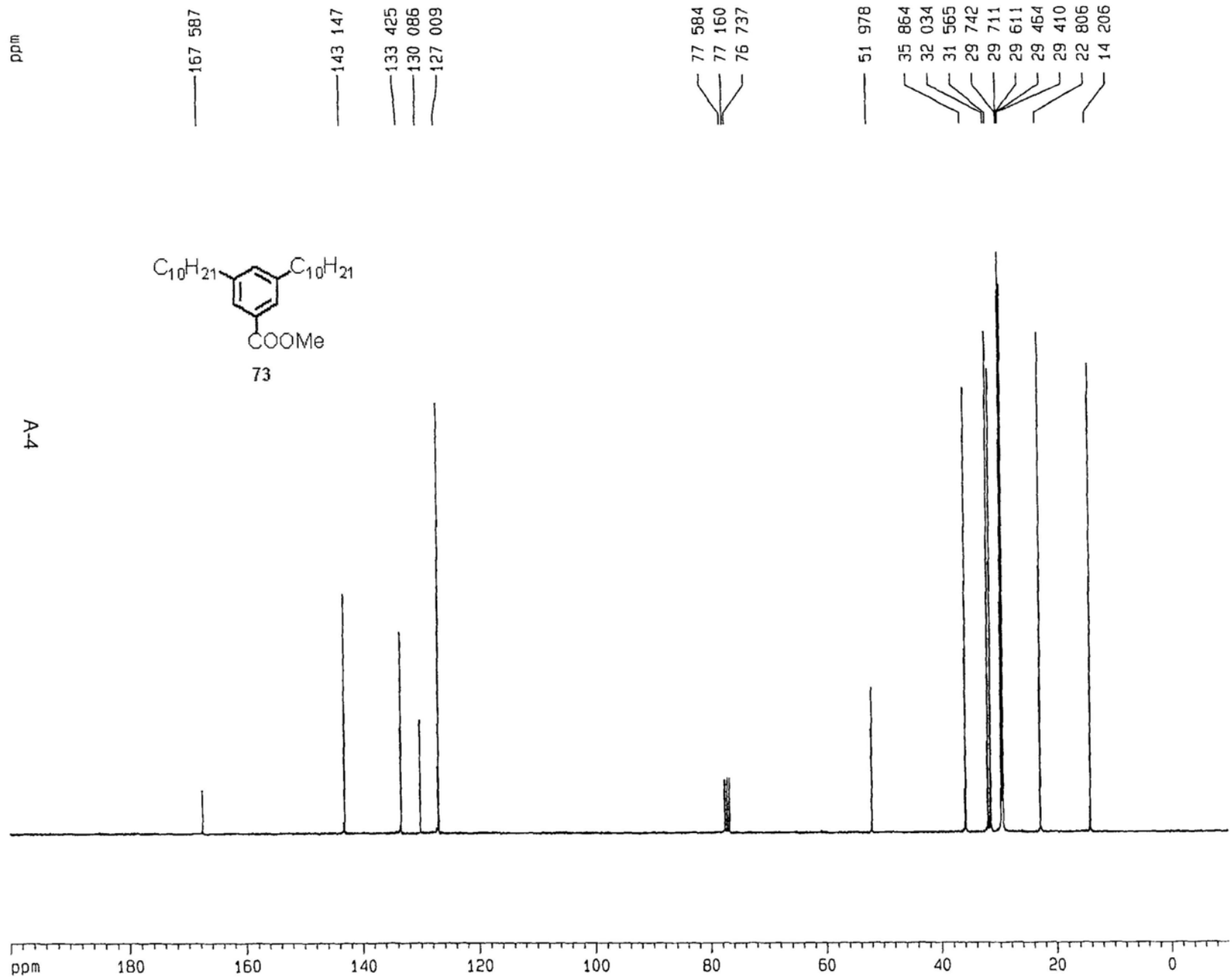

Current Data Parameters

NAME	jan032-c
EXPNO	1
PROCNO	1

F2 - Acquisition Parameters

Date_	20050525
Time	9 14
INSTRUM	dpx300
PROBHD	5 mm BBO BB-1H
PULPROG	zgdc
TD	65536
SOLVENT	CDCl3
NS	415
DS	0
SWH	22675 736 Hz
FIDRES	0 346004 Hz
AQ	1 4451188 sec
RG	8192
DW	22 050 usec
DE	6 00 usec
TE	296 2 K
D1	1 00000000 sec
d11	0 03000000 sec
MCREST	0 00000000 sec
MCWRK	0 01500000 sec

======== CHANNEL f1 ========

NUC1	13C
P1	3 00 usec
PL1	-6 00 dB
SFO1	75 4745111 MHz

======== CHANNEL f2 ========

CPDPRG2	waltz16
NUC2	1H
PCPD2	100 00 usec
PL2	120 00 dB
PL12	19 00 dB
SFO2	300 1315007 MHz

F2 - Processing parameters

SI	65536
SF	75 4677424 MHz
WDW	EM
SSB	0
LB	1 00 Hz
GB	0
PC	1 40

1D NMR plot parameters

CX	22 00 cm
CY	10 48 cm
F1P	200 000 ppm
F1	15093 55 Hz
F2P	-10 000 ppm
F2	-754 68 Hz
PPMCM	9 54545 ppm/cm
HZCM	720 37384 Hz/cm

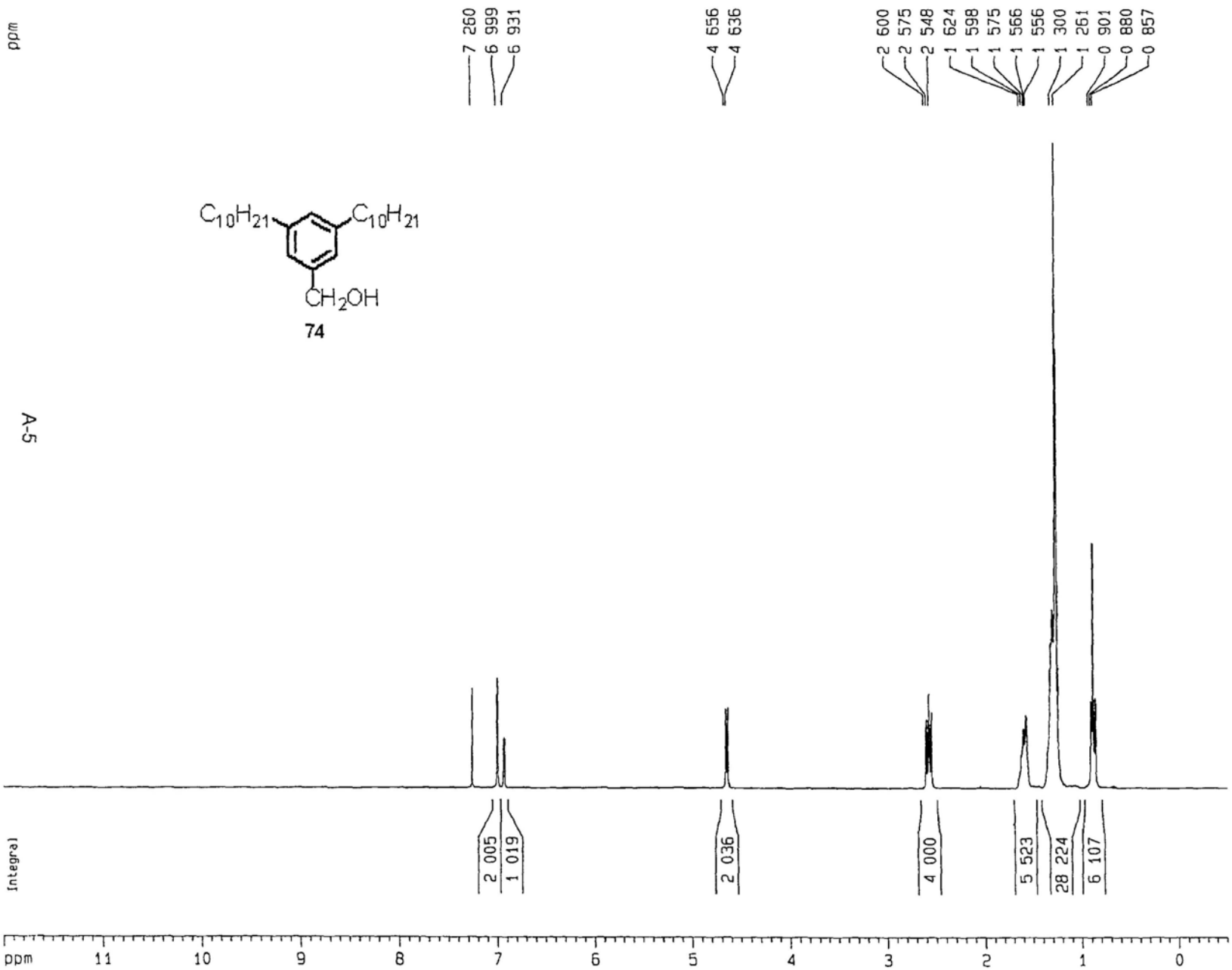

Current Data Parameters

NAME	jan033
EXPNO	1
PROCNO	1

F2 - Acquisition Parameters

Date_	20050727
Time	12 15
INSTRUM	dpx300
PROBHD	5 mm BBO BB-1H
PULPROG	zg
TD	32768
SOLVENT	CDCl3
NS	8
DS	0
SWH	8992 806 Hz
FIDRES	0 274439 Hz
AQ	1 8219508 sec
RG	203 2
DW	55 600 usec
DE	79 43 usec
TE	296 2 K
D1	5 00000000 sec
MCREST	0 00000000 sec
MCWRK	0 01500000 sec

======== CHANNEL f1 ========

NUC1	1H
P1	5 00 usec
PL1	-2 00 dB
SFO1	300 1312000 MHz

F2 - Processing parameters

SI	32768
SF	300 1300066 MHz
WDW	EM
SSB	0
LB	0 30 Hz
GB	0
PC	1 00

1D NMR plot parameters

CX	22 00 cm
CY	11 54 cm
F1P	12 000 ppm
F1	3601 56 Hz
F2P	-0 500 ppm
F2	-150 07 Hz
PPMCM	0 56818 ppm/cm
HZCM	170 52841 Hz/cm

C13

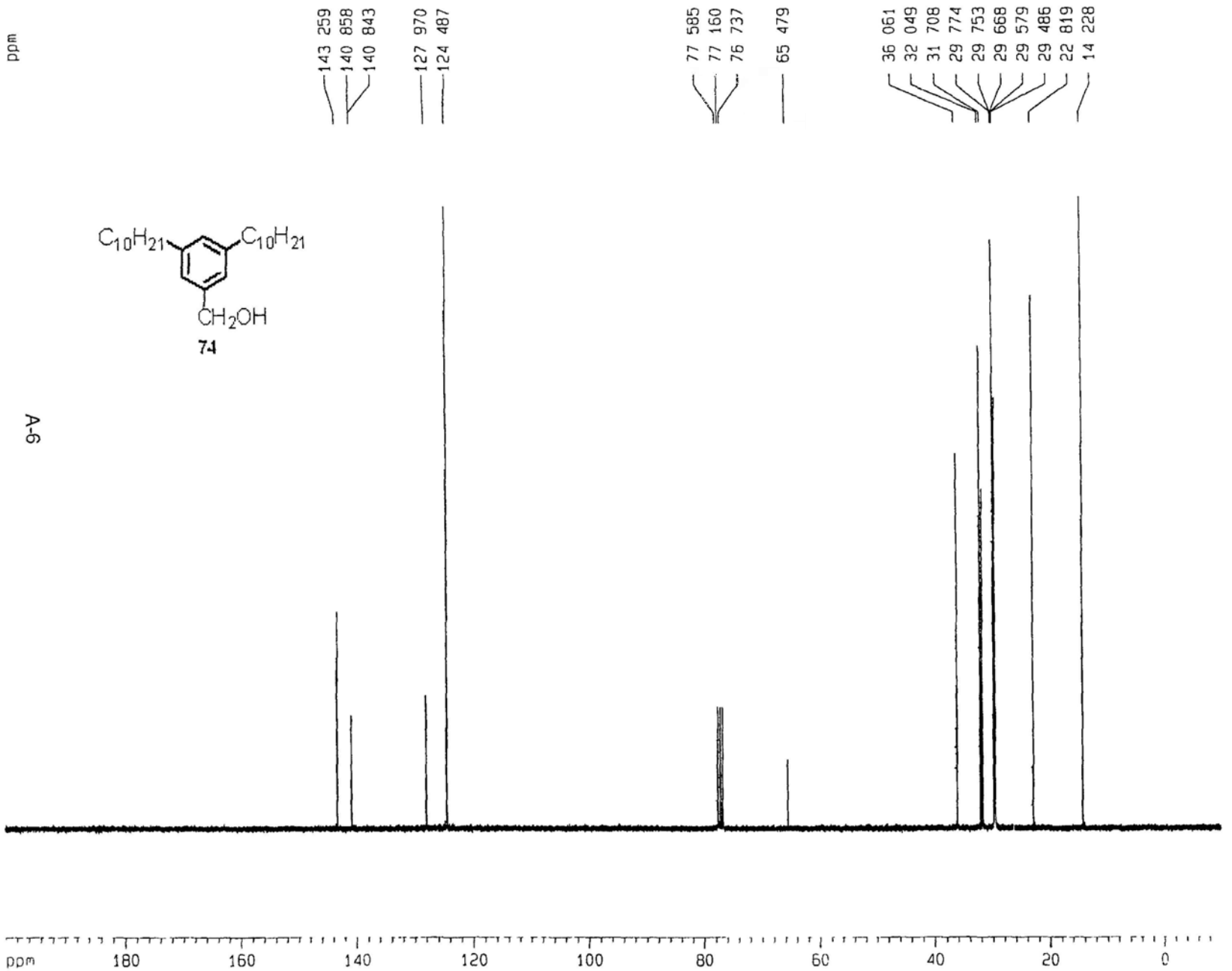

Current Data Parameters

NAME	G1-CH2OH-c
EXPNO	1
PROCNO	1

F2 - Acquisition Parameters

Date_	20050514
Time	9 28
INSTRUM	dpx300
PROBHD	5 mm BBO BB-1H
PULPROG	zgdc
TD	65536
SOLVENT	CDCl3
NS	198
DS	0
SWH	22675 736 Hz
FIDRES	0 346004 Hz
AQ	1 4451188 sec
RG	8192
DW	22 050 usec
DE	6 00 usec
TE	297 2 K
D1	10 00000000 sec
d11	0 03000000 sec
MCREST	0 00000000 sec
MCWRK	0 01500000 sec

======== CHANNEL f1 ========

NUC1	13C
P1	3 00 usec
PL1	-6 00 dB
SFO1	75 4745111 MHz

======== CHANNEL f2 ========

CPDPRG2	waltz16
NUC2	1H
PCPD2	100 00 usec
PL2	120 00 dB
PL12	19 00 dB
SFO2	300 1315007 MHz

F2 - Processing parameters

SI	65536
SF	75 4677453 MHz
WDW	EM
SSB	0
LB	0 00 Hz
GB	0
PC	1 40

1D NMR plot parameters

CX	22 00 cm
CY	11 59 cm
F1P	200 000 ppm
F1	15093 55 Hz
F2P	-10 000 ppm
F2	-754 68 Hz
PPMCM	9 54545 ppm/cm
HZCM	720 37384 Hz/cm

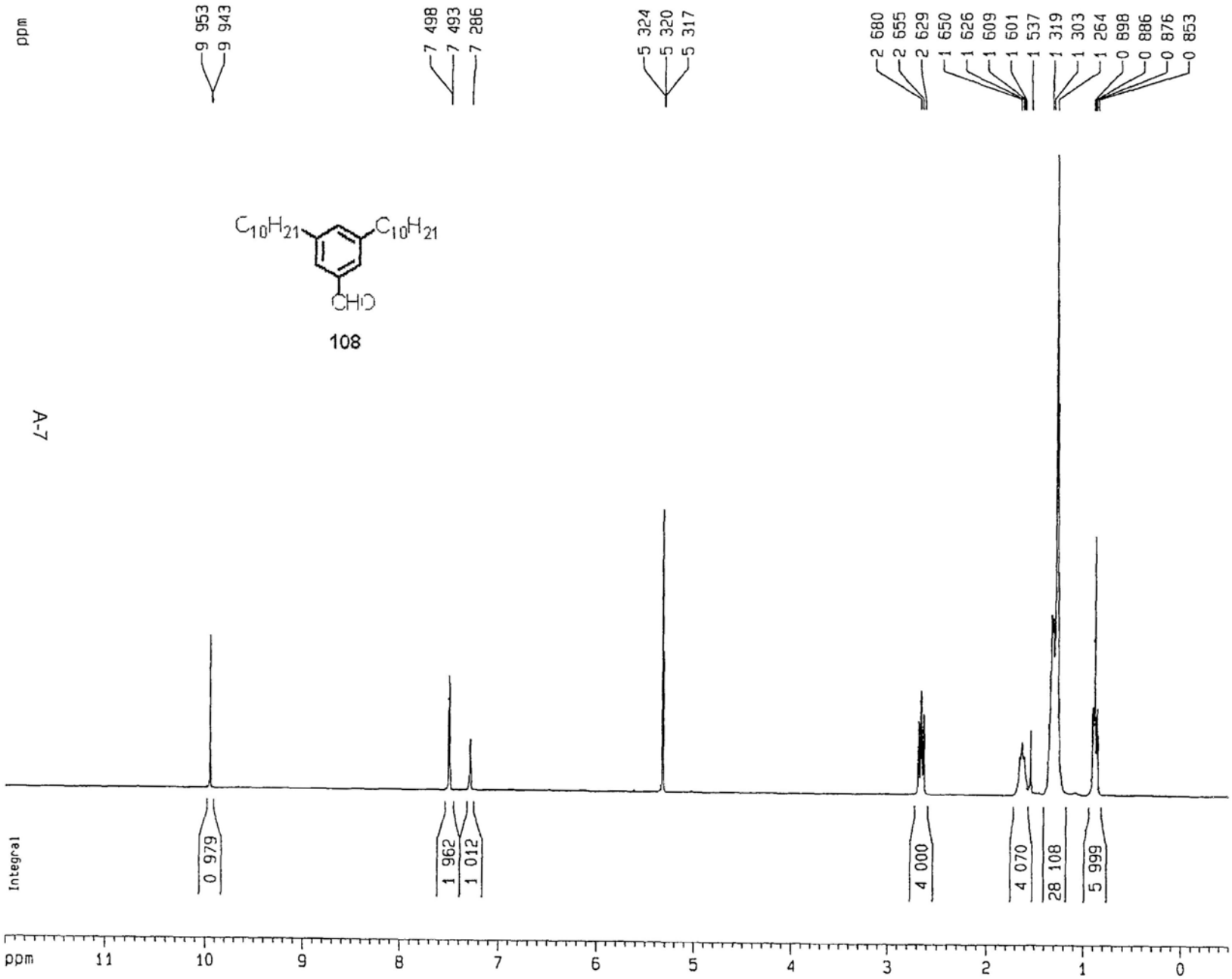

Current Data Parameters
NAME G1-CHO-dDCM
EXPNO 1
PROCNO 1

F2 - Acquisition Parameters
Date_ 20080312
Time 16 28
INSTRUM dpx300
PROBHD 5 mm BBO BB-1H
PULPROG zg
TD 32768
SOLVENT CD2Cl2
NS 16
DS 0
SWH 8992 806 Hz
FIDRES 0 274439 Hz
AQ 1 8219508 sec
RG 203 2
DW 55 600 usec
DE 79 43 usec
TE 295 2 K
D1 5 00000000 sec
MCREST 0 00000000 sec
MCWRK 0 01500000 sec

======== CHANNEL f1 ========
NUC1 1H
P1 5 00 usec
PL1 -2 00 dB
SFO1 300 1312000 MHz

F2 - Processing parameters
SI 32768
SF 300 1300108 MHz
WDW EM
SSB 0
LB 0 30 Hz
GB 0
PC 1 00

1D NMR plot parameters
CX 22 00 cm
CY 11 43 cm
F1P 12 000 ppm
F1 3601 56 Hz
F2P -0 500 ppm
F2 -150 07 Hz
PPMCM 0 56818 ppm/cm
HZCM 170 52841 Hz/cm

C13

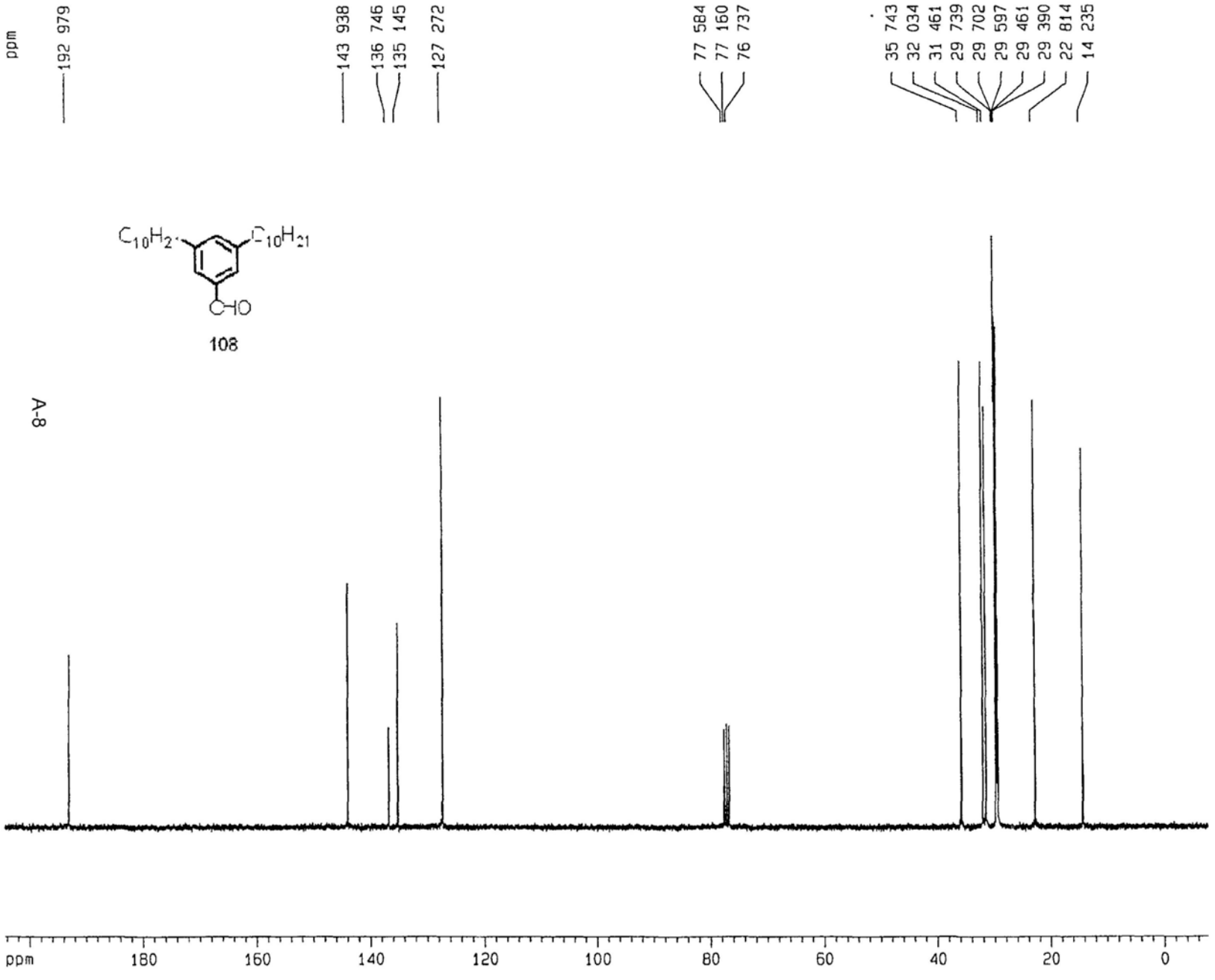


```
Current Data Parameters
NAME                 G1-CHO(c)
EXPNO                        1
PROCNO                       1

F2 - Acquisition Parameters
Date_               20061205
Time                   18 23
INSTRUM                dpx300
PROBHD   5 mm BBO BB-1H
PULPROG                 zgdc
TD                     65536
SOLVENT                CDCl3
NS                       220
DS                         0
SWH              22675 736 Hz
FIDRES           0 346004 Hz
AQ               1 4451188 sec
RG                  7298 2
DW                  22 050 usec
DE                   6 00 usec
TE                   0 0 K
D1               1 00000000 sec
d11              0 03000000 sec
MCREST           0 00000000 sec
MCWRK            0 01500000 sec

======== CHANNEL f1 ========
NUC1                    13C
P1                   3 00 usec
PL1                 -6 00 dB
SFO1            75 4745111 MHz

======== CHANNEL f2 ========
CPDPRG2              waltz16
NUC2                    1H
PCPD2              100 00 usec
PL2                120 00 dB
PL12                19 00 dB
SFO2           300 1315007 MHz

F2 - Processing parameters
SI                     65536
SF              75 4677410 MHz
WDW                       EM
SSB                        0
LB                   1 00 Hz
GB                         0
PC                    1 40

1D NMR plot parameters
CX                  22 00 cm
CY                  10 70 cm
F1P               204 375 ppm
F1                15423 75 Hz
F2P                -7 698 ppm
F2                -580 97 Hz
PPMCM             9 63972 ppm/cm
HZCM             727 48755 Hz/cm
```

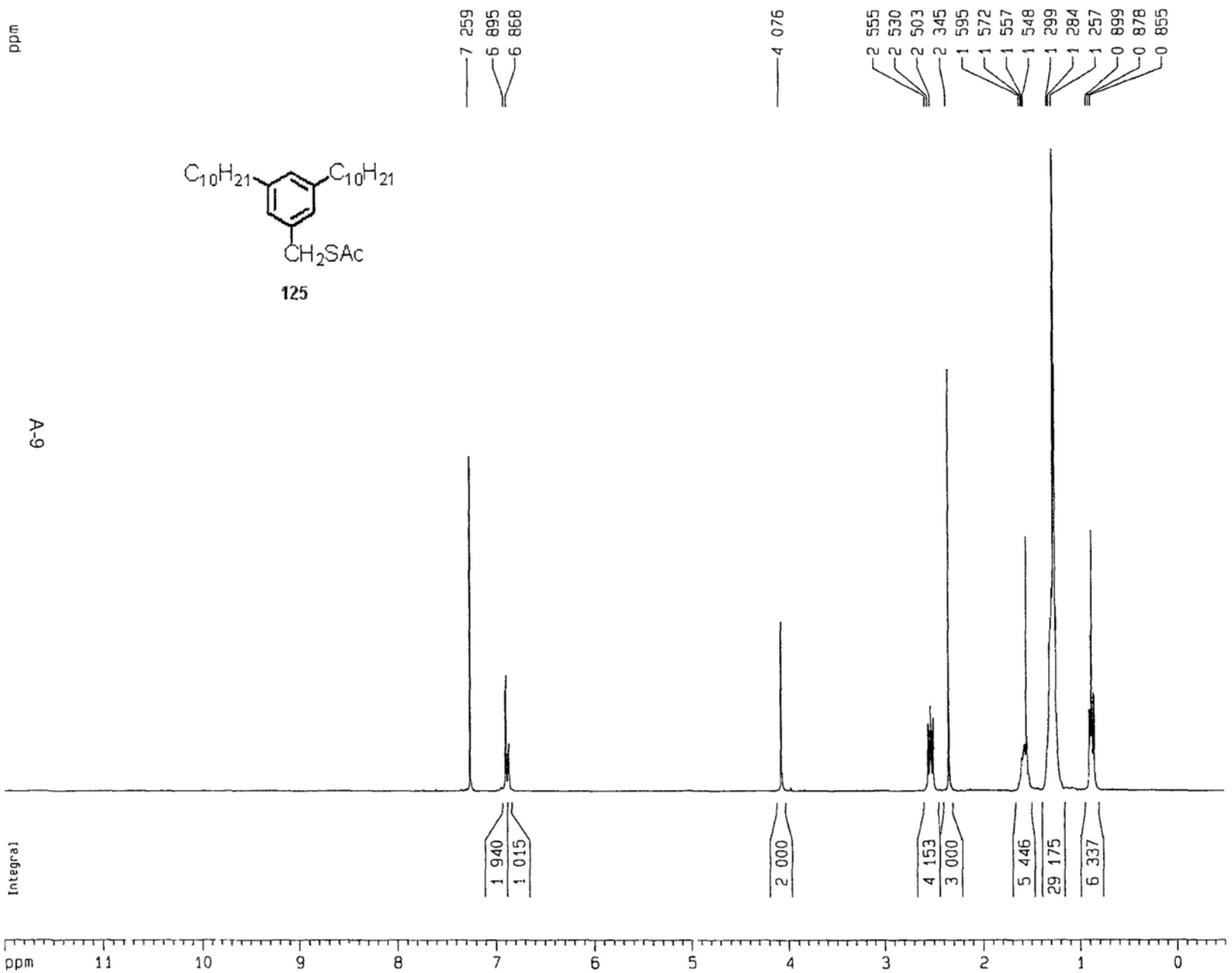

Current Data Parameters
NAME)an034-t1
EXPNO 1
PROCNO 1

F2 - Acquisition Parameters
Date_ 20070323
Time 21 19
INSTRUM dpx300
PROBHD 5 mm BBO BB-1H
PULPROG zg
TD 32768
SOLVENT CDCl3
NS 8
DS 0
SWH 8992 806 Hz
FIDRES 0 274439 Hz
AQ 1 8219508 sec
RG 362
DW 55 600 usec
DE 79 43 usec
TE 0 0 K
D1 5 00000000 sec
MCREST 0 00000000 sec
MCWRK 0 01500000 sec

======== CHANNEL f1 ========
NUC1 1H
P1 5 00 usec
PL1 -2 00 dB
SFO1 300 1312000 MHz

F2 - Processing parameters
SI 32768
SF 300 1300066 MHz
WDW EM
SSB 0
LB 0 30 Hz
GB 0
PC 1 00

1D NMR plot parameters
CX 22 00 cm
CY 11 47 cm
F1P 12 000 ppm
F1 3601 56 Hz
F2P -0 500 ppm
F2 -150 07 Hz
PPMCM 0 56818 ppm/cm
HZCM 170 52840 Hz/cm

C13

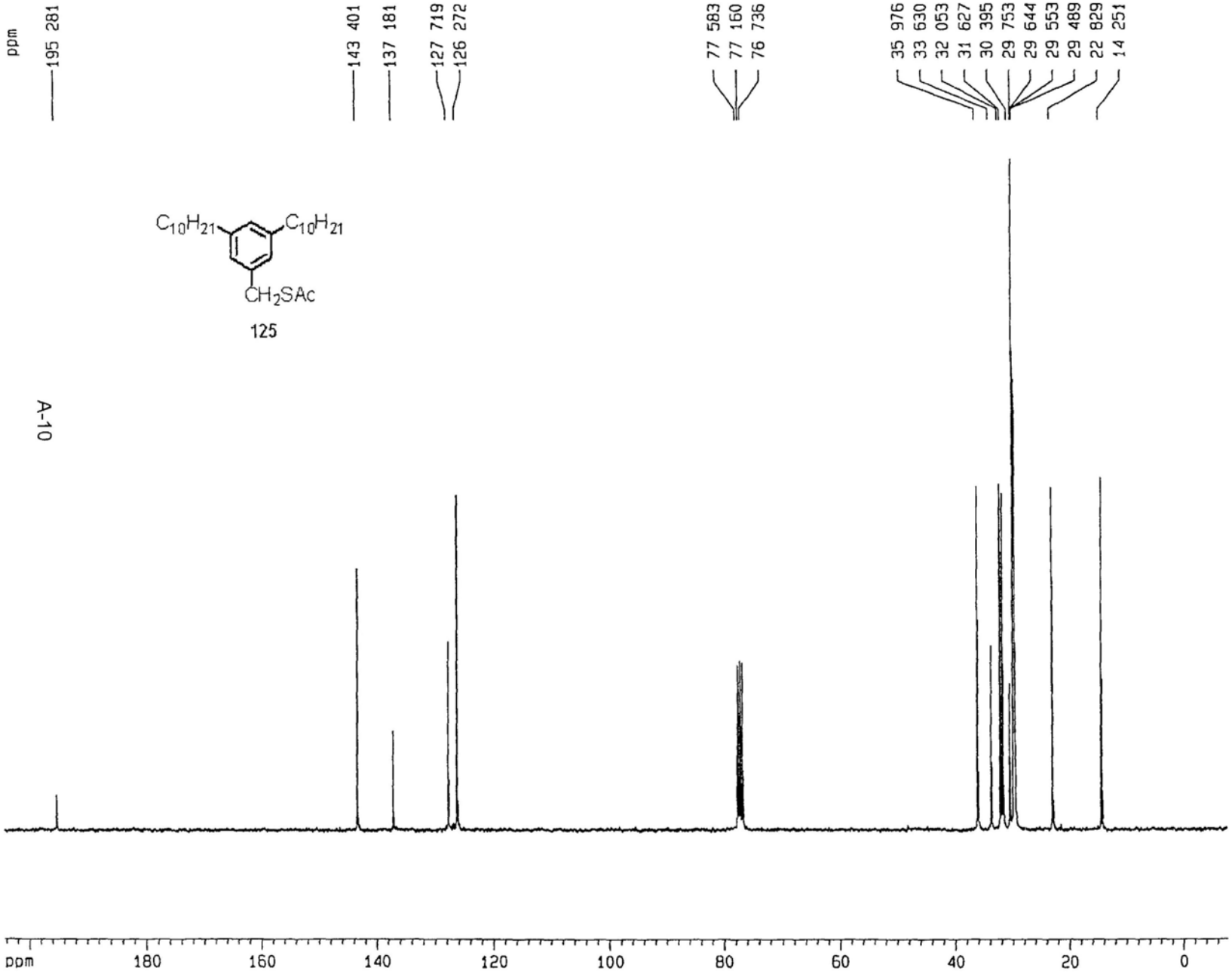

Current Data Parameters

NAME	jan034-c13
EXPNO	1
PROCNO	1

F2 - Acquisition Parameters

Date_	20050531
Time	18 18
INSTRUM	dpx300
PROBHD	5 mm BBO BB-1H
PULPROG	zgdc
TD	65536
SOLVENT	CDCl3
NS	519
DS	0
SWH	22675 736 Hz
FIDRES	0 346004 Hz
AQ	1 4451188 sec
RG	8192
DW	22 050 usec
DE	6 00 usec
TE	295 2 K
D1	1 00000000 sec
d11	0 03000000 sec
MCREST	0 00000000 sec
MCWRK	0 01500000 sec

======== CHANNEL f1 ========

NUC1	13C
P1	3 00 usec
PL1	-6 00 dB
SFO1	75 4745111 MHz

======== CHANNEL f2 ========

CPDPRG2	waltz16
NUC2	1H
PCPD2	100 00 usec
PL2	120 00 dB
PL12	19 00 dB
SFO2	300 1315007 MHz

F2 - Processing parameters

SI	65536
SF	75 4677434 MHz
WDW	EM
SSB	0
LB	3 00 Hz
GB	0
PC	1 40

1D NMR plot parameters

CX	22 00 cm
CY	12 00 cm
F1P	204 375 ppm
F1	15423 75 Hz
F2P	-7 698 ppm
F2	-580 97 Hz
PPMCM	9 63972 ppm/cm
HZCM	727 48755 Hz/cm

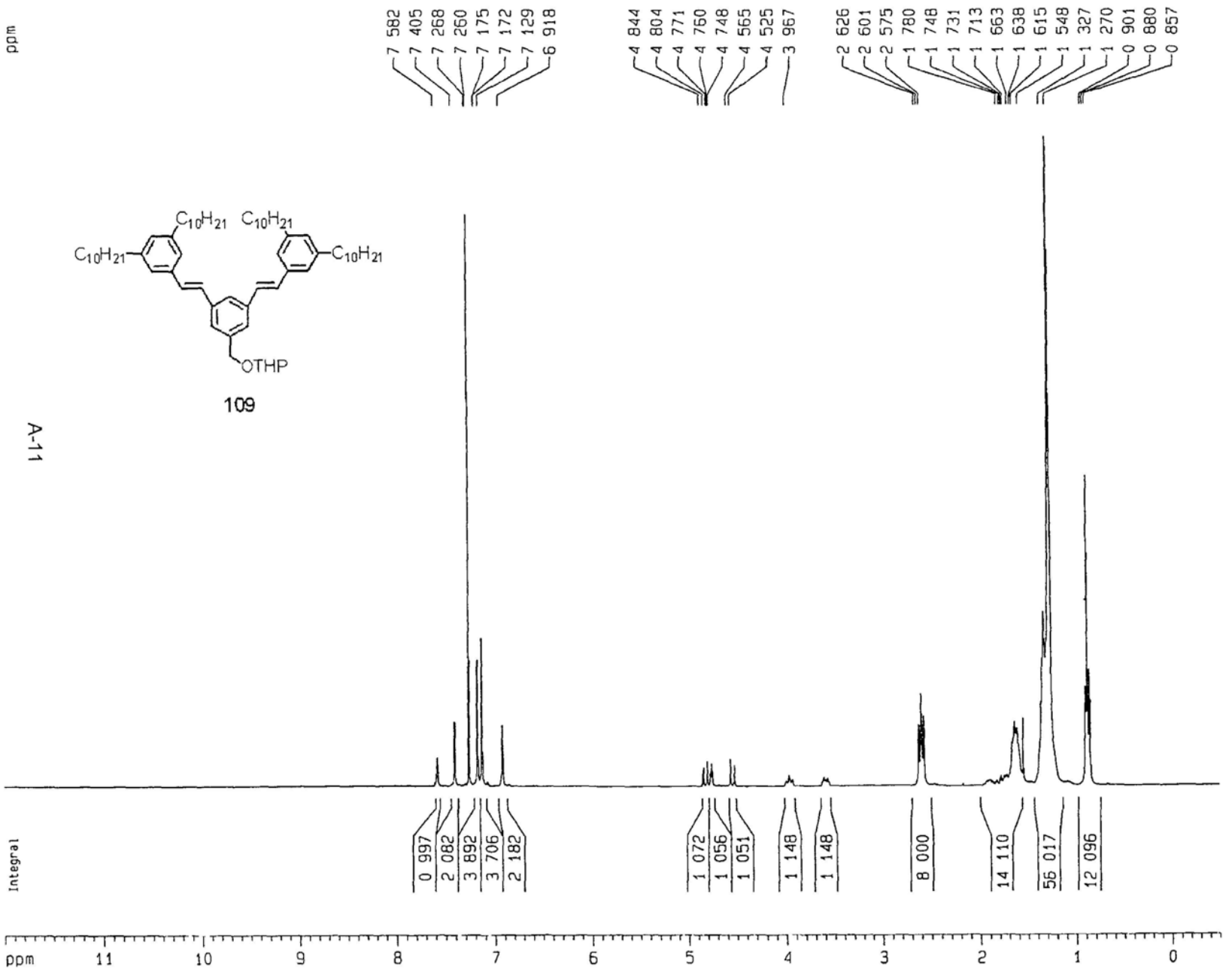

Current Data Parameters
NAME G2-C=C-OTHP
EXPNO 1
PROCNO 1

F2 - Acquisition Parameters
Date_ 20080408
Time 9 51
INSTRUM dpx300
PROBHD 5 mm BBO BB-1H
PULPROG zg
TD 32768
SOLVENT CDCl3
NS 32
DS 0
SWH 8992 806 Hz
FIDRES 0 274439 Hz
AQ 1 8219508 sec
RG 322 5
DW 55 600 usec
DE 79 43 usec
TE 295 2 K
D1 5 00000000 sec
MCREST 0 00000000 sec
MCWRK 0 01500000 sec

======== CHANNEL f1 ========
NUC1 1H
P1 5 00 usec
PL1 -2 00 dB
SFO1 300 1312000 MHz

F2 - Processing parameters
SI 32768
SF 300 1300066 MHz
WDW EM
SSB 0
LB 0 30 Hz
GB 0
PC 1 00

1D NMR plot parameters
CX 22 00 cm
CY 11 63 cm
F1P 12 000 ppm
F1 3601 56 Hz
F2P -0 500 ppm
F2 -150 07 Hz
PPMCM 0 56818 ppm/cm
HZCM 170 52840 Hz/cm

C13

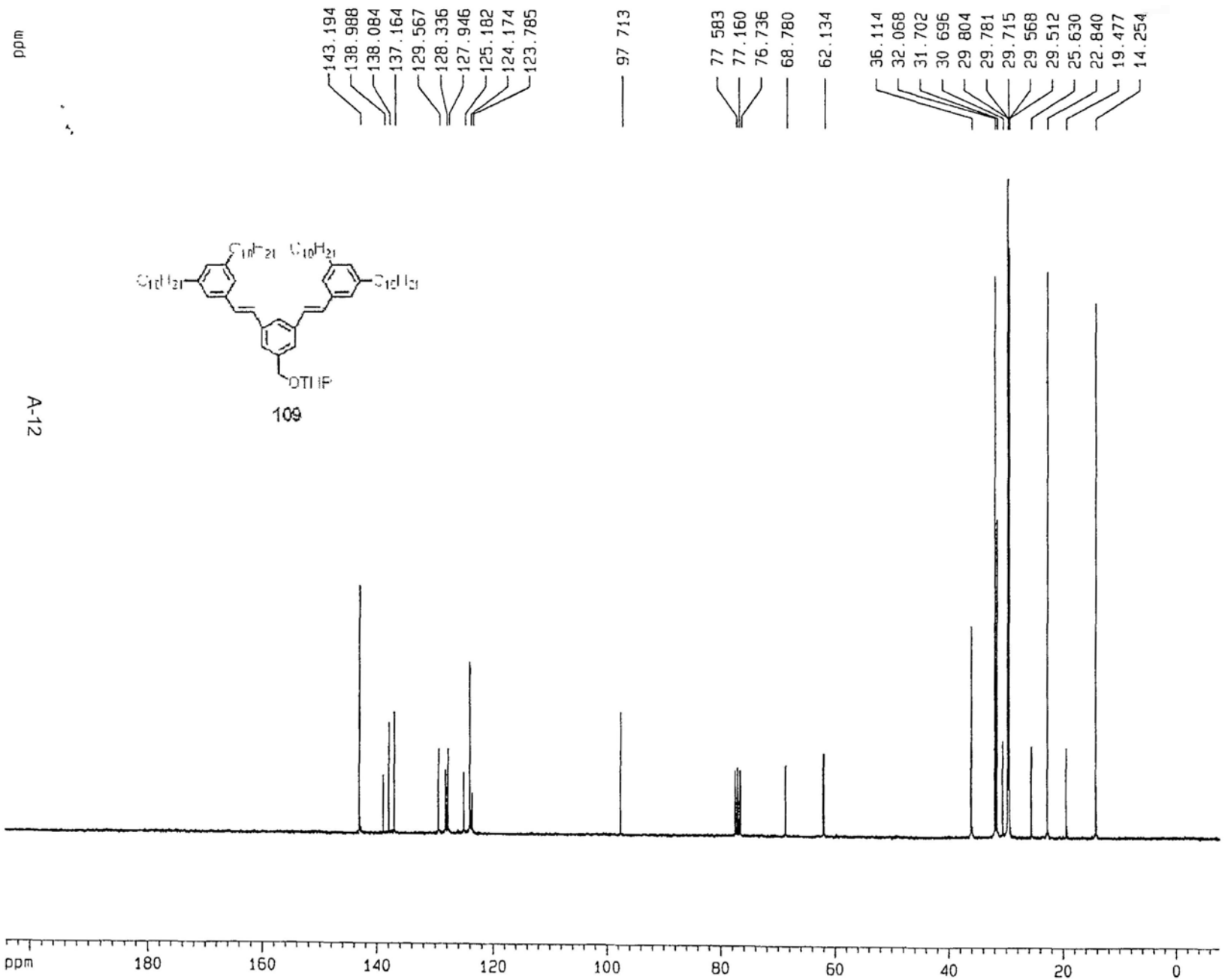

Current Data Parameters
NAME G2-C=C-OTHP-c
EXPNO 1
PROCNO 1

F2 - Acquisition Parameters
Date_ 20080313
Time 11.47
INSTRUM dpx300
PROBHD 5 mm BBO BB-1H
PULPROG zgdc
TD 65536
SOLVENT CDCl3
NS 200
DS 0
SWH 22675.736 Hz
FIDRES 0.346004 Hz
AQ 1.4451188 sec
RG 8192
DW 22.050 usec
DE 6.00 usec
TE 295.2 K
D1 1.00000000 sec
d11 0.03000000 sec
MCREST 0.00000000 sec
MCWRK 0.01500000 sec

======== CHANNEL f1 ========
NUC1 13C
P1 3.00 usec
PL1 -6.00 dB
SFO1 75.4745111 MHz

======== CHANNEL f2 ========
CPDPRG2 waltz16
NUC2 1H
PCPD2 100.00 usec
PL2 120.00 dB
PL12 19.00 dB
SFO2 300.1315007 MHz

F2 - Processing parameters
SI 65536
SF 75.4677519 MHz
WDW EM
SSB 0
LB 1.00 Hz
GB 0
PC 1.40

1D NMR plot parameters
CX 22.00 cm
CY 11.92 cm
F1P 204.375 ppm
F1 15423.75 Hz
F2P -7.698 ppm
F2 -580.97 Hz
PPMCM 9.63972 ppm/cm
HZCM 727.48761 Hz/cm

1H

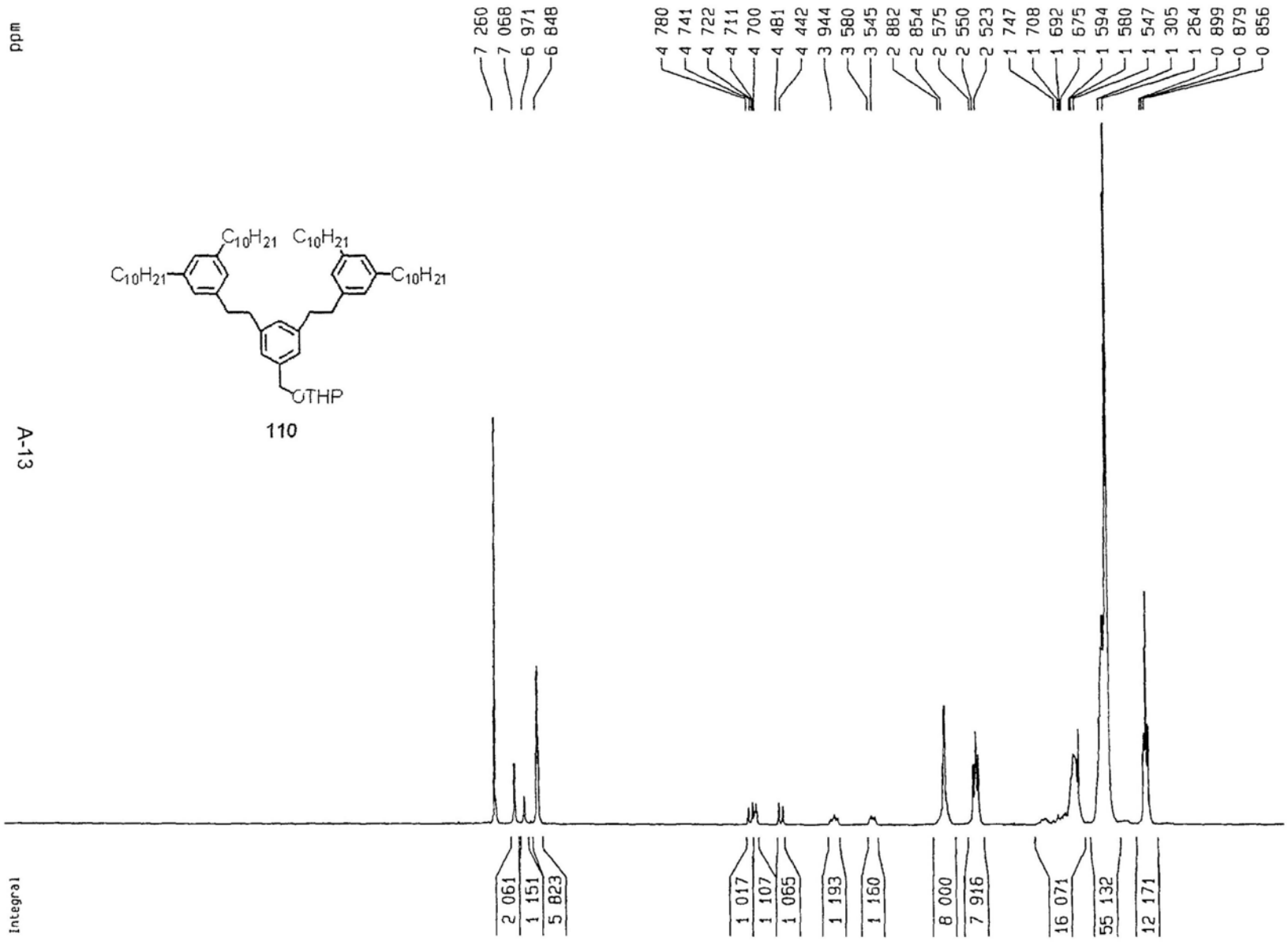


```
Current Data Parameters
NAME            G2-C-OTHP3
EXPNO                    1
PROCNO                   1

F2 - Acquisition Parameters
Date_            20080319
Time                15 41
INSTRUM           dpx300
PROBHD   5 mm BBO BB-1H
PULPROG                zg
TD                  32768
SOLVENT             CDCl3
NS                     16
DS                      0
SWH           8992 806 Hz
FIDRES        0 274439 Hz
AQ            1 8219508 sec
RG                 406 4
DW                55 600 usec
DE                79 43 usec
TE                295 2 K
D1           5 00000000 sec
MCREST       0 00000000 sec
MCWRK        0 01500000 sec

======== CHANNEL f1 ========
NUC1                   1H
P1                5 00 usec
PL1               -2 00 dB
SFO1        300 1312000 MHz

F2 - Processing parameters
SI                  32768
SF          300 1300060 MHz
WDW                    EM
SSB                     0
LB                0 30 Hz
GB                      0
PC                 1 00

1D NMR plot parameters
CX                22 00 cm
CY                12 00 cm
F1P              12 000 ppm
F1               3601 56 Hz
F2P               -0 500 ppm
F2               -150 07 Hz
PPMCM          0 56818 ppm/cm
HZCM          170 52841 Hz/cm
```

C13

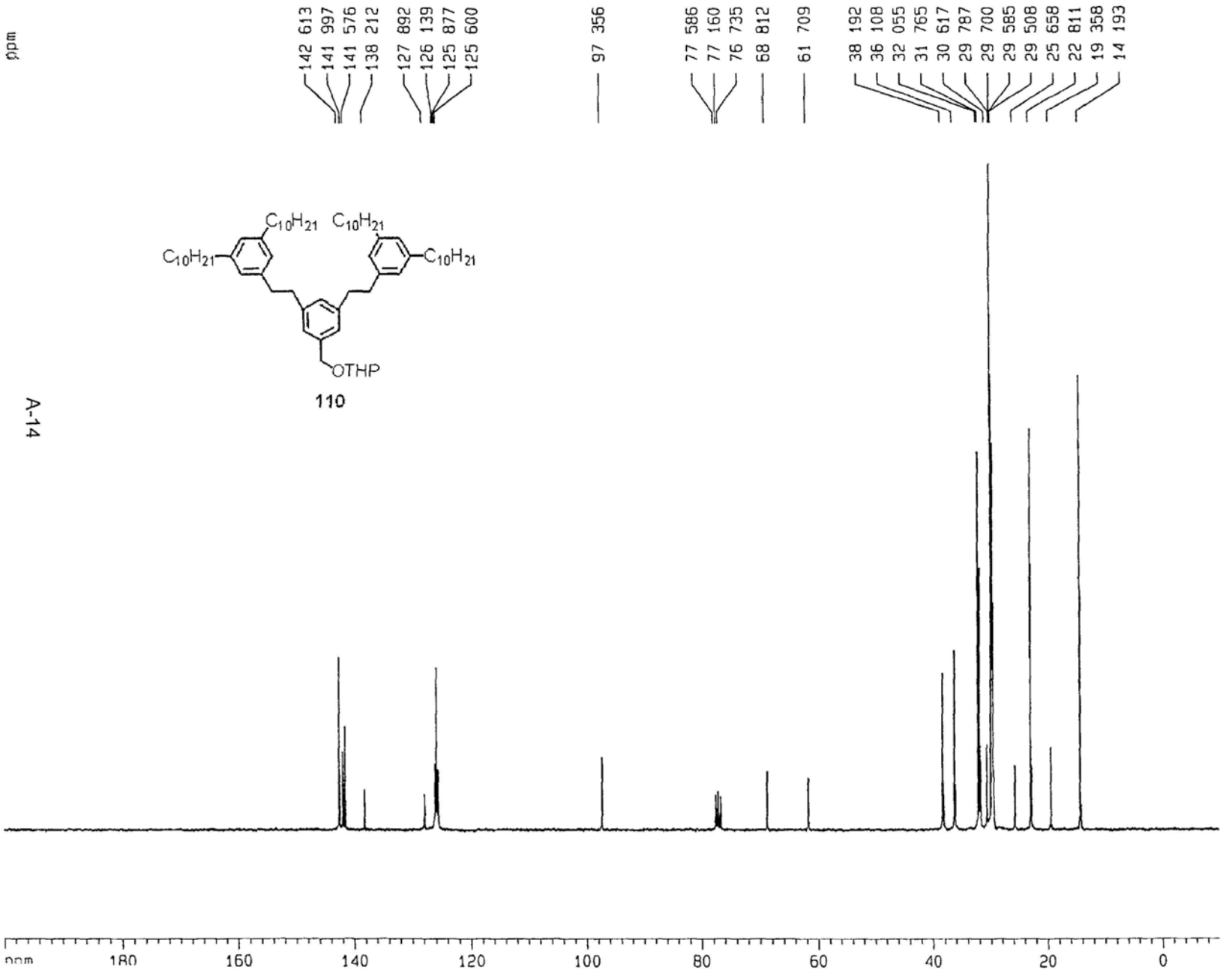

Current Data Parameters

NAME	G2-C-OTHP-c
EXPNO	1
PROCNO	1

F2 - Acquisition Parameters

Date_	20080319
Time	14 32
INSTRUM	dpx300
PROBHD	5 mm BBO BB-1H
PULPROG	zgdc
TD	65536
SOLVENT	CDCl3
NS	107
DS	0
SWH	22675 736 Hz
FIDRES	0 346004 Hz
AQ	1 4451188 sec
RG	3649 1
DW	22 050 usec
DE	6 00 usec
TE	296 2 K
D1	1 00000000 sec
d11	0 03000000 sec
MCREST	0 00000000 sec
MCWRK	0 01500000 sec

======== CHANNEL f1 ========

NUC1	13C
P1	3 00 usec
PL1	-6 00 dB
SFO1	75 4745111 MHz

======== CHANNEL f2 ========

CPDPRG2	waltz16
NUC2	1H
PCPD2	100 00 usec
PL2	120 00 dB
PL12	19 00 dB
SFO2	300 1315007 MHz

F2 - Processing parameters

SI	65536
SF	75 4677715 MHz
WDW	EM
SSB	0
LB	2 00 Hz
GB	0
PC	1 40

1D NMR plot parameters

CX	22 00 cm
CY	12 00 cm
F1P	200 000 ppm
F1	15093 55 Hz
F2P	-10 000 ppm
F2	-754 68 Hz
PPMCM	9 54545 ppm/cm
HZCM	720 37415 Hz/cm

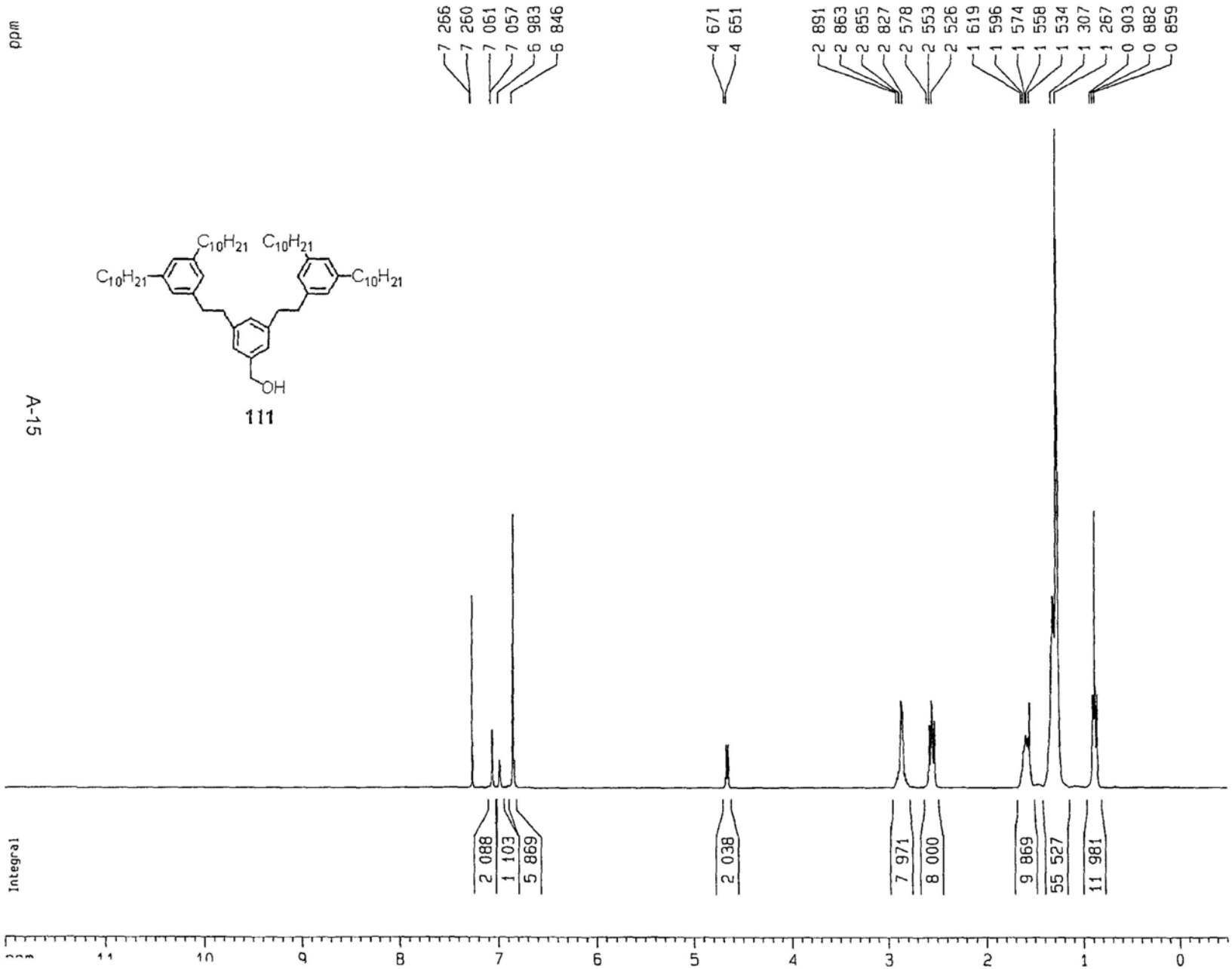

111

A-15

```
Current Data Parameters
NAME          G2-C-CH2OH
EXPNO                  1
PROCNO                 1

F2 - Acquisition Parameters
Date_          20080326
Time             16 45
INSTRUM          dpx300
PROBHD   5 mm BBO BB-1H
PULPROG              zg
TD                32768
SOLVENT           CDCl3
NS                   16
DS                    0
SWH          8992 806 Hz
FIDRES       0 274439 Hz
AQ           1 8219508 sec
RG                  181
DW              55 600 usec
DE              79 43 usec
TE               295 2 K
D1          5 00000000 sec
MCREST      0 00000000 sec
MCWRK       0 01500000 sec

======== CHANNEL f1 ========
NUC1                  1H
P1                5 00 usec
PL1               -2 00 dB
SFO1        300 1312000 MHz

F2 - Processing parameters
SI                32768
SF          300 1300066 MHz
WDW                  EM
SSB                   0
LB               0 30 Hz
GB                    0
PC                1 00

1D NMR plot parameters
CX               22 00 cm
CY               11 78 cm
F1P             12 000 ppm
F1             3601 56 Hz
F2P             -0 500 ppm
F2             -150 07 Hz
PPMCM          0 56818 ppm/cm
HZCM         170 52841 Hz/cm
```

C13

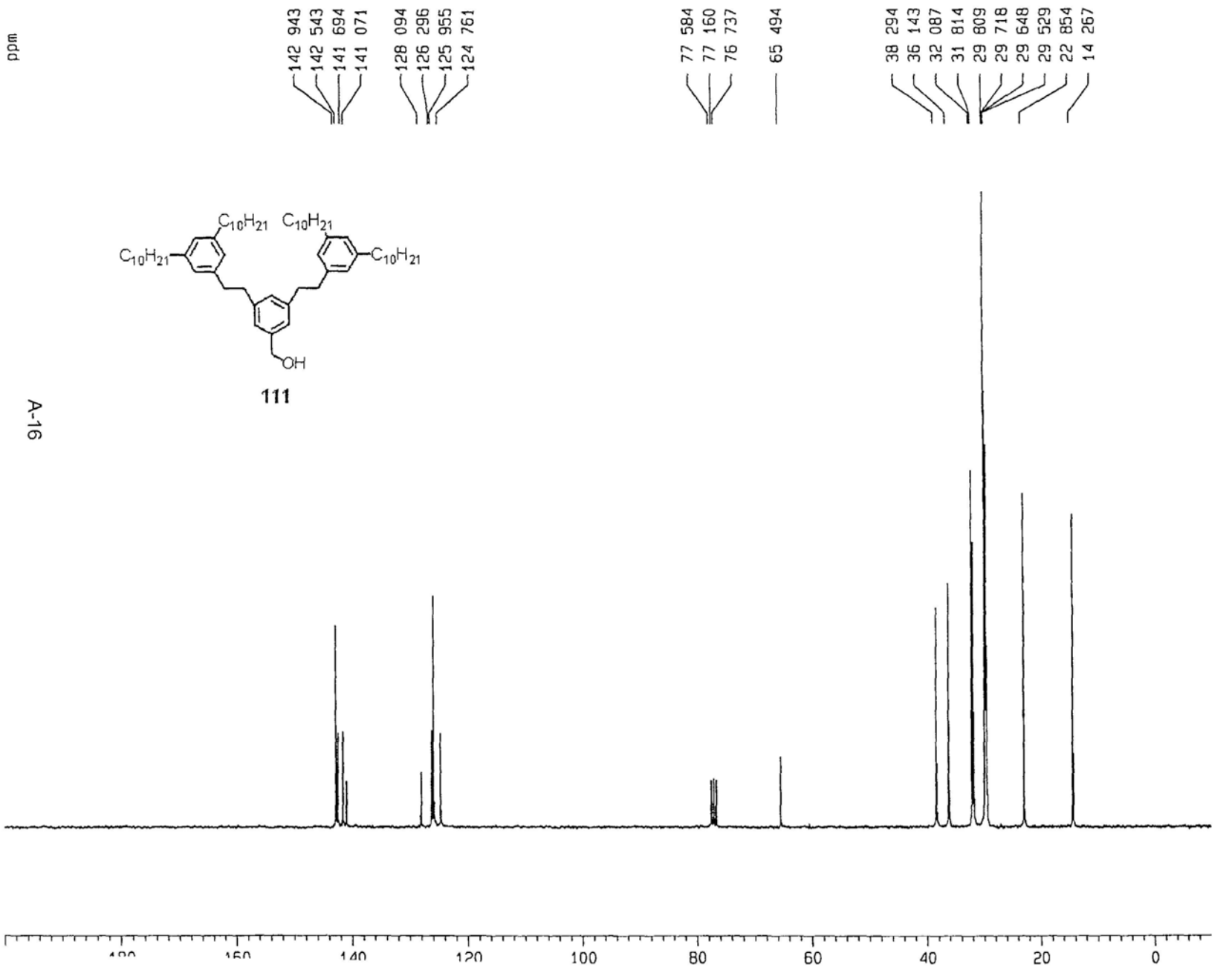


```
Current Data Parameters
NAME        G2 (C) CH2OH-c
EXPNO                   1
PROCNO                  1

F2 - Acquisition Parameters
Date_            20070821
Time               16 28
INSTRUM          dpx300
PROBHD   5 mm BBO BB-1H
PULPROG             zgdc
TD                 65536
SOLVENT            CDCl3
NS                    91
DS                     0
SWH          22675 736 Hz
FIDRES        0 346004 Hz
AQ            1 4451188 sec
RG                  8192
DW               22 050 usec
DE                6 00 usec
TE                 0 0 K
D1           1 00000000 sec
d11          0 03000000 sec
MCREST       0 00000000 sec
MCWRK        0 01500000 sec

======== CHANNEL f1 ========
NUC1                  13C
P1                 3 00 usec
PL1               -6 00 dB
SFO1        75 4745111 MHz

======== CHANNEL f2 ========
CPDPRG2          waltz16
NUC2                  1H
PCPD2           100 00 usec
PL2             120 00 dB
PL12             19 00 dB
SFO2       300 1315007 MHz

F2 - Processing parameters
SI                 65536
SF          75 4677519 MHz
WDW                   EM
SSB                    0
LB                 3 00 Hz
GB                     0
PC                 1 40

1D NMR plot parameters
CX                22 00 cm
CY                11 50 cm
F1P             200 000 ppm
F1             15093 55 Hz
F2P             -10 000 ppm
F2              -754 68 Hz
PPMCM           9 54545 ppm/cm
HZCM          720 37390 Hz/cm
```

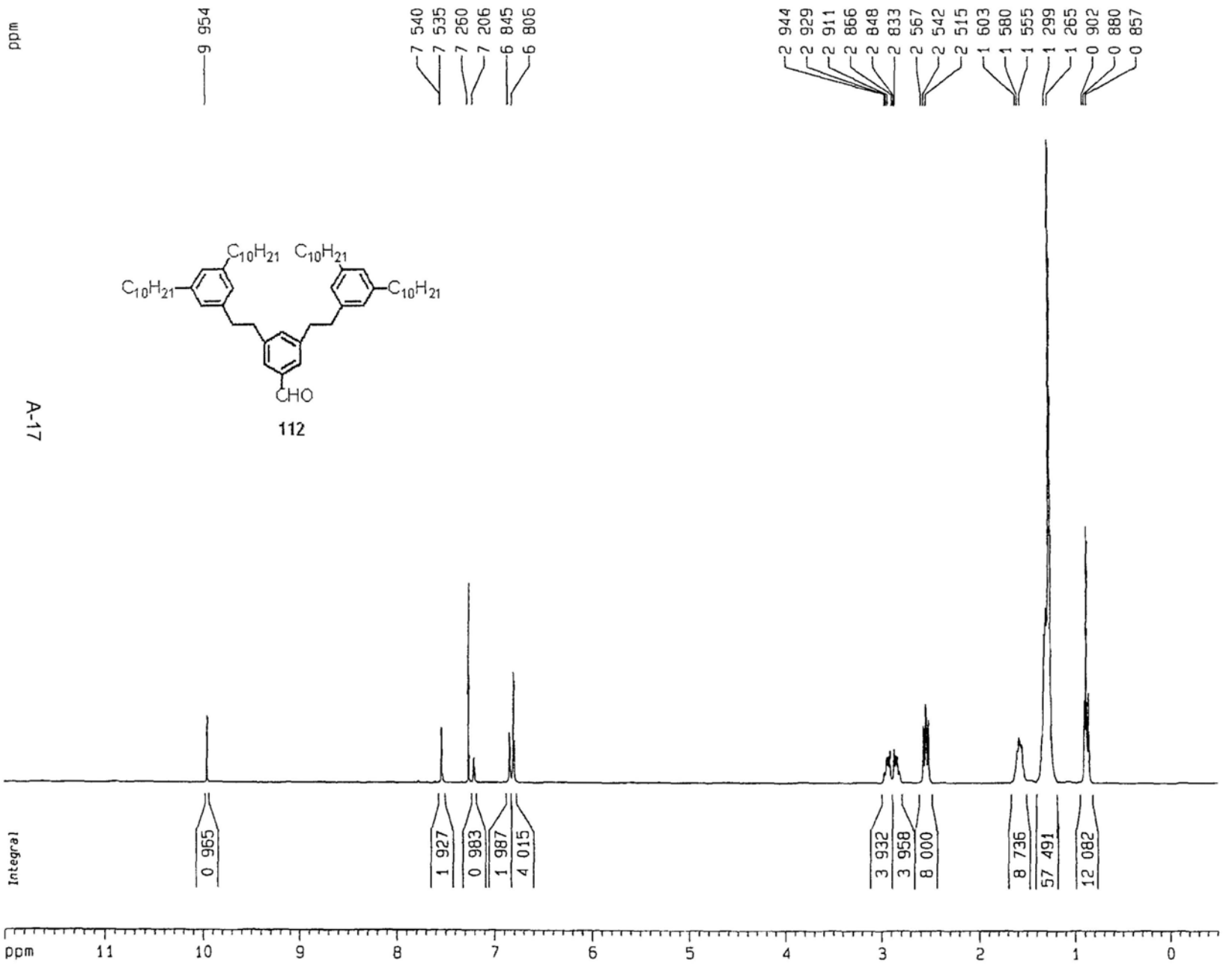

A-17

$C_{10}H_{21}$ $C_{10}H_{21}$ $C_{10}H_{21}$ $C_{10}H_{21}$ CHO

112

```
Current Data Parameters
NAME                  G2(C)CH01
EXPNO                         1
PROCNO                        1

F2 - Acquisition Parameters
Date_                  20080326
Time                      16 28
INSTRUM                 dpx300
PROBHD    5 mm BBO BB-1H
PULPROG                     zg
TD                       32768
SOLVENT                  CDCl3
NS                            8
DS                            0
SWH                8992 806 Hz
FIDRES             0 274439 Hz
AQ                 1 8219508 sec
RG                      724 1
DW                     55 600 usec
DE                     79 43 usec
TE                     295 2 K
D1                 5 00000000 sec
MCREST             0 00000000 sec
MCWRK              0 01500000 sec

======== CHANNEL f1 ========
NUC1                        1H
P1                       5 00 usec
PL1                      -2 00 dB
SFO1               300 1312000 MHz

F2 - Processing parameters
SI                       32768
SF                 300 1300063 MHz
WDW                         EM
SSB                          0
LB                       0 30 Hz
GB                           0
PC                       1 00

1D NMR plot parameters
CX                      22 00 cm
CY                      11 59 cm
F1P                    12 000 ppm
F1                   3601 56 Hz
F2P                    -0 500 ppm
F2                   -150 07 Hz
PPMCM                0 56818 ppm/cm
HZCM               170 52841 Hz/cm
```

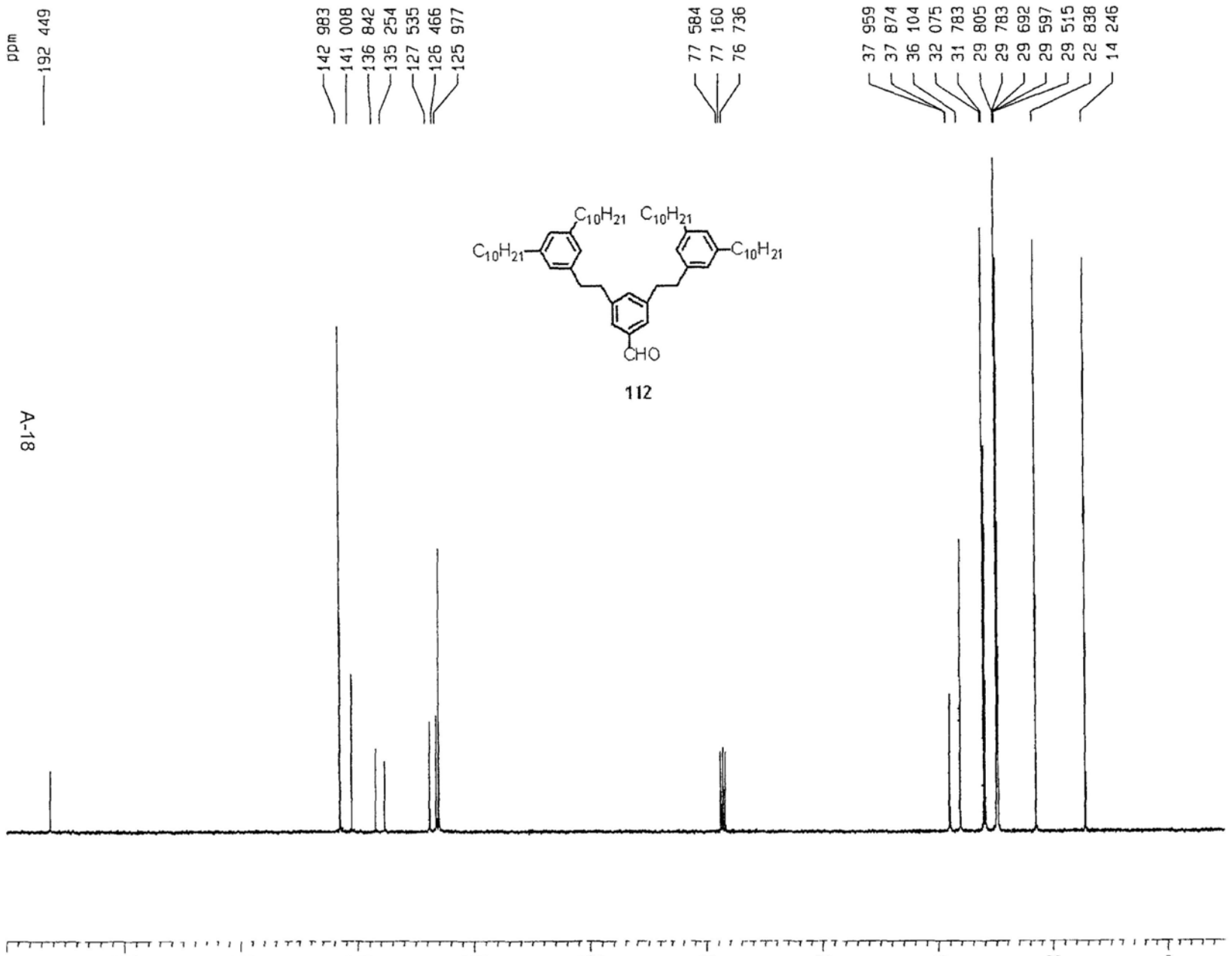

Current Data Parameters

NAME	G2-C-CHO(c)
EXPNO	1
PROCNO	1

F2 - Acquisition Parameters

Date_	20080220
Time	9 51
INSTRUM	dpx300
PROBHD	5 mm BBO BB-1H
PULPROG	zgdc
TD	65536
SOLVENT	CDCl3
NS	150
DS	0
SWH	22675 736 Hz
FIDRES	0 346004 Hz
AQ	1 4451188 sec
RG	8192
DW	22 050 usec
DE	6 00 usec
TE	298 2 K
D1	1 00000000 sec
d11	0 03000000 sec
MCREST	0 00000000 sec
MCWRK	0 01500000 sec

======== CHANNEL f1 ========

NUC1	13C
P1	3 00 usec
PL1	-6 00 dB
SFO1	75 4745111 MHz

======== CHANNEL f2 ========

CPDPRG2	waltz16
NUC2	1H
PCPD2	100 00 usec
PL2	120 00 dB
PL12	19 00 dB
SFO2	300 1315007 MHz

F2 - Processing parameters

SI	65536
SF	75 4677512 MHz
WDW	EM
SSB	0
LB	1 00 Hz
GB	0
PC	1 40

1D NMR plot parameters

CX	22 00 cm
CY	12 18 cm
F1P	200 000 ppm
F1	15093 55 Hz
F2P	-10 000 ppm
F2	-754 68 Hz
PPMCM	9 54545 ppm/cm
HZCM	720 37390 Hz/cm

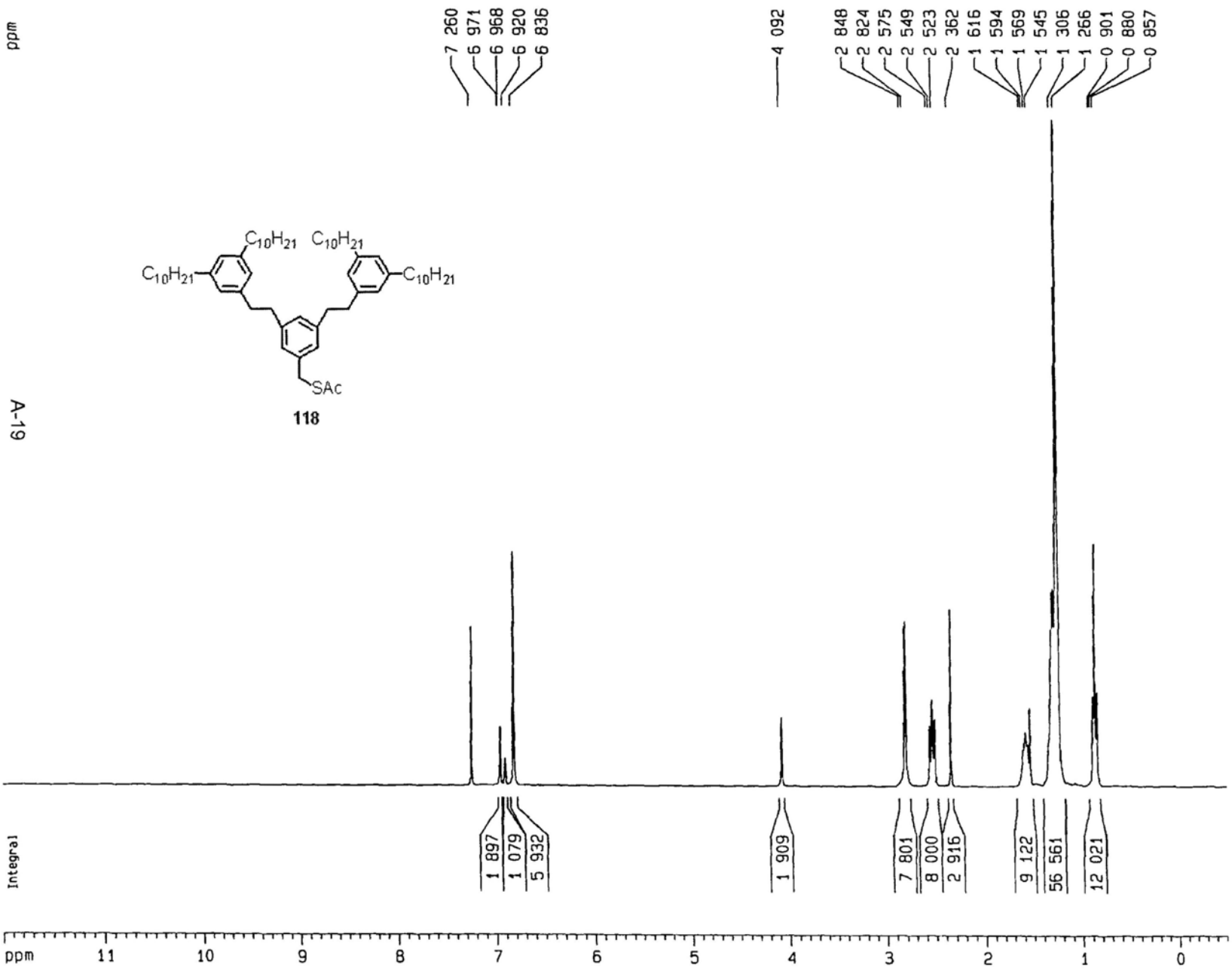

Current Data Parameters

NAME	G2-C-CH2SAc
EXPNO	1
PROCNO	1

F2 - Acquisition Parameters

Date_	20080620
Time	12 51
INSTRUM	dpx300
PROBHD	5 mm BBO BB-1H
PULPROG	zg
TD	32768
SOLVENT	CDCl3
NS	16
DS	0
SWH	8992 806 Hz
FIDRES	0 274439 Hz
AQ	1 8219508 sec
RG	256
DW	55 600 usec
DE	79 43 usec
TE	296 2 K
D1	5 00000000 sec
MCREST	0 00000000 sec
MCWRK	0 01500000 sec

======== CHANNEL f1 ========

NUC1	1H
P1	5 00 usec
PL1	-2 00 dB
SFO1	300 1312000 MHz

F2 - Processing parameters

SI	32768
SF	300 1300063 MHz
WDW	EM
SSB	0
LB	0 30 Hz
GB	0
PC	1 00

1D NMR plot parameters

CX	22 00 cm
CY	11 99 cm
F1P	12 000 ppm
F1	3601 56 Hz
F2P	-0 500 ppm
F2	-150 07 Hz
PPMCM	0 56818 ppm/cm
HZCM	170 52840 Hz/cm

C13

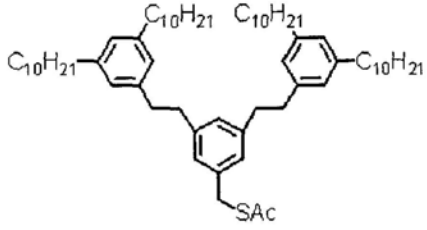

118

A-20


```
Current Data Parameters
NAME        G2(C)CH2SAc-c
EXPNO                   1
PROCNO                  1

F2 - Acquisition Parameters
Date_            20070828
Time                11 50
INSTRUM           dpx300
PROBHD   5 mm BBO BB-1H
PULPROG             zgdc
TD                 65536
SOLVENT             CDCl3
NS                    300
DS                      0
SWH           22675 736 Hz
FIDRES         0 346004 Hz
AQ            1 4451188 sec
RG                 1448 2
DW                22 050 usec
DE                 6 00 usec
TE                  0 0 K
D1           1 00000000 sec
d11          0 03000000 sec
MCREST       0 00000000 sec
MCWRK        0 01500000 sec

======== CHANNEL f1 ========
NUC1                   13C
P1                  3 00 usec
PL1                -6 00 dB
SFO1          75 4745111 MHz

======== CHANNEL f2 ========
CPDPRG2          waltz16
NUC2                   1H
PCPD2             100 00 usec
PL2               120 00 dB
PL12               19 00 dB
SFO2         300 1315007 MHz

F2 - Processing parameters
SI                  65536
SF           75 4677523 MHz
WDW                    EM
SSB                     0
LB                  3 00 Hz
GB                      0
PC                   1 40

1D NMR plot parameters
CX                 22 00 cm
CY                 11 70 cm
F1P              200 000 ppm
F1              15093 55 Hz
F2P              -10 000 ppm
F2               -754 68 Hz
PPMCM             9 54545 ppm/cm
HZCM            720 37390 Hz/cm
```

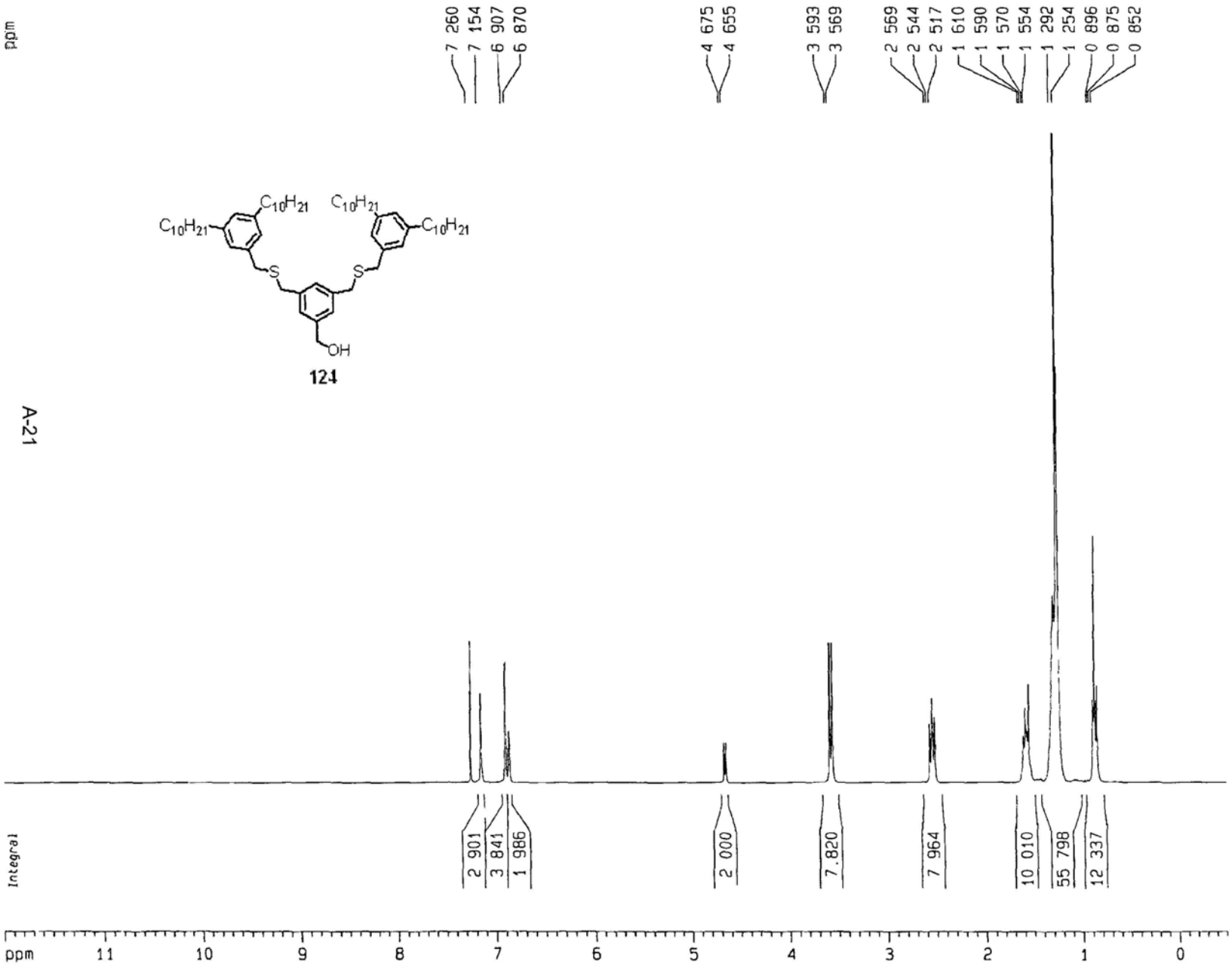

Current Data Parameters

NAME	G2-S-CH2OH
EXPNO	1
PROCNO	1

F2 - Acquisition Parameters

Date_	20090415
Time	11 24
INSTRUM	dpx300
PROBHD	5 mm BBO BB-1H
PULPROG	zg
TD	32768
SOLVENT	CDCl3
NS	32
DS	0
SWH	8992 806 Hz
FIDRES	0 274439 Hz
AQ	1 8219508 sec
RG	228 1
DW	55 600 usec
DE	79 43 usec
TE	295 2 K
D1	5 00000000 sec
MCREST	0 00000000 sec
MCWRK	0 01500000 sec

======== CHANNEL f1 ========

NUC1	1H
P1	5 00 usec
PL1	-2 00 dB
SF01	300 1312000 MHz

F2 - Processing parameters

SI	32768
SF	300 1300063 MHz
WDW	EM
SSB	0
LB	0 30 Hz
GB	0
PC	1 00

1D NMR plot parameters

CX	22 00 cm
CY	11 66 cm
F1P	12 000 ppm
F1	3601 56 Hz
F2P	-0 500 ppm
F2	-150 07 Hz
PPMCM	0 56818 ppm/cm
HZCM	170 52841 Hz/cm

C13

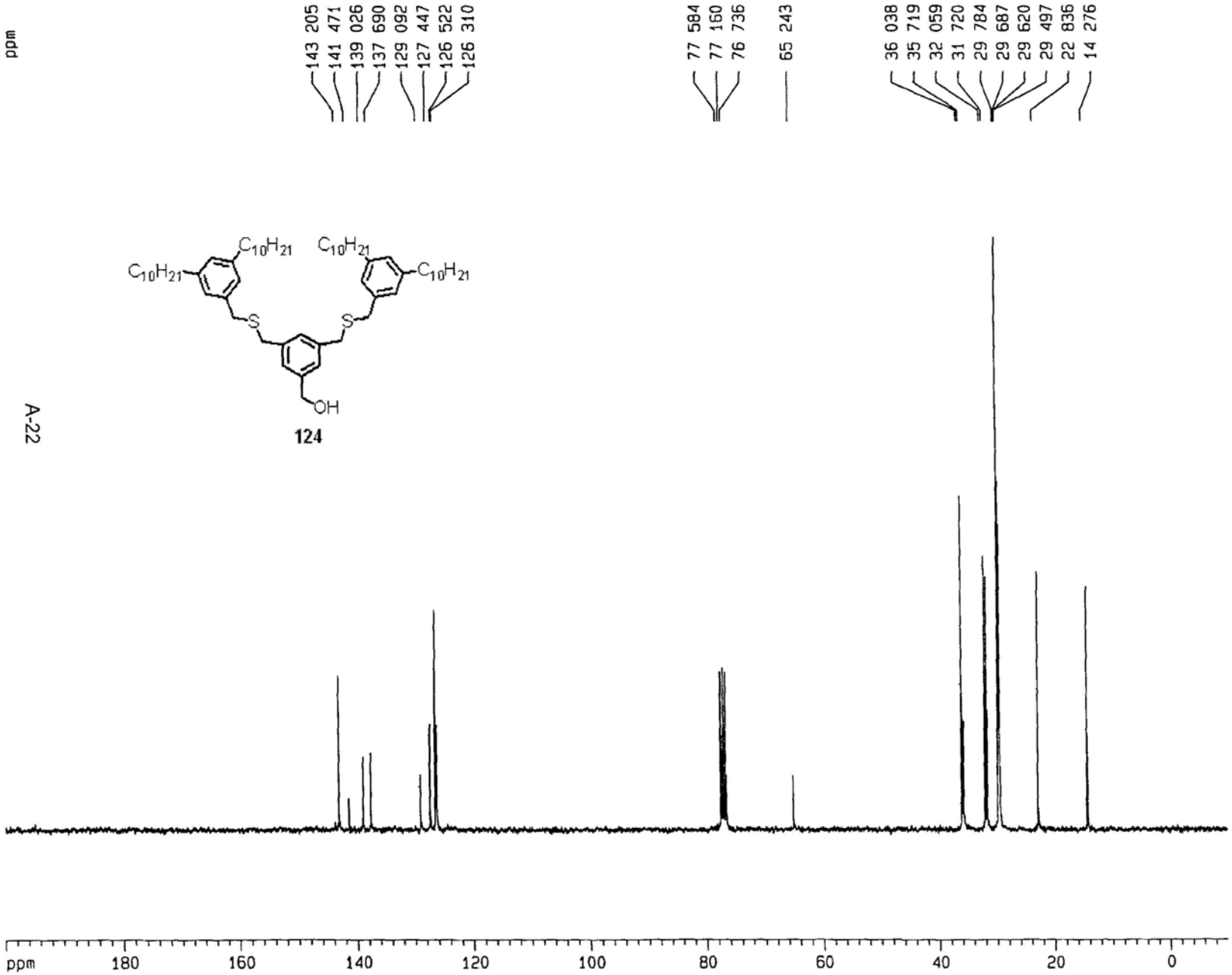

A-22

124

Current Data Parameters
NAME G2-S-CH2OH (c)
EXPNO 1
PROCNO 1

F2 - Acquisition Parameters
Date_ 20080521
Time 16 36
INSTRUM dpx300
PROBHD 5 mm BBO BB-1H
PULPROG zgdc
TD 65536
SOLVENT CDCl3
NS 320
DS 0
SWH 22675 736 Hz
FIDRES 0 346004 Hz
AQ 1 4451188 sec
RG 8192
DW 22 050 usec
DE 6 00 usec
TE 295 2 K
D1 1 00000000 sec
d11 0 03000000 sec
MCREST 0 00000000 sec
MCWRK 0 01500000 sec

======== CHANNEL f1 ========
NUC1 13C
P1 3 00 usec
PL1 -6 00 dB
SFO1 75 4745111 MHz

======== CHANNEL f2 ========
CPDPRG2 waltz16
NUC2 1H
PCPD2 100 00 usec
PL2 120 00 dB
PL12 19 00 dB
SFO2 300 1315007 MHz

F2 - Processing parameters
SI 65536
SF 75 4677414 MHz
WDW EM
SSB 0
LB 3 00 Hz
GB 0
PC 1 40

1D NMR plot parameters
CX 22 00 cm
CY 10 64 cm
F1P 200 000 ppm
F1 15093 55 Hz
F2P -10 000 ppm
F2 -754 68 Hz
PPMCM 9 54545 ppm/cm
HZCM 720 37384 Hz/cm

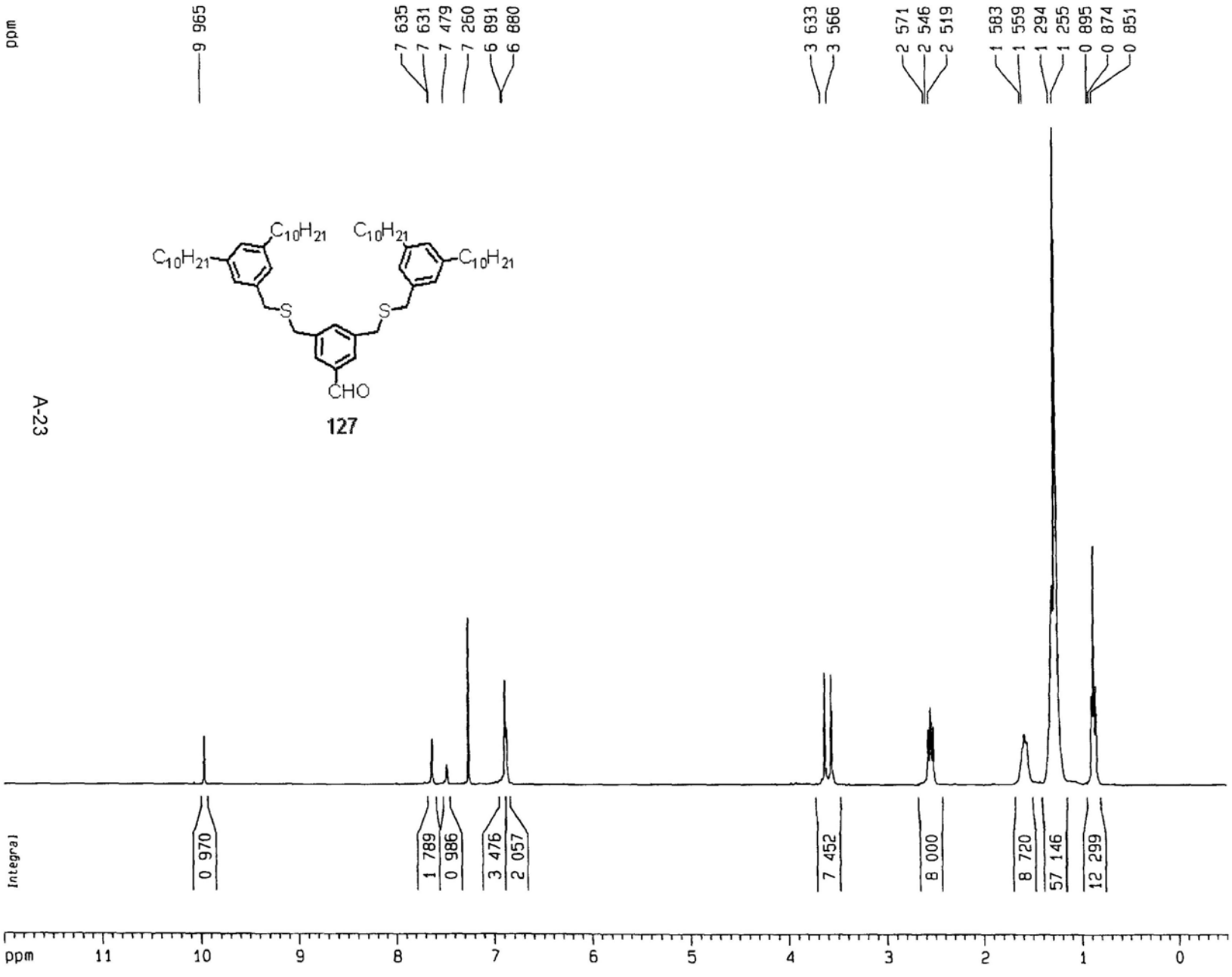

Current Data Parameters

NAME	G2-S-CHO
EXPNO	1
PROCNO	1

F2 - Acquisition Parameters

Date_	20080529
Time	13 39
INSTRUM	dpx300
PROBHD	5 mm BBO BB-1H
PULPROG	zg
TD	32768
SOLVENT	CDCl3
NS	16
DS	0
SWH	8992 806 Hz
FIDRES	0 274439 Hz
AQ	1 8219508 sec
RG	362
DW	55 600 usec
DE	79 43 usec
TE	296 2 K
D1	5 00000000 sec
MCREST	0 00000000 sec
MCWRK	0 01500000 sec

======== CHANNEL f1 ========

NUC1	1H
P1	5 00 usec
PL1	-2 00 dB
SF01	300 1312000 MHz

F2 - Processing parameters

SI	32768
SF	300 1300057 MHz
WDW	EM
SSB	0
LB	0 30 Hz
GB	0
PC	1 00

1D NMR plot parameters

CX	22 00 cm
CY	11 80 cm
F1P	12 000 ppm
F1	3601 56 Hz
F2P	-0 500 ppm
F2	-150 07 Hz
PPMCM	0 56818 ppm/cm
HZCM	170 52841 Hz/cm

C13

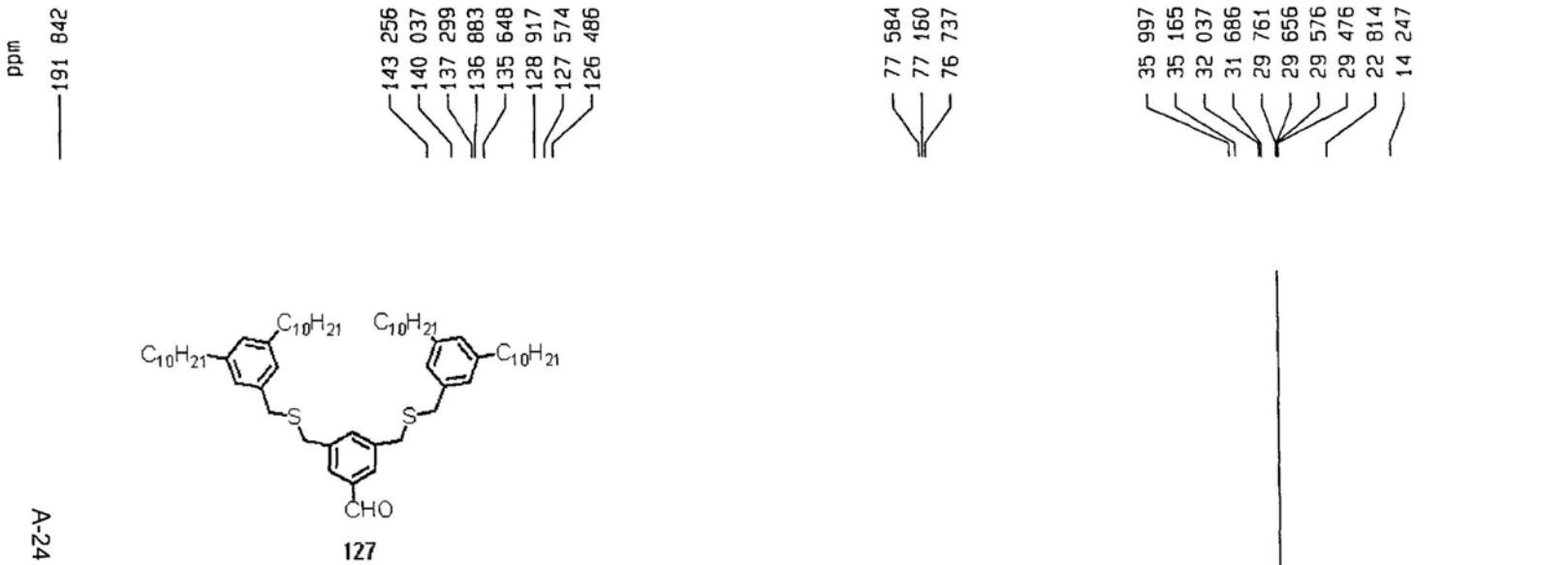

127

A-24

Current Data Parameters
NAME G2-S-CHO (c)
EXPNO 1
PROCNO 1

F2 - Acquisition Parameters
Date_ 20080530
Time 18 00
INSTRUM dpx300
PROBHD 5 mm BBO BB-1H
PULPROG zgdc
TD 65536
SOLVENT CDCl3
NS 100
DS 0
SWH 22675 736 Hz
FIDRES 0 346004 Hz
AQ 1 4451188 sec
RG 7298 2
DW 22 050 usec
DE 6 00 usec
TE 296 2 K
D1 1 00000000 sec
d11 0 03000000 sec
MCREST 0 00000000 sec
MCWRK 0 01500000 sec

======== CHANNEL f1 ========
NUC1 13C
P1 3 00 usec
PL1 -6 00 dB
SFO1 75 4745111 MHz

======== CHANNEL f2 ========
CPDPRG2 waltz16
NUC2 1H
PCPD2 100 00 usec
PL2 120 00 dB
PL12 19 00 dB
SFO2 300 1315007 MHz

F2 - Processing parameters
SI 65536
SF 75 4677454 MHz
WDW EM
SSB 0
LB 3 00 Hz
GB 0
PC 1 40

1D NMR plot parameters
CX 22 00 cm
CY 11 18 cm
F1P 200 000 ppm
F1 15093 55 Hz
F2P -10 000 ppm
F2 -754 68 Hz
PPMCM 9 54545 ppm/cm
HZCM 720 37384 Hz/cm

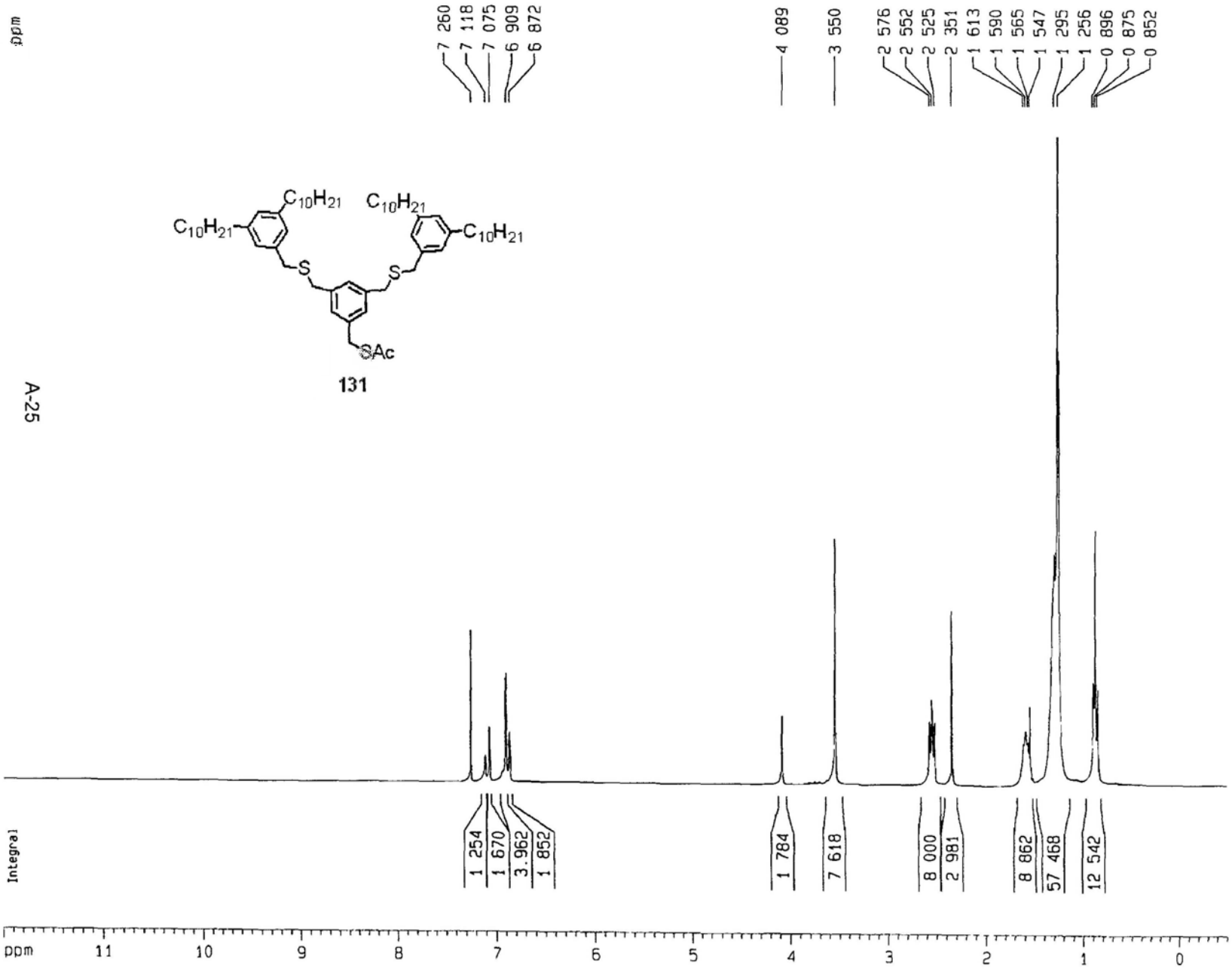

Current Data Parameters
NAME G2-S-CH2SAc
EXPNO 2
PROCNO 1

F2 - Acquisition Parameters
Date_ 20090408
Time 11 33
INSTRUM dpx300
PROBHD 5 mm BBO BB-1H
PULPROG zg
TD 32768
SOLVENT CDCl3
NS 128
DS 0
SWH 8992 806 Hz
FIDRES 0 274439 Hz
AQ 1 8219508 sec
RG 228 1
DW 55 600 usec
DE 79 43 usec
TE 294 2 K
D1 5 00000000 sec
MCREST 0 00000000 sec
MCWRK 0 01500000 sec

======== CHANNEL f1 ========
NUC1 1H
P1 5 00 usec
PL1 -2 00 dB
SF01 300 1312000 MHz

F2 - Processing parameters
SI 32768
SF 300 1300066 MHz
WDW EM
SSB 0
LB 0 30 Hz
GB 0
PC 1 00

1D NMR plot parameters
CX 22 00 cm
CY 11 69 cm
F1P 12 000 ppm
F1 3601 56 Hz
F2P -0 500 ppm
F2 -150 07 Hz
PPMCM 0 56818 ppm/cm
HZCM 170 52841 Hz/cm

C13

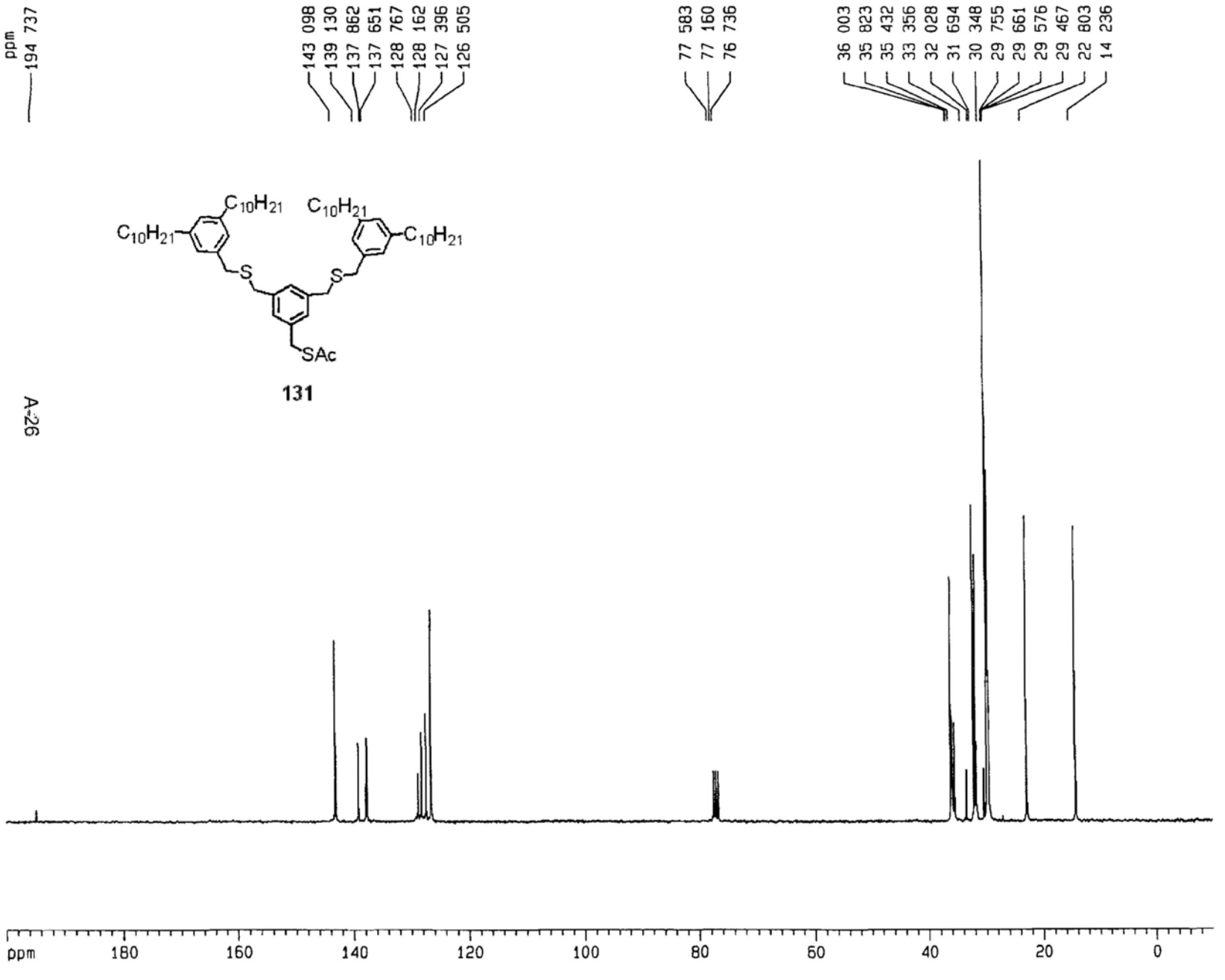

131

Current Data Parameters

NAME	G2-S-CH2SAc (c)
EXPNO	1
PROCNO	1

F2 - Acquisition Parameters

Date_	20080530
Time	18 24
INSTRUM	dpx300
PROBHD	5 mm BBO BB-1H
PULPROG	zgdc
TD	65536
SOLVENT	CDCl3
NS	200
DS	0
SWH	22675 736 Hz
FIDRES	0 346004 Hz
AQ	1 4451188 sec
RG	7298 2
DW	22 050 usec
DE	6 00 usec
TE	295 2 K
D1	1 00000000 sec
d11	0 03000000 sec
MCREST	0 00000000 sec
MCWRK	0 01500000 sec

======== CHANNEL f1 ========

NUC1	13C
P1	3 00 usec
PL1	-6 00 dB
SFO1	75 4745111 MHz

======== CHANNEL f2 ========

CPDPRG2	waltz16
NUC2	1H
PCPD2	100 00 usec
PL2	120 00 dB
PL12	19 00 dB
SFO2	300 1315007 MHz

F2 - Processing parameters

SI	65536
SF	75 4677484 MHz
WDW	EM
SSB	0
LB	3 00 Hz
GB	0
PC	1 40

1D NMR plot parameters

CX	22 00 cm
CY	12 00 cm
F1P	200 000 ppm
F1	15093 55 Hz
F2P	-10 000 ppm
F2	-754 68 Hz
PPMCM	9 54545 ppm/cm
HZCM	720 37390 Hz/cm

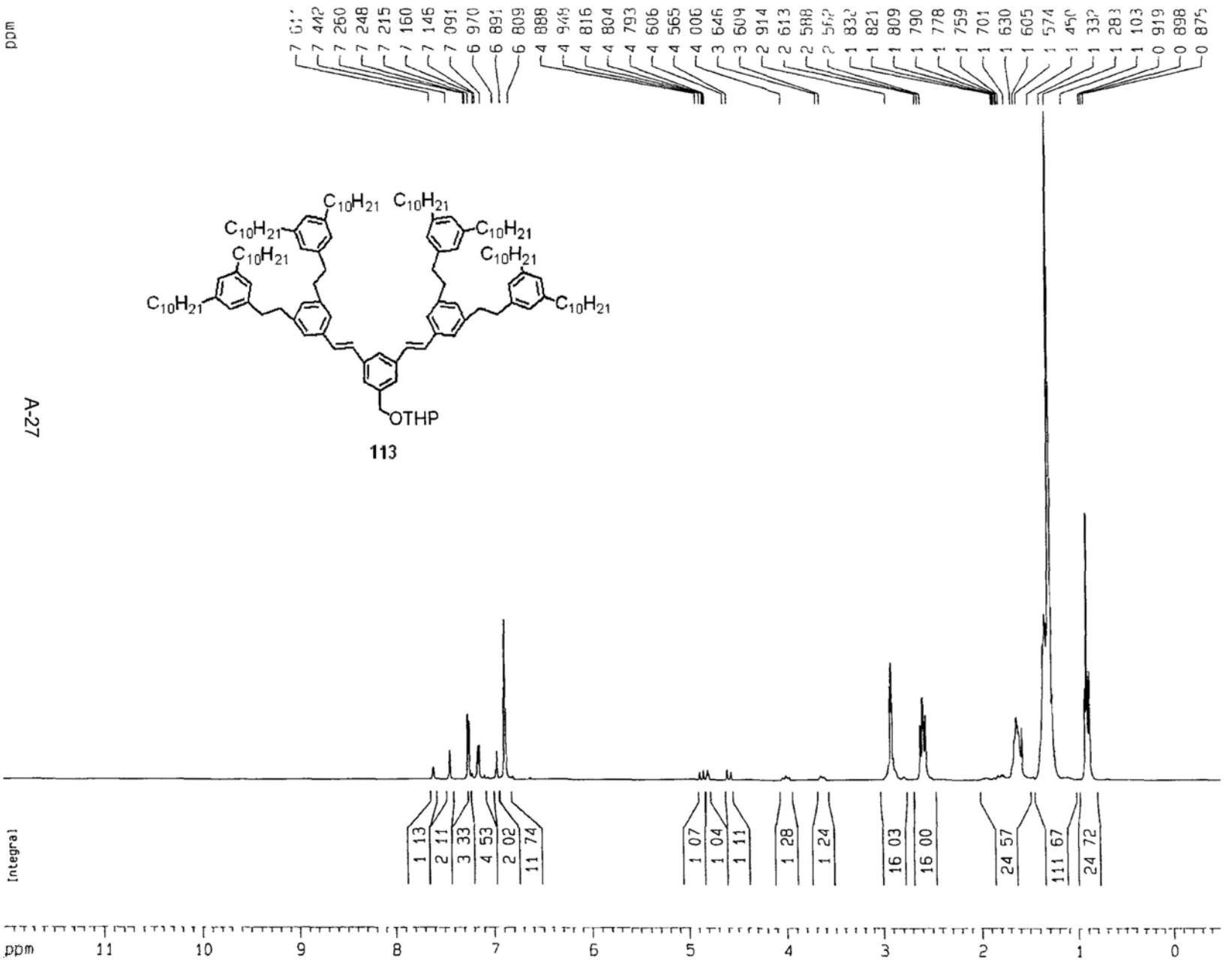

Current Data Parameters
NAME G3-C C≡C-OTHP
EXPNO 1
PROCNO 1

F2 - Acquisition Parameters
Date_ 20080421
Time 11 10
INSTRUM dpx300
PROBHD 5 mm BBO BB-1H
PULPROG zg
TD 32768
SOLVENT CDCl3
NS 16
DS 0
SWH 8992 806 Hz
FIDRES 0 274439 Hz
AQ 1 8219508 sec
RG 40 3
DW 55 600 usec
DE 79 43 usec
TE 295 2 K
D1 5 00000000 sec
MCREST 0 00000000 sec
MCWRK 0 01500000 sec

======== CHANNEL f1 ========
NUC1 1H
P1 5 00 usec
PL1 -2 00 dB
SFO1 300 1312000 MHz

F2 - Processing parameters
SI 32768
SF 300 1300057 MHz
WDW EM
SSB 0
LB 0 30 Hz
GB 0
PC 1 00

1D NMR plot parameters
CX 22 00 cm
CY 12 09 cm
F1P 12 000 ppm
F1 3601 56 Hz
F2P -0 500 ppm
F2 -150 07 Hz
PPMCM 0 56818 ppm/cm
HZCM 170 52841 Hz/cm

C13

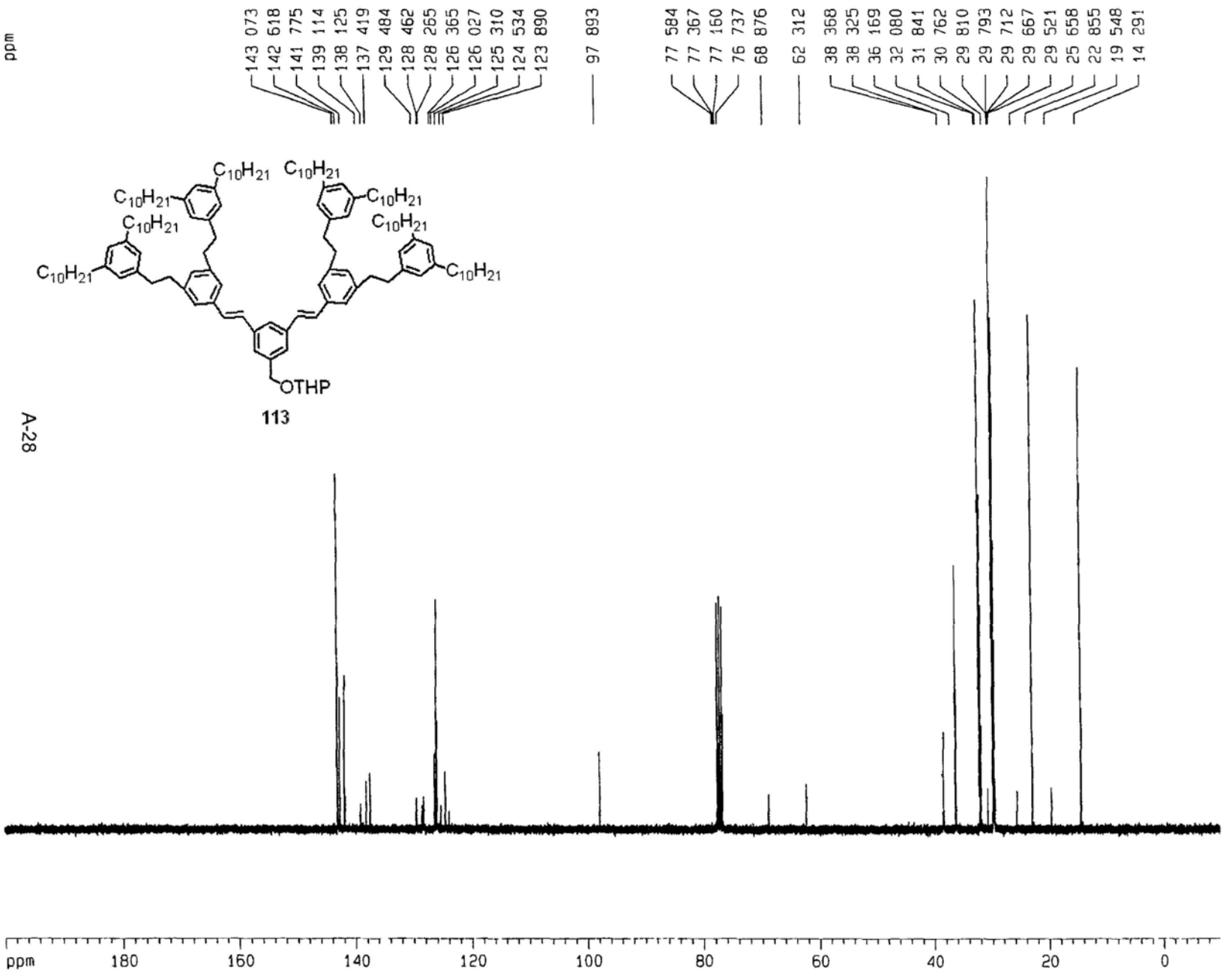

113

A-28

Current Data Parameters

NAME	G3 C C≡C-OTHP(c)
EXPNO	1
PROCNO	1

F2 - Acquisition Parameters

Date_	20080418
Time	11 01
INSTRUM	dpx300
PROBHD	5 mm BBO BB-1H
PULPROG	zgdc
TD	65536
SOLVENT	CDCl3
NS	1400
DS	0
SWH	22675 736 Hz
FIDRES	0 346004 Hz
AQ	1 4451188 sec
RG	8192
DW	22 050 usec
DE	6 00 usec
TE	296 2 K
D1	1 00000000 sec
d11	0 03000000 sec
MCREST	0 00000000 sec
MCWRK	0 01500000 sec

======== CHANNEL f1 ========

NUC1	13C
P1	3 00 usec
PL1	-6 00 dB
SF01	75 4745111 MHz

======== CHANNEL f2 ========

CPDPRG2	waltz16
NUC2	1H
PCPD2	100 00 usec
PL2	120 00 dB
PL12	19 00 dB
SF02	300 1315007 MHz

F2 - Processing parameters

SI	65536
SF	75 4677420 MHz
WDW	EM
SSB	0
LB	0 00 Hz
GB	0
PC	1 40

1D NMR plot parameters

CX	22 00 cm
CY	11 78 cm
F1P	200 000 ppm
F1	15093 55 Hz
F2P	-10 000 ppm
F2	-754 68 Hz
PPMCM	9 54545 ppm/cm
HZCM	720 37384 Hz/cm

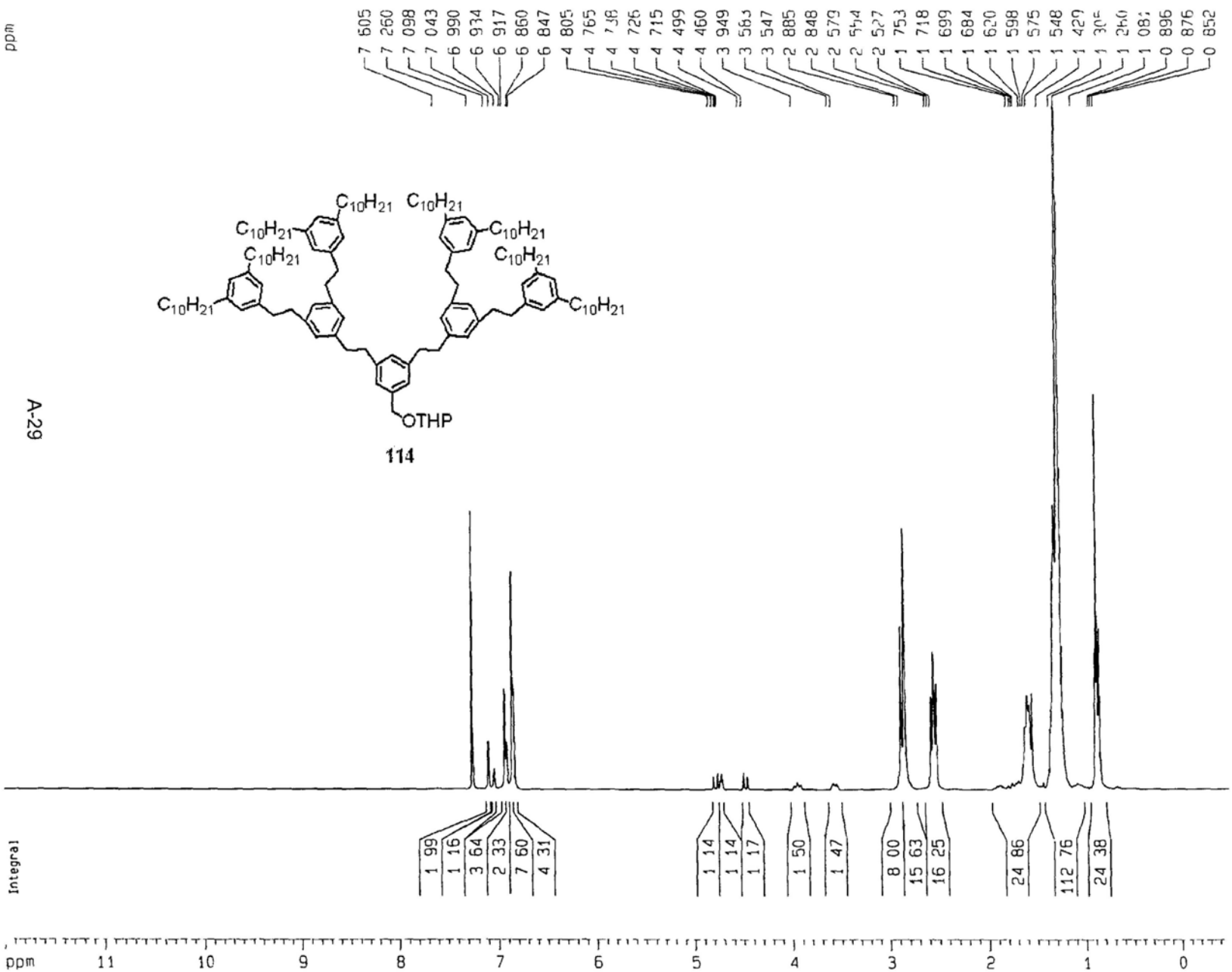

A-29

$C_{10}H_{21}$

114

Current Data Parameters

NAME	G3-CC-OTHP
EXPNO	1
PROCNO	1

F2 - Acquisition Parameters

Date_	20080421
Time	18 06
INSTRUM	dpx300
PROBHD	5 mm BBO BB-1H
PULPROG	zg
TD	32768
SOLVENT	CDCl3
NS	32
DS	0
SWH	8992 806 Hz
FIDRES	0 274439 Hz
AQ	1 8219508 sec
RG	181
DW	55 600 usec
DE	79 43 usec
TE	295 2 K
D1	5 00000000 sec
MCREST	0 00000000 sec
MCWRK	0 01500000 sec

======== CHANNEL f1 ========

NUC1	1H
P1	5 00 usec
PL1	-2 00 dB
SFO1	300 1312000 MHz

F2 - Processing parameters

SI	32768
SF	300 1300050 MHz
WDW	EM
SSB	0
LB	0 30 Hz
GB	0
PC	1 00

1D NMR plot parameters

CX	22 00 cm
CY	19 38 cm
F1P	12 000 ppm
F1	3601 56 Hz
F2P	-0 500 ppm
F2	-150 07 Hz
PPMCM	0 56818 ppm/cm
HZCM	170 52841 Hz/cm

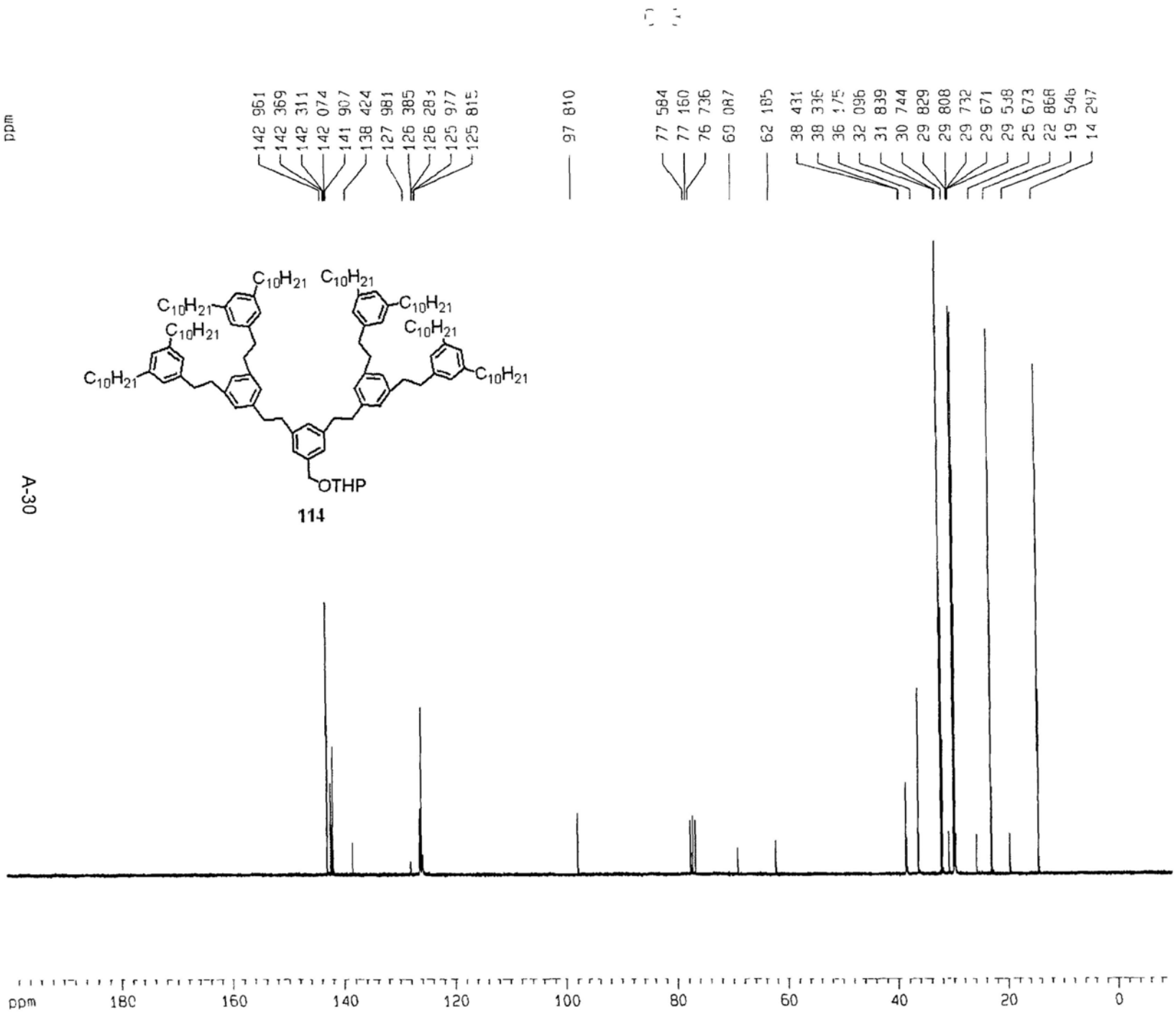

A-30

114

F2 - Acquisition Parameters

Date_	20080422
Time	10 06
INSTRUM	dpx300
PROBHD	5 mm BBO BB-1H
PULPROG	zgdc
TD	65536
SOLVENT	CDCl3
NS	361
DS	0
SWH	22675 736 Hz
FIDRES	0 346004 Hz
AQ	1 4451188 sec
RG	9195 2
DW	22 050 usec
DE	6 00 usec
TE	295 2 K
D1	1 00000000 sec
d11	0 03000000 sec
MCREST	0 00000000 sec
MCWRK	0 01500000 sec

======== CHANNEL f1 ========

NUC1	13C
P1	3 00 usec
PL1	-6 00 dB
SFO1	75 4745111 MHz

======== CHANNEL f2 ========

CPDPRG2	waltz16
NUC2	1H
PCPD2	100 00 usec
PL2	120 00 dB
PL12	19 00 dB
SFO2	300 1315007 MHz

F2 - Processing parameters

SI	65536
SF	75 4677518 MHz
WDW	EM
SSB	0
LB	0 00 Hz
GB	0
PC	1 40

1D NMR plot parameters

CX	22 00 cm
CY	12 00 cm
F1P	200 000 ppm
F1	15093 55 Hz
F2P	-10 000 ppm
F2	-754 68 Hz
PPMCM	9 54545 ppm/cm
HZCM	720 37390 Hz/cm

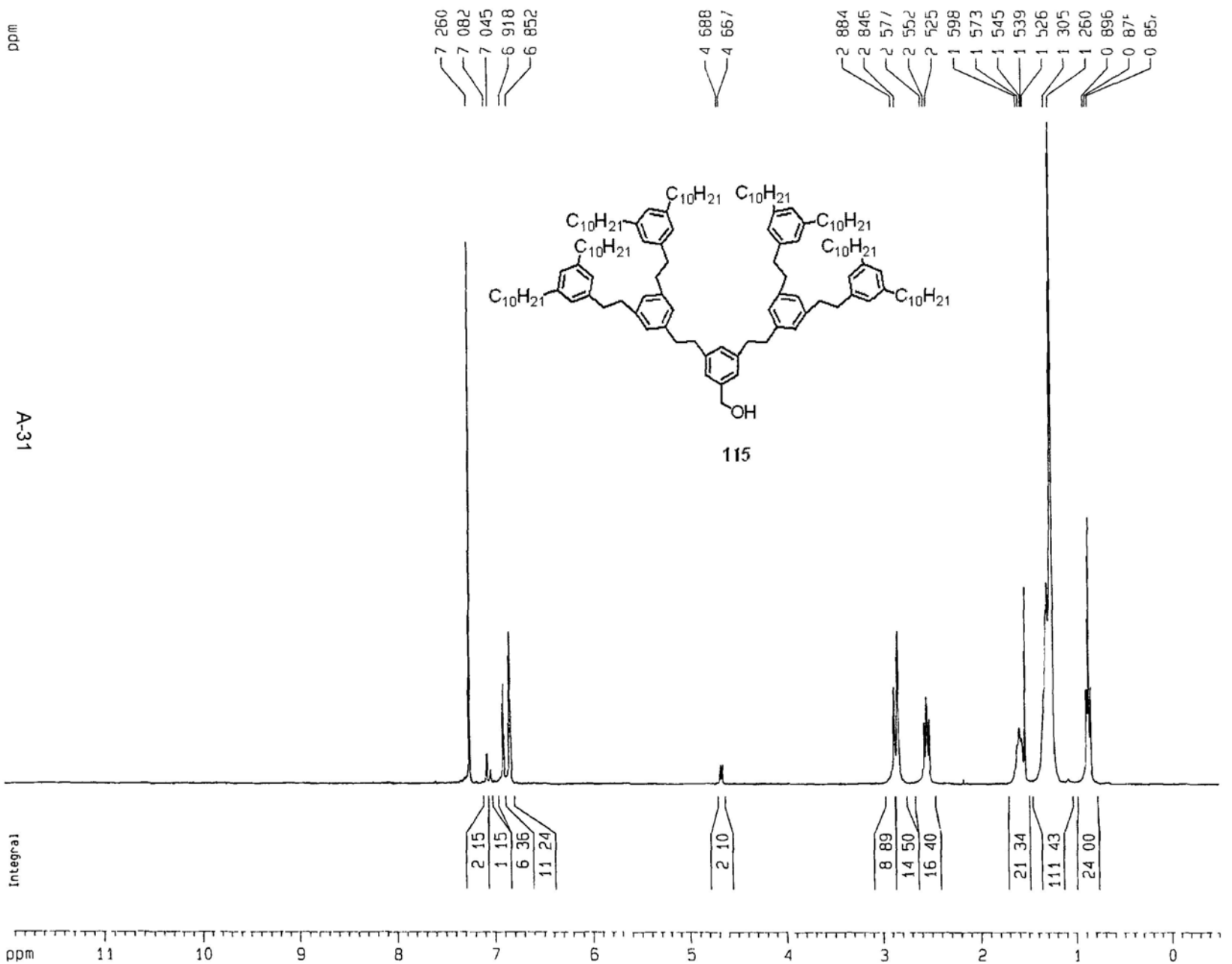

$C_{10}H_{21}$ $C_{10}H_{21}$ $C_{10}H_{21}$ $C_{10}H_{21}$ $C_{10}H_{21}$ $C_{10}H_{21}$ $C_{10}H_{21}$ OH

115

A-31

```
Current Data Parameters
NAME          G3-CC CH2OH
EXPNO                   1
PROCNO                  1

F2 - Acquisition Parameters
Date_          20080229
Time             10 56
INSTRUM          dpx300
PROBHD   5 mm BBO BB-1H
PULPROG              zg
TD                32768
SOLVENT           CDCl3
NS                    8
DS                    0
SWH           8992 806 Hz
FIDRES        0 274439 Hz
AQ            1 8219508 sec
RG              574 7
DW              55 600 usec
DE              79 43 usec
TE              298 2 K
D1            5 00000000 sec
MCREST        0 00000000 sec
MCWRK         0 01500000 sec

======== CHANNEL f1 ========
NUC1                  1H
P1                5 00 usec
PL1               -2 00 dB
SFO1        300 1312000 MHz

F2 - Processing parameters
SI                32768
SF          300 1300066 MHz
WDW                  EM
SSB                   0
LB               0 30 Hz
GB                    0
PC                1 00

1D NMR plot parameters
CX               22 00 cm
CY               11 94 cm
F1P             12 000 ppm
F1              3601 56 Hz
F2P              -0 500 ppm
F2              -150 07 Hz
PPMCM         0 56818 ppm/cm
HZCM         170 52841 Hz/cm
```

1H

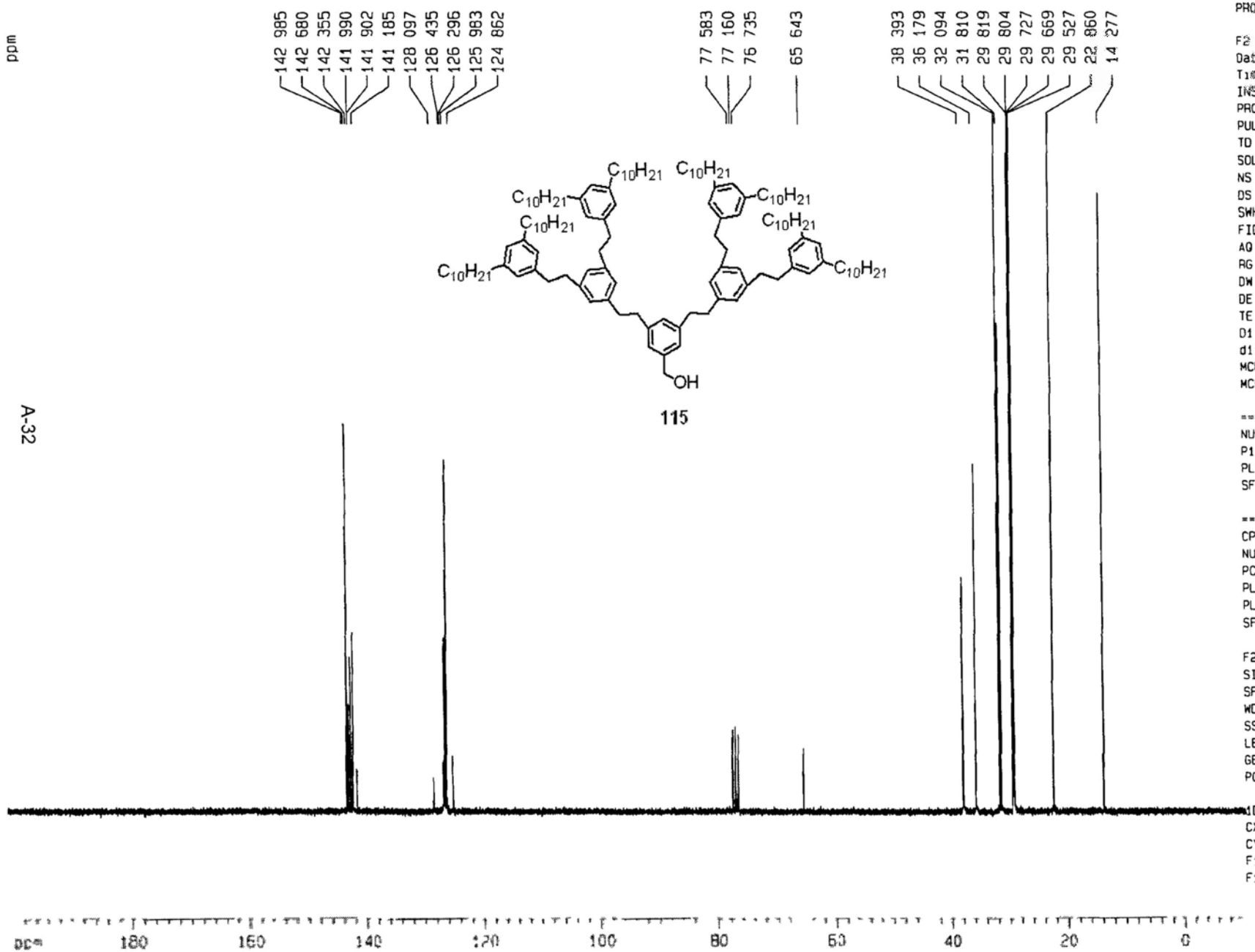

Current Data Parameters
NAME 63-CC-CH2OH-c
EXPNO 1
PROCNO 1

F2 - Acquisition Parameters
Date_ 20071101
Time 11 58
INSTRUM dpx300
PROBHD 5 mm BBO BB-1H
PULPROG zgdc
TD 65536
SOLVENT DMSO
NS 500
DS 0
SWH 22675 736 Hz
FIDRES 0 346004 Hz
AQ 1 4451188 sec
RG 1625 5
DW 22 050 usec
DE 6 00 usec
TE 0 0 K
D1 1 00000000 sec
d11 0 03000000 sec
MCREST 0 00000000 sec
MCWRK 0 01500000 sec

======== CHANNEL f1 ========
NUC1 13C
P1 3 00 usec
PL1 -6 00 dB
SFO1 75 4745111 MHz

======== CHANNEL f2 ========
CPDPRG2 waltz16
NUC2 1H
PCPD2 100 00 usec
PL2 120 00 dB
PL12 19 00 dB
SFO2 300 1315007 MHz

F2 - Processing parameters
SI 32768
SF 75 4677474 MHz
WDW EM
SSB 0
LB 0 00 Hz
GB 0
PC 1 40

1D NMR plot parameters
CX 23 00 cm
CY 18 51 cm
F1P 200 000 ppm
F1 15093 55 Hz
P -10 000 ppm
-754 68 Hz
MCM 9 13043 ppm/cm
CM 689 05334 Hz/cm

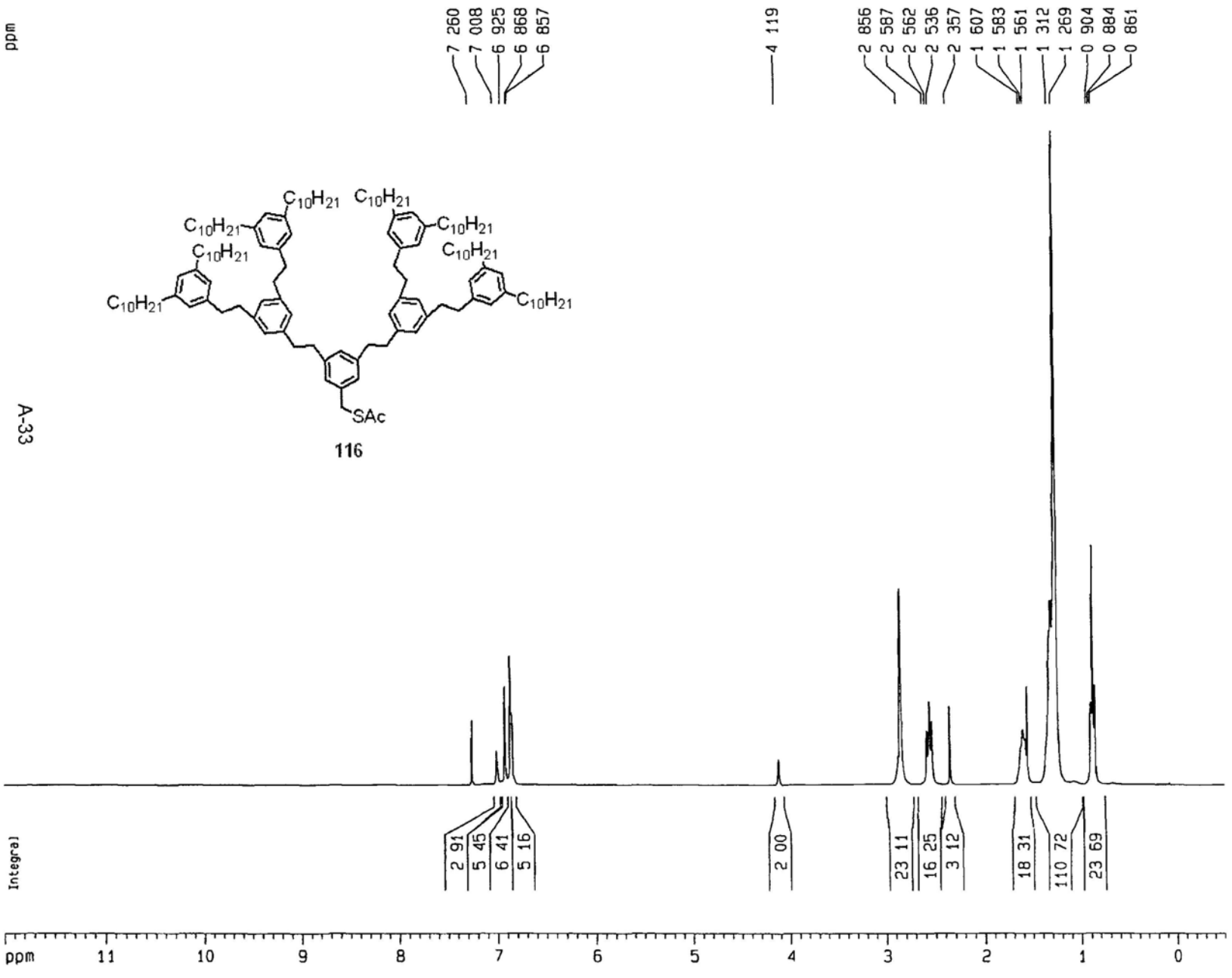

116

A-33

Current Data Parameters
NAME G3-CC-CH2SAc
EXPNO 1
PROCNO 1

F2 - Acquisition Parameters
Date_ 20080705
Time 11 34
INSTRUM dpx300
PROBHD 5 mm BBO BB-1H
PULPROG zg
TD 32768
SOLVENT CDCl3
NS 48
DS 0
SWH 8992 806 Hz
FIDRES 0 274439 Hz
AQ 1 8219508 sec
RG 101 6
DW 55 600 usec
DE 79 43 usec
TE 296 2 K
D1 5 00000000 sec
MCREST 0 00000000 sec
MCWRK 0 01500000 sec

======== CHANNEL f1 ========
NUC1 1H
P1 5 00 usec
PL1 -2 00 dB
SFO1 300 1312000 MHz

F2 - Processing parameters
SI 32768
SF 300 1300063 MHz
WDW EM
SSB 0
LB 0 30 Hz
GB 0
PC 1 00

1D NMR plot parameters
CX 22 00 cm
CY 11 74 cm
F1P 12 000 ppm
F1 3601 56 Hz
F2P -0 500 ppm
F2 -150 07 Hz
PPMCM 0 56818 ppm/cm
HZCM 170 52841 Hz/cm

C13

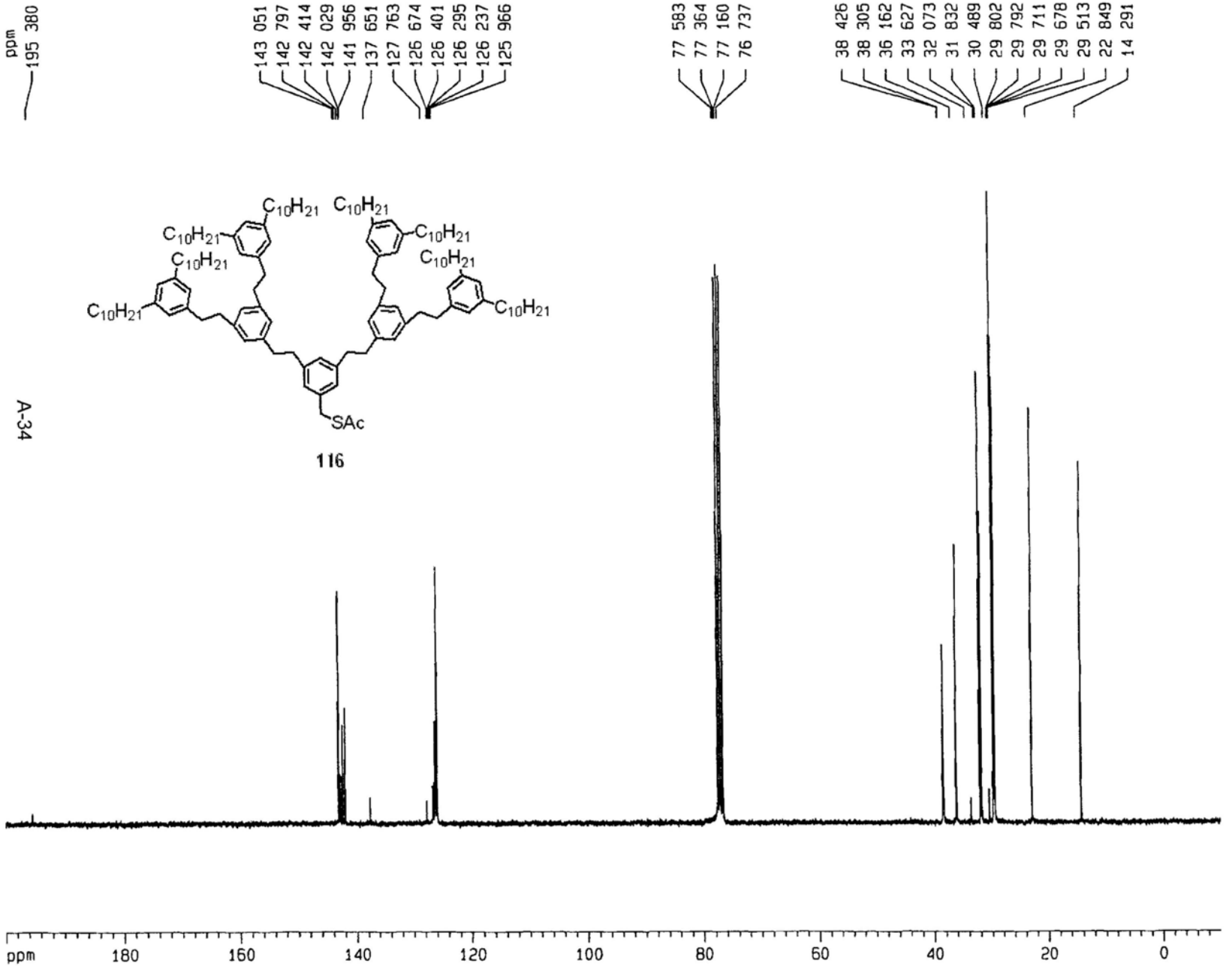

116

A-34

Current Data Parameters

NAME	G3-CC-CH2SAc-c
EXPNO	1
PROCNO	1

F2 - Acquisition Parameters

Date_	20080707
Time	18 20
INSTRUM	dpx300
PROBHD	5 mm BBO BB-1H
PULPROG	zgdc
TD	65536
SOLVENT	CDCl3
NS	6527
DS	0
SWH	22675 736 Hz
FIDRES	0 346004 Hz
AQ	1 4451188 sec
RG	8192
DW	22 050 usec
DE	6 00 usec
TE	295 2 K
D1	1 00000000 sec
d11	0 03000000 sec
MCREST	0 00000000 sec
MCWRK	0 01500000 sec

======== CHANNEL f1 ========

NUC1	13C
P1	3 00 usec
PL1	-6 00 dB
SFO1	75 4745111 MHz

======== CHANNEL f2 ========

CPDPRG2	waltz16
NUC2	1H
PCPD2	100 00 usec
PL2	120 00 dB
PL12	19 00 dB
SFO2	300 1315007 MHz

F2 - Processing parameters

SI	65536
SF	75 4677400 MHz
WDW	EM
SSB	0
LB	1 00 Hz
GB	0
PC	1 40

1D NMR plot parameters

CX	22 00 cm
CY	11 56 cm
F1P	200 000 ppm
F1	15093 55 Hz
F2P	-10 000 ppm
F2	-754 68 Hz
PPMCM	9 54545 ppm/cm
HZCM	720 37384 Hz/cm

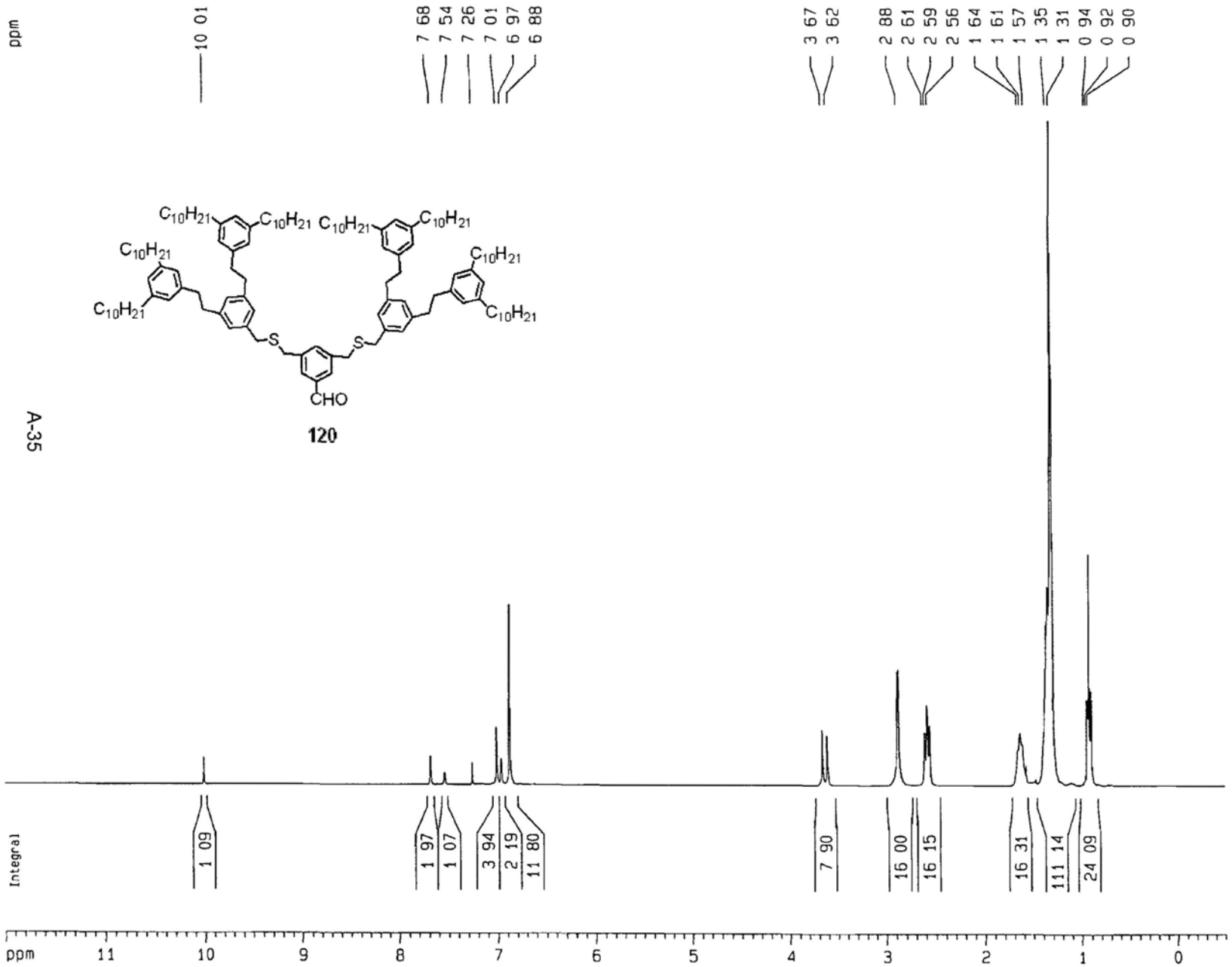

120

A-35

```
Current Data Parameters
NAME            G3-CS-CHO2
EXPNO                    1
PROCNO                   1

F2 - Acquisition Parameters
Date_            20080329
Time                12 09
INSTRUM           dpx300
PROBHD   5 mm BBO BB-1H
PULPROG                zg
TD                  32768
SOLVENT             CDCl3
NS                     16
DS                      0
SWH           8992 806 Hz
FIDRES        0 274439 Hz
AQ            1 8219508 sec
RG                 22 6
DW                55 600 usec
DE                79 43 usec
TE                296 2 K
D1            5 00000000 sec
MCREST        0 00000000 sec
MCWRK         0 01500000 sec

======== CHANNEL f1 ========
NUC1                    1H
P1                   5 00 usec
PL1                 -2 00 dB
SFO1         300 1312000 MHz

F2 - Processing parameters
SI                  32768
SF           300 1300063 MHz
WDW                    EM
SSB                     0
LB                 0 30 Hz
GB                      0
PC                 1 00

1D NMR plot parameters
CX                 22 00 cm
CY                 11 93 cm
F1P               12 000 ppm
F1               3601 56 Hz
F2P               -0 500 ppm
F2               -150 07 Hz
PPMCM          0 56818 ppm/cm
HZCM          170 52840 Hz/cm
```

C13

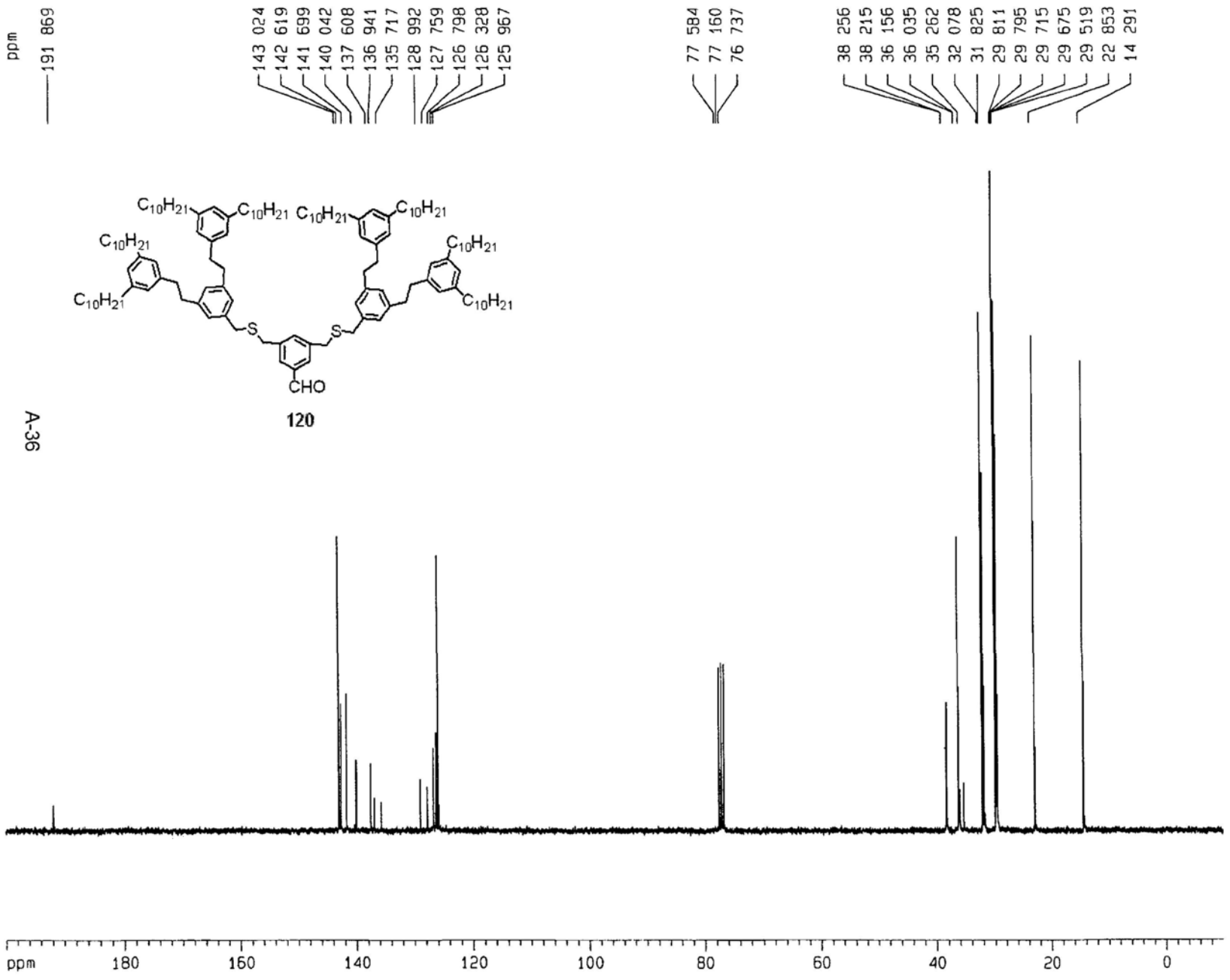

120

A-36

Current Data Parameters

NAME	G3-CS-CHO-c
EXPNO	1
PROCNO	1

F2 - Acquisition Parameters

Date_	20080329
Time	12 21
INSTRUM	dpx300
PROBHD	5 mm BBO BB-1H
PULPROG	zgdc
TD	65536
SOLVENT	CDCl3
NS	241
DS	0
SWH	22675 736 Hz
FIDRES	0 346004 Hz
AQ	1 4451188 sec
RG	8192
DW	22 050 usec
DE	6 00 usec
TE	295 2 K
D1	1 00000000 sec
d11	0 03000000 sec
MCREST	0 00000000 sec
MCWRK	0 01500000 sec

======== CHANNEL f1 ========

NUC1	13C
P1	3 00 usec
PL1	-6 00 dB
SF01	75 4745111 MHz

======== CHANNEL f2 ========

CPDPRG2	waltz16
NUC2	1H
PCPD2	100 00 usec
PL2	120 00 dB
PL12	19 00 dB
SF02	300 1315007 MHz

F2 - Processing parameters

SI	65536
SF	75 4677432 MHz
WDW	EM
SSB	0
LB	1 00 Hz
GB	0
PC	1 40

1D NMR plot parameters

CX	22 00 cm
CY	11 86 cm
F1P	200 000 ppm
F1	15093 55 Hz
F2P	-10 000 ppm
F2	-754 68 Hz
PPMCM	9 54545 ppm/cm
HZCM	720 37384 Hz/cm

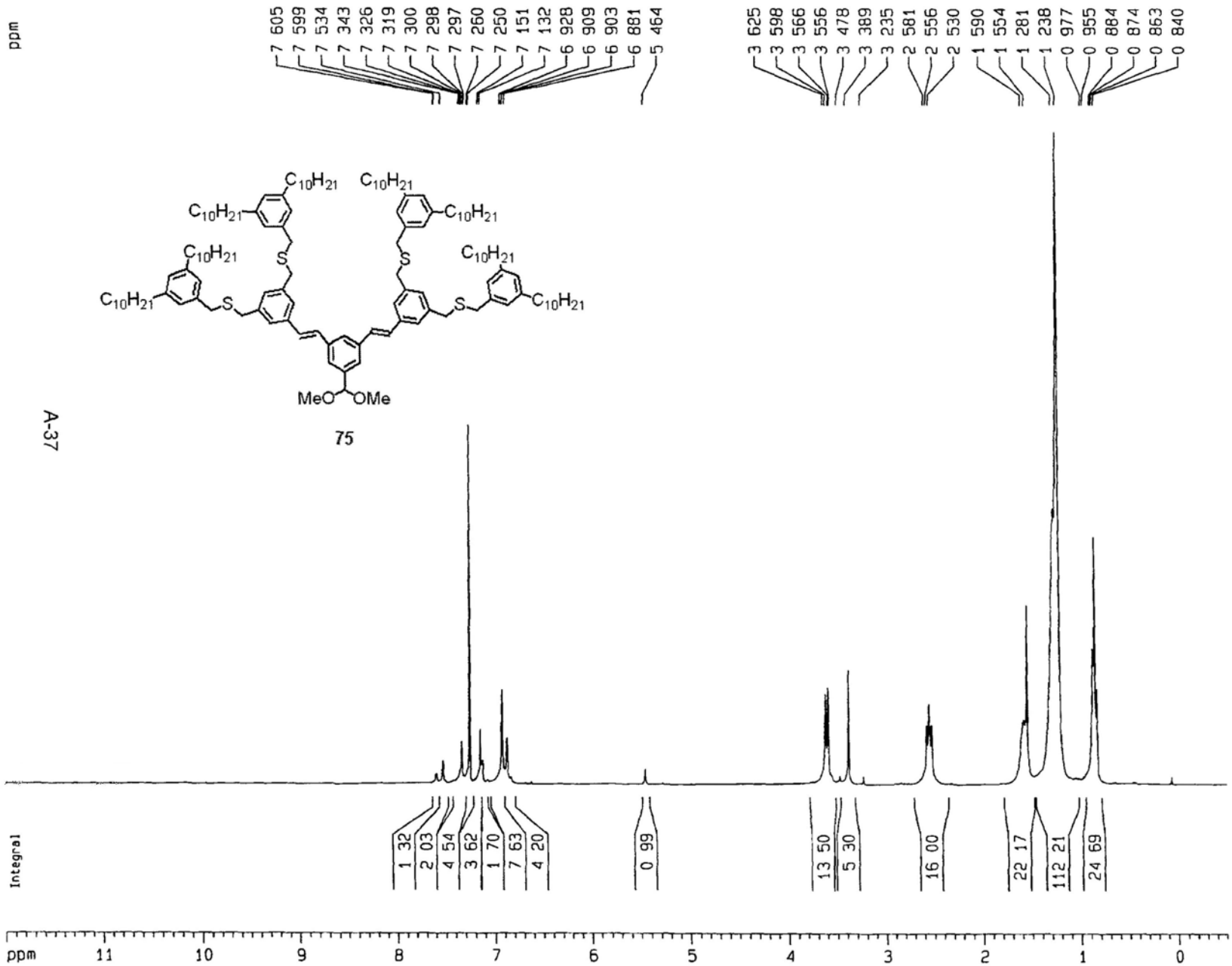

75

A-37

```
Current Data Parameters
NAME      G3-SC=C-CH(OMe)2
EXPNO                    2
PROCNO                   1

F2 - Acquisition Parameters
Date_              20090218
Time                 11 18
INSTRUM            dpx300
PROBHD   5 mm BBO BB-1H
PULPROG                zg
TD                  32768
SOLVENT             CDCl3
NS                     64
DS                      0
SWH             8992 806 Hz
FIDRES          0 274439 Hz
AQ              1 8219508 sec
RG                    181
DW                55 600 usec
DE                79 43 usec
TE                296 2 K
D1              5 00000000 sec
MCREST          0 00000000 sec
MCWRK           0 01500000 sec

======== CHANNEL f1 ========
NUC1                   1H
P1                  5 00 usec
PL1                -2 00 dB
SFO1          300 1312000 MHz

F2 - Processing parameters
SI                  32768
SF            300 1300063 MHz
WDW                    EM
SSB                     0
LB                 0 30 Hz
GB                      0
PC                 1 00

1D NMR plot parameters
CX                 22 00 cm
CY                 11 72 cm
F1P               12 000 ppm
F1                3601 56 Hz
F2P                -0 500 ppm
F2                -150 07 Hz
PPMCM           0 56818 ppm/cm
HZCM          170 52841 Hz/cm
```

C13

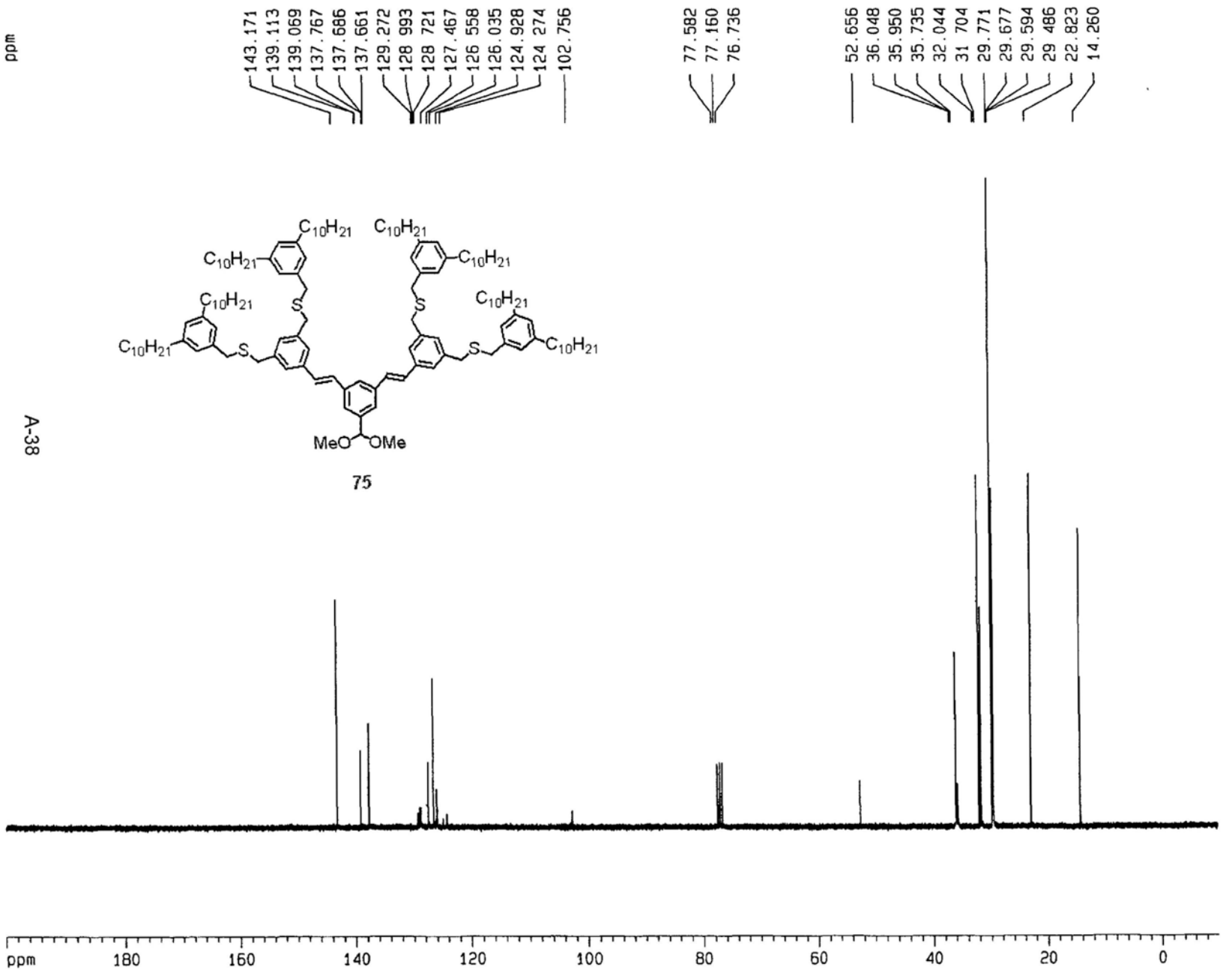

75

A-38

Current Data Parameters

NAME	G3-SC=C-CHOMe2 (c1)
EXPNO	1
PROCNO	1

F2 - Acquisition Parameters

Date_	20080618
Time	16 21
INSTRUM	dpx300
PROBHD	5 mm BBO BB-1H
PULPROG	zgdc
TD	65536
SOLVENT	CDCl3
NS	400
DS	0
SWH	22675 736 Hz
FIDRES	0 346004 Hz
AQ	1 4451188 sec
RG	8192
DW	22 050 usec
DE	6 00 usec
TE	296 2 K
D1	1 00000000 sec
d11	0 03000000 sec
MCREST	0 00000000 sec
MCWRK	0 01500000 sec

======== CHANNEL f1 ========

NUC1	13C
P1	3 00 usec
PL1	-6 00 dB
SFO1	75 4745111 MHz

======== CHANNEL f2 ========

CPDPRG2	waltz16
NUC2	1H
PCPD2	100 00 usec
PL2	120 00 dB
PL12	19 00 dB
SFO2	300 1315007 MHz

F2 - Processing parameters

SI	65536
SF	75 4677447 MHz
WDW	EM
SSB	0
LB	0 00 Hz
GB	0
PC	1 40

1D NMR plot parameters

CX	22 00 cm
CY	11 84 cm
F1P	200 000 ppm
F1	15093.55 Hz
F2P	-10 000 ppm
F2	-754 68 Hz
PPMCM	9 54545 ppm/cm
HZCM	720 37384 Hz/cm

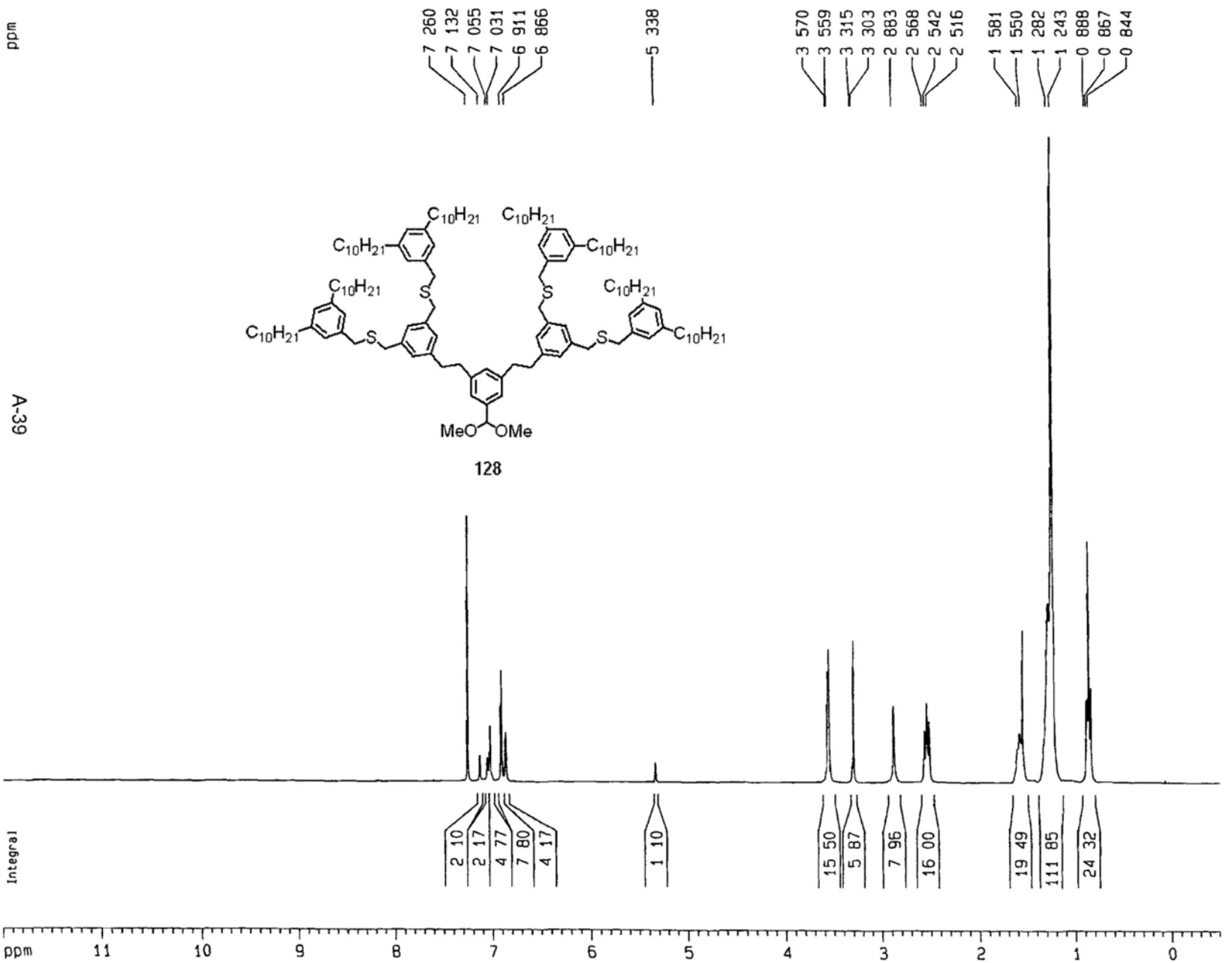

128

A-39

Current Data Parameters
NAME G3-SC-CHOMe2
EXPNO 1
PROCNO 1

F2 - Acquisition Parameters
Date_ 20080718
Time 11 39
INSTRUM dpx300
PROBHD 5 mm BBO BB-1H
PULPROG zg
TD 32768
SOLVENT CDCl3
NS 24
DS 0
SWH 8992 806 Hz
FIDRES 0 274439 Hz
AQ 1 8219508 sec
RG 256
DW 55 600 usec
DE 79 43 usec
TE 295 2 K
D1 5 00000000 sec
MCREST 0 00000000 sec
MCWRK 0 01500000 sec

======== CHANNEL f1 ========
NUC1 1H
P1 5 00 usec
PL1 -2 00 dB
SFO1 300 1312000 MHz

F2 - Processing parameters
SI 32768
SF 300 1300060 MHz
WDW EM
SSB 0
LB 0 30 Hz
GB 0
PC 1 00

1D NMR plot parameters
CX 22 00 cm
CY 11 66 cm
F1P 12 000 ppm
F1 3601 56 Hz
F2P -0 500 ppm
F2 -150 07 Hz
PPMCM 0 56818 ppm/cm
HZCM 170 52841 Hz/cm

C13

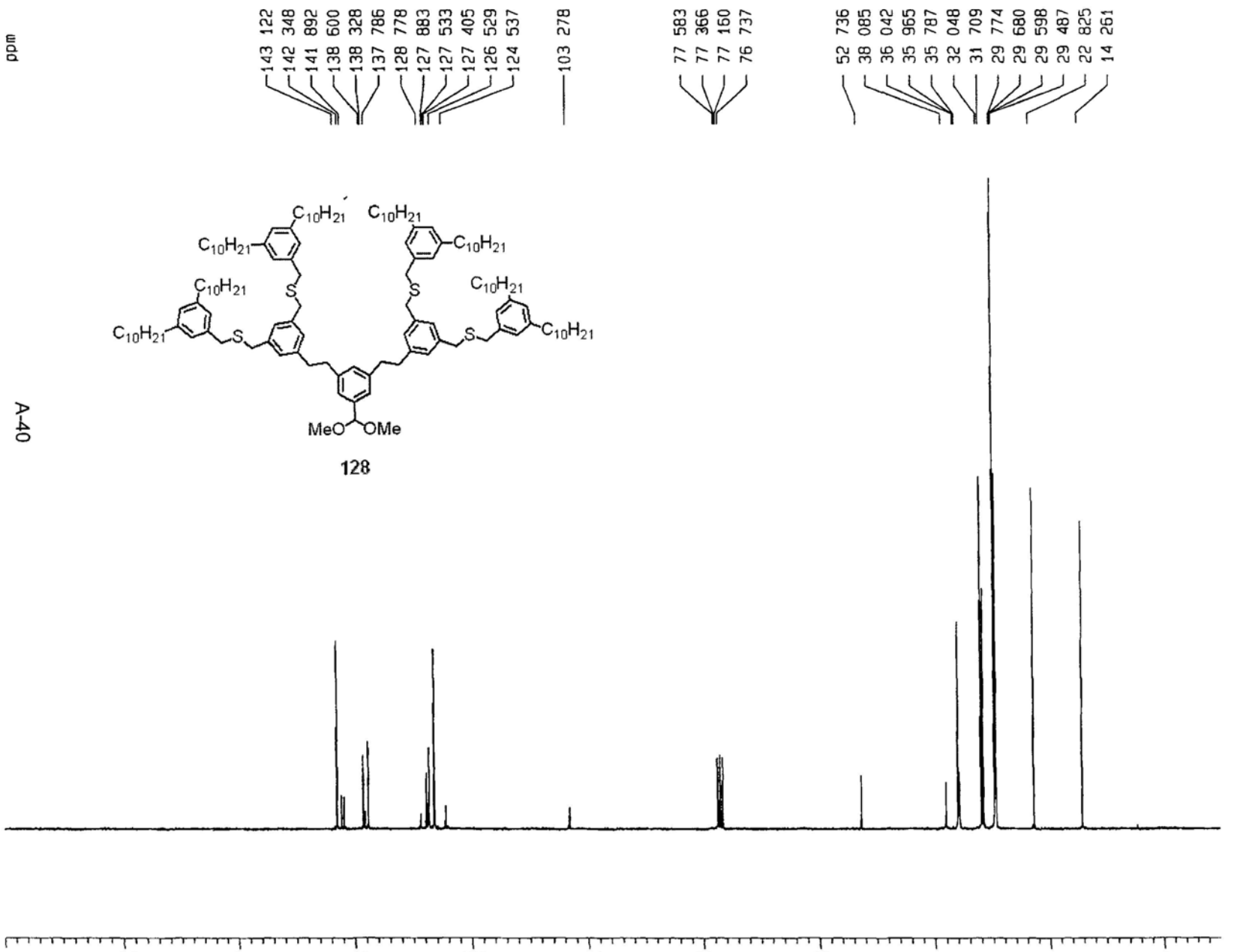

128

A-40

Current Data Parameters
NAME G3-SC-CHOMe2(c)
EXPNO 1
PROCNO 1

F2 - Acquisition Parameters
Date_ 20080715
Time 10 19
INSTRUM dpx300
PROBHD 5 mm BBO BB-1H
PULPROG zgdc
TD 65536
SOLVENT CDCl3
NS 500
DS 0
SWH 22675 736 Hz
FIDRES 0 346004 Hz
AQ 1 4451188 sec
RG 7298 2
DW 22 050 usec
DE 6 00 usec
TE 295 2 K
D1 1 00000000 sec
d11 0 03000000 sec
MCREST 0 00000000 sec
MCWRK 0 01500000 sec

======== CHANNEL f1 ========
NUC1 13C
P1 3 00 usec
PL1 -6 00 dB
SFO1 75 4745111 MHz

======== CHANNEL f2 ========
CPDPRG2 waltz16
NUC2 1H
PCPD2 100 00 usec
PL2 120 00 dB
PL12 19 00 dB
SFO2 300 1315007 MHz

F2 - Processing parameters
SI 65536
SF 75 4677452 MHz
WDW EM
SSB 0
LB 1 00 Hz
GB 0
PC 1 40

1D NMR plot parameters
CX 22 00 cm
CY 11 84 cm
F1P 200 000 ppm
F1 15093 55 Hz
F2P -10 000 ppm
F2 -754 68 Hz
PPMCM 9 54545 ppm/cm
HZCM 720 37384 Hz/cm

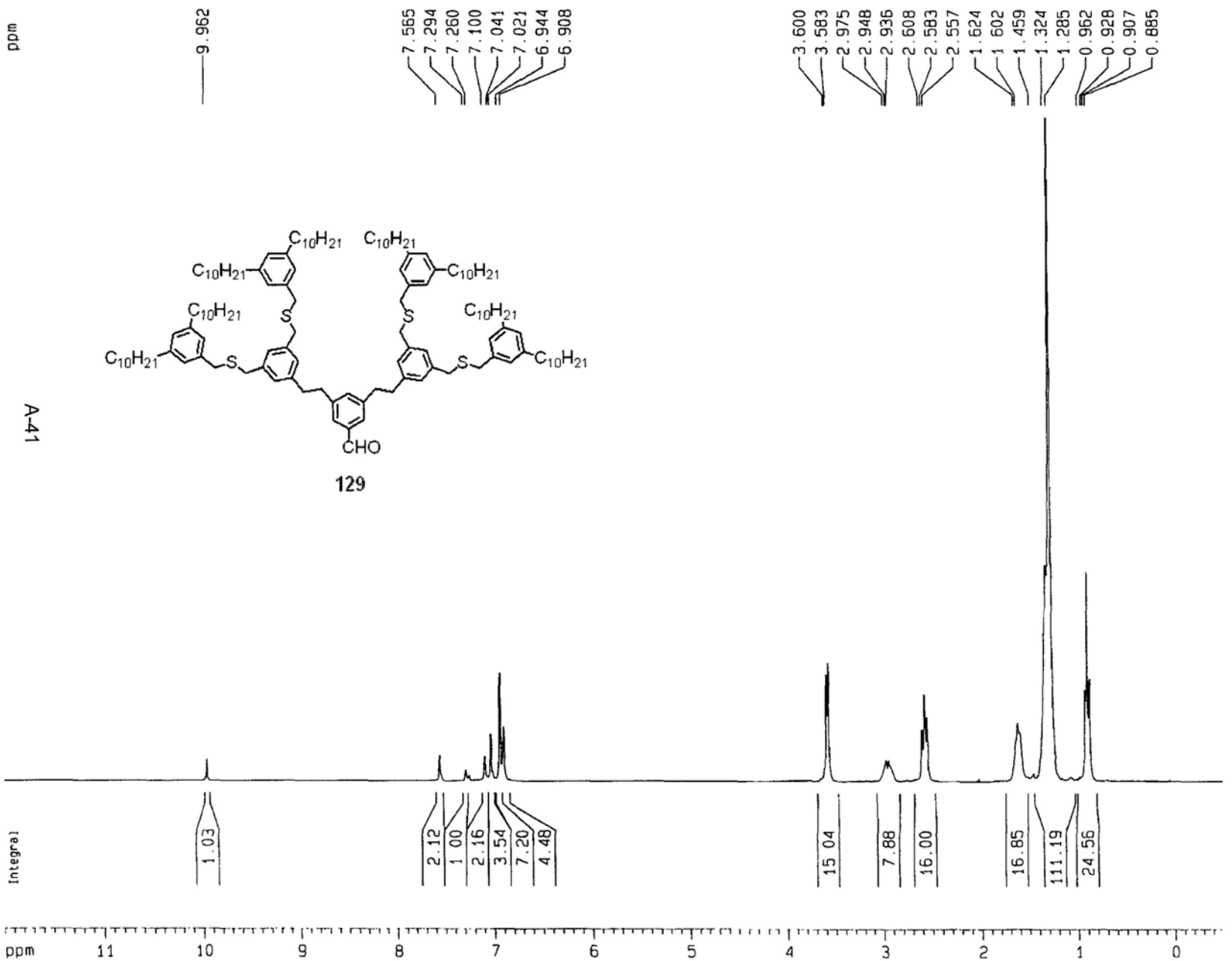

129

```
Current Data Parameters
NAME                  G3-SC-CHO
EXPNO                         1
PROCNO                        1

F2 - Acquisition Parameters
Date_                  20080718
Time                      11.47
INSTRUM                  dpx300
PROBHD    5 mm BBO BB-1H
PULPROG                     zg
TD                       32768
SOLVENT                  CDCl3
NS                           24
DS                            0
SWH                   8992.806 Hz
FIDRES                0.274439 Hz
AQ                    1.8219508 sec
RG                         20.2
DW                       55.600 usec
DE                       79.43 usec
TE                        295.2 K
D1                    5.00000000 sec
MCREST                0.00000000 sec
MCWRK                 0.01500000 sec

======== CHANNEL f1 ========
NUC1                         1H
P1                        5.00 usec
PL1                      -2.00 dB
SFO1                300.1312000 MHz

F2 - Processing parameters
SI                       32768
SF                  300.1300046 MHz
WDW                         EM
SSB                          0
LB                        0.30 Hz
GB                           0
PC                        1.00

1D NMR plot parameters
CX                       22.00 cm
CY                       12.01 cm
F1P                     12.000 ppm
F1                     3601.56 Hz
F2P                    -0.500 ppm
F2                     -150.07 Hz
PPMCM                 0.56818 ppm/cm
HZCM                170.52841 Hz/cm
```

C13

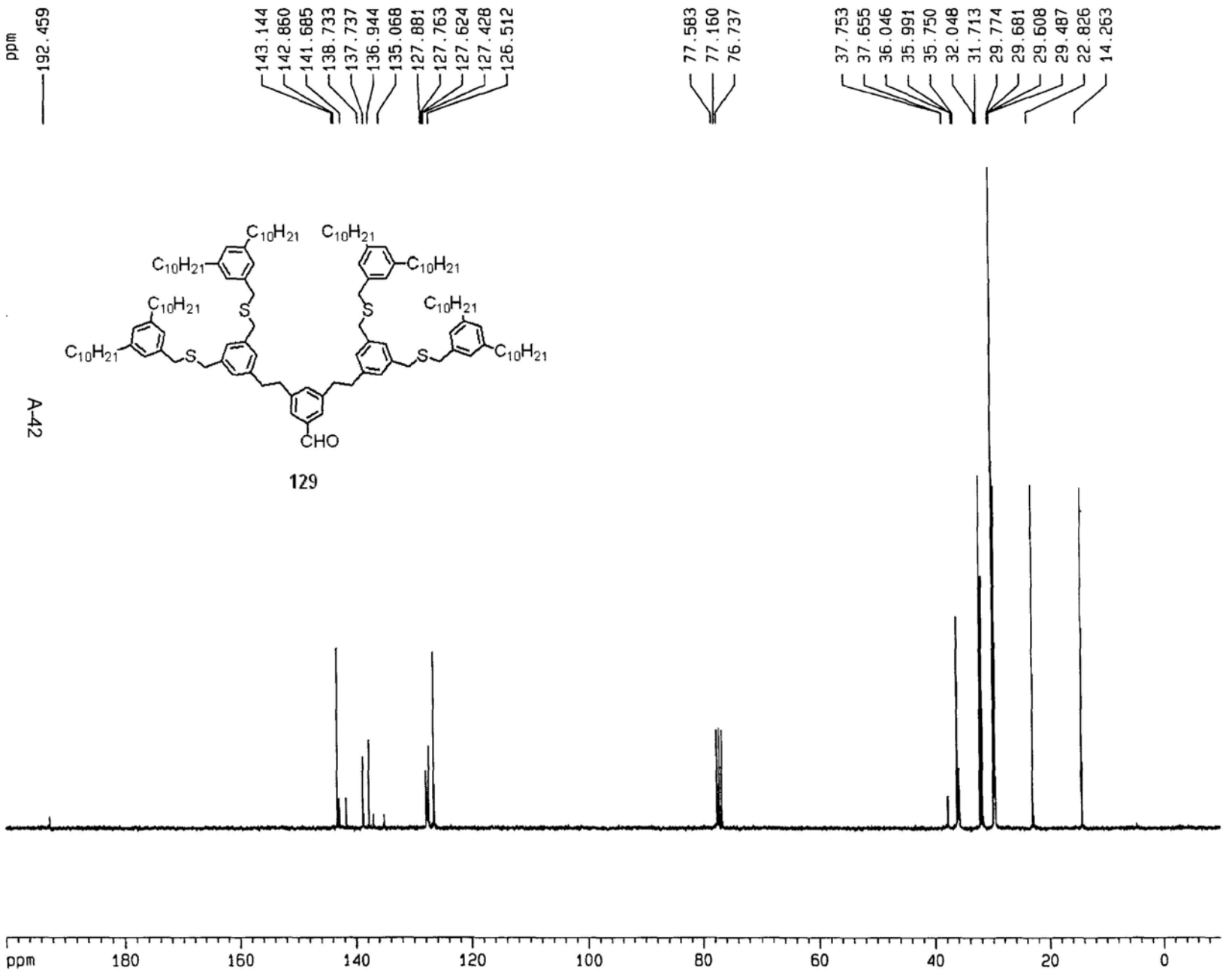

129

Current Data Parameters

NAME	G3-SC-CHO(c)
EXPNO	1
PROCNO	1

F2 - Acquisition Parameters

Date_	20080718
Time	11.58
INSTRUM	dpx300
PROBHD	5 mm BBO BB-1H
PULPROG	zgdc
TD	65536
SOLVENT	CDCl3
NS	300
DS	0
SWH	22675.736 Hz
FIDRES	0.346004 Hz
AQ	1.4451188 sec
RG	7298.2
DW	22.050 usec
DE	6.00 usec
TE	296.2 K
D1	1.00000000 sec
d11	0.03000000 sec
MCREST	0.00000000 sec
MCWRK	0.01500000 sec

======== CHANNEL f1 ========

NUC1	13C
P1	3.00 usec
PL1	-6.00 dB
SFO1	75.4745111 MHz

======== CHANNEL f2 ========

CPDPRG2	waltz16
NUC2	1H
PCPD2	100.00 usec
PL2	120.00 dB
PL12	19.00 dB
SFO2	300.1315007 MHz

F2 - Processing parameters

SI	65536
SF	75.4677436 MHz
WDW	EM
SSB	0
LB	1.00 Hz
GB	0
PC	1.40

1D NMR plot parameters

CX	22.00 cm
CY	11.97 cm
F1P	200.000 ppm
F1	15093.55 Hz
F2P	-10.000 ppm
F2	-754.68 Hz
PPMCM	9.54545 ppm/cm
HZCM	720.37384 Hz/cm

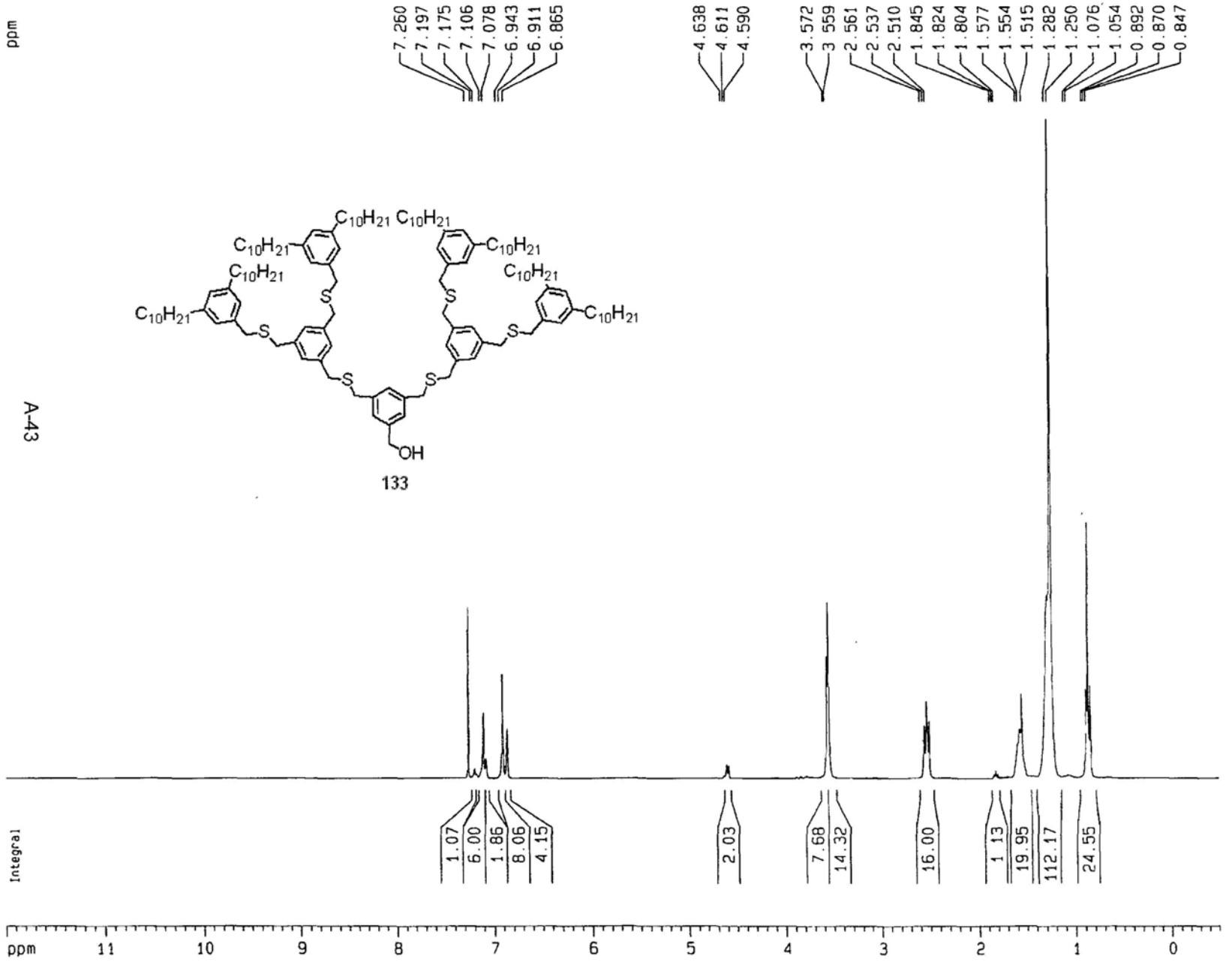

A-43

133

Current Data Parameters

NAME	G3-SS-CH2OH
EXPNO	1
PROCNO	1

F2 - Acquisition Parameters

Date_	20090319
Time	11.31
INSTRUM	dpx300
PROBHD	5 mm BBO BB-1H
PULPROG	zg
TD	32768
SOLVENT	CDCl3
NS	32
DS	0
SWH	8992.806 Hz
FIDRES	0.274439 Hz
AQ	1.8219508 sec
RG	203.2
DW	55.600 usec
DE	79.43 usec
TE	294.2 K
D1	5.00000000 sec
MCREST	0.00000000 sec
MCWRK	0.01500000 sec

======== CHANNEL f1 ========

NUC1	1H
P1	5.00 usec
PL1	-2.00 dB
SFO1	300.1312000 MHz

F2 - Processing parameters

SI	32768
SF	300.1300068 MHz
WDW	EM
SSB	0
LB	0.30 Hz
GB	0
PC	1.00

1D NMR plot parameters

CX	22.00 cm
CY	11.91 cm
F1P	12.000 ppm
F1	3601.56 Hz
F2P	-0.500 ppm
F2	-150.07 Hz
PPMCM	0.56818 ppm/cm
HZCM	170.52841 Hz/cm

C13

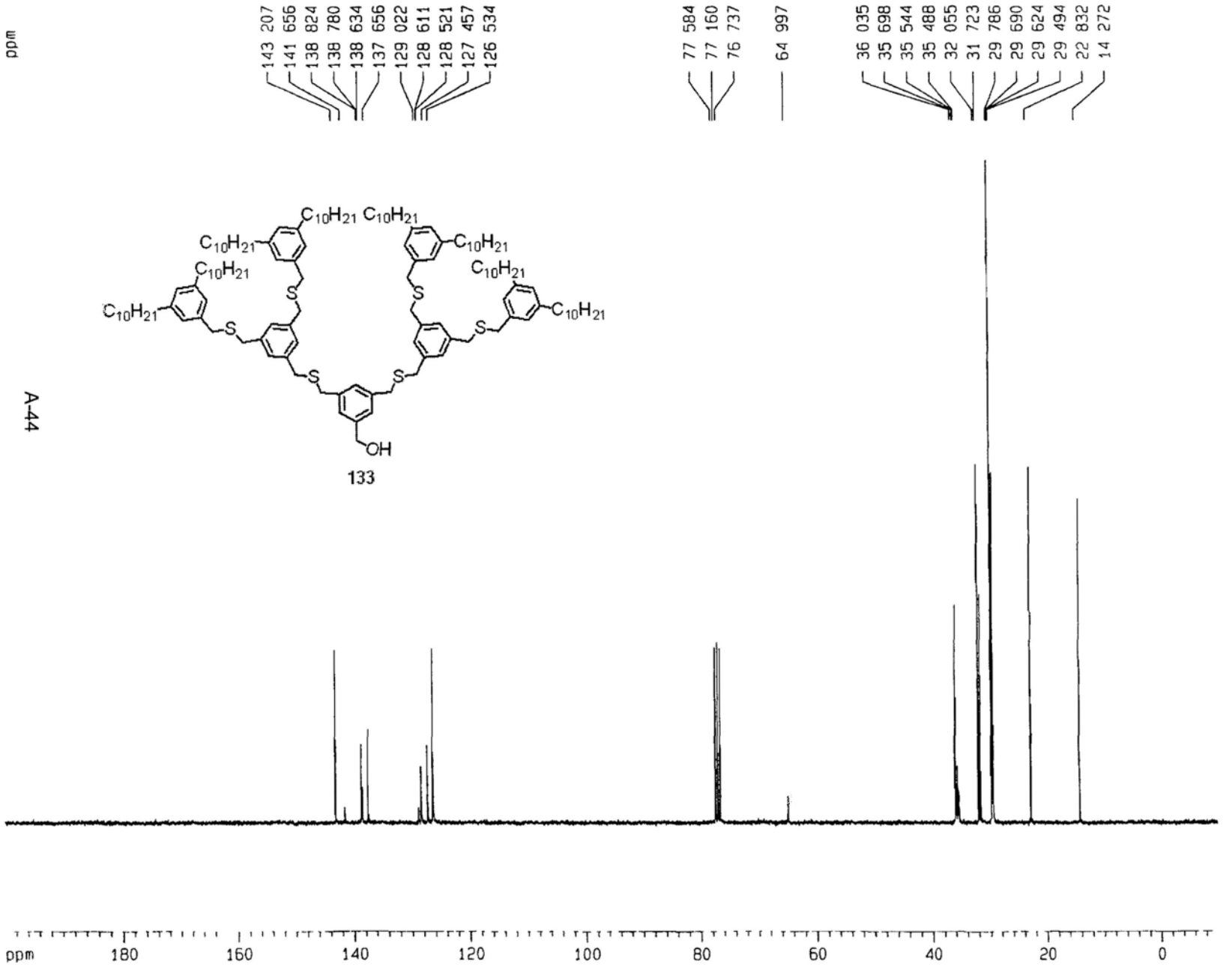

133

Current Data Parameters
NAME G3-SS-CH2OH(c)
EXPNO 1
PROCNO 1

F2 - Acquisition Parameters
Date_ 20090319
Time 11 52
INSTRUM dpx300
PROBHD 5 mm BBO BB-1H
PULPROG zgdc
TD 65536
SOLVENT CDCl3
NS 407
DS 0
SWH 22675 736 Hz
FIDRES 0 346004 Hz
AQ 1 4451188 sec
RG 8192
DW 22 050 usec
DE 6 00 usec
TE 296 2 K
D1 1 00000000 sec
d11 0 03000000 sec
MCREST 0 00000000 sec
MCWRK 0 01500000 sec

======== CHANNEL f1 ========
NUC1 13C
P1 3 00 usec
PL1 -6 00 dB
SFO1 75 4745111 MHz

======== CHANNEL f2 ========
CPDPRG2 waltz16
NUC2 1H
PCPD2 100 00 usec
PL2 120 00 dB
PL12 19 00 dB
SFO2 300 1315007 MHz

F2 - Processing parameters
SI 65536
SF 75 4677423 MHz
WDW EM
SSB 0
LB 1 00 Hz
GB 0
PC 1 40

1D NMR plot parameters
CX 22 00 cm
CY 12 00 cm
F1P 200 000 ppm
F1 15093 55 Hz
F2P -10 000 ppm
F2 -754 68 Hz
PPMCM 9 54545 ppm/cm
HZCM 720 37384 Hz/cm

1H

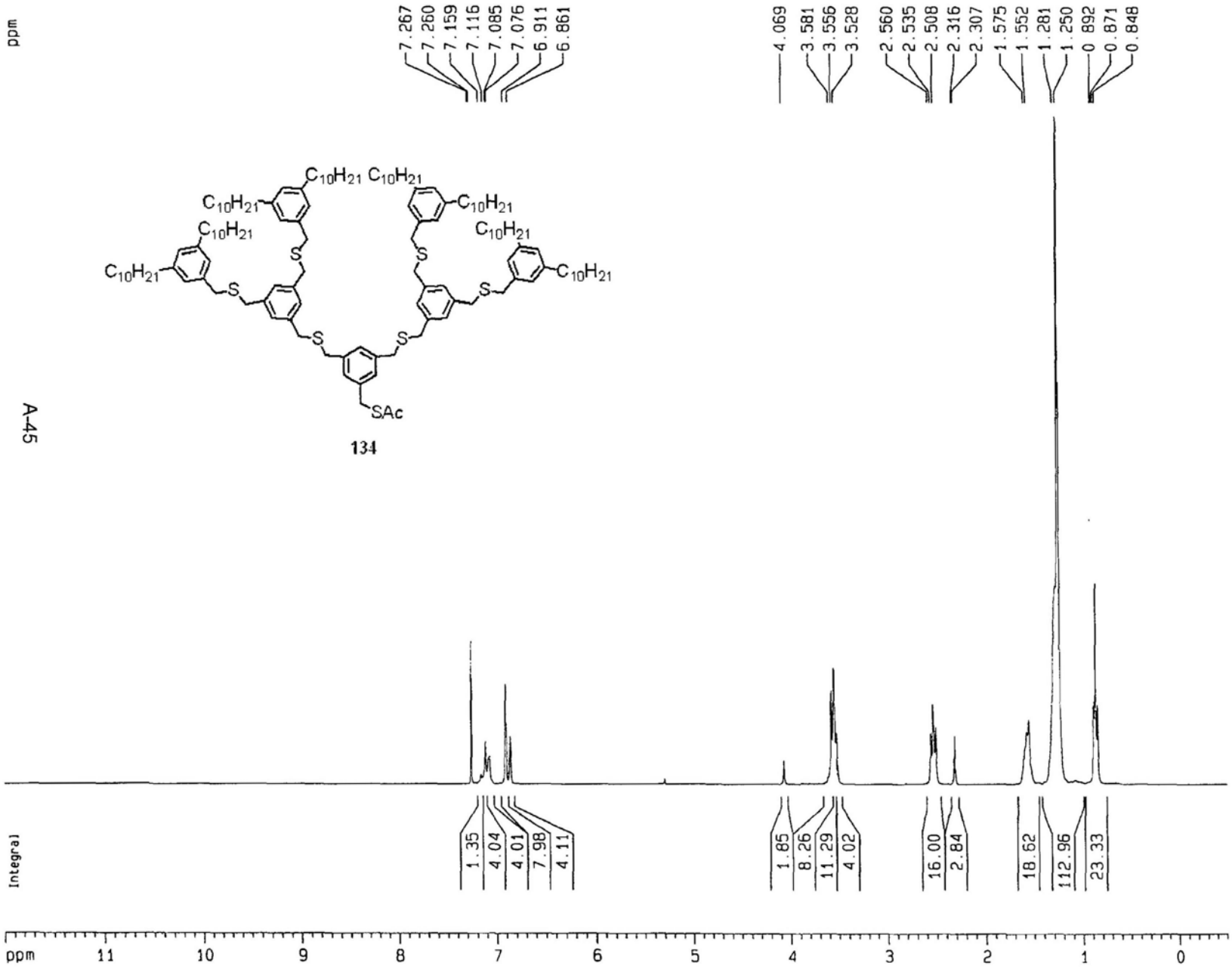

134

A-45

```
Current Data Parameters
NAME        G3-SS-CH2SAc
EXPNO                  1
PROCNO                 1

F2 - Acquisition Parameters
Date_           20090422
Time               11.52
INSTRUM          dpx300
PROBHD   5 mm BBO BB-1H
PULPROG              zg
TD                32768
SOLVENT           CDCl3
NS                   16
DS                    0
SWH          8992.806 Hz
FIDRES       0.274439 Hz
AQ           1.8219508 sec
RG                  256
DW             55.600 usec
DE             79.43 usec
TE             295.2 K
D1          1.00000000 sec
MCREST      0.00000000 sec
MCWRK       0.01500000 sec

======== CHANNEL f1 ========
NUC1                  1H
P1              5.00 usec
PL1             -2.00 dB
SFO1       300.1312000 MHz

F2 - Processing parameters
SI                32768
SF         300.1300066 MHz
WDW                  EM
SSB                   0
LB             0.30 Hz
GB                    0
PC                1.00

1D NMR plot parameters
CX               22.00 cm
CY               11.97 cm
F1P             12.000 ppm
F1             3601.56 Hz
F2P             -0.500 ppm
F2             -150.07 Hz
PPMCM          0.56818 ppm/cm
HZCM         170.52841 Hz/cm
```

C13

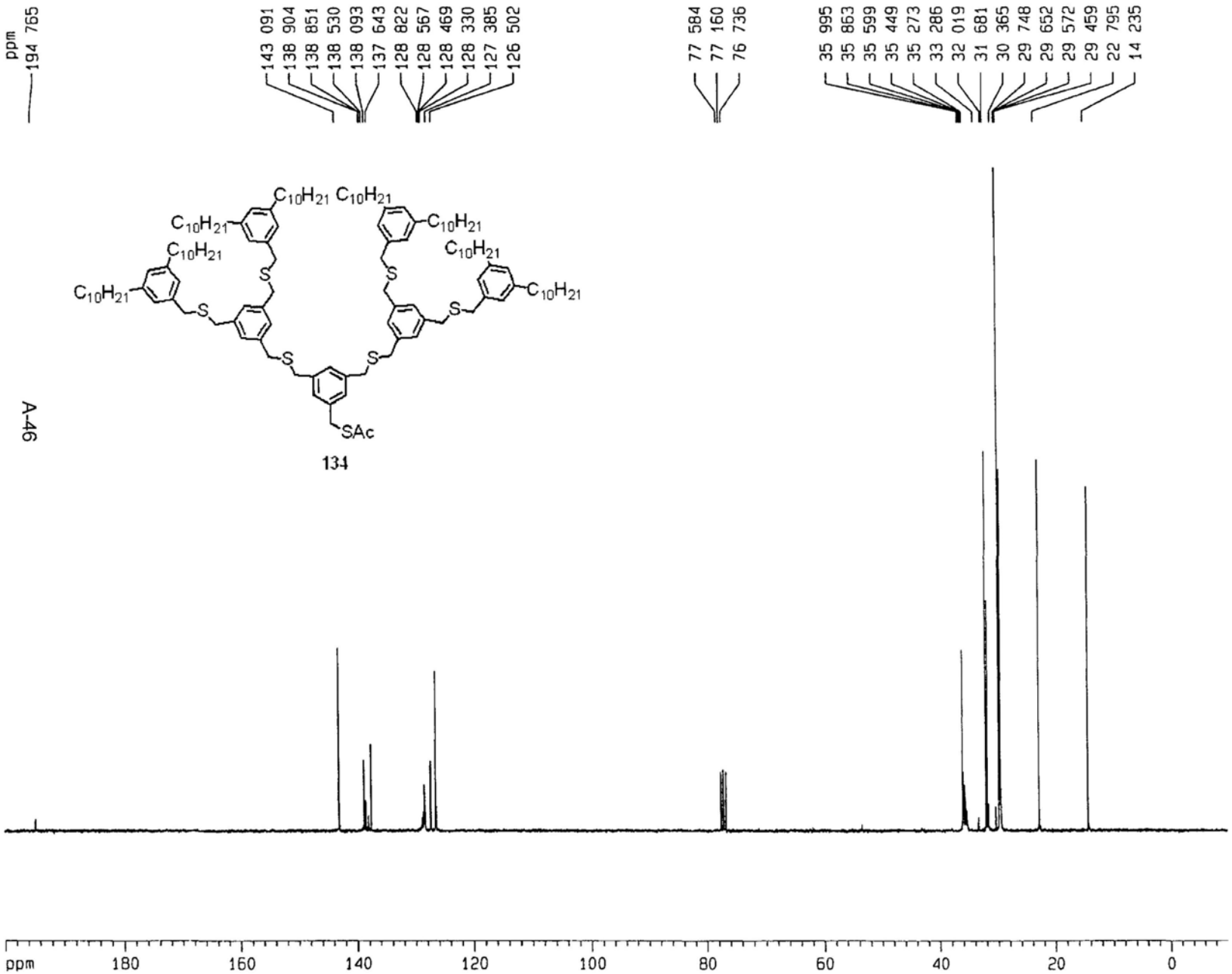

134

Current Data Parameters

NAME	G3-SS-CH2SAc (c)
EXPNO	1
PROCNO	1

F2 - Acquisition Parameters

Date_	20090422
Time	11 18
INSTRUM	dpx300
PROBHD	5 mm BBO BB-1H
PULPROG	zgdc
TD	65536
SOLVENT	CDCl3
NS	100
DS	0
SWH	22675 736 Hz
FIDRES	0 346004 Hz
AQ	1 4451188 sec
RG	4597 6
DW	22 050 usec
DE	6 00 usec
TE	296 2 K
D1	1 00000000 sec
d11	0 03000000 sec
MCREST	0 00000000 sec
MCWRK	0 01500000 sec

======== CHANNEL f1 ========

NUC1	13C
P1	3 00 usec
PL1	-6 00 dB
SF01	75 4745111 MHz

======== CHANNEL f2 ========

CPDPRG2	waltz16
NUC2	1H
PCPD2	100 00 usec
PL2	120 00 dB
PL12	19 00 dB
SF02	300 1315007 MHz

F2 - Processing parameters

SI	65536
SF	75 4677499 MHz
WDW	EM
SSB	0
LB	1 00 Hz
GB	0
PC	1 40

1D NMR plot parameters

CX	22 00 cm
CY	12 00 cm
F1P	200 000 ppm
F1	15093 55 Hz
F2P	-10 000 ppm
F2	-754 68 Hz
PPMCM	9 54545 ppm/cm
HZCM	720 37390 Hz/cm

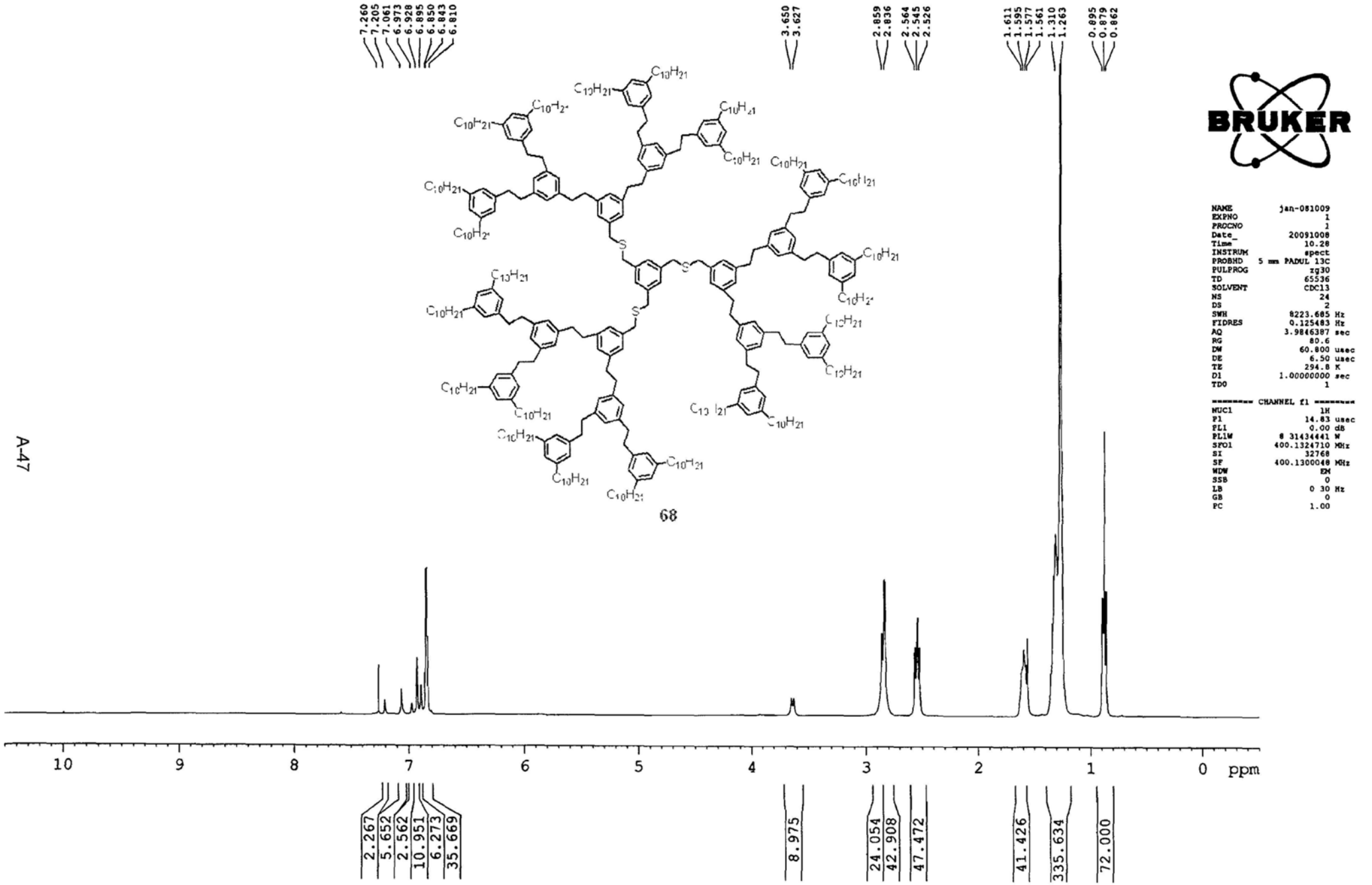
7.260
7.205
7.061
6.973
6.928
6.895
6.850
6.843
6.810
3.650
3.627
2.859
2.836
2.564
2.545
2.526
1.611
1.595
1.577
1.561
1.310
1.263
0.895
0.879
0.862
BRUKER
NAME jan-081009
EXPNO 1
PROCNO 1
Date_ 20091008
Time 10.28
INSTRUM spect
PROBHD 5 mm PADUL 13C
PULPROG zg30
TD 65536
SOLVENT CDCl3
NS 24
DS 2
SWH 8223.685 Hz
FIDRES 0.125483 Hz
AQ 3.9846387 sec
RG 80.6
DW 60.800 usec
DE 6.50 usec
TE 294.8 K
D1 1.00000000 sec
TD0 1
======== CHANNEL f1 ========
NUC1 1H
P1 14.83 usec
PL1 0.00 dB
PL1W 8.31434441 W
SFO1 400.1324710 MHz
SI 32768
SF 400.1300048 MHz
WDW EM
SSB 0
LB 0.30 Hz
GB 0
PC 1.00
68
A-47
10
9
8
7
6
5
4
3
2
1
0 ppm
2.267
5.652
2.562
10.951
6.273
35.669
8.975
24.054
42.908
47.472
41.426
335.634
72.000

C13

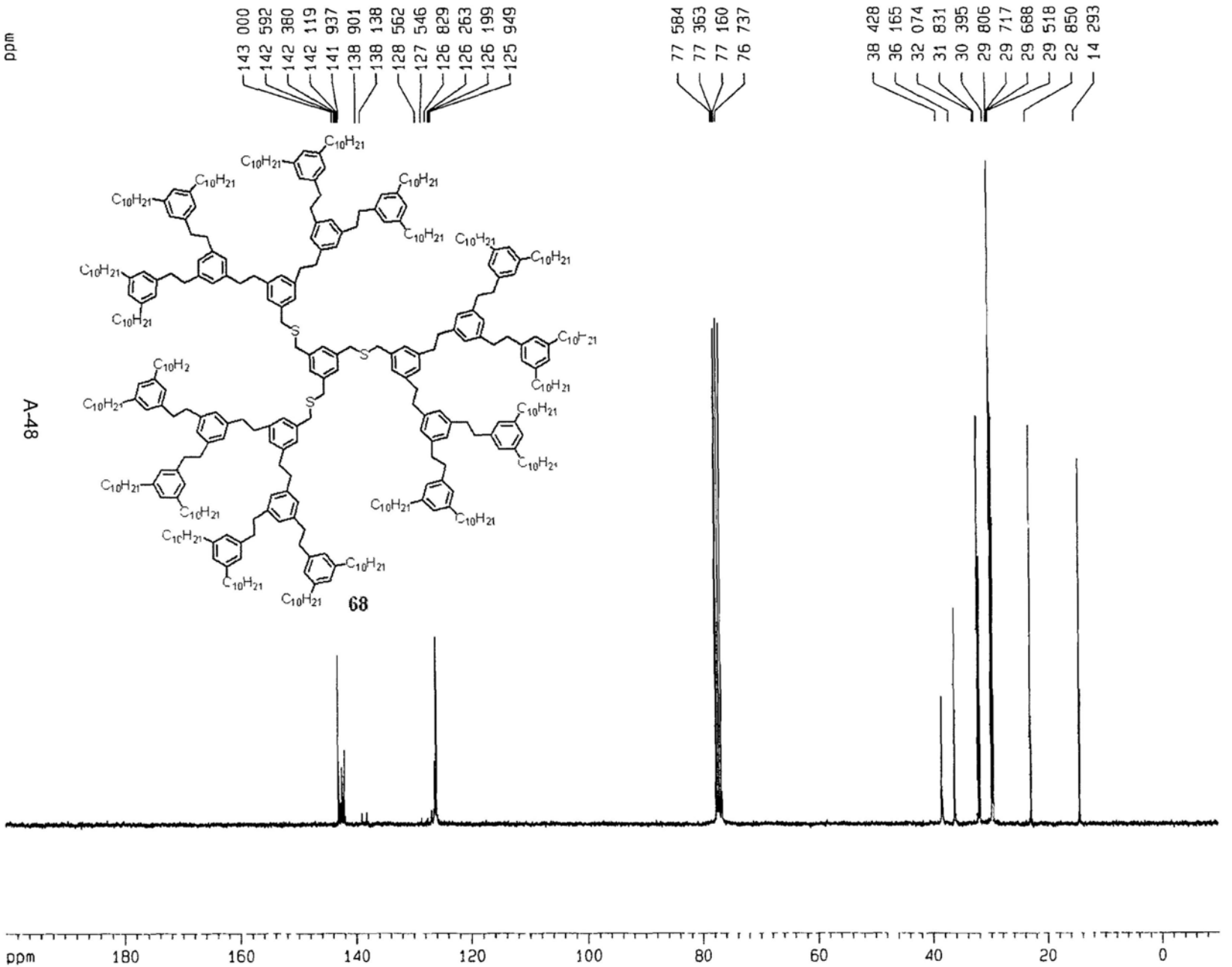

Current Data Parameters
NAME G3-CCS-dendrimer(c)
EXPNO 1
PROCNO 1

F2 - Acquisition Parameters
Date_ 20091008
Time 14 16
INSTRUM dpx300
PROBHD 5 mm BBO BB-1H
PULPROG zgdc
TD 65536
SOLVENT CDCl3
NS 4166
DS 0
SWH 22675 736 Hz
FIDRES 0 346004 Hz
AQ 1 4451188 sec
RG 2298 8
DW 22 050 usec
DE 6 00 usec
TE 295 2 K
D1 1 00000000 sec
d11 0 03000000 sec
MCREST 0 00000000 sec
MCWRK 0 01500000 sec

======== CHANNEL f1 ========
NUC1 13C
P1 3 00 usec
PL1 -6 00 dB
SFO1 75 4745111 MHz

======== CHANNEL f2 ========
CPDPRG2 waltz16
NUC2 1H
PCPD2 100 00 usec
PL2 120 00 dB
PL12 19 00 dB
SFO2 300 1315007 MHz

F2 Processing parameters
SI 65536
SF 75 4677404 MHz
WDW EM
SSB 0
LB 1 00 Hz
GB 0
PC 1 40

1D NMR plot parameters
CX 22 00 cm
CY 12 00 cm
F1P 200 000 ppm
F1 15093 55 Hz
F2P -10 000 ppm
F2 -754 68 Hz
PPMCM 9 54545 ppm/cm
HZCM 720 37384 Hz/cm

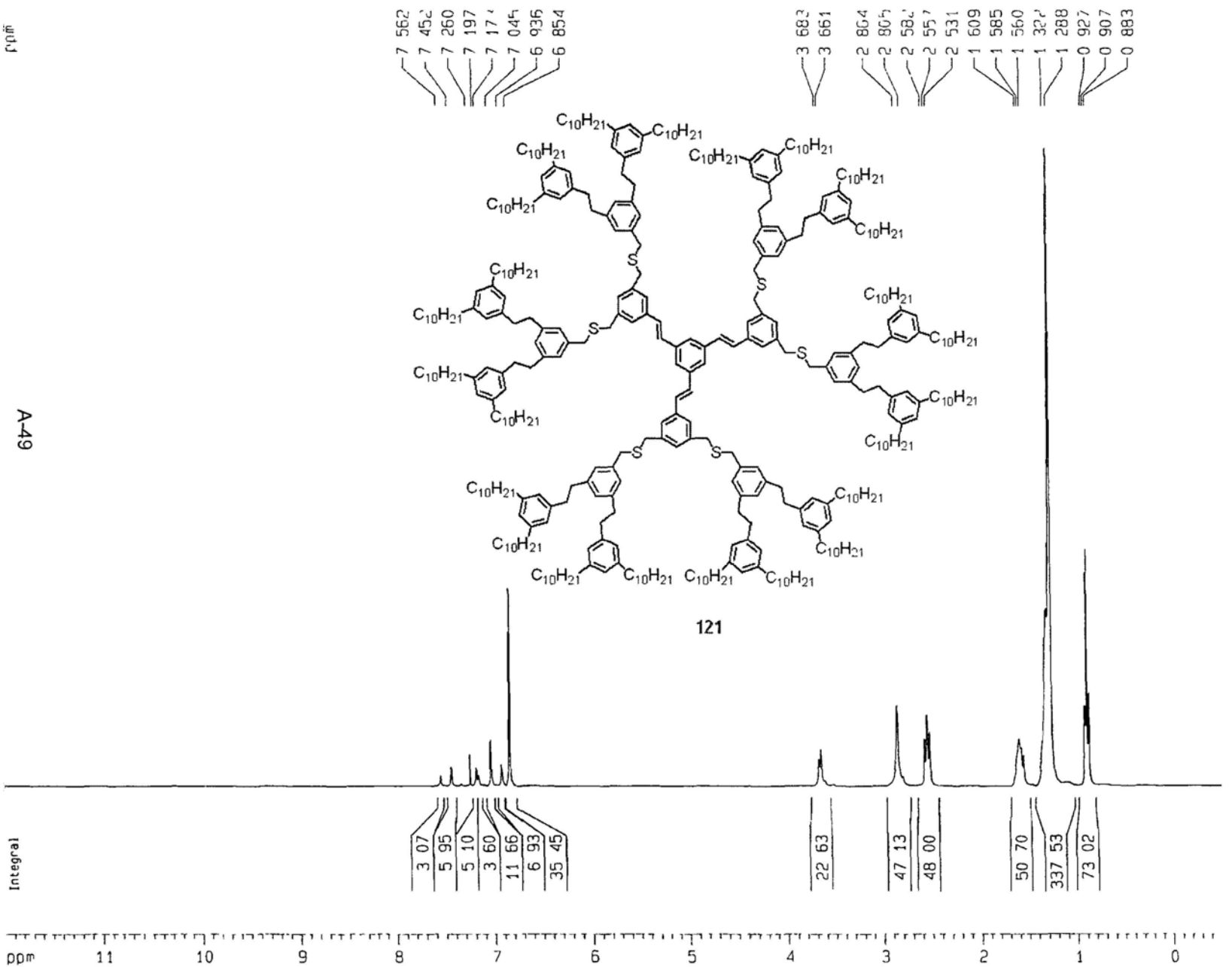

A-49

```
Current Data Parameters
NAME      G3-CSC=C den(h
EXPNO               1
PROCNO              1

F2 - Acquisition Parameters
Date_          20080422
Time             14 02
INSTRUM          dpx300
PROBHD   5 mm BBO BB-1H
PULPROG             zg
TD               32768
SOLVENT          CDCl3
NS                  16
DS                   0
SWH          8992 806 Hz
FIDRES       0 274439 Hz
AQ           1 8219508 sec
RG                28 5
DW              55 600 usec
DE              79 43 usec
TE              296 2 K
D1           5 00000000 sec
MCREST       0 00000000 sec
MCWRK        0 01500000 sec

======== CHANNEL f1 ========
NUC1                1H
P1               5 00 usec
PL1              -2 00 dB
SFO1       300 1312000 MHz

F2 - Processing parameters
SI               32768
SF         300 1300063 MHz
WDW                 EM
SSB                  0
LB               0 30 Hz
GB                   0
PC                1 00

1D NMR plot parameters
CX              22 00 cm
CY              11 45 cm
F1P             12 000 ppm
F1            3601 56 Hz
F2P             -0 500 ppm
F2            -150 07 Hz
PPMCM         0 56818 ppm/cm
HZCM        170 52841 Hz/cm
```

C13

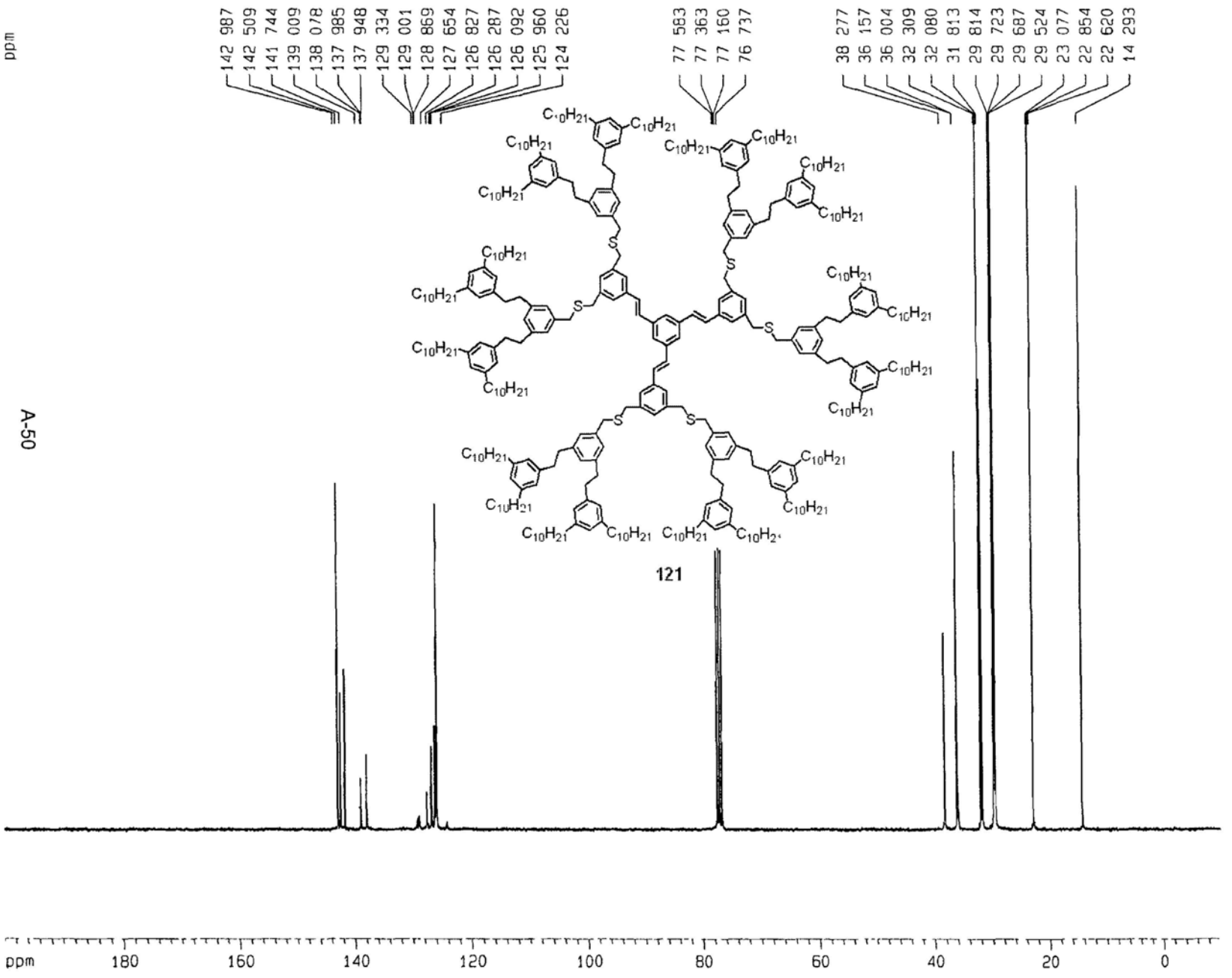

Current Data Parameters
NAME G3-CSC-C-der (C)
EXPNO 1
PROCNO 1

F2 - Acquisition Parameters
Date_ 20080422
Time 14 00
INSTRUM dpx300
PROBHD 5 mm BBO BB-1H
PULPROG zgdc
TD 65536
SOLVENT CDCl3
NS 2832
DS 0
SWH 22675 736 Hz
FIDRES 0 346004 Hz
AQ 1 4451188 sec
RG 8192
DW 22 050 usec
DE 6 00 usec
TE 296 2 K
D1 1 00000000 sec
d11 0 03000000 sec
MCREST 0 00000000 sec
MCWRK 0 01500000 sec

======== CHANNEL f1 ========
NUC1 13C
P1 3 00 usec
PL1 -6 00 dB
SFO1 75 4745111 MHz

======== CHANNEL f2 ========
CPDPRG2 waltz16
NUC2 1H
PCPD2 100 00 usec
PL2 120 00 dB
PL12 19 00 dB
SFO2 300 1315007 MHz

F2 - Processing parameters
SI 65536
SF 75 4677422 MHz
WDW EM
SSB 0
LB 1 00 Hz
GB 0
PC 1 40

1D NMR plot parameters
CX 22 00 cm
CY 19 87 cm
F1P 200 000 ppm
F1 15093 55 Hz
F2P -10 000 ppm
F2 -754 68 Hz
PPMCM 9 54545 ppm/cm
HZCM 720 37384 Hz/cm

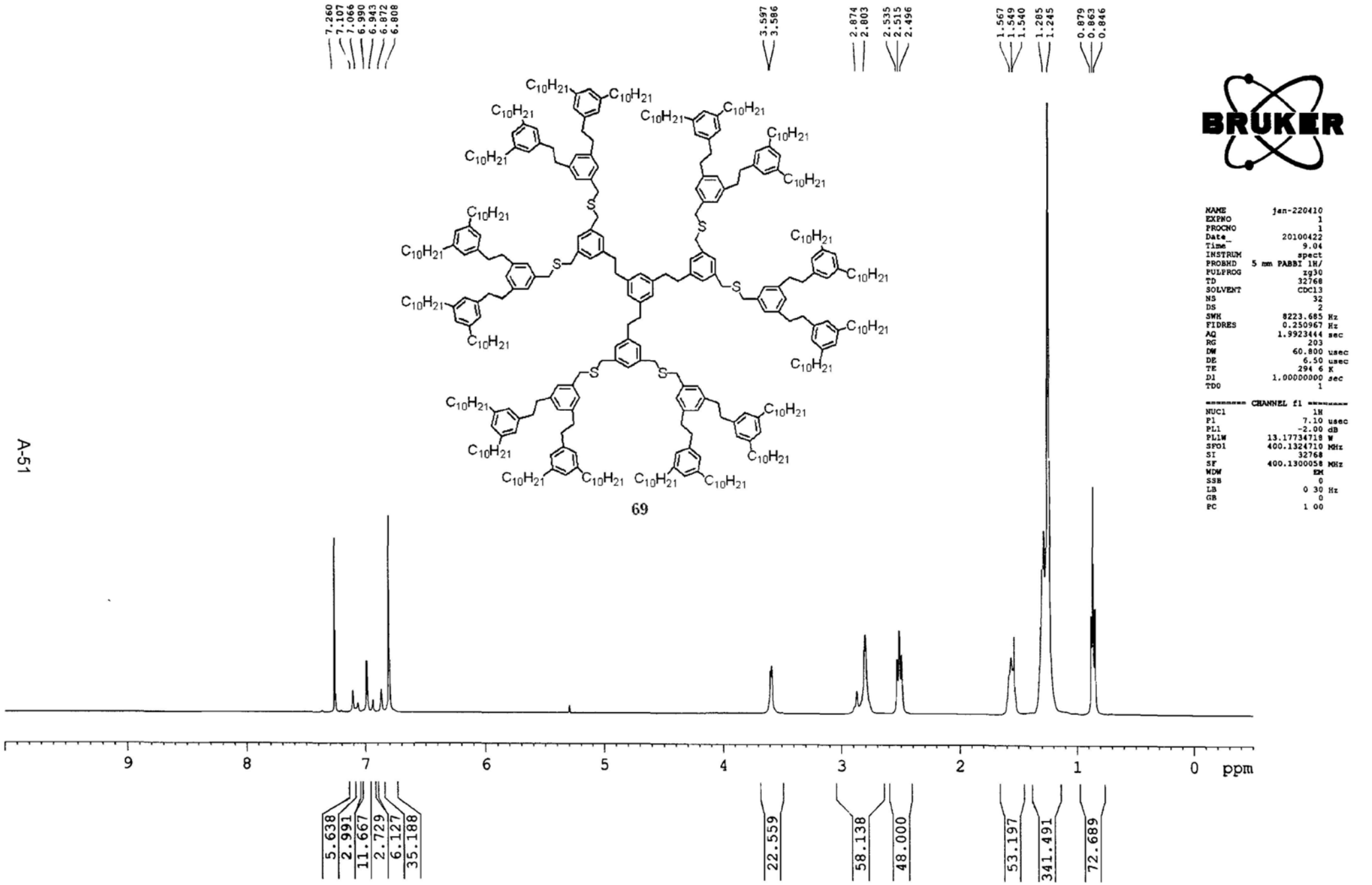
7.260
7.107
7.066
6.990
6.943
6.872
6.808
3.597
3.586
2.874
2.803
2.535
2.515
2.496
1.567
1.549
1.540
1.285
1.245
0.879
0.863
0.846
BRUKER
NAME jan-220410
EXPNO 1
PROCNO 1
Date_ 20100422
Time 9.04
INSTRUM spect
PROBHD 5 mm PABBI 1H/
PULPROG zg30
TD 32768
SOLVENT CDCl3
NS 32
DS 2
SWH 8223.685 Hz
FIDRES 0.250967 Hz
AQ 1.9923444 sec
RG 203
DW 60.800 usec
DE 6.50 usec
TE 294.6 K
D1 1.00000000 sec
TD0 1
CHANNEL f1
NUC1 1H
P1 7.10 usec
PL1 -2.00 dB
PL1W 13.17734718 W
SFO1 400.1324710 MHz
SI 32768
SF 400.1300058 MHz
WDW EM
SSB 0
LB 0.30 Hz
GB 0
PC 1.00
9
8
7
6
5
4
3
2
1
0
ppm
5.638
2.991
11.667
2.729
6.127
35.188
22.559
58.138
48.000
53.197
341.491
72.689

69

A-51

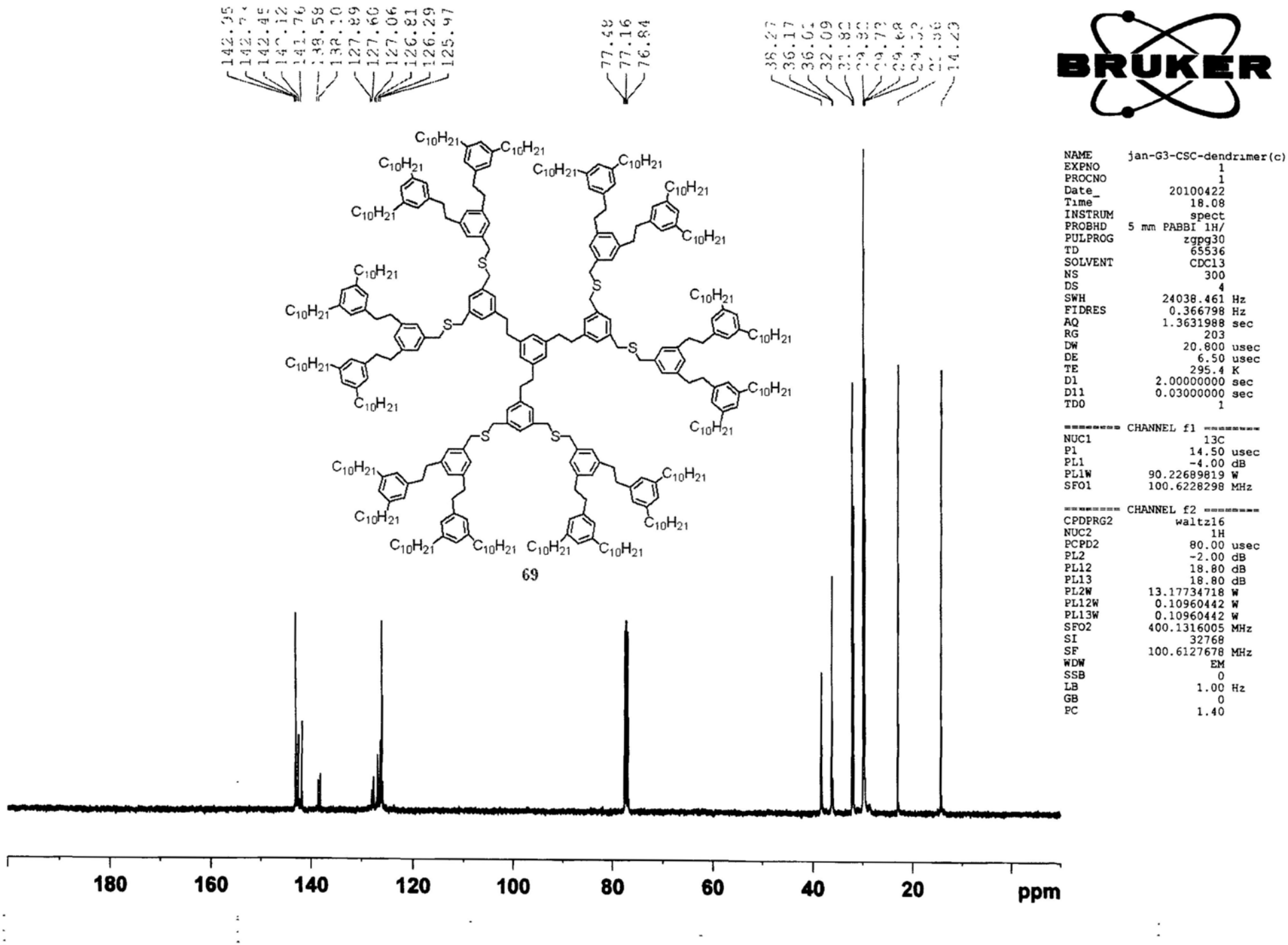

NAME	jan-G3-CSC-dendrimer(c)
EXPNO	1
PROCNO	1
Date_	20100422
Time	18.08
INSTRUM	spect
PROBHD	5 mm PABBI 1H/
PULPROG	zgpg30
TD	65536
SOLVENT	CDCl3
NS	300
DS	4
SWH	24038.461 Hz
FIDRES	0.366798 Hz
AQ	1.3631988 sec
RG	203
DW	20.800 usec
DE	6.50 usec
TE	295.4 K
D1	2.00000000 sec
D11	0.03000000 sec
TD0	1
======== CHANNEL f1 ========	
NUC1	13C
P1	14.50 usec
PL1	-4.00 dB
PL1W	90.22689819 W
SFO1	100.6228298 MHz
======== CHANNEL f2 ========	
CPDPRG2	waltz16
NUC2	1H
PCPD2	80.00 usec
PL2	-2.00 dB
PL12	18.80 dB
PL13	18.80 dB
PL2W	13.17734718 W
PL12W	0.10960442 W
PL13W	0.10960442 W
SFO2	400.1316005 MHz
SI	32768
SF	100.6127678 MHz
WDW	EM
SSB	0
LB	1.00 Hz
GB	0
PC	1.40

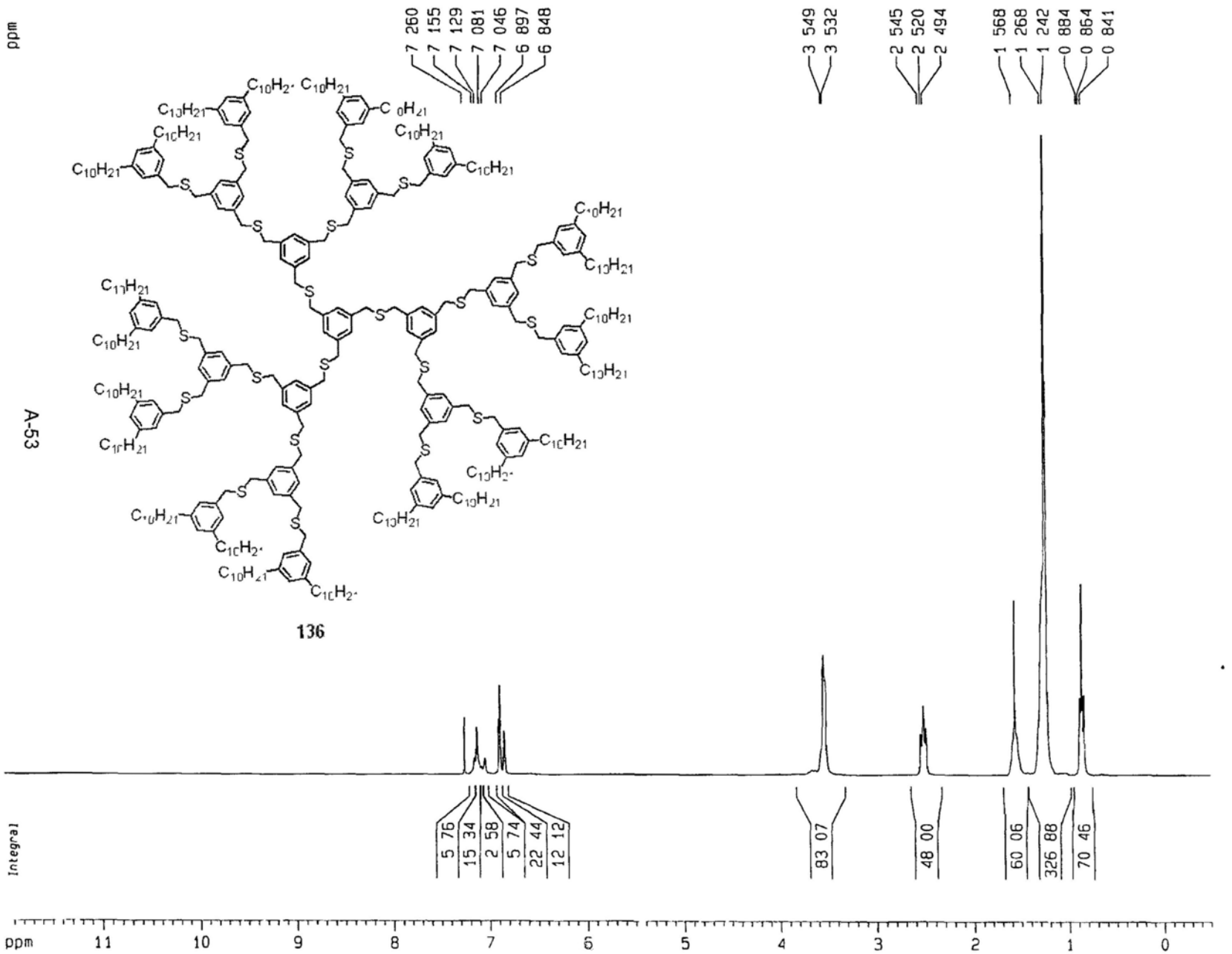

136

A-53

Current Data Parameters
NAME G3-SSS-dendrimer
EXPNO 1
PROCNO 1

F2 - Acquisition Parameters
Date_ 20090424
Time 9 38
INSTRUM dpx300
PROBHD 5 mm BBO BB-1H
PULPROG zg
TD 32768
SOLVENT CDCl3
NS 16
DS 0
SWH 8992 806 Hz
FIDRES 0 274439 Hz
AQ 1 8219508 sec
RG 90 5
DW 55 600 usec
DE 79 43 usec
TE 295 2 K
D1 5 00000000 sec
MCREST 0 00000000 sec
MCWRK 0 01500000 sec

======== CHANNEL f1 ========
NUC1 1H
P1 5 00 usec
PL1 -2 00 dB
SFO1 300 1312000 MHz

F2 - Processing parameters
SI 32768
SF 300 1300066 MHz
WDW EM
SSB 0
LB 0 30 Hz
GB 0
PC 1 00

1D NMR plot parameters
CX 22 00 cm
CY 11 64 cm
F1P 12 000 ppm
F1 3601 56 Hz
F2P -0 500 ppm
F2 -150 07 Hz
PPMCM 0 56818 ppm/cm
HZCM 170 52841 Hz/cm

C13

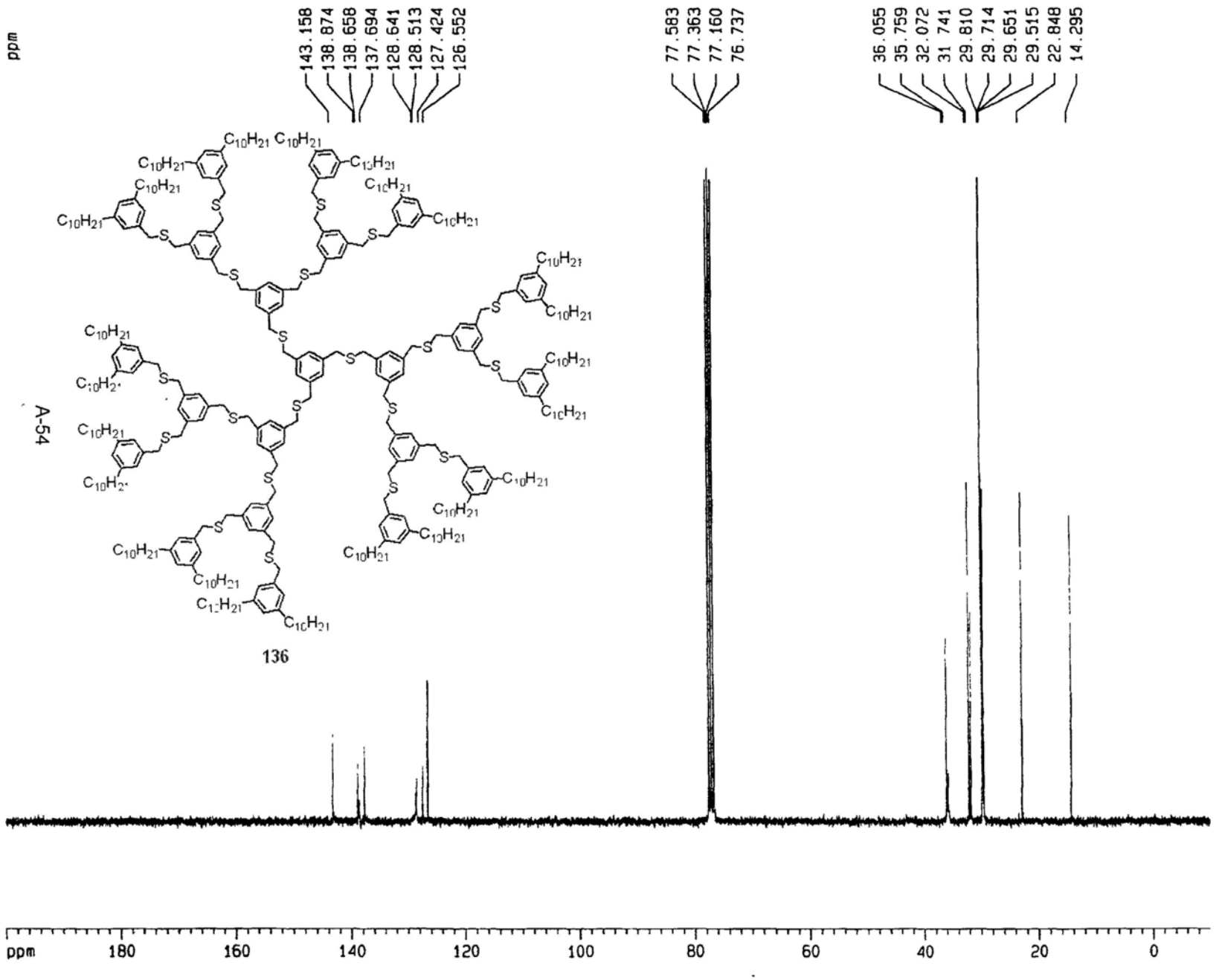

Current Data Parameters
NAME G3-SSS-den(c)
EXPNO 1
PROCNO 1

F2 - Acquisition Parameters
Date_ 20090424
Time 15.54
INSTRUM dpx300
PROBHD 5 mm BBO BB-1H
PULPROG zgdc
TD 65536
SOLVENT CDCl3
NS 1610
DS 0
SWH 22675.736 Hz
FIDRES 0.346004 Hz
AQ 1.4451188 sec
RG 8192
DW 22.050 usec
DE 6.00 usec
TE 296.2 K
D1 1.00000000 sec
d11 0.03000000 sec
MCREST 0.00000000 sec
MCWRK 0.01500000 sec

======== CHANNEL f1 ========
NUC1 13C
P1 3.00 usec
PL1 -6.00 dB
SFO1 75.4745111 MHz

======== CHANNEL f2 ========
CPDPRG2 waltz16
NUC2 1H
PCPD2 100.00 usec
PL2 120.00 dB
PL12 19.00 dB
SFO2 300.1315007 MHz

F2 - Processing parameters
SI 65536
SF [illegible]
WDW EM
SSB 0
LB 1.00 Hz
GB 0
PC 1.40

1D NMR plot parameters
CX 22.00 cm
CY 12.00 cm
F1P 200.000 ppm
F1 15093.55 Hz
F2P -10.000 ppm
F2 -754.68 Hz
PPMCM 9.54545 ppm/cm
HZCM 720.37384 Hz/cm

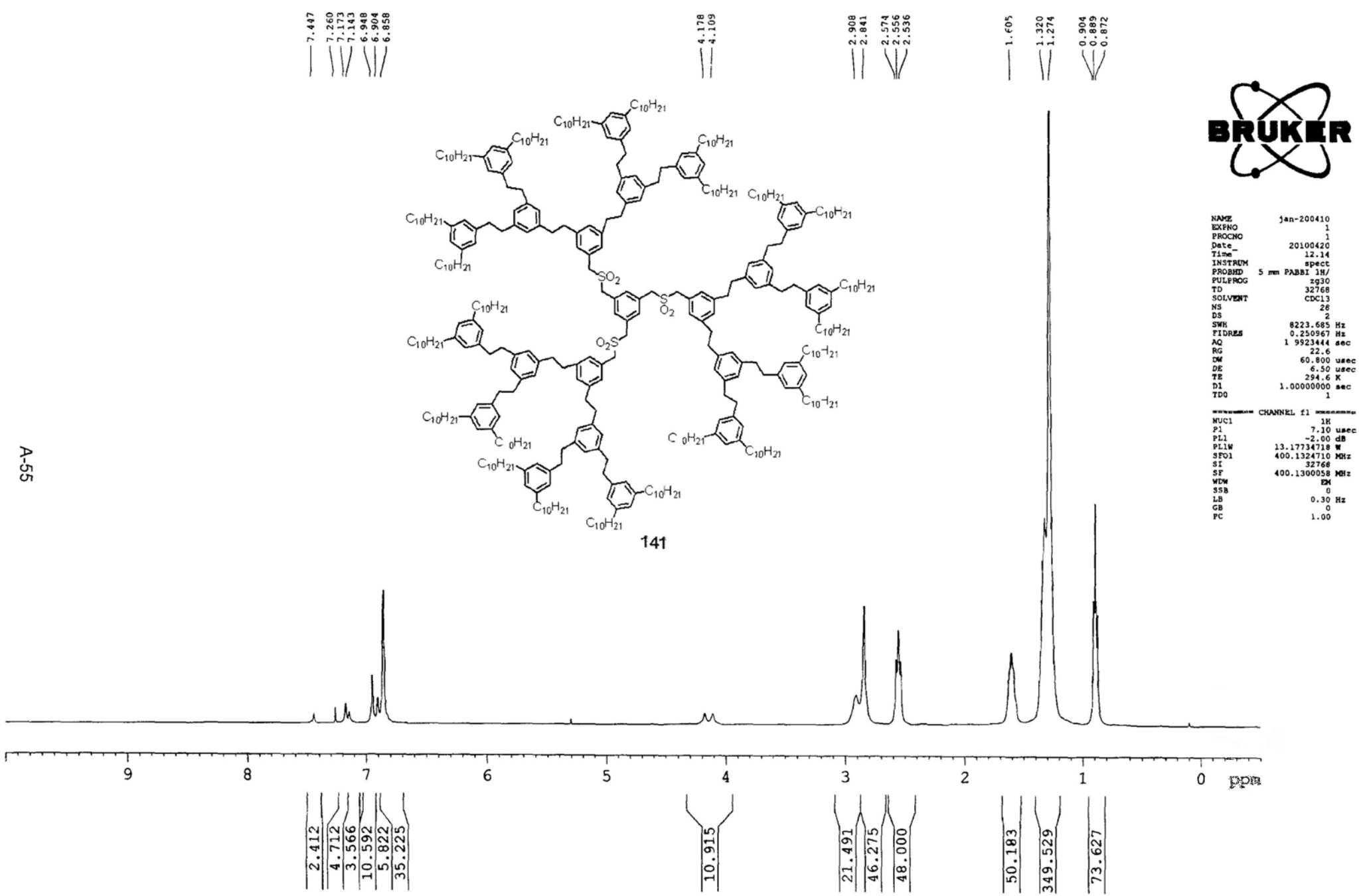
7.447
7.260
7.173
7.143
6.948
6.904
6.858
4.178
4.109
2.908
2.841
2.574
2.556
2.536
1.605
1.320
1.274
0.904
0.889
0.872
BRUKER
NAME jan-200410
EXPNO 1
PROCNO 1
Date_ 20100420
Time 12.14
INSTRUM spect
PROBHD 5 mm PABBI 1H/
PULPROG zg30
TD 32768
SOLVENT CDCl3
NS 26
DS 2
SWH 8223.685 Hz
FIDRES 0.250967 Hz
AQ 1.9923444 sec
RG 22.6
DW 60.800 usec
DE 6.50 usec
TE 294.6 K
D1 1.00000000 sec
TD0 1
CHANNEL f1
NUC1 1H
P1 7.10 usec
PL1 -2.00 dB
PL1W 13.17734718 W
SFO1 400.1324710 MHz
SI 32768
SF 400.1300058 MHz
WDW EM
SSB 0
LB 0.30 Hz
GB 0
PC 1.00
141
9
8
7
6
5
4
3
2
1
0
ppm
2.412
4.712
3.566
10.592
5.822
35.225
10.915
21.491
46.275
48.000
50.183
349.529
73.627

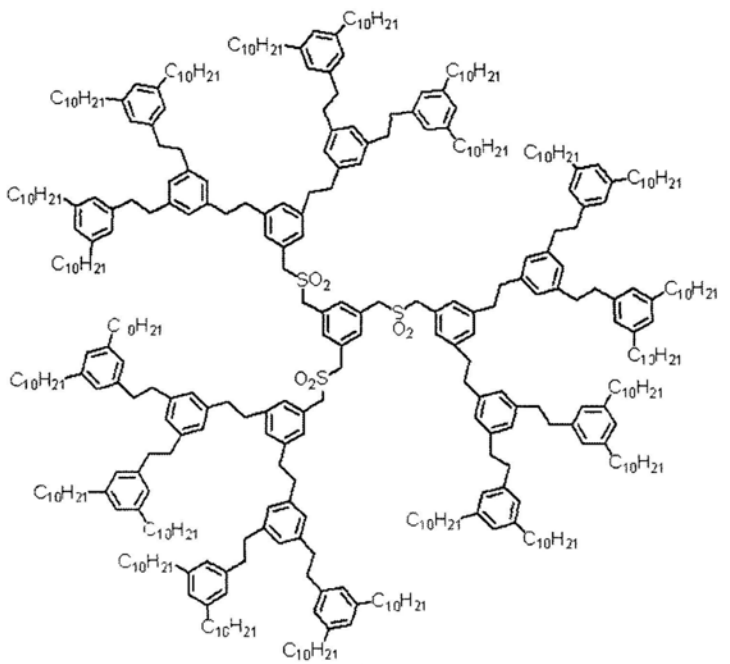

141

NAME	jan-G3-3SOc-den(c)
EXPNO	1
PROCNO	1
Date_	20100422
Time_	9.13
INSTRUM	spect
PROBHD	5 mm PABBI 1H/
PULPROG	zgpg30
TD	32768
SOLVENT	CDCl3
NS	1044
DS	4
SWH	24038.461 Hz
FIDRES	0.733596 Hz
AQ	0.6816244 sec
RG	203
DW	20.800 usec
DE	6.50 usec
TE	294.7 K
D1	2.00000000 sec
D11	0.03000000 sec
TD0	1
======== CHANNEL f1 ========	
NUC1	13C
P1	14.50 usec
PL1	-4.00 dB
PL1W	90.22689819 W
SFO1	100.6228298 MHz
======== CHANNEL f2 ========	
CPDPRG2	waltz16
NUC2	1H
PCPD2	80.00 usec
PL2	-2.00 dB
PL12	18.80 dB
PL13	18.80 dB
PL2W	13.17734718 W
PL12W	0.10960442 W
PL13W	0.10960442 W
SFO2	400.1316005 MHz
SI	32768
SF	100.6127575 MHz
WDW	EM
SSB	0
LB	1.00 Hz
GB	0
PC	1.40

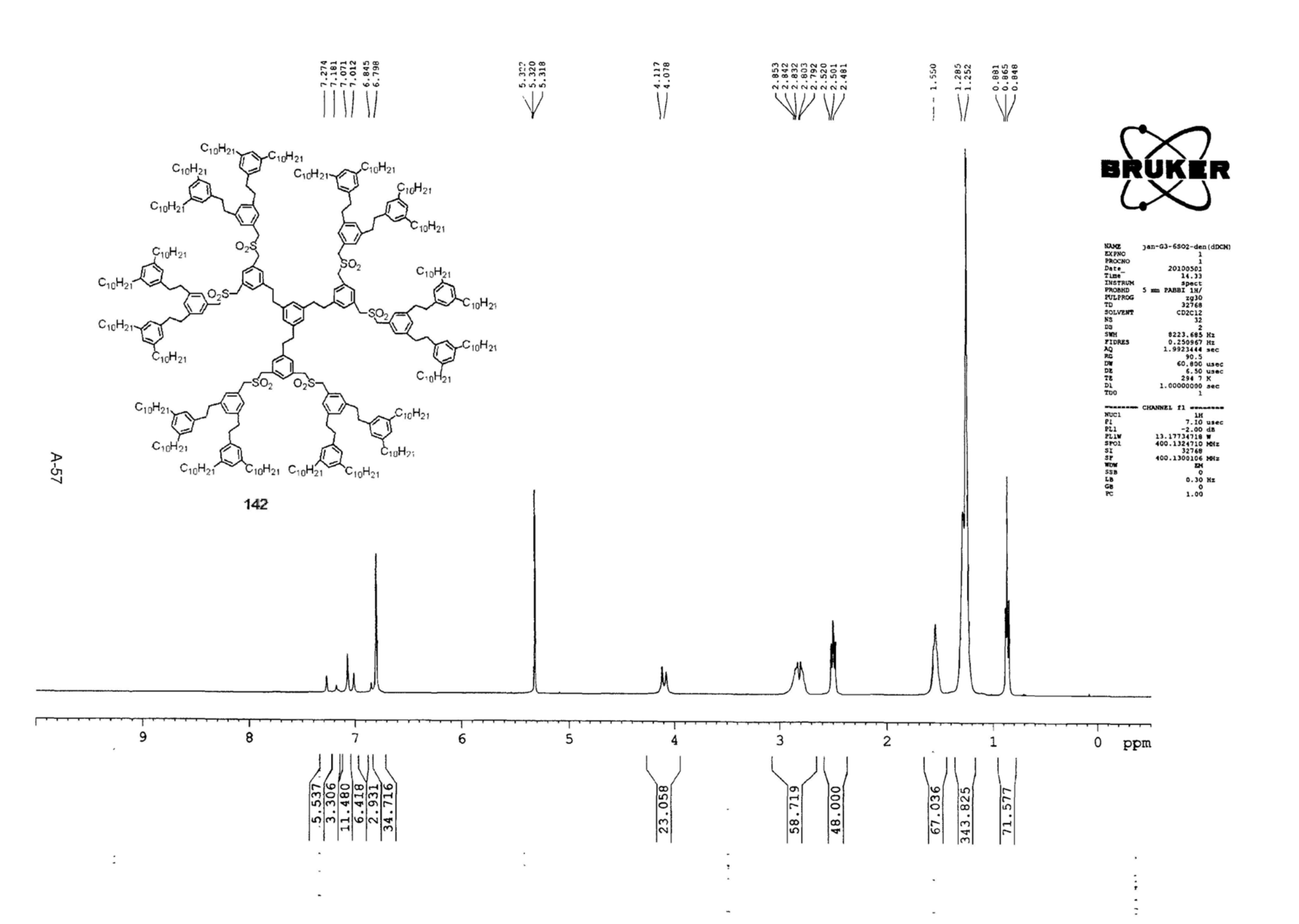
7.274
7.181
7.071
7.012
6.845
6.798
5.322
5.320
5.318
4.117
4.078
2.853
2.842
2.832
2.803
2.792
2.520
2.501
2.481
1.550
1.285
1.252
0.881
0.865
0.848
BRUKER
NAME jan-G3-6SO2-den(dDCM)
EXPNO 1
PROCNO 1
Date_ 20100501
Time 14.33
INSTRUM spect
PROBHD 5 mm PABBI 1H/
PULPROG zg30
TD 32768
SOLVENT CD2Cl2
NS 32
DS 2
SWH 8223.685 Hz
FIDRES 0.250967 Hz
AQ 1.9923444 sec
RG 90.5
DW 60.800 usec
DE 6.50 usec
TE 294.7 K
D1 1.00000000 sec
TD0 1
CHANNEL f1
NUC1 1H
P1 7.10 usec
PL1 -2.00 dB
PL1W 13.17734718 W
SFO1 400.1324710 MHz
SI 32768
SF 400.1300106 MHz
WDW EM
SSB 0
LB 0.30 Hz
GB 0
PC 1.00
142
A-57
9
8
7
6
5
4
3
2
1
0
ppm
5.537
3.306
11.480
6.418
2.931
34.716
23.058
58.719
48.000
67.036
343.825
71.577

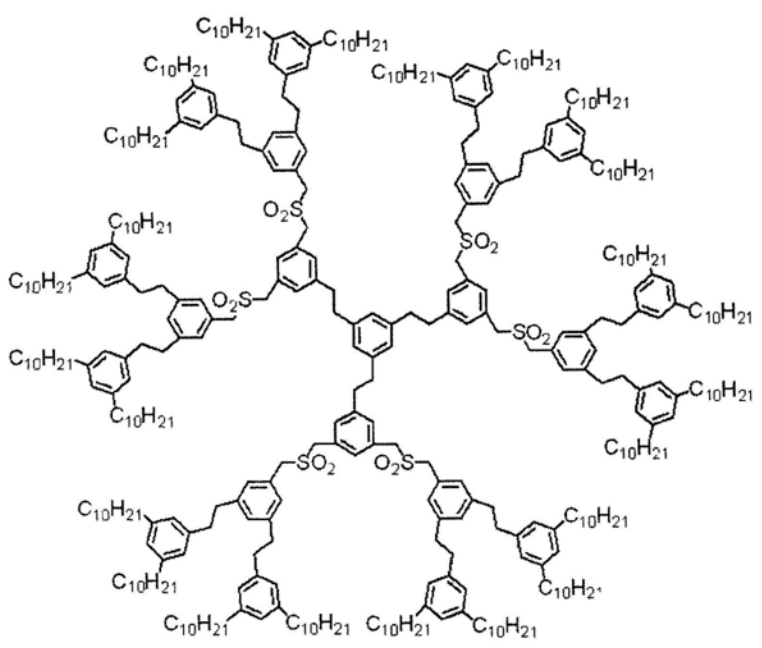

142

NAME	jan-G3-6SO2-den(c)
EXPNO	1
PROCNO	1
Date_	20100429
Time	18.22
INSTRUM	spect
PROBHD	5 mm PABBI 1H/
PULPROG	zgpg30
TD	65536
SOLVENT	CDCl3
NS	1155
DS	4
SWH	24038.461 Hz
FIDRES	0.366798 Hz
AQ	1.3631988 sec
RG	203
DW	20.800 usec
DE	6.50 usec
TE	295.2 K
D1	2.00000000 sec
D11	0.03000000 sec
TD0	1
======== CHANNEL f1 ========	
NUC1	13C
P1	14.50 usec
PL1	-4.00 dB
PL1W	90.22689819 W
SFO1	100.6228298 MHz
======== CHANNEL f2 ========	
CPDPRG2	waltz16
NUC2	1H
PCPD2	80.00 usec
PL2	-2.00 dB
PL12	18.80 dB
PL13	18.80 dB
PL2W	13.17734718 W
PL12W	0.10960442 W
PL13W	0.10960442 W
SFO2	400.1316005 MHz
SI	32768
SF	100.6127575 MHz
WDW	EM
SSB	0
LB	1.00 Hz
GB	0
PC	1.40

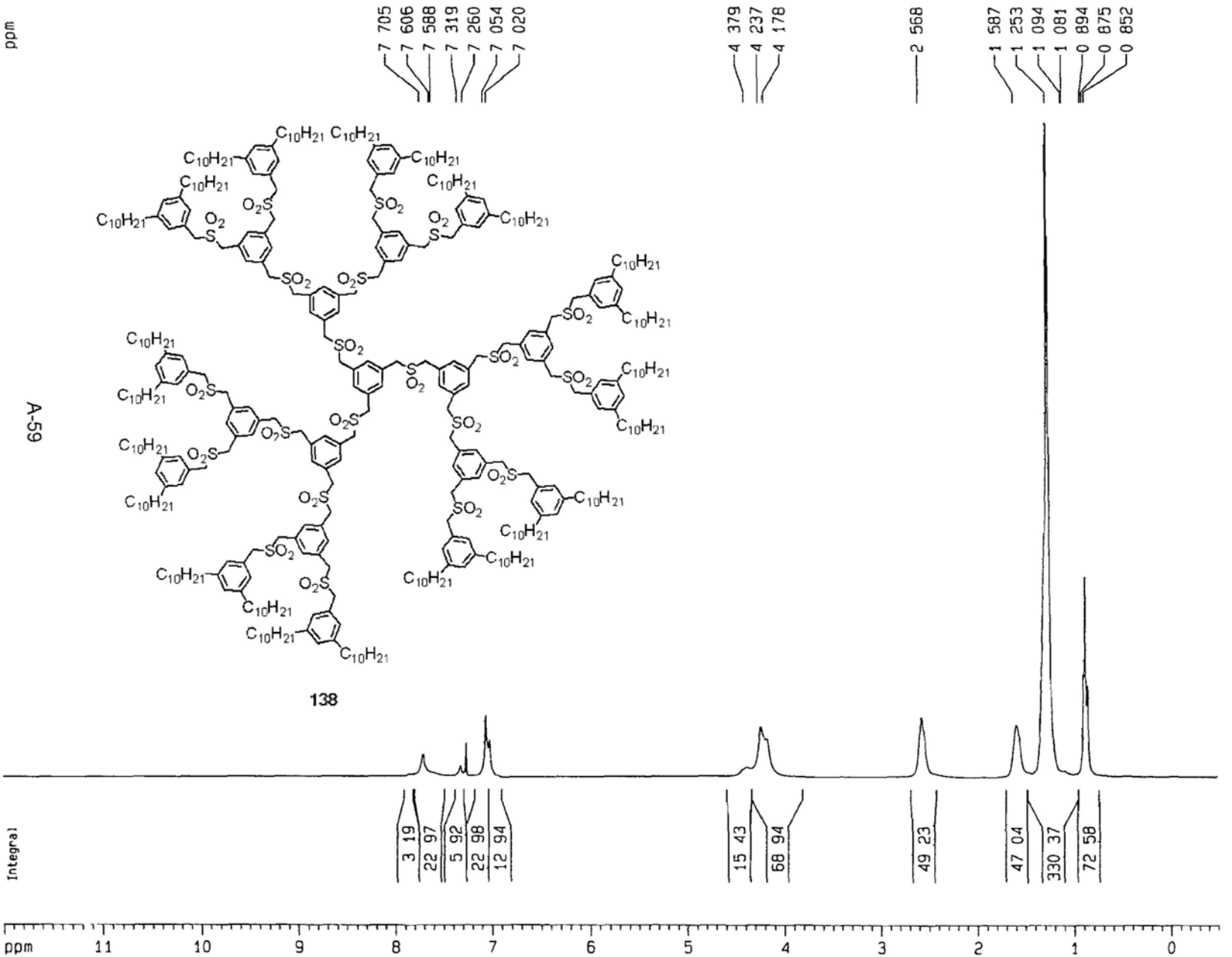


```
Current Data Parameters
NAME      G3-21SO2-dendrimer
EXPNO                      1
PROCNO                     1

F2 - Acquisition Parameters
Date_              20090807
Time                 18 07
INSTRUM              dpx300
PROBHD   5 mm BBO BB-1H
PULPROG                 zg
TD                   32768
SOLVENT              CDCl3
NS                     128
DS                       0
SWH              8992 806 Hz
FIDRES           0 274439 Hz
AQ               1 8219508 sec
RG                      32
DW                 55 600 usec
DE                 79 43 usec
TE                 294 2 K
D1               5 00000000 sec
MCREST           0 00000000 sec
MCWRK            0 01500000 sec

======== CHANNEL f1 ========
NUC1                    1H
P1                 5 00 usec
PL1                -2 00 dB
SFO1          300 1312000 MHz

F2 - Processing parameters
SI                   32768
SF            300 1300071 MHz
WDW                     EM
SSB                      0
LB                 0 30 Hz
GB                       0
PC                  1 00

1D NMR plot parameters
CX                 22 00 cm
CY                 11 85 cm
F1P               12 000 ppm
F1                3601 56 Hz
F2P                -0 500 ppm
F2                -150 07 Hz
PPMCM           0 56818 ppm/cm
HZCM          170 52840 Hz/cm
```

C13

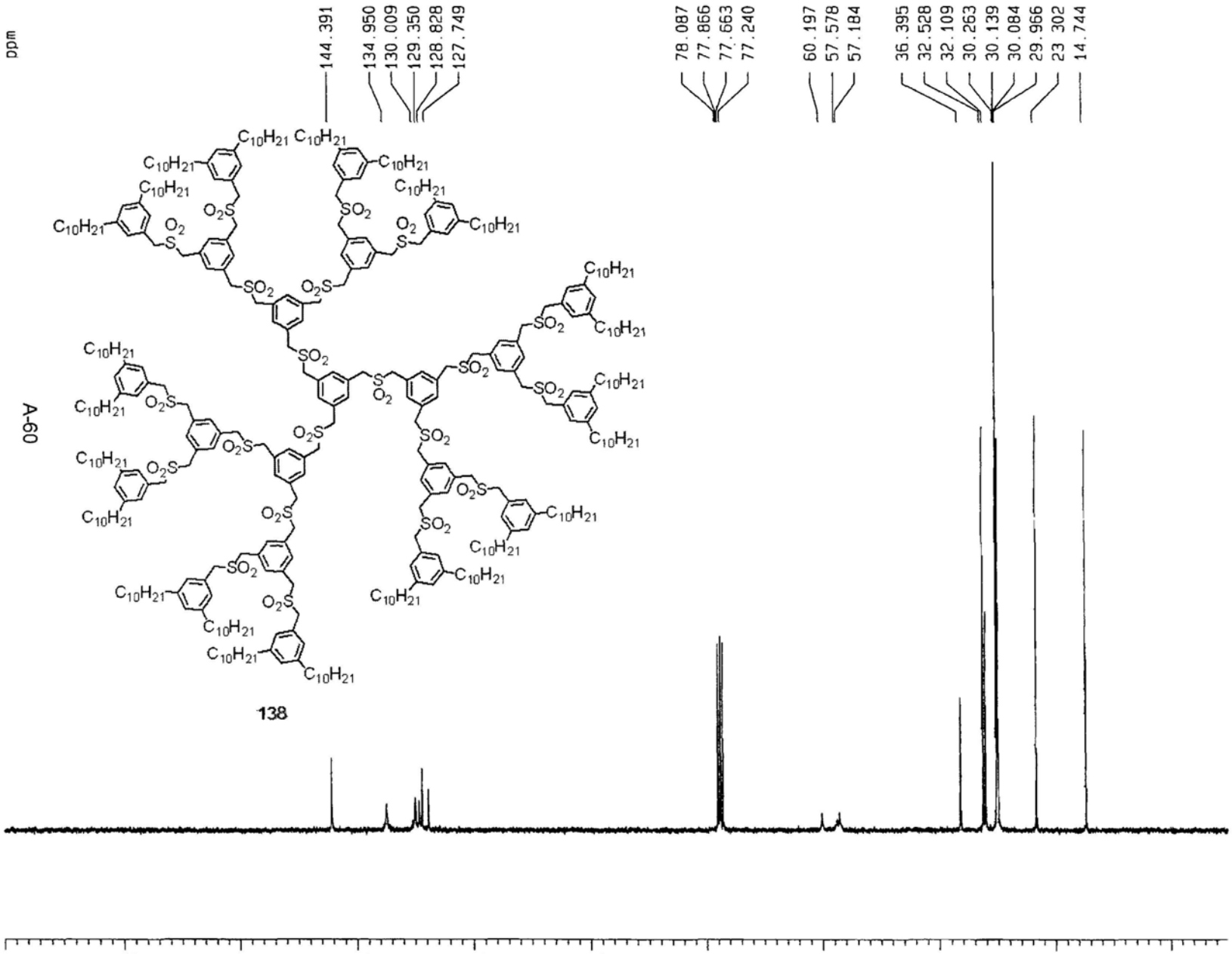


```
Current Data Parameters
NAME          G3-21SO2-den
EXPNO                    1
PROCNO                   1

F2 - Acquisition Parameters
Date_              20090807
Time                 14.20
INSTRUM              dpx300
PROBHD   5 mm BBO BB-1H
PULPROG               zgdc
TD                   65536
SOLVENT              CDCl3
NS                     508
DS                       0
SWH            22675.736 Hz
FIDRES          0.346004 Hz
AQ              1.4451188 sec
RG                 10321.3
DW                22.050 usec
DE                 6.00 usec
TE                295.2 K
D1              1.00000000 sec
d11             0.03000000 sec
MCREST          0.00000000 sec
MCWRK           0.01500000 sec

======== CHANNEL f1 ========
NUC1                  13C
P1                 3.00 usec
PL1                -6.00 dB
SFO1          75.4745111 MHz

======== CHANNEL f2 ========
CPDPRG2           waltz16
NUC2                  1H
PCPD2            100.00 usec
PL2               120.00 dB
PL12               19.00 dB
SFO2          300.1315007 MHz

F2 - Processing parameters
SI                   65536
SF            75.4677053 MHz
WDW                     EM
SSB                      0
LB                  1.00 Hz
GB                       0
PC                    1.40

1D NMR plot parameters
CX                  22.00 cm
CY                  12.00 cm
F1P               200.000 ppm
F1              15093.54 Hz
F2P               -10.000 ppm
F2               -754.68 Hz
PPMCM              9.54545 ppm/cm
HZCM             720.37347 Hz/cm
```

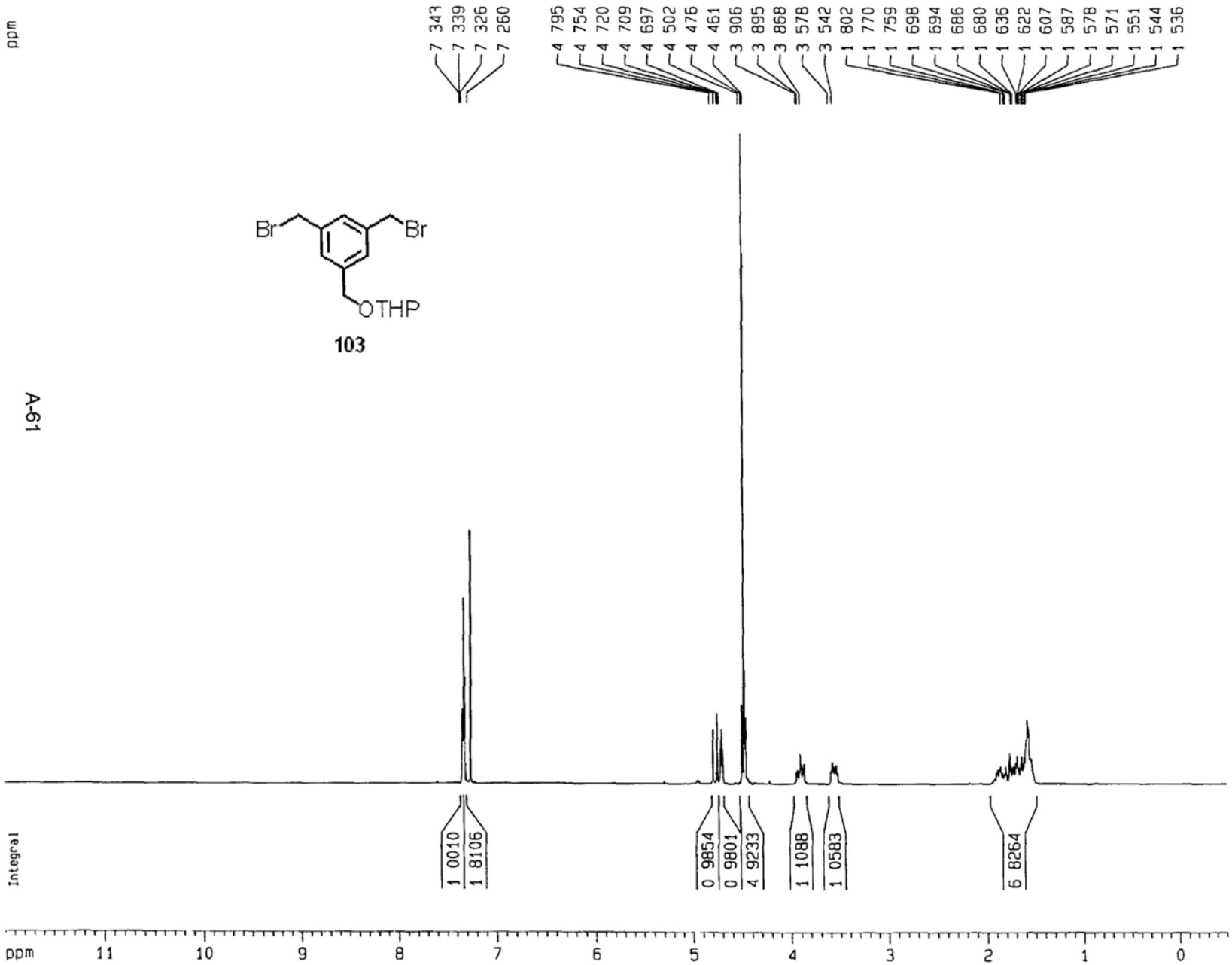

Current Data Parameters
NAME t-01CH2Br-OTHP
EXPNO 1
PROCNO 1

F2 - Acquisition Parameters
Date_ 20080409
Time 15 50
INSTRUM dpx300
PROBHD 5 mm BBO BB-1H
PULPROG zg
TD 32768
SOLVENT CDCl3
NS 8
DS 0
SWH 8992 806 Hz
FIDRES 0 274439 Hz
AQ 1 8219508 sec
RG 256
DW 55 600 usec
DE 79 43 usec
TE 296 2 K
D1 5 00000000 sec
MCREST 0 00000000 sec
MCWRK 0 01500000 sec

======== CHANNEL f1 ========
NUC1 1H
P1 5 00 usec
PL1 -2 00 dB
SFO1 300 1312000 MHz

F2 - Processing parameters
SI 32768
SF 300 1300063 MHz
WDW EM
SSB 0
LB 0 30 Hz
GB 0
PC 1 00

1D NMR plot parameters
CX 22 00 cm
CY 11 77 cm
F1P 12 000 ppm
F1 3601 56 Hz
F2P -0 500 ppm
F2 -150 07 Hz
PPMCM 0 56818 ppm/cm
HZCM 170 52841 Hz/cm

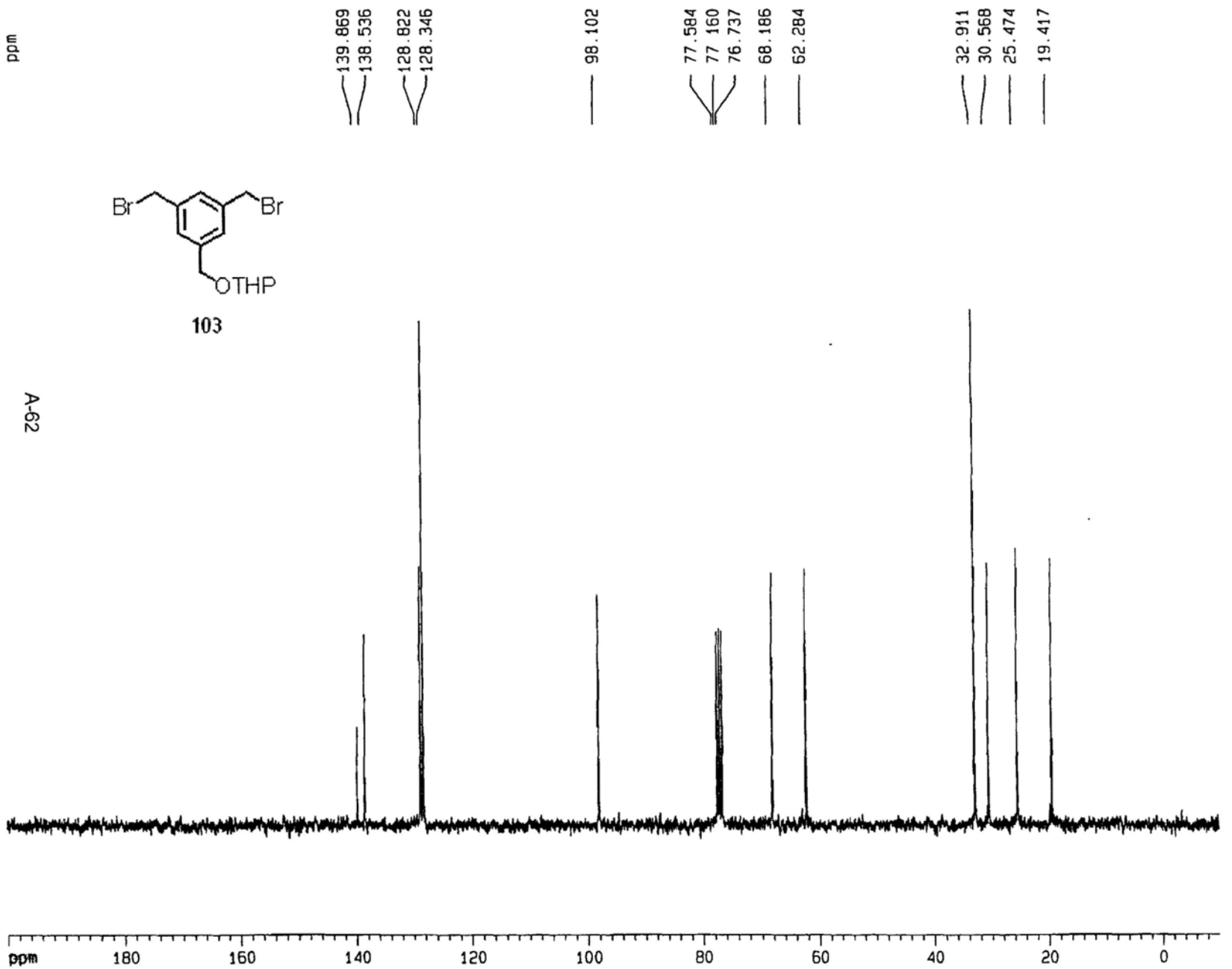

Current Data Parameters
NAME dlCH2Br-OTHP-c1
EXPNO 2
PROCNO 1

F2 - Acquisition Parameters
Date_ 20081202
Time 18.33
INSTRUM dpx300
PROBHD 5 mm BBO BB-1H
PULPROG zgdc
TD 65536
SOLVENT CDCl3
NS 32
DS 0
SWH 22675 736 Hz
FIDRES 0.346004 Hz
AQ 1.4451188 sec
RG 6502
DW 22 050 usec
DE 6.00 usec
TE 296 2 K
D1 1.00000000 sec
d11 0.03000000 sec
MCREST 0.00000000 sec
MCWRK 0.01500000 sec

======== CHANNEL f1 ========
NUC1 13C
P1 3 00 usec
PL1 -6.00 dB
SFO1 75.4745111 MHz

======== CHANNEL f2 ========
CPDPRG2 waltz16
NUC2 1H
PCPD2 100.00 usec
PL2 120 00 dB
PL12 19.00 dB
SFO2 300 1315007 MHz

F2 - Processing parameters
SI 65536
SF 75.4677462 MHz
WDW EM
SSB 0
LB 3.00 Hz
GB 0
PC 1.40

1D NMR plot parameters
CX 22.00 cm
CY 9.39 cm
F1P 200.000 ppm
F1 15093 55 Hz
F2P -10.000 ppm
F2 -754.68 Hz
PPMCM 9.54545 ppm/cm
HZCM 720.37384 Hz/cm

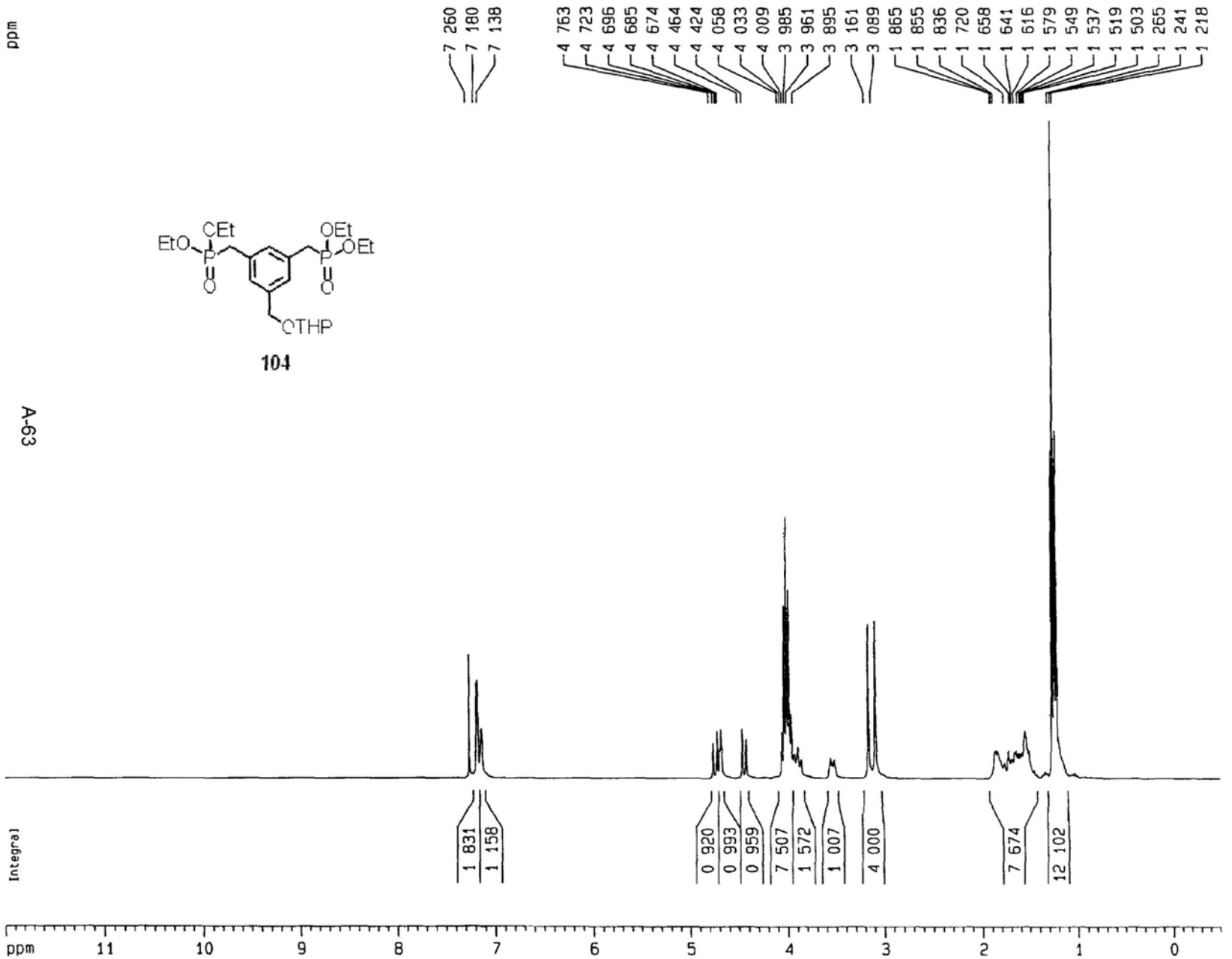

Current Data Parameters

NAME	d1POEt2-OTHP1
EXPNO	1
PROCNO	1

F2 - Acquisition Parameters

Date_	20080805
Time	16 30
INSTRUM	dpx300
PROBHD	5 mm BBO BB-1H
PULPROG	zg
TD	32768
SOLVENT	CDCl3
NS	32
DS	0
SWH	8992 806 Hz
FIDRES	0 274439 Hz
AQ	1 8219508 sec
RG	574 7
DW	55 600 usec
DE	79 43 usec
TE	295 2 K
D1	5 00000000 sec
MCREST	0 00000000 sec
MCWRK	0 01500000 sec

======== CHANNEL f1 ========

NUC1	1H
P1	5 00 usec
PL1	-2 00 dB
SFO1	300 1312000 MHz

F2 - Processing parameters

SI	32768
SF	300 1300063 MHz
WDW	EM
SSB	0
LB	0 30 Hz
GB	0
PC	1 00

1D NMR plot parameters

CX	22 00 cm
CY	11 97 cm
F1P	12 000 ppm
F1	3601 56 Hz
F2P	-0 500 ppm
F2	-150 07 Hz
PPMCM	0 56818 ppm/cm
HZCM	170 52841 Hz/cm

C13

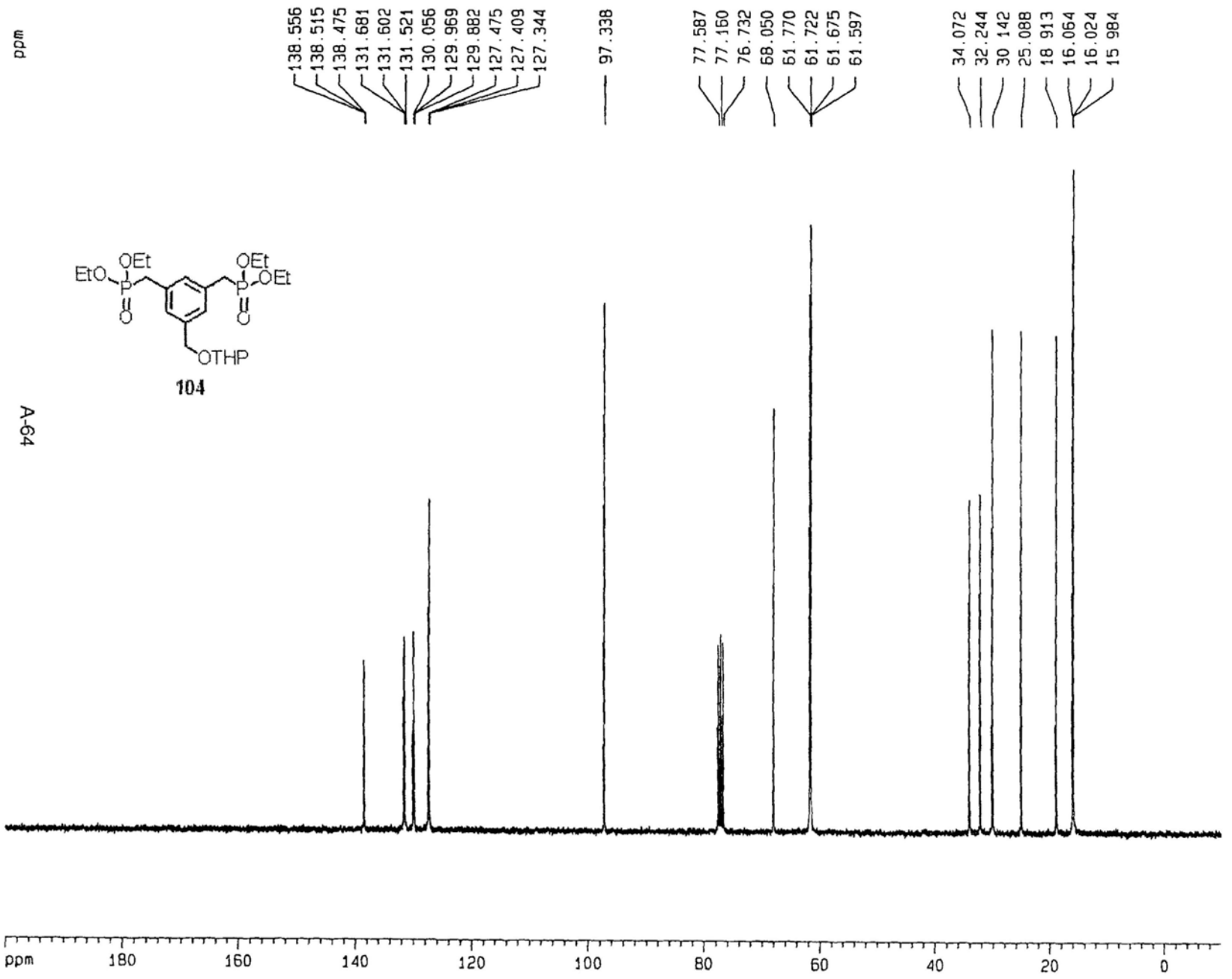

Current Data Parameters
NAME d1POEt-OTHP(c)
EXPNO 1
PROCNO 1

F2 - Acquisition Parameters
Date_ 20080731
Time 17 17
INSTRUM dpx300
PROBHD 5 mm BBO BB-1H
PULPROG zgdc
TD 65536
SOLVENT CDCl3
NS 300
DS 0
SWH 22675.736 Hz
FIDRES 0 346004 Hz
AQ 1.4451188 sec
RG 8192
DW 22 050 usec
DE 6 00 usec
TE 296 2 K
D1 1 00000000 sec
d11 0.03000000 sec
MCREST 0 00000000 sec
MCWRK 0 01500000 sec

======== CHANNEL f1 ========
NUC1 13C
P1 3 00 usec
PL1 -6 00 dB
SFO1 75 4745111 MHz

======== CHANNEL f2 ========
CPDPRG2 waltz16
NUC2 1H
PCPD2 100 00 usec
PL2 120 00 dB
PL12 19 00 dB
SFO2 300 1315007 MHz

F2 - Processing parameters
SI 65536
SF 75 4677630 MHz
WDW EM
SSB 0
LB 1 00 Hz
GB 0
PC 1 40

1D NMR plot parameters
CX 22 00 cm
CY 12.00 cm
F1P 200 000 ppm
F1 15093 55 Hz
F2P -10 000 ppm
F2 -754 68 Hz
PPMCM 9.54545 ppm/cm
HZCM 720 37408 Hz/cm